3-D MODELING OF PILED RAFT FOUNDATION

Anup Sinha

A Thesis
in
The Department of
Building, Civil and Environmental Engineering

Presented in Partial Fulfillment of the Requirements
for the Degree of Doctor of Philosophy at
Concordia University
Montreal, Quebec, Canada

March 2013

CONCORDIA UNIVERSITY
SCHOOL OF GRADUATE STUDIES

This is to certify that the thesis prepared

By: Anup Sinha

Entitled: 3-D Modeling of Piled Raft Foundation

and submitted in partial fulfillment of the requirements for the degree of

DOCTOR OF PHILOSOPHY (CIVIL ENGINEERING)

complies with the regulations of the University and meets the accepted standards with respect to originality and quality.

Signed by the final examining committee:

Dt. D. Dysart-Gale — Chair

Dr. H. Mitri — External Examiner

Dr. A. k. Elhakeem — External to Program

Dr. K. Galal — Examiner

Dr. A. Zsaki — Examiner

Dr. A. Hanna — Thesis Supervisor

Approved by

Chair of Department or Graduate Program Director

March 15, 2013

Dean of Faculty

ABSTRACT

3-D Modeling of Piled Raft Foundation

Anup Sinha, Ph.D.

Concordia University, 2013

Piled-raft-foundation is a new concept, which has received increasing recognition in recent years. Current design practice is based on conventional group pile or block failure theory, that ignore the bearing contribution from the raft. Moreover, the pile group theory is incapable of predicting the differential settlement of the raft, which is beyond the capability of any available analytical method in the literature.

The objective of this thesis is to develop analytical models capable to predict the settlement of each individual pile in the group under the raft. Accordingly, the differential settlement within the pile raft can be estimated. In this investigation, three independent models will be developed to perform as follows; first, the load sharing model that estimates the load components of the raft and the pile group in the system, the second model is to estimate the maximum settlement of the top of the raft and the third model is to estimate the differential settlement among the pile-raft-foundation.

To develop these analytical models, the three dimensional numerical models developed in ABAQUS platform, was extensively used. The extent of stress influence zone, sensitivity analysis of the governing parameters, time increment of the analysis step were performed in advance. The modified Drucker – Pager cap plasticity was used to model the soil continuum. The influence of pile cross-sectional shape (square, octagonal and circular)

on soil bearing behavior was examined to check the suitability of using the 8-noded hexahedron 3D brick element. Parametric studies were performed to observe the influence of raft and pile geometry (e.g length, size, spacing of pile and thickness of raft) on the foundation bearing behavior. The raft bearing contribution and its top deflection pattern under various loading and pile-raft configuration were also investigated. The multiple regression analysis technique, using statistical software MINITAB, along with the theory of solid mechanics was used to develop the analytical models for load sharing, maximum and differential settlement. Design theories and recommendation for future work are presented.

ACKNOWLEDGEMENT

I am grateful to Dr. A. Hanna, Professor of Civil Engineering, for supervising my research works. I would like to express my gratitude to him for his encouragement and continuous support in carrying out this work and in preparing this Thesis.

I would like to express my gratitude to Dr. H.G. Poulos, P. Clancy, R. Kztzenbach, D Sen and special gratefulness to Dr. Oliver Reul for their support and information during the progress of this research.

The financial support through Dr. A. Hanna and Concordia University Retired Faculty and Stuff Graduate Award are also gratefully acknowledged.

To my son - Arnab, wife - Mukti, Mother

and

to the Soul of my Father

TABLE OF CONTENTS

LIST OF FIGURES

Chapter 2

Chapter 3

Chapter 4

LIST OF TABLES

List of symbols

Latin symbols

B_r raft breadth

C cap area [Butterfield et al. 1971]

c soil cohesion

c_u undrained soil cohesion

D pile diameter

d soil cohesion in *p-t* plane

dC element of the cap area [Butterfield et al. 1971]

D_p pile diameter

d_p pile diameter

dS pile shaft element [Butterfield et al. 1971]

E modulus of elasticity

E_c concrete modulus of elasticity

E_r raft modulus of elasticity

E_s soil modulus of elasticity

f friction factor for pile soil interface

F_c cap surface

F_s shear failure yield surface

F_t smooth transition curve surface

G shear modulus of elasticity

I stress invariant

J stress tensor invariant

K	shape parameter of yield surface for cap plasticity
k	stiffness factor
K’	effective earth coefficient
k_p	stiffness factor of pile
k_{pr}	stiffness factor for pile raft
k_r	stiffness factor of raft
L	pile length
L_p	pile length
L_r	raft length
n	number of piles
${}_nI_{ij}$	influence factor [Davis & Poulos 1972]
p	equivalent normal stress
P	total load (concentrated)
p_a	evolution parameter
p_b	uniforms normal stress at shaft base element [Davis & Poulos 1972]
p_b	volumetric plastic strain
p_c	uniforms normal stress under cap element [Davis & Poulos 1972]
P_G	total load on the pile group [Davis & Poulos 1972]
$P_{i,j}$	load on element *i, j* [Davis & Poulos 1972]
$p_{i,j}$	uniforms shear stress acting along shaft element *i, j* [Davis & Poulos 1972]
P_p	load carried by pile group
P_r	load carried by raft
q	Von Mises equivalent stress

Q_c cap bearing capacity [Butterfield et al. 1971]

q_E yield stress in triaxial tension

q_K yield stress in triaxial compression

Q_s shaft bearing capacity [Butterfield et al. 1971]

R cap eccentricity

r third invariant of deviator stress

r_0 pile radius [Randolph 1983]

R^2 Pearson's coefficient of determination

R_a ratio of area

R_c cap reduction factor [Davis & Poulos 1972]

R_G group reduction factor [Davis & Poulos 1972]

r_m maximum radius of influence of a pile [Randolph 1983]

s pile spacing

S pile tip area [Butterfield et al. 1971]

s_p pile spacing

t deviator stress

T raft thickness

t_r raft thickness

w total load

W(P) total vertical displacement due to load P [Butterfield et al. 1971]

w_c displacement of cap [Randolph 1983]

w_{cp} displacement of cap-pile [Randolph 1983]

w_p displacement of pile

w_r settlement of raft

w_{rp} settlement of raft-pile

y centre point settlement

z depth in soil mass

Greek symbols

α empirical adhesion factor

α_{cp} cap pile interaction factor [Randolph 1983]

α_{pc} pile cap interaction factor [Randolph 1983]

α_{pr} pile raft interaction factor

α_{pr} pile raft interaction factor

α_r interaction factor [Davis & Poulos 1972]

α_{rij} α_r of equivalent cap unit [Davis & Poulos 1972]

α_{rp} raft pile interaction factor

β soil angle of friction in *p-t* plane

β_n regression coefficient

δ soil pile frictional angle

ε statistical error in regression analysis

ε strain

ζ influence of pile geometry and soil homogeneity [Randolph et al. 1978]

ν Poisson's ratio

ν_c Poisson's ratio of concrete

ν_r Poisson's ratio of raft

ν_s Poisson's ratio of soil

ρ degree of homogeneity of soil [Randolph et al. 1978]

ρ_i vertical displacement of element *i* [Davis & Poulos 1972]

σ normal stress

σ'_z effective vertical stress at depth z

τ shear stress

τ_o shear stress

Φ_c normal stress to raft soil interface [Butterfield et al. 1971]

Φ_s normal and share stress to pile soil interface [Butterfield et al. 1971]

Chapter 1

INTRODUCTION

1.1 Introduction

The function of any foundation is to transmit the load to the soil in order to provide safety, reliability and serviceability to the structure. Current practice is to provide a deep foundation, when the shallow foundation is not sufficient to provide adequate safety and reliability. However, a combination of the shallow and deep foundation can be a cost effective design approach. The pile raft foundation is such a combination of a deep pile group and a shallow raft foundation, which has gained increasing recognition in very recent years.

It is evident from the available literature that the piled raft foundation was constructed about fifty years ago and the attempt to capture its behavior was started in the early eighties, which has intensified in the last few years, but no appropriate design strategy has been formulated yet. This is because of the complex interactions among the raft, pile and soil, which is three dimensional in nature and cannot be captured by any analytical method so far developed. With the advancement of computer technology and numerical code, the researchers are now trying to model the complex behavior of pile raft foundation.

1.2 Research Objectives

The pile group in deep foundation is provided with a cap or raft that gives a combined pile raft foundation. However, the conventional design approach, based on pile group or block failure theory, ignores the bearing contribution from the raft to the soil, resulting in a conservative estimate of the foundation performance.

The objective of this work is therefore to investigate the raft contribution to the bearing behavior of the pile raft foundation. This has been determined by establishing a load sharing or interaction factor to estimate the load shared by each of the pile group and raft.

Another major objective is to estimate the settlement of each of the piles in the group under the raft and thereby estimate the differential settlement of pile raft foundation. This unrevealed phenomenon is associated with the estimation of maximum settlement within the foundation system. Therefore, the analytical model for the maximum settlement within the foundation system and for the differential settlement is the primary goals of this thesis.

To develop the above analytical model, necessary literature review was conducted and numerical models were developed in advance. As mentioned earlier, the problem is complex and three dimensional in nature, the numerical models therefore, was developed in 3D finite element software. Necessary studies were performed to reduce the resource cost of the numerical analysis. Comprehensive parametric studies were performed for various pile and raft configuration in order to capture the foundation behavior properly.

Besides the above mentioned studies, recommendations were made for future researchers to reveal the unexplored behavior and characteristics for pile raft foundation.

1.3 Organization of the Thesis

The complex pile raft foundation behavior has not yet been captured by so far developed analytical method. The available literature has been reviewed and summarized in Chapter 2, in order to present the related development and the investigations need to be done.

Chapter 3 consists of the numerical model development and parametric studies. This chapter describes the various components of the numerical model and their development. The numerical model validation with the reported one has been cited thereafter. The developed numerical model was then simulated for the parametric studies in order to capture the behavior of the foundation.

The analytical model for load sharing, maximum and differential settlement is presented in chapter 4. In this chapter, the necessary mathematical and statistical theories were utilized to develop the analytical model with the simulated data obtained from the ABAQUS output. Statistical software MINITAB was used for multiple regression analysis in order to develop the analytical model for maximum settlement. These models were validated and a design strategy was formulated in this chapter.

The conclusions of the whole work were summarized in chapter 5 and necessary recommendations were made for future researches. References were added at the end of chapter 5.

Chapter 2

LITERATURE REVIEW

2.1 Introduction

Foundation of any structure transmits the total structural load to the soil. To serve this purpose satisfactorily, it should be designed properly to satisfy the strength, serviceability, constructability and economic requirements. Investigation on all the components related to these requirements, is now in progress, in order to develop an effective foundation design approach.

The conventional foundation design strategy is to provide a deep foundation (e.g. Pile, Drilled Shaft, Caisson etc.), when the shallow foundation (e.g. Isolated Column, Combined, Raft etc.) is not sufficient to withstand the entire structural load. Attempts are now in progress to combine the shallow and deep foundation, in order to achieve a cost effective design process. The main objective is not only the load sharing between these two components but also to restrict the total and differential settlement within acceptable limit. This is an emerging field of foundation engineering, as even if the Raft foundation has adequate factor of safety against ultimate bearing capacity failure but it may not be safe from excessive settlement (Davis 1972). To offset this limitation and thereby to fulfill this structural serviceability requirement from total as well as differential settlement, Raft foundation is combined with relatively fewer piles than that would require in a pure pile foundation.

Documented literature reports that the first attempt to combine this shallow and deep foundation was started at about half century from now. Leonardo Zeevaert is the pioneer

(Poulos 2005), who first recommended the combination of shallow and deep foundation for the compressible volcanic clay of Mexico City (Zeevaert 1957). He should be accredited as the successful introducer of pile raft foundation for the construction of "Tower Latino Americana" in Mexico City (Zeevaert 1957).

Various analysis methods for pile raft foundation have been developed and researchers are trying to develop a suitable model, in order to simulate the complex pile-raft-soil interaction in a representative manner. Randolph (1983) referred Butterfield and Banerjee's (1971) attempt as the "first" to analyze this complex interaction. However, this analysis was for small pile group. Davis & Poulos in 1972 developed an analysis technique for pile raft foundation of any size, but the most commonly accepted analysis technique was developed by Randolph in 1994. Besides these important works, notable contribution to the simplified analysis of pile raft foundation is made by Hooper (1973), Burland et al (1977), Hain et al (1979), Sommer et al (1985), Franke et al (1994), Poulos (2002, 2005), Ai and Yan (2005).

Alternative design and analysis approaches for this type is also investigated by means of modeling the piled raft foundation, in the form of plate loaded spring. Griffith et al. (1991), Clancy P et al (1993), Poulos H G (1994), Horikoshi et al (1998). Russo G (1998), Kim K N et al (2001), Kitiyodom P et al (2002, 2003 & 2005) are the important contributor to investigate the complex pile raft foundation behavior.

The advancement of computer technology and its high speed processor provides greater computing facility for numerical methods in geotechnical engineering. This computational advancement helps the researchers to perceive the complex foundation behavior with more convenience. Brown may be accredited for introducing the numerical method in geotechnical engineering in 1969. However, Banarjee and Berfield introduced the numerical analysis for pile cap foundation in 1971. Hooper, in 1973, first used the Finite Element Method (FEM) to analyze the complex behavior of piled raft foundation. Notable contribution to analysis the behavior was made by Hain and Lee (1978), Sommer H et al. (1985), Burland B et al (1986), Kuwabara F (1989), Randolph M F (1991, 1993, 1996, 2003, 2004), Poulos H G (1993, 1994) Ta and Small (1997, 1996), Katzenbach (1998), Russo G (1998), Prakoso W (2001), Sanctis L (2002, 2006), Reul O (1998, 2003, 2004, 2006), Wang S T (2005, 2006), Chow H S W (2001, 2006) and Small (2001, 2006).

The development of various methods is mainly due to the inadequate perception of the complex pile-raft-soil interaction, Each method comes with its own sets of assumptions, boundary and limiting conditions; based on various geological conditions (soil strata and its nature, soil type and their properties, moisture level etc.), structural requirements and considerations (stiff or elastic raft, floating or end bearing pile and their arrangement), and environmental condition. To reach the ultimate goal of utilizing the full capacity of pile and raft at ultimate state, researchers are investigating the different aspects from various viewpoints.

The development of various models (elastic, elasto-plastic, visco-plastic etc) by means of various numero-geotechnical methods along with the conventional is introduced to analyze and simulate the complex piled raft foundation behavior. Each model is developed again, for different soil condition (homogeneous, non-homogeneous, layered, compensated etc).

The subsequent sections of this chapter will highlight the various aspect of pile-raft foundation, which is compiled on the basis of available documented English literature. Since, any design is guided by the design philosophy (i.e. the design considerations, approaches, methods and purposes), the literature review is proceeded accordingly to review all the aspect of design consideration (e.g issue, assumption, favorable and unfavorable considerations etc), parametric study, safety and reliability concept.

2.2 Design Philosophy

2.2.1 Design Philosophy

The above section indicates that numerous works have been done and still in progress to develop a definite design strategy. Researchers use their own design philosophy to formulate the design process for pile raft foundation. Randolph (1994a) categorized the various design philosophy into three different design approaches.

a) The conventional approach, in which, foundation is designed as a pile group with regular spacing over the entire foundation area, to carry the major portion of the load (60 – 75% of the total structural load) and allowance is made for the raft to transmit some load directly to the ground.

The conventional approach has the limitation that any design by this philosophy will remain inevitably in elastic regime, where the piles are loaded below their shaft capacity and piles are evenly distributed over the whole foundation area. The shaft capacity of the group pile is "extremely difficult and has not resolved yet" (Das 2007). Moreover, the allowance for the raft to transmit the load is not defined in this approach, which they let it for engineering judgment.

b) Creep Piling approach, proposed by Hansbo and Kalstrom (1983), in which, piles are designed to operate at a working load, at which significant creep starts to occur (typically at about 70 – 80% of its ultimate load bearing capacity). To reduce the net contact pressure between the raft and soil, adequate piles are added in order to reduce the pre-consolidation pressure of the clay.

The creep piling approach again sets the limitation of operating the pile, below the creep load, which is, as mentioned above, as 70% to 80% of ultimate load bearing capacity. However, the ultimate capacity is based on conventional group theory, which is under investigation. Moreover, the reduction of net contact pressure between raft and soil by means of pile addition, will refrain the raft from transmitting load to its full capacity directly to the soil.

c) Differential settlement control approach, in which, pile supports are designed tactfully in order to minimize differential settlement rather than reducing average settlement significantly.

The differential settlement control approach could be the economical one, as piles are located strategically to reduce the differential settlement. It will require less number of piles, in comparison to the other two approaches. However, to cause the differential settlement to occur, the utilization of ultimate bearing capacity of each of the single individual pile in the group is required, which has not established yet and cannot be captured by any so far developed analytical method. The goal, to use the ultimate bearing capacity according to the requirement of raft-pile-soil interaction, can be achieved by the numero-geotechnical methods by simulating the complex nature of pile raft foundation.

2.2.2 Design Considerations

Katzenbach et al. (2005) termed piled raft foundation as a Combined Piled Raft Foundations (CPRF), which is consists of three bearing elements, - piles, raft and subsoil. The stiffness of raft and pile, the soil properties, the dimension and strategy of pile location, play the significant role in the design of a pile raft foundation system. Figure 2.1 illustrate a general piled raft foundation with its overall forces and moments. The following design issues must be taken into consideration, in order to develop a successful pile raft foundation.

1. Ultimate geotechnical capacity under vertical, lateral and moment loadings
2. Maximum and total settlements.
3. Differential settlement and angular rotation
4. Lateral movement and stiffness
5. Load shearing between the piles and raft
6. Raft moment and shear for the structural design of raft and its stiffness

7. Pile loads and moments for the structural design of the piles and its stiffness.

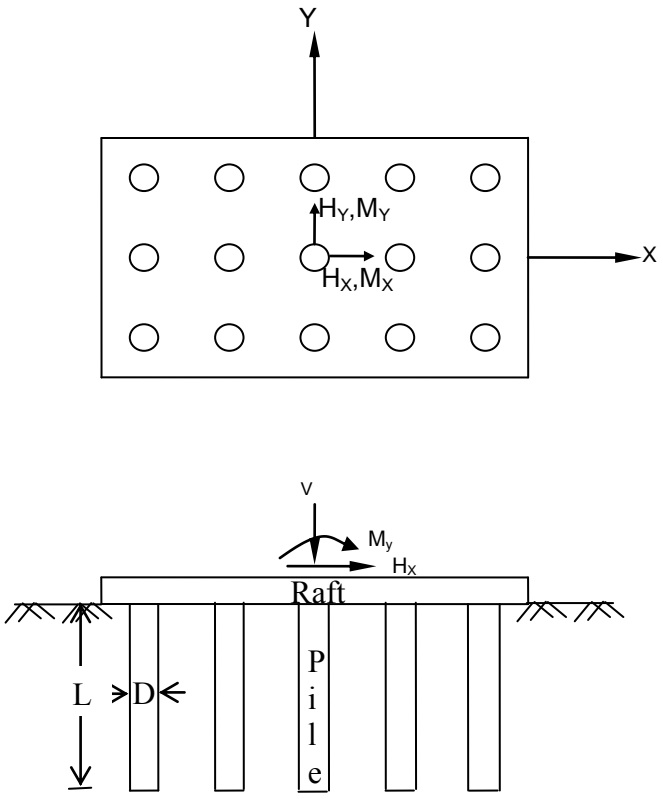

Figure 2.1 Piled Raft foundation system.

A sound prediction of a piled raft foundation behavior implies a full interaction between piles, raft and soil. Hence, the following factors must be considered.

1. The raft characteristics (its relative stiffness – flexibility, rigidity, shape - dimension).
2. Piles characteristics (number, layout, length, diameter, stiffness)
3. Applied load characteristics (concentrated or distributed load and its level related to the ultimate capacity)

4. Soil characteristics (soil profile, layers and their stiffness, the ultimate soil bearing capacity)

Therefore, it is essential to develop a design method for pile raft foundation, which includes the following capabilities

1. Piles-raft-soil interaction in a logical manner, including the interaction of raft-raft, pile-pile, raft-pile, pile-raft, raft-soil, pile-soil.
2. Variation of number, location and characteristics of the pile
3. Load shearing of pile and raft
4. Full utilization of the ultimate pile load capacity in compresion and tension as well as the nonlinear load deflection behavior of the foundation.

2.2.3 Favorable and Unfavorable Condition

Poulos examined a number of idealized soil profiles for piled raft foundation and suggested (1991) the following situations may be favorable

1. A uniform soil layer of relatively stiff clay.
2. A uniform soil profile of relatively dense sand.

Consequently, the following situation may be unfavorable for applying a piled raft foundation

1. Presence of relatively soft clay in the soil profile near the surface.
2. Presence of relatively loose sand in soil profile near the surface.
3. Presence of soft compressive layer in a soil profile at relatively shallow depth

4. Soil profiles, which are likely to undergo consolidation settlement due to external causes.
5. Soil profiles, which are likely to undergo swelling movement due to external causes.

2.2.4 Design Process

The design process of piled raft foundation consists of two stages. The preliminary stage assesses the feasibility of using a pile raft and the required number of pile, to satisfy design requirements. It involves the estimation of ultimate geotechnical properties (vertical loading, Lateral loading, Moment loading,), load settlement behavior, pile loads, raft moments and shears. This stage requires a little or no application of computer.

The detail design stage come into effect when the preliminary design stage assures the feasibility of a pile raft foundation. This is performed to obtain optimum number, location and configuration of piles, and to compute the detailed distribution of settlement, bending moment and shear force in the raft and piles. It involves the application of different models, geotechnical numerical methods, safety and reliability analysis.

2.3 Methods of Analysis

2.3.1 Introduction

The introduction of this chapter indicates that from the beginning of this type of foundation, researchers are trying to develop a suitable design method in various approaches. To perform a critical review, these works have been categorized under three major group i.e. simplified analysis method, approximate numerical analysis method and numerical analysis method.

2.3.2 Simplified Analysis Method

The simplified analysis method involves the development of mathematical model, based on established theory and principles, which can be performed by simple hand calculation without extensive use of computer. Researchers are still investigating to develop a standard mathematical model that includes all the capabilities as mentioned in section 2.2.2. Three fundamental approaches to analyze pile raft foundation are available in English literature, which are summarized in the subsequent sections.

(A) Butterfield and Banerjee Approach

Butterfield and Banerjee (1971) were the "first" (Randolph 1983) to estimate the load sharing between the pile and cap, and the corresponding settlement behavior for various pile configuration (pile number, size and space) and cap type (Contacting or Floating). The analysis technique adopted the Mindlin's solution (1936) for a point load embedded in the interior of a semi-infinite elastic solid. By distributing such point load over the pile

cap, integral equation was developed for the vertical displacement of all points in the medium and expressed in terms of stress intensities.

The analysis was on small floating pile group (1,2,3,2x2,5 and 3x3) with rigid cap (floating and contacting), subjected to a point load in an elastic soil medium of semi-infinite depth. The total vertical displacement *W(P)* due to the load P can be expressed as

$$W(P) = \int_C \varphi_C K(P, Q_C) dC + \int_S \varphi_S K(P, Q_S) dS \qquad (2.1)$$

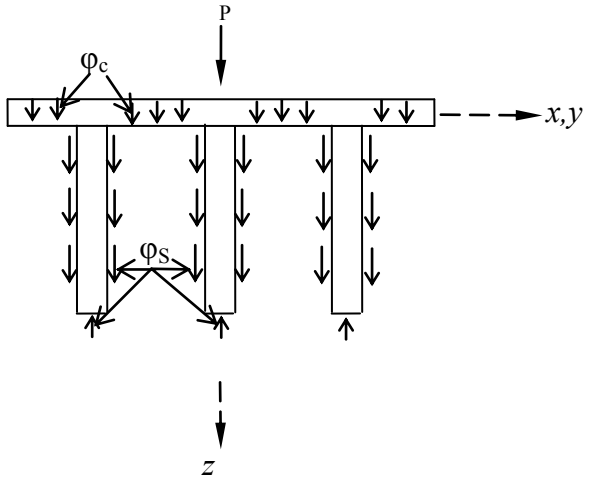

Figure 2.2 General arrangements (Butterfield and Banerjee 1971)

Where, the first portion of above equation includes the vertical displacement on the cap soil interface, due to the fictitious normal direct stress φ_c on element *dC* of effective cap area C (i.e. total cap area less area occupied by N piles). The second portion includes the vertical displacement due to fictitious shear and direct stress φ_s, acting at pile soil interface of pile shaft element *dS* and base area (S). The terms $K(P, Q_c)$ and $K(P, Q_s)$ can be obtained from Mindlin's equation. (Mindlin's 1936; Butterfield and Banerjee 1971.a)

The above solution does not take into account the radial displacement compatibility at the pile shaft and soil continuum interface. Butterfield and Banerjee (1971.a) showed that

this has negligible effect on load sharing and displacement. The above analysis is applicable to pile group of any geometry with rigid cap. However, for compressible pile, the above equation can be written in matrix form by dividing the various interfaces into discrete elements.

This elastic analysis calculates only the total settlement. It does not include the interaction between pile and cap within the cap, which influence the shear redistribution and bending moment of the raft element.. The assumed identical fictitious stress intensity φ_s, along pile shaft and on pile tip, may not be the same. The determination of load sharing is not explicit and the larger matrix formation due to more discrete elements will involve more calculating effort.

(B) Davis and Poulos Approach

Davis and Poulos (1972) performed an elastic analysis of pile-raft interaction, considering soil as semi-infinite elastic medium. The analysis is based on the interaction between two units, where, each unit consists of a rigid floating pile connected with a rigid circular cap, which is subjected to a point load. The rectangular or square mat would be the combination of such units covering the same area of the circular cap.

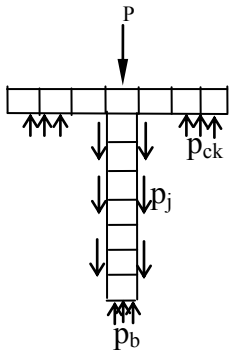

Figure 2.3 Analysis considerations (after Davis & Poulos 1972)

In this analysis, pile length is divided into 'n' cylindrical element, each is subjected to an uniform shear stress p, acting around the surface, and the bottom circle is acted upon by a uniform vertical pressure p_b. The pile cap is also divided into 'v' annuli, each is uniformly loaded by a vertical stress, p_c. The soil displacement at a typical element i is calculated from elastic stress-strain relationship as follows

$$\rho_i = \frac{d}{E_s}\left(\sum_{j=1}^{n}({}_1I_{ij} + {}_2I_{ij})p_j + p_b({}_1I_{ib} + {}_2I_{ib}) + \sum_{k=1}^{n} p_{ck}({}_1I_{ik} + {}_2I_{ik})\right) \qquad (2.2)$$

Here, stress is expressed in terms of two groups of influence factors. One group (${}_1I_{ij}$, ${}_2I_{ij}$, ${}_1I_{ib}$, ${}_2I_{ib}$) is for vertical displacement due to point load in semi infinite mass and it is calculated from Mindlins equation. The other group of influence factor (${}_1I_{ik}$, ${}_2I_{ik}$) for vertical displacement, due to surface point load, is calculated by Boussinesq's equation (Notation ${}_1I_{ij}$ is the influence factor for vertical displacement at i due to shear stress on element j of pile 1 and ${}_2I_{ij}$ is due to element j of pile 2. ${}_1I_{ib}$, ${}_2I_{ib}$ are the same at i due to vertical stress on base of pile 1 & 2 respectively. ${}_1I_{ik}$ is also the same at i due to uniform stress on annular k of pile 1 and ${}_2I_{ik}$ is due to element j of pile 2)

This analysis assumes incompressible pile and cap; hence the settlement of each element of a pile cap unit is same. Again, since a free standing pile is under consideration, the soil displacement is the same to that of the pile-cap unit. Above equation is used to evaluate the settlement of two pile-cap unit for various pile and cap dimension and configuration. Another interaction factor, α_r, was introduced to generalize the above expression for various pile configuration as follows.

$$\alpha_r = \frac{Additional\ \ settlement\ \ due\ to\ adjacent\ unit}{Settlement\ \ of\ \ a\ single\ \ pile}$$

The above analysis can be used for any pile-raft system, considering the system consists of several pile-cap units, each having an equivalent circular cap area that would be occupied by the raft of a single pile. So, for a system comprises of *m* equivalent units, the settlement of a typical unit can be written by applying superposition principles as.

$$\rho_i = \bar{\rho}_1 \left(\sum_{j=1\ j\neq i}^{n} \bar{P}_j \alpha_{rij} + \bar{P}_i \right) \tag{2.3}$$

and the total settlement of the system can be given by, $\rho = R_G P_G \rho_1$ (2.4)

where, $\alpha_{rij} = \alpha_r$ of the equivalent pile-cap unit

$$P_G = \sum_{j=1}^{n} \bar{P}_j, \qquad where, \bar{P}_j \text{ is the load on unit } j$$

$$\rho_1 = \bar{\rho}_1 / R_c \quad where, \rho_1 \text{ is the settlement of a free standing pile under unit load and } \bar{\rho}_1 \text{ is the settlement of a single pile cap unit under unit load}$$

and group reduction factor R_G

$$R_G = \frac{Settlement\ of\ system}{Settlement\ of\ a\ single\ unit\ carrying\ same\ total\ load}$$

Davis and Poulos in 1980 rewrite the same analysis and proved its validity by means of an example.

Two interaction factors are used to express the interaction between two independent pile-cap units and the stress around the pile shaft is considered as uniform. However, the equivalent circular cap-pile unit concept lacks the accountability of the total integrated raft as a whole. The shear distribution around the equivalent cap periphery along with the bending moment effect is totally ignored. The structural integrity of cap contributes to the

shear redistribution to a greater extent. Load sharing between the foundation elements is not explicit in the analysis and radial action was totally ignored. Application of Mindlin's and Bousinesq's equation remains the analysis procedure in elastic regime. The load displacement curves for the interaction of two rigid circular pile cap unit were obtained first, and then these curves were superimposed to predict for all the pile cap units. However, this elastic superposition theory is valid, only when the piles are located along a circumference and subjected to the same load (Mendonca et al. 2000).

(C) Randolph Approach

Randolph (1983) developed the simplest analysis method for a single pile cap unit and showed its applicability for a 3x3 pile group raft foundation, which has a good agreement with Butterfield and Banerjee (1971). The analysis was on a unit of rigid floating pile, which is attached to a rigid circular cap and the soil was considered as elastic semi-infinite mass.

On the basis of the relationship between displacement (w_o) of pile shaft and locally induced shear stress (τ_0, where, $\tau_o = Gw_o/\zeta r_o$), two pile cap interaction factors were developed as below.

$$The\ cap\ \ pile\ interaction\ \ factor,\ \ \alpha_{cp} = 1 - \frac{\ln(r_c / r_0)}{\zeta} \qquad (2.5)$$

$$The\ pile\ \ cap\ interaction\ \ factor, \alpha_{pc} = \frac{r_c}{4L}\left[\left(1 - \frac{1}{2(1-\nu)} + \left(2 + \frac{1}{(1-\nu)}\right).\sinh^{-1}(L/r_c)\right)\right] \qquad (2.6)$$

where, the parameter ζ includes the influence of pile geometry and relative homogeneity of the soil. Randolph and Wroth (1978) expressed the parameter as, $\zeta = ln(r_m/r_o)$, where,

r_m is the maximum radius of influence of pile, which is related to the pile length as $r_m = 2.5\rho(1-\nu)L$ and to the degree of homogeneity (ρ) of the soil

The above two interaction factors were then applied to correlate the stiffness (k), settlement (w) and load (P) carried by pile and cap as follows

$$\begin{bmatrix} 1/k_p & \alpha_{pc}/k_c \\ \alpha_{cp}/k_p & 1/k_c \end{bmatrix} \begin{bmatrix} P_p \\ P_c \end{bmatrix} = \begin{bmatrix} w_p \\ w_c \end{bmatrix} \tag{2.7}$$

This analysis was for a rigid pile-cap unit, therefore, $w_p=w_c$ ($=w_{cp}$ for the combined unit) and to satisfy the reciprocal theorem the above "matrix expected to be symmetric" (i.e. $\alpha_{cp}/k_p = \alpha_{pc}/k_c$). Considering this approximation the above flexibility matrix (equation 2.7) can be solved for the overall stiffness and load sharing as follows

$$k_{pc} = \frac{k_p + (1-2\alpha_{cp})k_c}{1-\alpha_{cp}{}^2 k_c/k_p} \tag{2.8}$$

$$\text{and} \quad \frac{P_c}{P_c+P_p} = \frac{(1-\alpha_{cp})k_c}{k_p + (1-2\alpha_{cp}/k_c)} \tag{2.9}$$

This elastic analysis can calculate only the total settlement of a single pile cap unit, with direct estimation of load, carried by each components of the foundation. However, Randoph (1983) concluded that the above relations for stiffness, settlement and load sharing are applicable for large pile group of any size, where the equivalent cap radius is calculated from the raft area associated with each pile.

Clancy and Randolph (1993) investigated the validity of this analytical approach by means of numerical Finite Element Method (FEM) and found its excellent agreement with a single pile cap unit. For larger pile group, the numerical analysis indicates that the

value of α_{rp} increases as the size of pile group increase, but tends towards a constant value of $\alpha_{rp} = 0.8$, which is independent of pile spacing, slenderness ratio and stiffness ratio.

In 1996, Clancy and Randolph reported a more extensive investigation on the raft-pile interaction factor (α_{rp}) convergence with increased pile group size. The same rectangular plate bending finite element numerical approach of 1993 were used, but for increased number of piles as shown in figure 2.4 below.

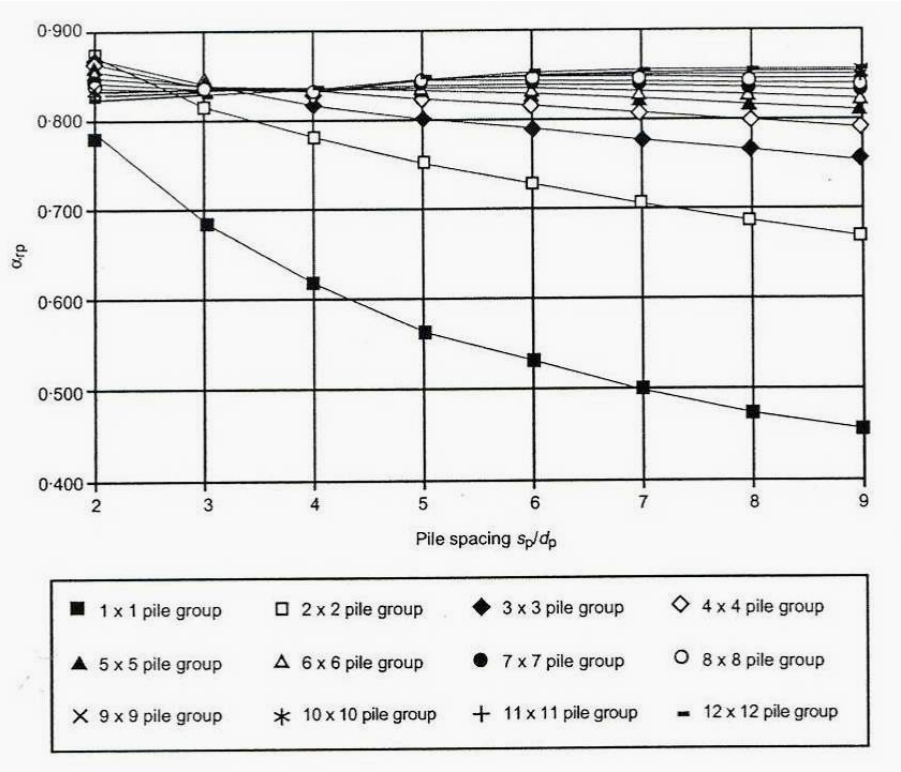

Figure 2.4 Values of interaction factor α_{rp} for various size with $L_p/d_p = 25$, $K_{ps} = 1000$ and $k_{rs} = 10$ (Clancy and Randolph 1996)

This investigation lead towards the modification of α_{rp} = 0.85, instead of 0.80 (1993) and equations 2.8 & 2.9 take the form

$$k_{pr} = \frac{1 - 0.7k_r / k_p}{1 - 0.723k_r / k_p} k_p \tag{2.10}$$

$$\frac{P_r}{P_r + P_p} = \frac{0.15k_r / k_p}{1 - 0.7k_r / k_p} \tag{2.11}$$

This simplified analysis method is widely accepted due to its simplicity and explicit expressions of load sharing and stiffness of the foundation components. The application of one interaction factor (α_{rp}), which is easy to calculate, widen the acceptability of this approach. However the method provides only the total settlement and like Davis and Poulos approach, it is based on a single cap unit, therefore, the limitations regarding its applicability for the whole pile raft foundation remains under question. Although, Clancy and Randolph tried to validate its applicability for larger pile raft by means of numerical application as explained above, but more investigation is required to establish n universal interaction factor.

The simplified analysis methods mentioned above, considered soil as a semi-infinite elastic medium, in which rigid pile & rigid cap was subjected to a point load. The load effect is determined by means of Mindlin's or combinations of Mindlin's and Boussinesq's equations, which are elastic in nature.

Butterfield and Banerjee's approach was for the total settlement and for the pile group of any size; however, the analysis was based on a single point load. Davis-Poulos and

Randolph methods are based on a unit, consists of rigid circular cap which is attached to a rigid pile. The behavior (interaction, load-settlement) of a single pile-cap unit is different from those of a piled raft foundation. Analysis, based on single pile cap unit did not include the effect of structural integrity, especially, the stresses (both flexural and shear) around the cap periphery within the raft material. Moreover, all these methods predict total settlement, and provide no information on differential settlement, for which the pile-raft foundation is sought for.

2.3.3 Approximate Numerical Analysis

The Approximate Numerical Method (Poulos, Russo), also known as Hybrid Analytical Method (Griffith, Clancy, Horikoshi, Randolph, Kitiyodem), is an alternative analysis approach, where the foundation behavior is investigated by means of modeling the piled raft foundation, in the form of plate loaded spring. This method reduces the rigorous numerical analysis by including analytical solution with some approximation. It requires fewer equations to solve than the finite element method, and "the time consuming numerical integration of the boundary element method are not necessary" (Clancy et al. 19996), Therefore, a great saving in computer memory utilization makes the foundation analysis more convenient and less expensive.

Griffith et al. (1991) modeled the raft as a two dimensional thin plate, pile as one dimensional rod element and soil as a vertical spring at each node. Clancy et al. (1993) incorporate the non-linear pile-pile interaction in the same model, whereas Horikoshi et al. (1998) applied this model for nonhomogeneous multilayered soil. Kitiyodem et al. (2002) modified this model by providing two more spring in horizontal plane at each

node. In 2003 he made this model suitable for non-homogenous multilayered soil and in 2005 he applied it for the ground movement effect induced by tunneling.

Poulos (1994) modeled piles as interactive springs and soil as elastic continuum. Russo (1998) modeled the piles as nonlinear spring on elastic continuum, while Kim et al (2001) considered soil as Winkler spring and piles as coupled spring. All these works are reviewed with their salient distinct feature in the subsequent sections.

(A) Strip on Spring Approach

Poulos (1991) investigated the behavior of a pile strip foundation, considering the strip as a number of beams of equal length, and piles as springs of equivalent stiffness in an elastic continuum of soil mass. This method utilized the boundary element method for strip, together with some results from simplified analysis (Randolph approach above) for axial pile response, in order to simulate the piles behavior. This model was suggested for piled raft, considering the foundation as a combination of a number of pile strip footings of equal length. The effects of the parts of raft outside the strip section (being analyzed) were taken into account by computing the free field-soil settlements due to these parts.

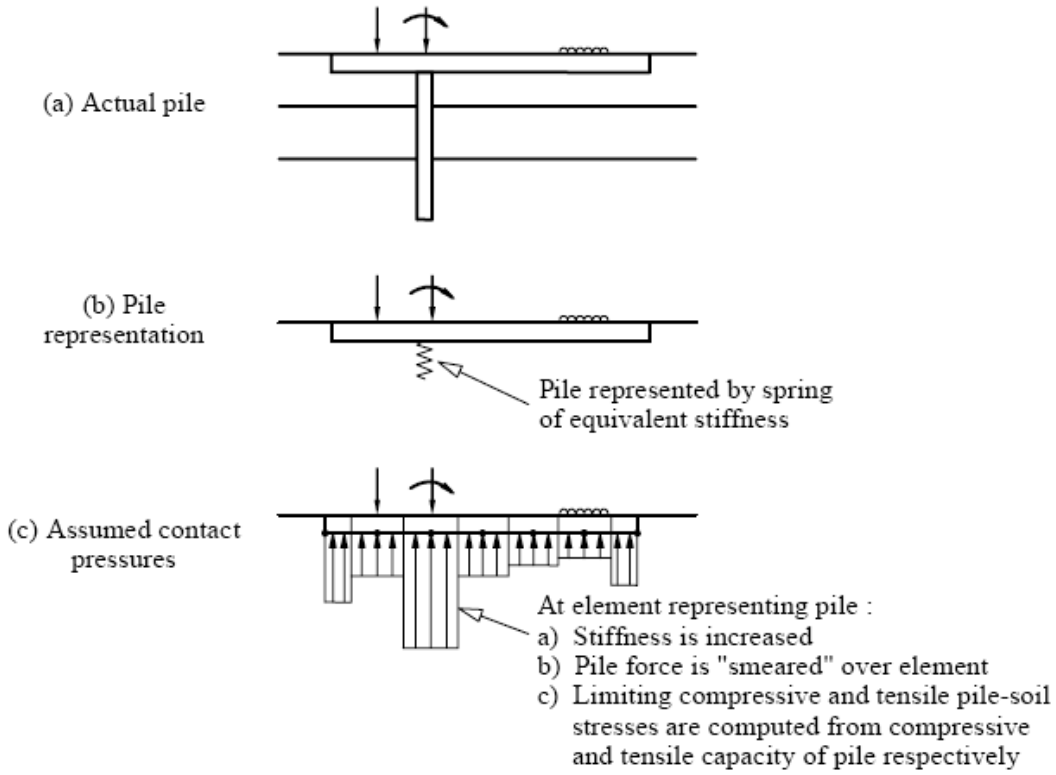

Figure 2.5 Modeling of piled strip foundation via GASP analysis (Poulos, 1991)

Computer program GASP (Geotechnical Analysis of Strip with Piles) was used to simulate the load settlement behavior. However, this method did not consider the torsional moments within the raft. It may not give consistent settlement at a point, if strip in two directions through that point is analyzed. This is because of the consideration that the pile raft is a number of pile strip, which in turns, is a number of beam element of equal length, therefore, the behavior in breadth direction is ignored. Moreover, the behavior of piles under a discrete beam, cannot be identical with the pile group action under a mat. Therefore, this type of analysis can produce unrealistic settlement behavior for piled raft foundation.

(B) Plate on Spring Approach

This type of analysis consider raft as an elastic thin plate, piles as rod elements or interacting springs those support the plate, and soil as an elastic continuum or springs with suitable stiffness at the nodes. All type of vertical, lateral and moment loading effects, as well as, layered soil non-homogeneity is included in the model by means of suitable analytical approximation.

Individual modeling of piled raft foundation components have been performed by many researchers, considering suitable approximation. Griffiths et al. (1991) modeled the foundation, considering raft as thin plate element, piles as axially loaded one dimensional (1-D) finite rod element. The discrete load transfer (or *t-z*) spring is coupled to each node of this rod element, in order to model the soil response. The soil deformation around the pile shaft was idealized as the shearing of concentric cylinders, and the base response was analyzed separately, as a rigid punch on the surface of a semi-infinite half space. These two parts of the analysis were combined by means of displacement compatibility at the base of the pile. The three types of interactions, namely, pile-soil-pile, pile-soil-raft and raft-soil-raft are demonstrated using Mindlin's elastic theory.

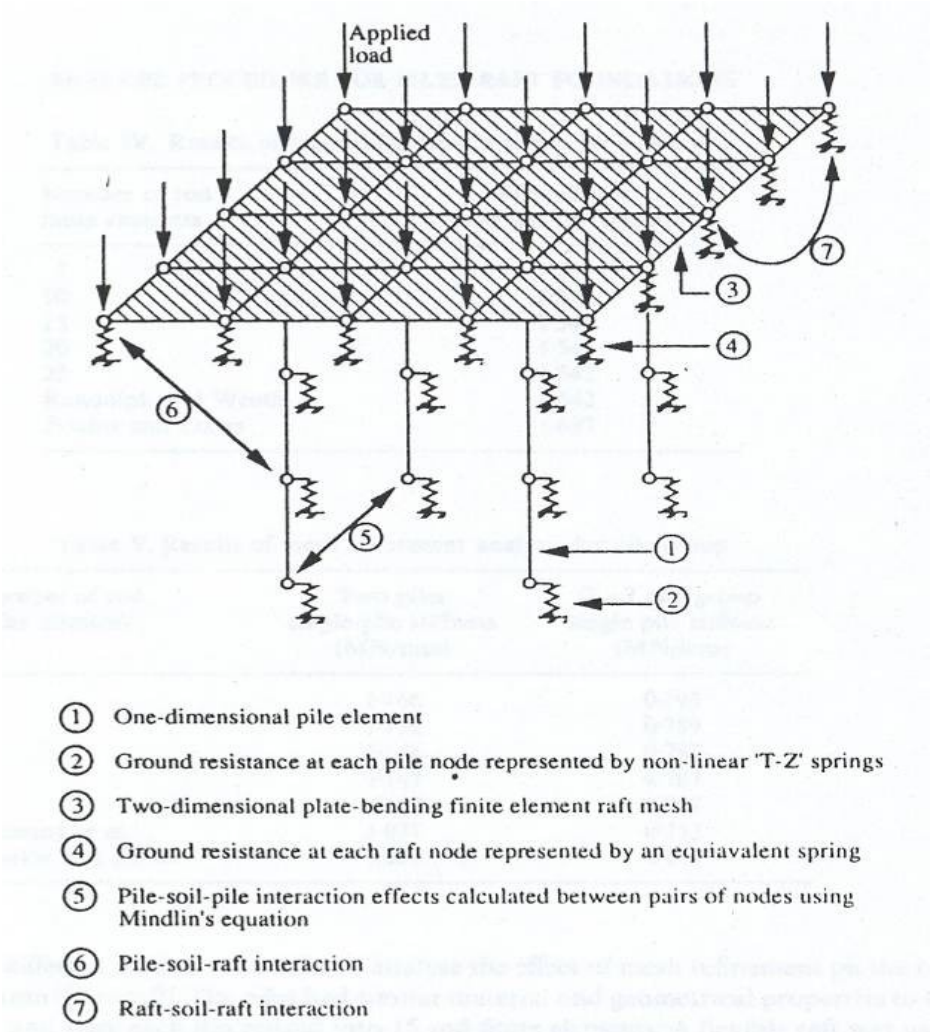

Figure 2.6 Numerical representation of piled raft (Clancy et al (1993)

This analysis used the raft-soil stiffness ratio from the finite element analysis of Hains and Lee (1978), where raft was considered as thin plate, while pile & soil (homogenous/non-homogenous) as a pile reinforced continuum. Moreover, the pile modeling as a finite element rod, was adopted from Chow's (1986, 1987) work, which were for pairs of pile and ignored cap effect. The inclusion of the raft soil stiffness ratio, together with the adoption of Chow's model for this purpose, might restrict the applicability of this model to simulate the actual pile raft foundation.

Clancy et al. (1993) extended Griffith's (1991) work to include non-linear variation of the shear modulus. This yields to the derivation of a formula that involves the secant shear modulus. It should be mentioned that Griffith's (1991) work considered only the linear *t-z* response. Interaction between piles through the soil was calculated using Mindlin's elastic continuum solution. It calculates the displacement of an interior point of a semi-infinite linear elastic half space, due to a point load at another point in the half space. The Raft was modeled as a combination of two dimensional (2-D) thin plate bending finite elements of suitable rectangular area, and the average settlement, under a uniformly loaded rectangular area, is calculated from the equivalent soil spring response. These two separate analyses for raft and pile were then combined via common nodes at the connecting points (figure 2.6 above). Interaction between pile nodes and raft nodes are calculated using Mindlin's (1936) elastic solution in a point to point fashion.

Clancy's work (1993) is an extension of Griffith's (1991) work, hence, the limitation concerning the raft-soil stiffness ratio and pile modeling remain as inherent there. Moreover, both of them considered only the vertical loading and linear ideal elastic homogenous soil condition.

Horikoshi et al. (1998) extended the work of Griffith (1991) and Clancy (1993) for non homogenous soils, by considering a "representative soil modulus" for the pile raft foundation. The representative soil modulus, to incorporate the non-homogeneity, was adopted from the "equivalent pier" concept of Poulos and Davis (1980). In this concept, the pile group is replaced by an equivalent pier, while, the soil region, in which piles

were embedded, is considered as an equivalent continuum. The young's modulus of the equivalent continuum was taken as the average value of the soils in that region. To estimate the behavior, the pile raft interaction factor and pile raft stiffness factor were adopted from Randolph (1983), as mentioned in equation 2.5 and 2.8 respectively.

The conversion of the non-homogenous layer into an equivalent continuum by averaging the Young's modulus of the soil layers, and the adoption of pile raft interaction factor as well as stiffness factor from Randolph (1983), might put the models under question. The limitations of these factors have already been discussed earlier in this chapter. Moreover, this model, based on equivalent pier approach, can estimate only the average settlement of the pile group but not the differential settlement.

Poulos (1994) presented an "approximate numerical analysis" method for this type of foundation, in which raft, pile and soil are modeled as thin plate, interacting spring of approximate stiffness and equivalent elastic continuum respectively. He employed a finite difference method (FDM) for the plate and allowed for various interactions by means of approximate elastic solutions. In fact, it is an extension work of strip on spring approach, which is described earlier (figure 2.5). However, necessary allowances were made to incorporate the raft effect and to analyze the piled raft foundation behavior by his own developed GARP (Geotechnical Analysis of Raft with Piles).

He employed the raft stiffness from Hain and Lee (1978), where, raft was considered as a thin plate on a pile-soil reinforced continuum, rather than on "interactive spring" and

"equivalent elastic continuum". He also included the pile-pile interaction factor from the approximate solution of Randolph (1981), which was extended later by Randolph et al. (1992), to include the interaction effect of pile group of large spacing. However, Randolph (1981) developed this interaction factor for fixed headed piles (restrained against rotation) in order to determine the elastic response of flexible piles, subjected to lateral loading. Moreover, to model the pile behavior, Poulos used his own developed DEFPIG computer program (1980), which was developed for the analysis of single piles and for the computation of interaction factors between pairs of piles.

Russo G (1998) presented an "approximate numerical method", in which, raft of any flexibility, subjected to any combination of vertical, distributed or concentrated loading, is modeled as a two dimensional thin plate elastic body. Soil was modeled as an elastic continuum and piles were modeled as interacting nonlinear springs (figure 2.7). Boussinesq's equation was used to calculate the nodal soil displacement at the interface between raft and soil. The displacement at the pile-soil in the node was determined by computer program NAPRA (Numerical Analysis of Piled RAft), by using Chin's (1970) hyperbolic load settlement curve for single pile to incorporate non-linear behavior. The compatibility equation was then applied to determine the load shearing, stiffness of the foundation components as well as bending moment of the raft.

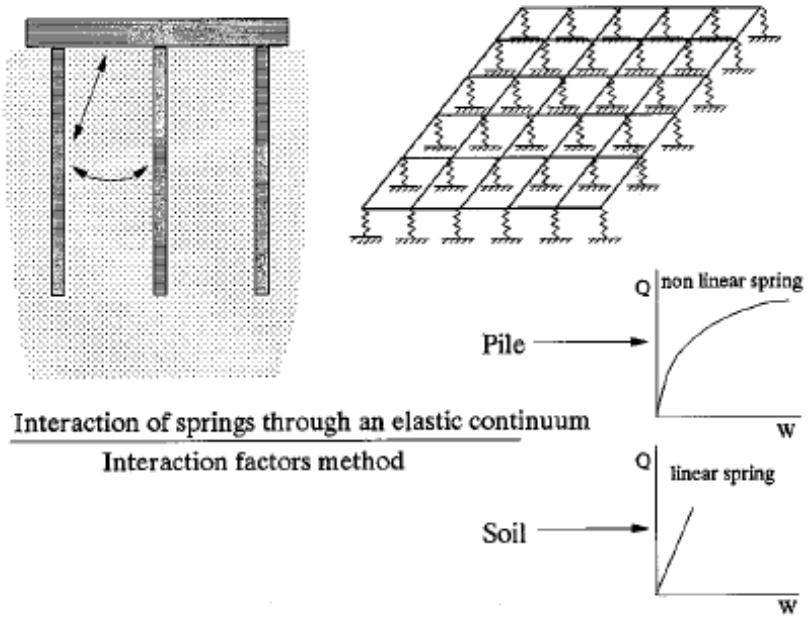

Figure 2.7 Basic features of the model for a piled raft (Russo 1998)

Russo's approach applied the compatibility equation between a nodal displacement determined by Boussinesqu's elastic equation and the non linear hyperbolic load settlement curve of Chin's may have some inconsistency in setting the compatibility. Chine's hyperbolic load settlement curve is for single pile. Therefore, pile-pile interaction is applied only to the elastic component of pile settlement, while the nonlinear component of settlement of a pile is assumed to arise only from the loading on that particular pile.

Moreover, Chin (1970) developed the hyperbolic curve for free standing pile without cap. The same free standing pile without cap was used to develop the pile-pile interaction factor by Randolph and Wroth (1979), which Russo modified to incorporate in this analysis.

Kim et al. (2001) developed "an optimization scheme" to minimize differential settlements by modeling raft, soil and pile as Mindlin's plate, Winkler spring and coupled spring respectively. The optimization is performed with respect to the location of the pile. The interaction is expressed by means of flexibility characteristics equation, based on the discretized stiffness equations for different components of the piled raft foundation.

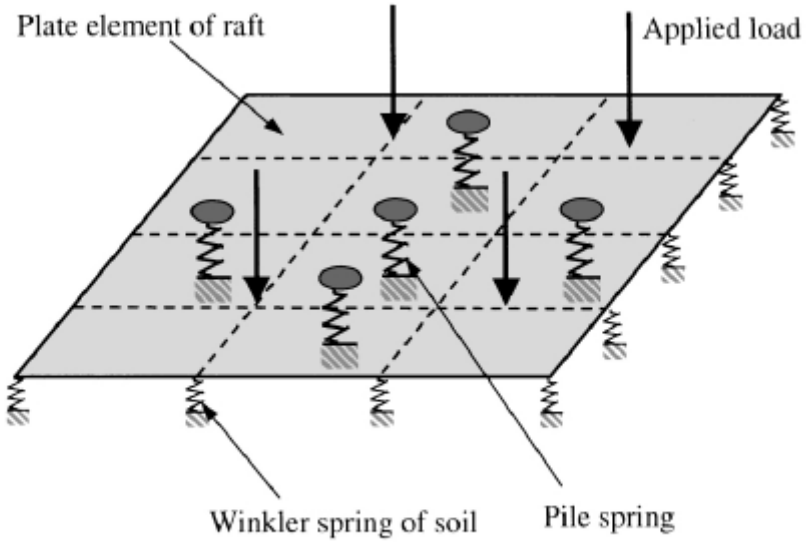

Figure 2.8 Finite element model of piled raft foundation (Kim et al. 2001)

The formulation developed in this analysis to express the interaction between the piles, utilized the coupled spring concept of Randolph and Wroth (1979). Randolph and Wroth (1979) concept was developed for free standing group pile, that ignores the influence of cap interaction for the group. Moreover, the interaction between piles and the cap is neglected, because the Winkler spring constant is evaluated from the modulus of sub-grade reactions. Therefore, the formulation may overestimate the stiffness of the piled raft foundation. The differential settlement estimation is not explicit; however, the overall flatness of the deflected shape of the raft may provide an indirect measurement of the differential settlement.

Kitiyodem P et al (2002) performed an approximate numerical analysis by modeling raft as thin plate, piles as elastic beam and soil as spring. This model incorporates the effect of lateral loading, along with vertical and moment loading, for any flexibility of raft. To incorporate the lateral action, two additional springs in horizontal plane were attached at each node of the piles and rafts. The purpose is to account for bending of piles, lateral resistances to the piles, and the shear resistance between the raft base and the soil surface (figure 2.9). Compatibility equation for displacement is applied at the head of each pile, which means, the flexible thin plate element of raft and the elastic beam element of pile is combined through the node of the pile head. Computer program PRAB (Piled Raft Analysis for Batter pile) was used to simulate the behavior.

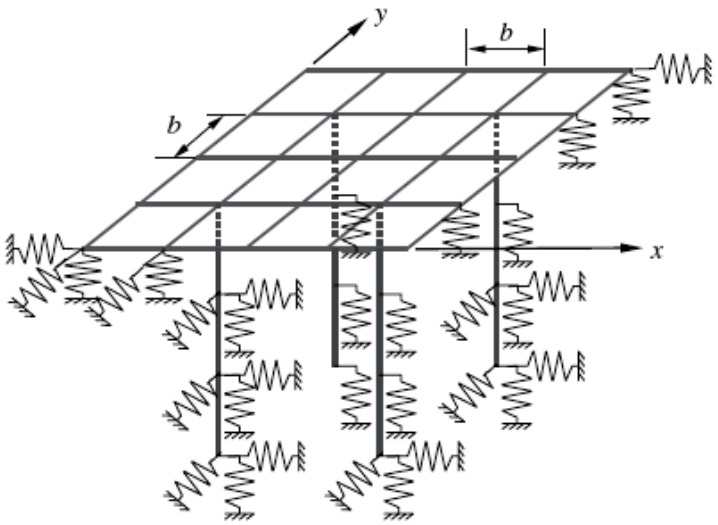

Figure 2.9 Plate-beam-spring modeling of applied raft foundation (Kitiyodem 2002)

Kitiyodem P et al (2002) employed Muki's (1960) solution to estimate raft stiffness's in all the three directions (K^R_x, K^R_y & K^R_z), Randolph and Wroth's (1978) solution to estimate piles vertical stiffness (K^P_z) and Mindlin's equation to estimate pile horizontal stiffness's (K^P_x & K^P_y). All these three solutions are on the basis of elastic theory and their limitations to apply for the pile raft foundation has already been discussed in the

previous paragraph. Moreover, he utilized the pile raft interaction factor from Randolph (1983), both for the lateral and vertical load effect calculation. However, Randolph developed the interaction factor for a single pile cap unit as demonstrated in article 2.3.1 of this chapter. Kitiyodem also extended the application of this model for batter pile foundation.

In 2003, Kitiyodem et al. extended this model further to incorporate the non-homogenous soil layer. The non-homogenous soil layer was converted into an equivalent soil mass, whose equivalent shear modulus and Poisson's ratio were derived from Fraser and Wardle (1976). Fraser and Wardle (1976) converted the non-homogeneous multilayered soil system into an approximate equivalent homogenous soil layer, by weighting the elastic parameters according to their approximate contribution to vertical settlement. More specifically, the inverse of equivalent soil elastic modulus ($1/E_{seq}$) is simply the average of the individual layers ($1/E_{si}$) weighted elastic modulus. Similarly, soil layers with unequal Poisson's ratios were converted into an equivalent layer of Poisson's ratio by using a "special scale" developed, which is based on the settlement criteria. Fraser and Wardle developed this conversion technique to determine the flexible raft behavior on layered soil, where, the raft was subjected to uniform loading, and for column loading. They suggested for the rigorous computer analysis. The parametric study, performed by them, using this model indicates the model as conservative, because it underestimates the foundation settlement as compared to the more rigorous finite element method.

Table 2.1 below summarizes the salient features of these hybrid models, which is a versatile tool to analyze the complex piled raft behavior in a less rigorous method. It requires less computing resources, which is very effective in analyzing large piled-raft foundation.

The models under this approach produce the elastic analysis, because the basic principles are based on the elastic theory of Mindlin's, Boussinesques and spring concept. The thin plate theory, used to model the raft, is purely two dimensional, and it does not consider the torsional moment, flexure and horizontal shear stress within the raft. It does not allow for transverse shear strain (Russo 1998, Kim 2001). The differential settlement is estimated from the deflected shape of the raft, therefore, the differential settlement within the same thin plate cannot be estimated and more discretization is required. Selvadurai APS (1979) clearly indicated the cases, where the thin plate theory is inadequate, as stated below.

01. "Plate subjected to localized or concentrated loadings and abrupt changes in the intensity of the external loading.
02. Edges and re-entrant corners of plates, openings with dimensions comparable with the raft thickness and abrupt changes in the flexural rigidity of the plate.
03. Plate, in which the lateral deflections are large compared with the thickness of the plate".

Small (2001) concluded that "the use of simple Plate on spring model is erroneous and recommended that their use should be discontinued". This is because

1. The springs are independent and do not interact. Therefore, the compression of one spring does not influence other parts of the foundation. To illustrate this, consider the case of a uniformly loaded raft. Such a raft will undergo a uniform displacement and therefore, there will be no bending moment in the raft. This is obviously wrong, as it is observed that such a loading would make a rectangular raft (for example) to deform into a dished shape, and the raft would then carry bending moments.

2. It is difficult to establish the stiffness values for the springs, those are used in analysis, because the spring constants are dependent on the scale of the foundation. For example, if a modulus of subgrade reaction is determined from a plate loading test, the load deflection behavior is specific to the size of plate used in that test. It should not be applied to loaded areas that are different in size from that of the plate.

3. A Winkler or spring model cannot directly take account of soil layering.

4. A vertical loading on a foundation may cause lateral displacements. A spring model cannot be used for such predictions.

Table 2.1 Salient Features of Approximate Numerical Analysis Method.

References	Model			Remarks
(A) Strip on spring	**Strip**	**Pile**	**Soil**	
Poulos (1991)	A number of beam of equal length	Spring	Elastic continuum	Homogenous soil and vertical loading
(B) Plate on spring	**Raft**	**Pile**	**Soil**	
Griffith et al. (1991)	2D thin plate	1D rod element	Vertical spring at each node of pile and raft	Homogenous soil and vertical loading
Clancy et al. (1993)	Do	Do	Do	Non-linear interaction between piles are considered
Horikoshi et al. (1998)	Do	Do	Do	Non-homogenous/ multilayered soil was converted by Davis and Poulos method
Poulos (1994)	Do	Interactive spring	Elastic continuum	FDM is applied
Russo (1998)	Do	Nonlinear spring	Elastic continuum	Nonlinear interaction between pile is considered
Kim et al (2001)	Mindlin's Plate	Coupled spring	Winkler spring	Homogenous soil and vertical loading
Kitiyodem (2002)	2D thin plate	Elastic beam	3 spring at each node. 2 in horizontal and 1 in vertical plane	To account for lateral load and action
Kitiyodem (2003)	Do	Do	Do	Non-homogenous/ multilayered soil was converted by Fraser and Wardle method
Kitiyodem (2005)	Do	Do	Do	Applied the model for piled raft foundation subjected to ground movement, induced by tunneling

2.3.4 Numerical Analytical Method (FEM, BEM, FLM etc)

The numerical methods employed to simulate the complex piled raft foundation are mainly the Finite Element Method (FEM), Boundary Element Method (BEM), Finite Layer Method (FLM), Finite Difference Method (FDM) or a combination of two or more of these methods. These numerical methods involved more discretization of the foundation elements and require large computation memory with high speed processors.

Boundary Element Method

In Boundary Element Methods, both the raft and the piles within the system are discretized, and elastic theory is used. Raft is discretized as a two dimensional thin plate and represented by integral equation. Soil, on the other hand, is treated as elastic homogenous layer, in which piles are embedded.

Conceptually, it works by constructing a "mesh" over the modeled surface, which have been formulated as integral equation (i.e. in boundary integral form). The interface between the soil and the foundation (piles and raft) is divided in to elements and an approximate Green function, such that due to Mindlin's, is used to relate the displacement of each element to the traction on the other elements. Corresponding equations are written for the structural response of the foundation, using either a finite difference or a finite element approach. The two sets of equations, together with those for overall equilibrium, gives the value of unknown tractions. Therefore, the settlement and load distribution throughout the foundation can be calculated.

The early works of Butterfield & Banerjee (1971) and Davis & Poulos (1972), as mentioned in section 2.3.2, are the limiting case of a rigid raft on a homogenous elastic continuum.

Kuwabara (1989) performed elastic boundary element analysis on small piled raft, founded on a homogenous elastic soil mass. Square group of identical compressible piles are connected to a square rigid raft, which is taken either free standing or in contact with the surface of the half space. It was found that under elastic condition, the raft carried only a small proportion of the load at normal pile spacing.

Poulos (1993) extended Kuwabara's (1989) analysis to allow for the effects of the free-field soil movements and for limiting contact pressures between raft and soil, as well as for the development of the ultimate compression and tension load in the piles. His investigation was only for a pile group consists of four piles with rigid cap. However, the limitation of rigid raft and axial load remained as in the other approach of this category.

Russo (1998) compared the findings of Butterfield and Banerjee's (1971) analysis with that of Kubwara's in terms of settlements and load sharing. Good agreement between these two methods were found in terms of settlement for various values of the pile spacing, slenderness ratio (L/d) and compressibility ($K_{ps)}$ as shown in figure 2.10. In contrast, the dimensionless plot of the load sharing between the piles and the raft versus the spacing of the piles (Figure 2.11) shows a large and discouraging disagreement. The portion of the total applied load supported by the piles, as obtained by Kuwabara, is

significantly higher than that calculated by ButterÞeld and Banerjee. This variation in load shearing between the two sets of results is due to their different approaches and approximations in the numerical techniques.

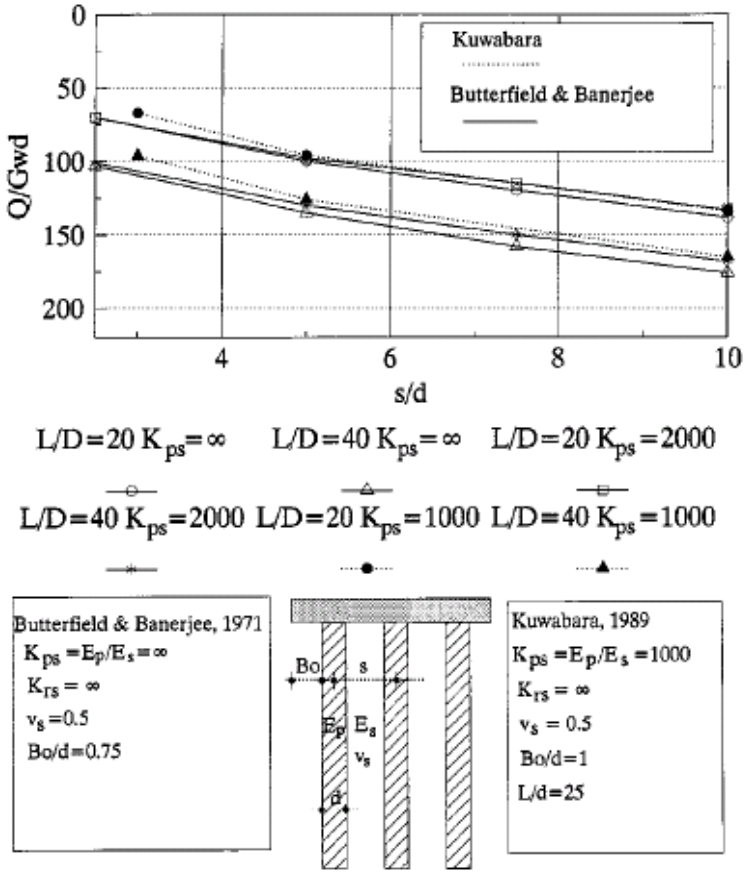

Figure 2.10 Settlements calculated by Kuwabara (1989) and Butterfield & Banerjee (1971)

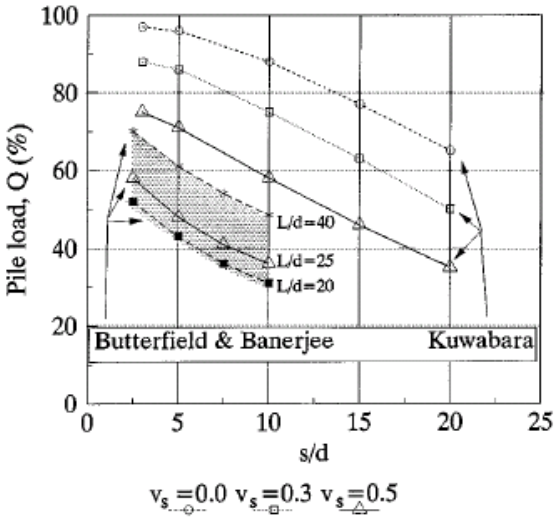

Figure 2.11 Load shared calculated by Kuwabara (1989) and by Butterfield and Banerjee (1971)

Mendonca et al. (2000) performed a Boundary Element Analysis for flexible piled raft foundation. The raft is assumed as thin plate and represented by integral equations, pile is represented by single element with three nodal points and the traction along it is approximated by a second degree polynomial equation. Soil is treated as an elastic linear homogeneous half space, represented by integral equation using Mindlin's fundamental solution. A uniform traction is assumed in plate-pile interface and the traction along the shaft of the pile is uniformly distributed around its periphery. Raft is subjected to only the vertical static load (figure 2.12).

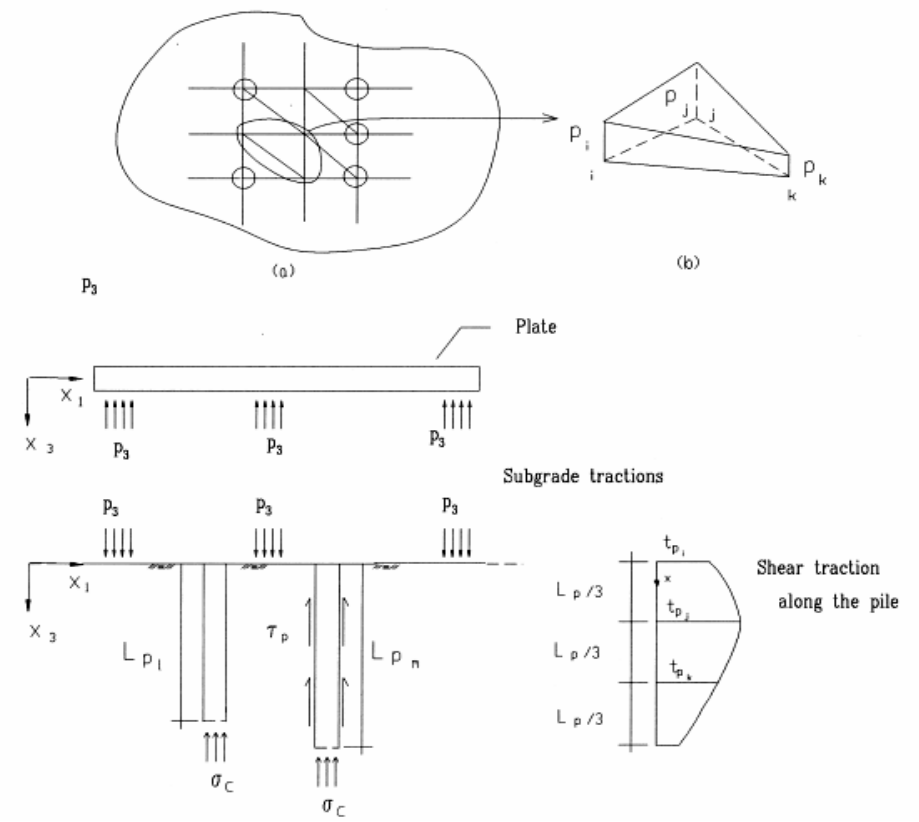

Figure 2.12 Plate-pile-soil interaction tractions (Mendonca et al. 2000)

The analysis of Mendonca et al. (2000) is a purely Boundary Element Method that introduced the raft flexibility. All the previous work in this method was done for rigid raft. However, it could be limited its application only to the small piled raft foundation. This is due to the fact that the computational time and memory requirement tends to grow according to the square of problem size. It could be more efficient for small surface volume ratio than finite element method in terms of computational resources.

The boundary Element Method is applicable only to the linear homogenous medium, for which the Green's function is applicable (Banerjee et al. 1986). The Green's functions, or

fundamental solutions, are often problematic to integrate as they are based on a solution of the system equations, subject to a singular load. Integration of such singular fields is viable for planer surface and therefore, raft is considered as two dimensional thin plate in all the analysis by this method. However, the limitation of considering two dimensional thin plate is already discussed in section 2.3.3. Therefore, it could be concluded like Russo and Viggiani (1997) that the complete Boundary Element Method solutions are possible only for relatively simple problems.

Finite Difference Method

Poulos (1994) employed Finite Difference Method (FDM) to analyze the raft behavior of a piled raft foundation. The rectangular rigid raft of constant stiffness was discretized into nodes and elements, for which, the equation of plate bending was expressed in incremental finite difference form. At this stage, Poulos concluded that the published theorem for the Finite Difference Coefficient are in "error", especially for the edges and corner of the raft, and do not satisfy vertical equilibrium. However he made some approximation to overcome this limitation.

This analysis considers the concentrated and applied moment load as uniformly distributed load. Load displacement curves were used to obtain the vertical displacement of the soil at the junctions of the piles. The load displacement curves for the interaction of two rigid circular cap pile unit were initially obtained and then applied for all pile cap unit by super position theory as mentioned in section 2.3.3. However, this elastic

superposition theory is valid, only when the piles are located along a circumference and subjected to the same load (Mendonca et al. 2000). The limitations of 2-D thin plate theory and other approximations used, have already been discussed in section 2.3.3.

Besides the work of Poulos (1994), no more analysis using Finite Difference Method was found in available published documents. This may be due to the lack in the development of a reliable Finite Difference Method formulation, as mentioned by Poulos (1994).

Finite Element Method

Simplified or 2-D FEM

In fact, all the simplified or two dimensional finite element analysis involved the representation of piled raft as an axi-symmetric or a two dimensional plain strain problem. In both cases, significant approximations were made. Many computer programs (FLAC, PLAXIS, AMPS etc.) are available to simulate the behavior.

Hooper (1973) was the first, to use the Finite Element Method (FEM) in analyzing the complex behavior of piled raft foundation of Hyde Park Cavalry Barracks on London clay. This linear elastic axi-symmetric finite element analysis precluded the rigid raft and pile consideration of Banerjee et al. (1971) and Davis et al. (1972). Attempts were made to incorporate soil layering, while the linear soil isotropy was expressed in terms of empirical equations. This analysis assumed that soil modulus of elasticity increased linearly with depth, and Poisson's ratio was constant at 0.5 for undrained and 0.1 for

drained condition. The analytical results were found to have a good agreement with the parameters, measured six years after the construction. However, this 2-D axi-symmetric analysis considered only the vertical uniformly distributed load, soil as a single phase medium and attempt to account for the soil layering was made by introducing modulus of sub-grade reaction value, which is based on plate load testing.

Sommer et al. (1985) used the finite element analysis technique for the static design of a tall building on Frankfurt clay in Germany. The finite element mesh consists of 960 elements and the soil deformation was simulated by nonlinear elastic constitutive law of Duncan/Change (1970). The load settlement behavior of this building was under observation, as it was equipped with the geotechnical measuring devices. However, the initial measurements had reasonable agreement with the computed values.

Burland et al. (1986) performed 2-D plain strain finite element analysis for the Queen Elizabeth conference centre on London clay. Raft was considered as rectangular plate element, subjected to equivalent uniformly distributed loading on elastic half space and was modeled by eight nodded isoparametric element. The computed results were compared with the measured parameters of heave and settlement during the construction process. However, the long term effects were not reported in any other available publications and the analysis has the common limitations of 2-D finite element analysis.

Prakoso et al. (2001) proposed a general design methodology for the optimum pile raft design. This design methodology was developed on the basis of a two dimensional plain

strain analysis of a vertically loaded pile raft. The geotechnical finite element code PLAXIS were used with six nodded triangular elements. The parametric study were performed for both elastic and elasto-plastic soil and validated with boundary and 3-D finite element analysis of other researchers. Sanctis et al.(2001) pointed out the limitations of this 2-D plain strain analysis and remarked that "only 3-D finite element analysis is suitable for the development of optimum design methodology".

G. Hassen et al. (2006) developed an elasto-plastic multiphase model in order to simulate the load settlement behavior of piled raft foundation subjected to combine (vertical and horizontal) loading. This 2-D plain strain problem were simulated numerically by the superposition of two 2-D continuous media, called matrix phase (surrounded soil mass) and reinforcement (pile reinforced zone) phases, respectively. Six nodded triangular finite elements were used to represent both of these phases in light and dense network, as shown in figure 2.13 below. This linear elasto-plastic model assumed a perfect bonding between soil and reinforced concrete in piles and in slab. The output remains unverified with some field measurement or with the accepted publications. The analysis was performed on two phase only, although it was claimed to be applicable for multiphase.

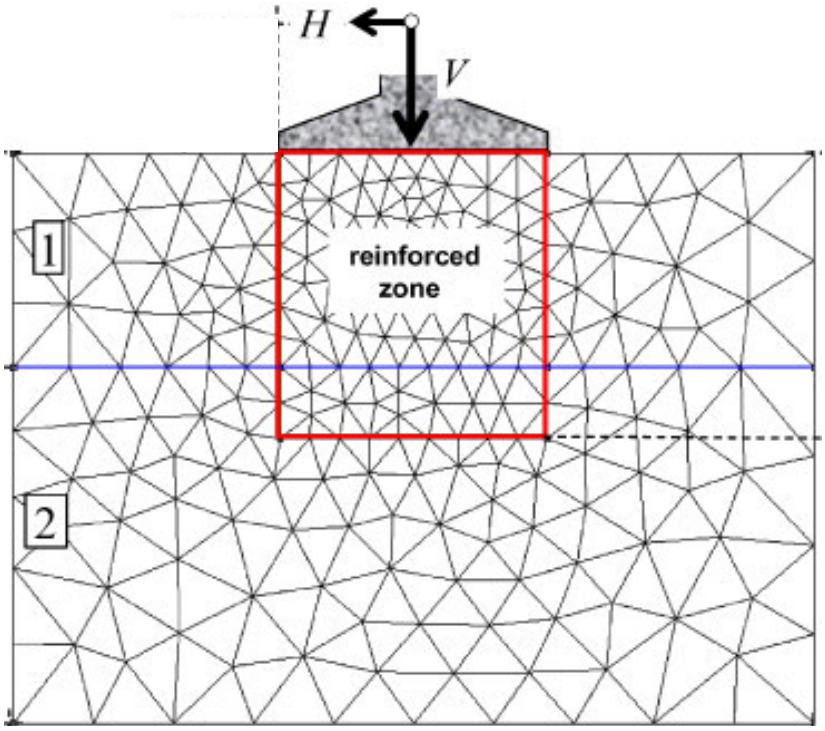

Figure 2.13 Finite element mesh of the two phase for simulating piled raft foundation behavior (Hassen et al. 2006)

The main problem of this simplified finite element analysis are that, only regular loading pattern can be analyzed, and like plate on spring approach, it cannot give the torsional moment in the raft. All the analyses are performed considering soil as a single phase medium. Although, Hassen et al.(2006) attempted for two phase medium approach.

3-D FEM

The advancement in computational resources paved the way to simulate the piled raft foundation by means of three dimensional finite element method, which was considered as "completely unsuitable" for piled raft foundation, as mentioned by Hooper in the CIRIA (Construction Industry Research and Information Association, London) report 1983. In contrast, Novak et al. (2005) mentioned the complex piled raft foundation

problem cannot be modeled correctly by the simplified method. The codes for 3-D FEM analysis are now available, more powerful and can be performed on personal computer.

Ottaviani (1975) is the "first" (Poulos et al. 1997), who applied 3-D finite element analysis to pile and pile raft foundation. The three dimensional axi-symmetric elements were used to study the load transfer mechanism, stress distribution and displacement (settlement) of a vertically loaded single and pile groups (3x3 and 5x3), with and without cap, embedded in a homogeneous linearly elastic soil medium. The analysis was simplified by means of assumptions and approximations (e.g. piles are considered square in cross section, constant rigidity for concrete of piles and cap material, soil is linear, elastic and homogeneous). The analysis was for small pile group and does not provide any information for differential settlement.

Katzenbach et al. (1997a) simulated the soil-structure interaction of piled raft foundation by means of an axi-symmetric 3-D finite element analysis. The linear elastic raft was modeled with shell elements. Linear elastic pile and elasto-plastic (based on Drucker-Prager 1952 model) isotropic soil continuum were represented by 3-D isoparametric shell elements. The load settlement behavior was validated by the static load test result for Sony Centre, Berlin, Germany (figure 2.14. As a consequence, the authors (1997b) extended their simulation for Commerzbank tower in Frankfurt, Germany with this model to estimate the load sharing between the raft and pile, and the interactions between the piles. Katzenbach et al. (1998) performed another analysis on the same numerical model but the elastic raft was replaced by the rigid raft, and the interaction factors, distribution

of the load and skin friction for different number, location and length of piles were presented. However, this study was not validated with any measured or with other research works. The same numerical model, with its approximations and assumptions, was used by the authors (2005) for assessing the settlement of City tower, Frankfurt, Germany, which was also equipped with geotechnical monitoring devices in order to study its in-situ behavior.

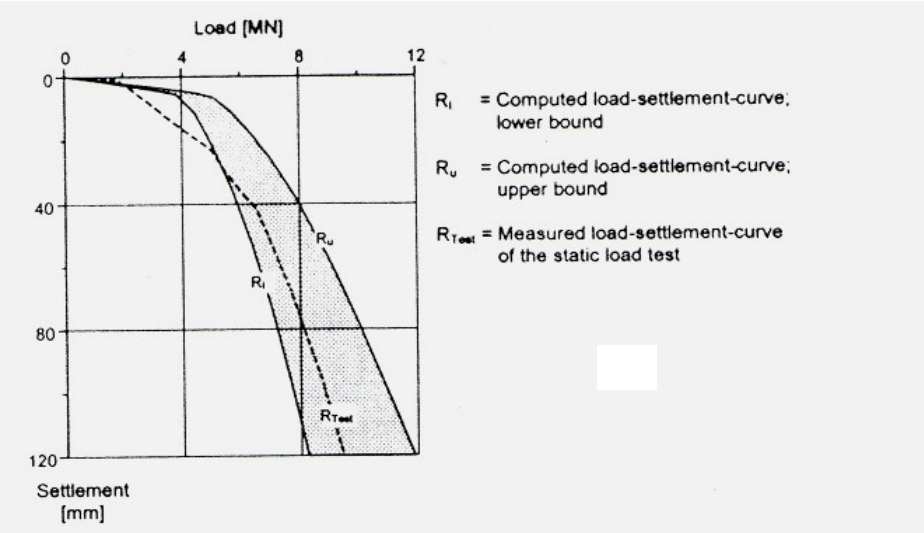

Figure 2.14 Comparison of measured and estimated load settlement behavior of Sony Centre, Frankfurt, Germany

Reul et al. (2000) performed the 3-D finite element analysis of three piled raft foundation (Messeturm, Torhaus, Westend 1 building in Germany) on over-consolidated clay and compared the results with the measured values in terms of load sharing, total and differential settlement. These analysis were performed on the numerical model developed by Katzenbach et al. (1997). The soil and piles were represented by first-order solid hexahedron (brick) and raft was by shell element. The circular piles have been replaced by square piles with the same shaft circumference. The contact between structure and soil

was considered as perfectly rough. The structural loads were considered as uniformly distributed over the raft. As a consequence of good agreement of this model with the measured one, Reul (2004) applied this model to investigate the foundation behavior, specially, the pile resistance for various pile position and load level and recommended that design optimization can be achieved by increasing pile length rather than increasing number of pile.

Garcia et al. (2006) plugged the viscohypoplastic model of Niemunis (1996, 2003) for soil continuum in Reul's (2000) numerical model. A very good agreement was found with the measured settlement and load distribution for the Messeturm tower on Frankfurt, Germany. This constitutive viscohypoplastic model is capable of modeling the small strain nonlinearity of clayey soil. The model has some assumptions and Garcia et al. (2006) made some approximation to incorporate this constitutive model into above mentioned 3-D finite element model by means of computer program ABAQUS. Moreover, this model considers the soil isotropy of constant stiffness, ignores the primary consolidation effect. To precise the creep intensity, over consolidation ratio (OCR) was considered smaller than 2.0. Since, the soil structure contact surface was considered rough, the replacement of circular pile by rectangular may limit the model adequacy to represent realistic behavior of the foundation.

Besides these major groups of German researcher, individual investigations are observed in recent years. Sanctis et al (2006) performed a 3-D FEM analysis by ABAQUS to evaluate the bearing capacity of a vertically loaded piled raft on Italian soft clay. This

axi-symmetric, displacement controlled analysis considered smooth contact between rigid raft and elasto-plastic soil. This analysis concluded that the bearing capacity of pile raft is the summation of the capacity of an un-piled raft and a pile group, "which can be simply evaluated in the conventional way". However, this is a controversial conclusion to the other researchers and practical measured values of the foundation behavior.

Maharaj (2003) studied the load settlement behavior of piled raft foundation by 3-D nonlinear finite element analysis. The elastic raft, subjected to uniformly distributed load and supported by elastic pile in stiff clay, was modeled by hexahedron 8-noded brick elements. This axi-symmetric analysis adopted the Drucker-Prager (1952) yield criterion to include the nonlinear behavior of the elasto-plastic soil. The load settlement behavior, total and differential settlement as well as parametric studies were done. As a consequence, he (2004) focused on the effect of raft and pile stiffness on load settlement behavior of the same model. The output of all of these analyses (2003 & 2004) was validated by comparing with the result of Trochanis et al. (1991), which was done for freestanding single or pair of square pile without any cap or raft. Moreover, the 3-D axi-symmetric finite element pile analysis of Trochanis et al. (1991) was modeled by solid 3-D quadratic isoparametric 27 node elements (nine nodes per face) by means of ABAQUS. The model was checked with some previous studies which are nor on the basis of analytical, laboratory or instrumented piled raft analysis

Novac et al. (2005) performed a linear elastic three dimensional finite element analysis for the load settlement behavior of piled raft foundation and found good agreement for

the measured value of two case studies (Westend I of Frankfurt, Germany and Urawa of Japan) on over consolidated stiff clay. The 3-D tetrahedron Flex Mesh elements were used to construct the model by means of computer programs AMPS (2004) to analyze the behavior of the system. The piled raft was modeled as reinforced concrete and was inserted into the soil domain as shown in figure 2.15 below.

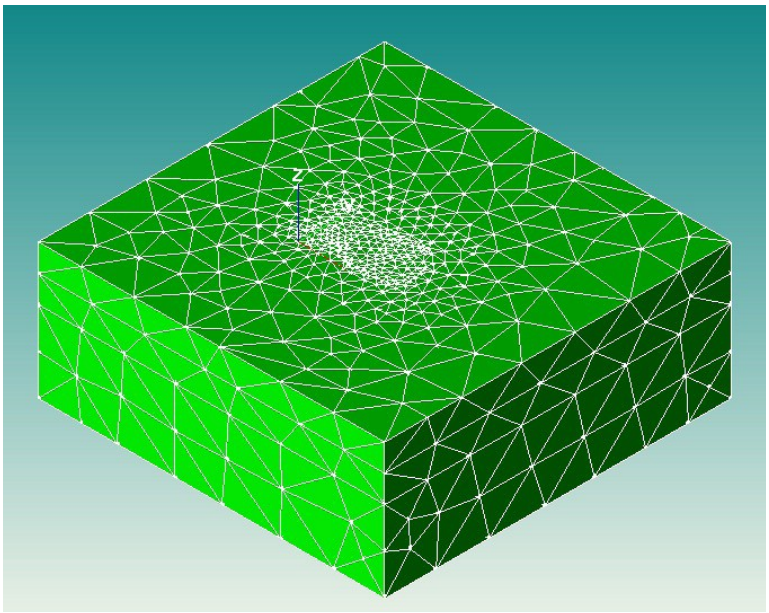

Figure 2.15 3-D mesh model of pile, raft and soil behavior (Novac et al. 2005)

Vasquez et al. (2006) replaced the linear elastic soil constitutive law from Novac et al. (2005) model by nonlinear soil constitutive equations of Mohr Coulomb model as extended by Zienkiewiez (2001). The same cases were studied as in Novac et al. (2005). However, both of them studied the settlement of the centre pile assuming a dish shape settlement of the slab.

The significance of 3D FEM analysis is that, detailed stress distribution for the foundation system can be revealed for investigation. All these study investigated only the vertical load effect on soil continuum and considered soil as a single phase medium, although, soil is a three phase medium that contain gas, liquid and solid.

Hybrid Method

Hybrid Method, as the name implies, combines two or more methods to simulate the complex piled raft foundation behavior. The purpose of combining two or more numero-geotechnical method is to reduce the mathematical interpretation and thereby to reduce the computer memory and time consumption requirements. The approximate numerical analysis described in the section 2.3.3 is also hybrid analysis but those are limited to the size of the problem as discussed earlier.

FEM+BEM

Hain and Lee (1978), Franke et al, (1994), Russo and Viggiani (1998) combined boundary element for the piles and finite element analysis for the raft. The main advantage of BEM is that the nonlinearity may be simulated by stepwise linear incremental procedure.

Hain and Lee (1978) developed a hybrid numerical model, combining the 2-D finite element analysis for the raft (rigid and flexible), and boundary element model for pile-soil medium. This elastic analysis considered raft as a series of 2-D thin plate and adopted the interaction factor concept to reduce the computation effort, while piles are

given by load transfer curves, taken from Davis and Poulos (1968, 1972). The limitations of superposition of the elastic load transfer curves of Davis and Poulos (1968, 1972) have been discussed in section 2.3.2. The model was verified with the measured data (just after construction) of La Azteca building of Mexico City and Hyde Park Cavarely of London. The analysis considered only the vertical component of load and assumed a sliding ball joint between raft and pile. Therefore, moment effect was ignored along with the effect of lateral loading as well as horizontal component of vertical loading. Moreover, it ignored the reinforcing effect due to pile in soil layer. The limitations of 2-D thin plate finite element and boundary element were described in the previous sections.

Frank et al. (1994) developed a hybrid numerical model, termed as "mixed technique" to simulate the three dimensional nature of the problem. The raft is modeled as 2-D finite element in bending plate, supported by springs of soil and pile element with sufficient stiffness. Nonlinear pile-soil interaction (around shaft as well as base of pile) was modeled by boundary element method and the pile slip effect as well as locked stresses was taken into consideration. The measured parameters showed concordance with the computed values at lower depth and load, but for greater values, it declined. This is due to the assumptions, approximations and methods of interpretation of the model.

Russo (1998) simulated the piled raft foundation by means of a 2-D thin plate finite element analysis for raft and boundary element analysis for piles. The pile-pile interaction factors among piles were calculated by means of boundary element analysis by means of computer code. The review of this literature has been done in section 2.3.2.

Mendonca et al. (2003) modified their pure boundary element analysis (2000) by replacing the boundary element analysis technique of raft with the finite element analysis technique. The raft is modeled as thin bending plat by flat triangular elements of Discrete Kirchoff Theory (DKT), which made the raft analysis a two dimensional bending plate finite element analysis in nature. This elastic analysis considered the pile and raft flexibility on linear elastic soil medium and only the static vertical loading were treated. This analysis provides information on soil lateral displacement, however, the modulus of sub-grade reaction is assumed to vary linearly. The settlement and moment distribution were studied, however, the intrinsic problem of two dimensional finite element as well as boundary element method remain the same.

FEM+FLM

Small J C could be accredited as a pioneer for introducing finite layer method in pile group (Ta & Small 1995) and piled raft (Ta & Small 1996). To overcome the limitation of conventional finite layer and finite element method incapability of analyzing incompressible materials, Small and Booker (1984, 1986) introduced exact finite layer flexibility matrix. This finite layer matrix is capable of analyzing the layered elastic materials. He extended this finite layer analysis for strip loading (1984), circular and rectangular loading (1986). As a consequence of this development and modification of finite layer analysis technique, Ta and Small reported their analysis for pile group behavior (1995) and piled raft behavior (1996).

Ta and Small (1996) performed the analysis combining the finite element analysis (for raft and pile) and finite layer analysis (for elastic isotropic layered soil). The axi-symmetric raft analysis considered the two dimensional thin plate bending elements, while, pile elements were represented by elastic beam elements. The elastic transversely isotropic (isotropic in x, z plane) soil layer is divided into multiple layers with their associated properties and then, the modified finite layer method of Small and Booker (1984, 1986) were used. The vertical load effect (stress and displacements) on soil were expressed in terms of double Fourier transformations. The plane strain-stress relationship and boundary conditions were applied to solve the unknowns. The results are expressed in terms of load distribution along the pile shaft, load sharing between the raft and piles and claimed it as an effective time saving method of pile raft analysis.

Ta and small (1997) extended their above mentioned work of 1996 to faster the analysis process up to 100 times and thereby make its use in large group of pile raft foundation (previous one was performed only for 3x3 and 4x4 pile group). In this case, he considered some approximation (e.g. raft elements were considered as of identical square elements with their displacement at center, the surface displacement of soil at any point is approximated by a polynomial). The great speed up was achieved by the typical identical square raft element and the use of a single polynomial equation to compute the load on other piles or rafts, which does not require to be computed for each pile element and each element of the raft.

Zhang and Small (2000) extended the above model to include the effect of horizontal loading (the previous works was only for vertical loading) along with the vertical loading for an off ground cap supported pile group in layered soil. The horizontal load effect in elastic soil mass was expressed in terms of Hankel Transforms (also known as Fourier-Bessel's transform), while the vertical load effect was in terms of double Fourier transforms like before. The analysis shows good agreement for small pile group (2x2) and differs greatly for a group of 4x4 piles when compared to other published results. This elastic model for rigid off ground cap supported pile group was used to perform parametric study.

Zhang and Small (2002) extended their model of 2000 to analyze the behavior of a rigid raft in contact with soil and supported by rigid pile group. The model was verified with the finite element analysis and found good agreement for closer pile spacing of a small pile group. However the parametric study was done only either for vertical loading or for horizontal loading and not for the combined loading.

Small (2001) reported an extension of the work of Zhang and Small (2000), where two horizontal point load were applied to the head of each pile, instead of single point load of Zhang and Small (2000). He found that the raft rotates under the horizontal loading and does not undergo any vertical movement at its centre. A reasonable close agreement was found when comparing with the finite element analysis, but great disagreement appeared when compared with the measured data from Yamashita and Kakurai (1991). However, the author claimed the analysis as, "of correct order of magnitude".

Chow and Small (2005) investigated the pile raft behavior for varying pile length and diameter within the pile group and with the aforementioned model under vertical loading. All the previous study by this type of hybrid method was performed for typical pile of equal length and equal diameter in the group.. This method is about five times faster than the finite element method. The author's pointed out the disparity on comparison with the finite element method was due to the assumptions used (e.g. horizontal loads and movement were neglected, rigid joints between raft and pile head was assumed as smooth base of raft on pile group) and approximations involved in this method.

The major problem is in the computation method of interaction factor. The interaction factor is developed on the basis of interaction between a pair of pile, where one pile is loaded and another is kept unloaded to estimate the interaction. Obviously, this approach neglects the stiffening effect of other piles in the group. This model is based on the Small and Booker transformation for strip, circular and rectangular loading. However, no transformation for point loading has been discussed. This theory considered the transverse soil isotropy that ignores the presence of pile and the effect of soil stiffness due to pile reinforcement in that layer. The use of polynomial for the horizontal soil layer may have some limitations; because the soil layer is infinite in horizontal direction. Moreover, this elastic analysis consists of two dimensional finite element plate bending analysis for raft, and the limitations have already been discussed.

As a means of summarizing the capabilities of some of the various methods mentioned above, Table 2.1 lists the methods and summarizes their ability to predict the response of the foundation system.

2.3.5 Variational Approach

An alternative approach was investigated by the researchers to overcome the limitations of existing numerical method (e.g. discretization, time and computer resources requirements of numerical method) by employing the work energy principles. Chow, Yong and Shen (2001) introduced this new concept to analyze the piled raft foundation.

The application of work energy principle was found to be used first, by Selvadurai (1979) in shallow foundation and by Chow, Yong and Shen (1997, 1999) in deep foundation to analysis the settlement behavior of group pile. The first paper of Chow et al (1997) investigated the behavior of a pile group with cap not in contact with soil, where the load transfer curves were used to model the elastic soil. Their second paper (1999) is also for off ground capped pile group, where soil was modeled as an isotropic elastic half space. They reported in 2000 the extension of the above works for the analysis of pile-cap interaction for a pile group with rigid cap in contact with soil. They extended this model for pile group with flexible raft in 2001. This analysis (2001) is in good agreement with Clancy and Randolph (1993) and gave significantly lower value, when compared with the measured value of two instrumented building.

The basic concept of this approach is that the raft is assumed to rest on a elastic half space, reinforced by pile group. The pile deformation and raft deflection are represented by a finite series, developed on the basis of potential energy. A stiffness matrix of the pile group-soil system is developed at the raft and pile group–soil interface.. This stiffness matrix is then combined with that of the raft analysis on the basis of minimum potential energy principle in order to obtain the behavior of the piled raft foundation.

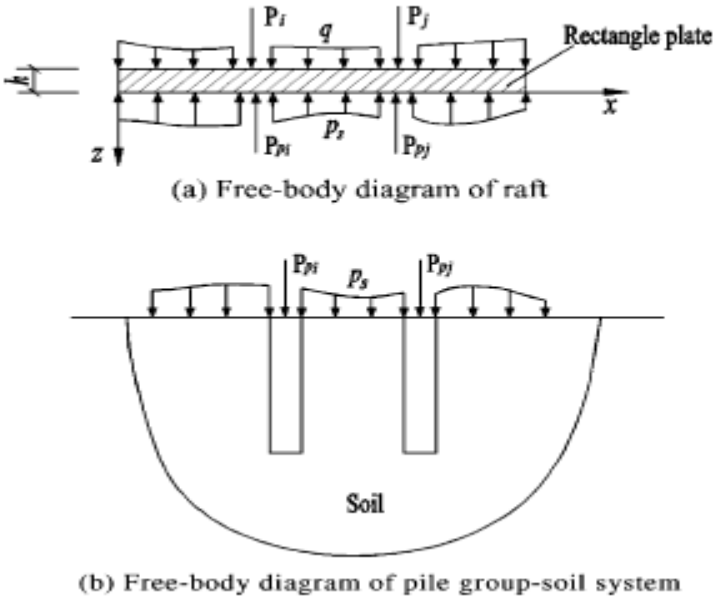

Figure 2.16 Concept of variational approach (Liang et al. 2004)

Liang and Chen (2004) brought some modification to the model of Chow et al (2001) to make it simple and faster. This modification was done assuming raft pile connection as a sliding ball joint and raft & pile group-soil interface as smooth. Because of these assumptions, the interface displacement can be represented either by the raft deflection or by the pile group-soil surface deflection. This is done by the application of minimum potential energy principles as mentioned above, where the raft deflection, flexural

moment and contact stress distribution can be expressed in the forms of simultaneous linear equation and can be solved analytically. The stiffness matrix for the pile group-soil system, subjected to vertical pressure force only (because of the assumptions), is developed from the free body of the pile group-soil system by using the principle of superposition. The model showed good agreement for rigid raft, when compared with the analysis result of Butterfield and Banerjee (1971). It also has good agreement for flexible raft, when compared with the analysis result of Clancy and Randolph (1993). In both cases, small pile groups were taken into consideration.

The main advantage of this method is that, no discretization of pile, soil and raft is required. The interaction between piles and soil are evaluated by a simplified approximate analytical solution. Hence, the computational time and computer storage space requirements are substantially less than those required by the conventional boundary or finite element method.

However, the variational approach is an elastic approach, that considered soil as isotropic, linearly elastic continuum and only vertical load component was taken into account. Raft strain energy was calculated from elastic thin plate theory, which ignores the torsional resistance. The horizontal or lateral load effect of vertical component of contact stress was ignored. Small et al. (2002) reported that this method as incapable of dealing with flexible raft of any stiffness. The results were compared with Butterfield & Banerjee (1971) and Clancy & Randolph (1993) - which were for 2x2 and 3x3 pile

groups only. The simplified assumptions involved in Liang and Chen (2004) report ignored the pile head restrainment with the raft or cap, and the raft surface roughness.

2.4 Field Study & Case History

2.4.1 Introduction

The objective of this section is to summarize the field study and case history data, which is essential to validate experimental, numerical and analytical model. In general, the field measurement data is essential for quality control, to develop maintenance and rehabilitation program for the respective structure and to predict the probable impact on the neighborhood. These are urgent for the safety and reliability aspects of the structures. However, at the beginning of this section, some earlier structure constructed on pile raft foundation was described and then the structures, mentioned by various researchers, were described in terms of their foundation parameters.

2.4.2 Early Piled Raft Foundation

Clarke and Watson (1936) reported that the "Juvenile Block of Ward Road Prison, Shanghai, China", constructed on interconnected wood pile during 1932–33, could be considered as the first building of this category. The same was mentioned by Terzaghi K (1936). Zeevaert (1957a) claimed that the construction of 14^{th} storied "Tower Latino Americana" in Mexico City was started in 1949, and "introduced a new and interesting problem in Foundation Engineering". The "Tower Latino Americana" was founded on reinforced concrete raft (1114 sq. meter), supported by 361 concrete end bearing piles (length 33.5 meter each). However, the "La Aztecca" office building of Mexico City is

the first ‘after construction measured settlement building’, as reported by Zeevaert (1957b) and was used by many researchers as a reference. This building was constructed during 1954-55 on 2.5 meter thick raft, and supported by 83 reinforced concrete piles of 18.0 meter length and 400 mm diameter (figure 2.17). These two buildings were constructed on highly compressible volcanic clay of Mexico City, where sub-soil improvements along with necessary engineering judgments were applied for their design and construction.

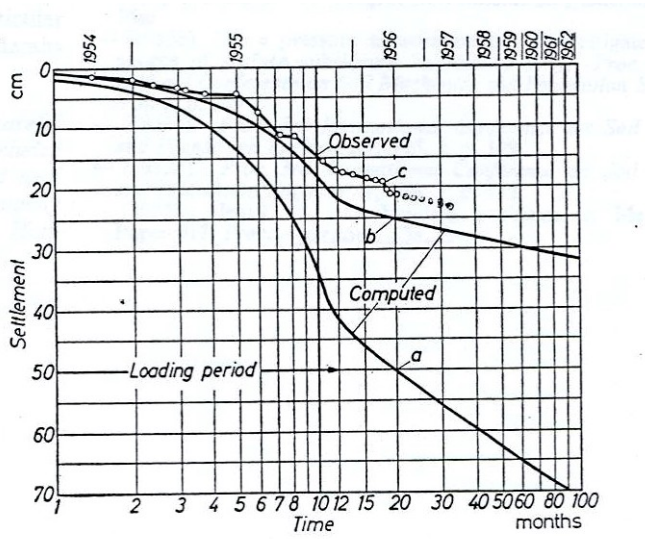

Figure 2.17 Observed and measured settlement for La Azteca office building in Mexico City (Zeevaert 1957b)

2.4.3 Piled Raft of the First Generation

Hooper (1973) reported the measured behavior of Hyde Park Cavarly Barracks on London clay. The updated measured parameters of this building were used by subsequent researchers (e/g Hains et al. 1978, Hooper 1979,) in order to compare with those of their developed models. Similarly, the Dashwood House, National Westminster Bank Tower and Queen Elizabeth II Conference Center on London clay were referred by many of the

investigator to compare their model parameter with the measured parameter of these geotechnical instrumented buildings. Table 2.2 summarizes the data for these structures, founded on London clay.

Table 2.2 Field measurement of some case history on London clay.

Building	Hyde Park Cavalry Tower Block	Dashwood House	National Westminster Bank Tower	Queen Elezabeth II conference centre
Construction Period	1967-70	1972-75	1972-79	1981-86
Storey	29	15		
Height (m)	90	61	185	34.5
Effective load (MN)	228	286	1442	
Raft Area (m^2)	618	1102	2290	2260
Raft thickness (max), (m)	1.52	1.5	2 - 4.5	2.0
Raft Depth (max) (m)	8.8			13.7
No of Piles	51	462	375	8/21
Pile length (m)	24.9	15.0	26.5	16/4.4
Pile Diameter (m)	0.91	0.485	1.2	1.8/4.0
No of instrumented pile	3	9	4	1
Pile load resistance (measured) (MN)	3.03	0.24-0.79		6.36
Settlement (max measured) (mm)	21.2	33*	40*	20*
Time after construction to measured settlement (yr)	5.94			
References	Hooper (1973, 1979) Hain et al. (1979)	Hight & Green (1976,1977) Hooper (1979)	Haws et al. (1973), Hooper (1979)	Burland et al. (1986), Price et al. (1986)

Besides the above instrumented structures, the 42 storied QVI building, Perth, Australia, constructed in 1991 and supported by 280 piles (20 meter length, 0.8 meter diameter), was referred by Smith et al. (1990) and Randolph et al. (1994). The five storied office buildings of Urawa suburb of Tokyo city, Japan was taken as case study by Yamashita et

al. (1998), Novak et al. (2001). However, detailed measured behaviors of these structures are unavailable and the same is true for other few referred structures.

2.4.4 Piled Raft of the Second Generation

The foundations of all the aforementioned and early age structures were designed on conventional group pile approach with some engineering judgments. The same conventional deep foundation approach (that ignored raft contribution to the foundation behavior) was also used in Germany and even in Frankfurt before the 'new era' in Foundation Engineering started with the construction of Messe-Torhaus building in Frankfurt clay (El-Mossallamy, 2002). The German constructed their first piled raft foundation for Messe-Torhaus building in the over consolidated Frankfurt clay during 1983-85, which was designed on completely new piled raft concept (where load carried by both pile group and raft were taken into account), together with finite element calculation (El-Mossallamy 2002). Since then, the majority of the piled raft foundation in Germany has been and is being constructed in the over-consolidated Frankfurt clay. This is due to the recent requirement of sky scrapers in Frankfurt because of the booming industrialization and respective office tower requirement for the new European financial capital, Frankfurt (Katzenbach 2005).

The German design guide line 'KPP-Richtlinie', in conformity with the Euro code EC 7, classified the piled raft foundation as the structure of highest geotechnical category (Category 3 in Euro-code and GK3 in German). For this category, the foundation

behavior has to be monitored and the field measurements need to be continuously compared with the theoretical model developed for this purpose. Therefore, geotechnical measurement devices were installed and geodetic surveying has been carried out for all high rise structure constructed in Frankfurt (Katzenbach 2005). Typical measurement devices include 'load cell' at the pile top and bottom tip, 'strain gauge' along the pile shaft, 'contact pressure cell' and 'pore pressure cell' under the raft, and 'multipoint borehole extensometer' in the bore hole. The capabilities and limitations of measuring devices for pile raft foundation behavior were discussed in Schwab et al. (1991). Table 2.3 below summarizes the pile raft foundation behavioral data from the instrumented structures on Frankfurt clay.

Table 2.3 Field measurements of piled raft foundation in Frankfurt clay, Germany

Building	Constr-uction Period	H (m)	P_{eff} (MN)	Raft			Pile			Measured				References
				A_R (m^2)	t_R (m)	Z_R (m)	N_P	L_P (m)	D_P (m)	N_{IP}	P_P (MN)	S (mm)	Time* (yr)	
American Express	1991-92	75	723	3575	2.0	14.0	35	20.0	0.9	6	2.7 - 5.1	55	1	Reul (2000)
Congress Centre	1995-97	52	1440	10200	2.7	14.2	141	12.5 34.5	1.3	12	2.4 - 5.9	58	0	Reul (2000)
Eurotheum	1997-99	110	425	1893	2.5	13.0	25	25 30	1.5	4	2.6 - 4.7	29	1	Katzenbach (1998,2005)
Forum-Kastor	1994-97	95	750	2830	3.0	13.5	26	20 30	1.3	3	5.0 - 12.6	55	0	Mossallamy (1999)
Forum Pollux	1994-97	130	760	1920	3.0	13.5	22	30	1.3	3	7.4 - 11.7	70	0	Mossallamy (1999)
Japan Centre	1994-96	115	630	1920	3.5	15.8	25	22	1.3	6	7.9 - 13.8	65	1	Mossallamy (1999)
Main Tower	1996-99	199	1470	3800	3.8	21.0	112	30	1.5	17	1.4 - 8.0	25	0	Katzenbach (1998)
Messeturm	1988-91	256	1570	3457	6.0	14.0	64	26.9 34.9	1.3	12	5.8 - 20.1	144	8	Sommer, Poulos, Katchenbach etc
Torhaus	1983-85	130	2x200	2x429	2.5	3.0	2x42	20	0.9	6	1.7 - 6.9	140	2	Sommer (1985), Reul (2003)
Westend I	1990-93	208	950	2940	4.7	14.5	40	30	1.3	6	9.2 - 14.9	120	3	Novak (2005), Poulos (2001), Frank (1994)
Haus des Wirtschaft	1997-99	68	605	5120	2.0	8.5	47	25.	1.2	6	1.4 - 3.1	25	0	Reul (2000)
Frankfurter Welle	1998 -01	55		25000	1.0 - 2.2		102	20 25	0.9	6	-	-	-	Hamsley (2000)

Notation used

H = Building height above ground
P_{eff} = Effective load (Settlement influencing load - uplift)
A_R = Area of Raft
t_R = Area of Raft
Z_R = Raft top depth below ground level
N_P = Number of pile
L_P = Length of pile
D_P = Diameter of pile
N_{IP} = No. of instrumented pile
P_P = Measured pile load
S = Measured settlement
* = Time of last measurement

2.5 Parametric Study

2.5.1 Introduction

The study of this complex three-dimensional foundation involves a number of geometrical, mechanical and their bi-product parameters. The geometrical parameters are related to pile geometry (e.g. pile length, diameter, areas, number & spacing) and raft geometry (raft length, breadth and thickness). Whereas, the mechanical properties includes the soil properties (e.g modulus of elasticity, Poisson's ratio etc/) and the bi-product parameters can include the various interaction factors (e.g. pile-raft, pile-soil, raft-soil and vice versa) and other derived parameters.

Researchers expressed their investigations output in terms of the combination of these parameters, sometimes in dimensional units and sometimes in dimensionless unit. Poulos (2001b) reported the influence of varying raft thickness, pile length and its number, and load type on the four aspects of piled raft foundation. These four aspects are total settlement, differential settlement, raft bending moment and load proportion carried by the piles and raft. For simplicity, the literature review on parametric study was performed on the basis of these four aspects of pile raft foundation, as described in the subsequent sections.

2.5.2 Raft Thickness and Size

Influence of raft thickness

Poulos (2001b) summarized his study of 2001a for the influence of raft thickness variation on maximum and differential settlement, raft moment, and load sharing for a

particular load of 12 MN (figure 2.18). The similar identical behavior can be found in Anagnostopoulos et al. (1998) and in Clancy et al. (1996) for larger number of piles. The study showed that the maximum settlement is not greatly affected by raft thickness except for thin rafts, whereas the differential settlement decreases significantly with increasing raft thickness. On the other hand, the maximum moment in the raft and percentage of the total load carried by the piles increases with increasing raft thickness. This study concluded that increasing raft thickness is effective in reducing the differential settlement. Moreover, increasing raft thickness is very effective in resisting the punching shear from both piles and column loadings. The diminishing trends of all the four curves with increased raft thickness indicate the presence of certain limiting value of raft thickness. This limiting raft thickness could be an important parameter for the optimistic design of this type of foundation. The similar trends of the curves were found by Prakoso et al. (2001). Some investigators expressed the behavior in terms of raft stiffness, which is a function of raft thickness.

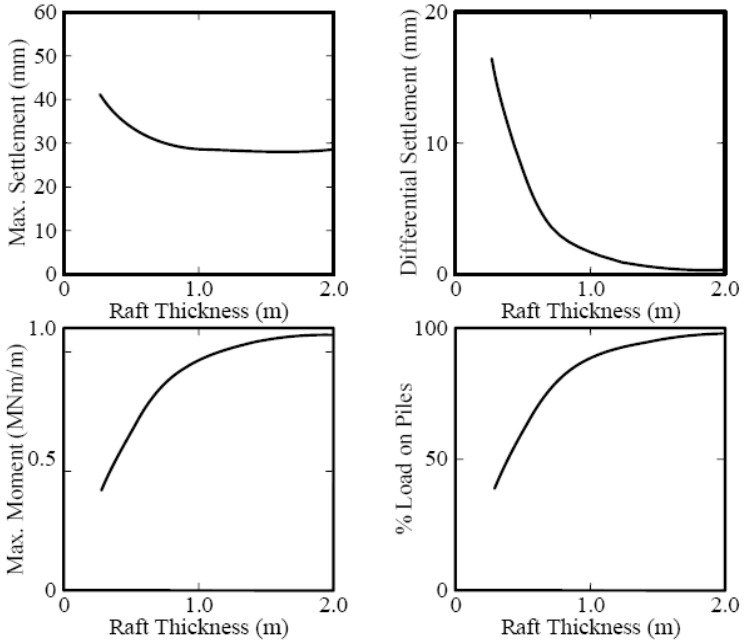

Figure 2.18 Effect of raft thickness on foundation performance. (Raft with 9 piles, 10m long subjected to a load of 12 MN)

2.5.3 Pile Number and Configuration

Influence of Number of Piles and Spacing

The pile number dictates the pile spacing, which has significant influence on the behavior of piled raft foundation. Poulos (2001b) reported a study on the load settlement behavior for varying pile number and found a linear increment relationship between the ultimate load bearing capacity and number of pile. Conversely, a reverse relation (as expected) is observed between the settlement and increased number of piles (figure 2.19), but after a certain limit, the additional number of piles has less or no influence on settlement reduction. Poulos termed this phenomenon as “law of diminishing returns” and obviously, it contributes to the concept of design optimization. The same observations can be found from the parametric study of Clancy et al (1996), Russo et al. (1997) and Horikoshi et al. (1998).

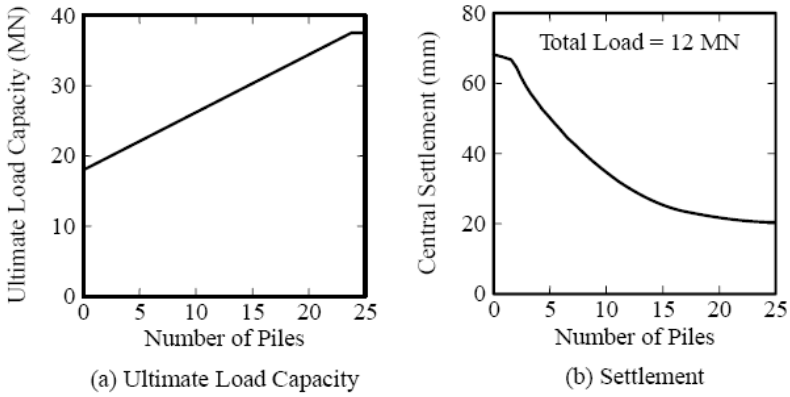

(a) Ultimate Load Capacity (b) Settlement

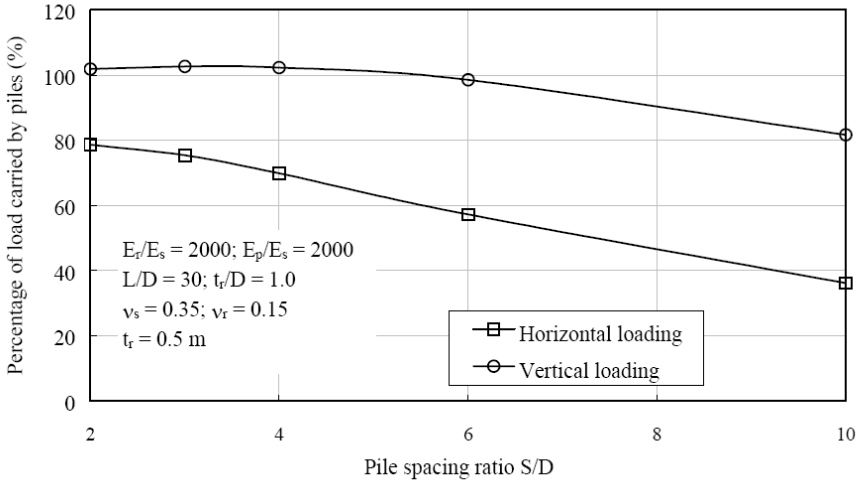

(c) Influence of pile spacing ratio on load carried by

Figure 2.19 Effect of number of piles on load settlement behavior of piled raft foundation

The direct linear relationship between ultimate load capacity and number of pile for the foundation, in turns, leads the piled raft foundation behavior toward a pure pile group behavior. However, the increased pile spacing reduces the load proportion carried by the pile (figure 2.19c) and increase the load proportion carried by the raft. This is due to the load distribution over or through the raft itself. Chow et al. (2001) have the similar observation.

Influence of Pile Group Area

The conventional practice is to leave a half pile space outside of the exterior pile. Sacntis et al. (2002) and Prakoso et al. (2001) reported that fully piled raft ($B_g = B_R$) is more effective in reducing average settlement (figure 2.20a). On the other hand, the ratio of the width of pile group to raft, in the range of 0.4 – 0.6, is very effective in reducing the differential settlement (figure 2.20b) for most of the pile raft (Prakoso et al. 2001, Horikoshi et al. 1997, Randolph 1994). However, a little variation is observed in Samctis et al. (2002) report as shown in figure 2.20c, which may be due to the variations in methods, assumptions, conditions and considerations, but the curve pattern is same in both cases. A pile group to raft width ratio (B_g/B_R) of 0.4-0.6 was also found effective in reducing the raft bending moment (figure 2.20d) as obtained from the study of Prakoso et al. (2001). The raft carried more load than the pile group for the case of equal pile group and raft area (figure 2.20e). However, the raft carrying capacity diminishes for larger pile length. The critical pile length for a desired load portion to be carried by the raft, could be investigated to develop an optimum piled raft design.

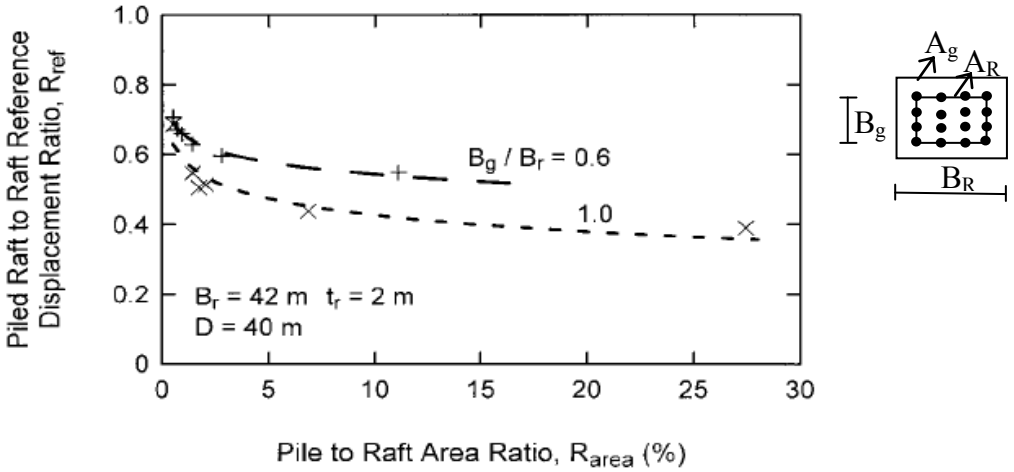

Figure 2.20a Influence of pile group size on average settlement

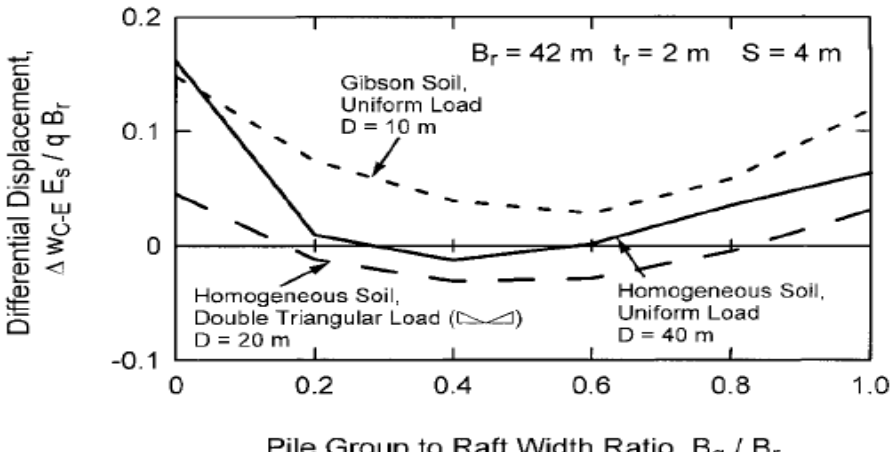

Figure 2.20b Influence of pile group size on differential settlement (Prakoso et al.2001)

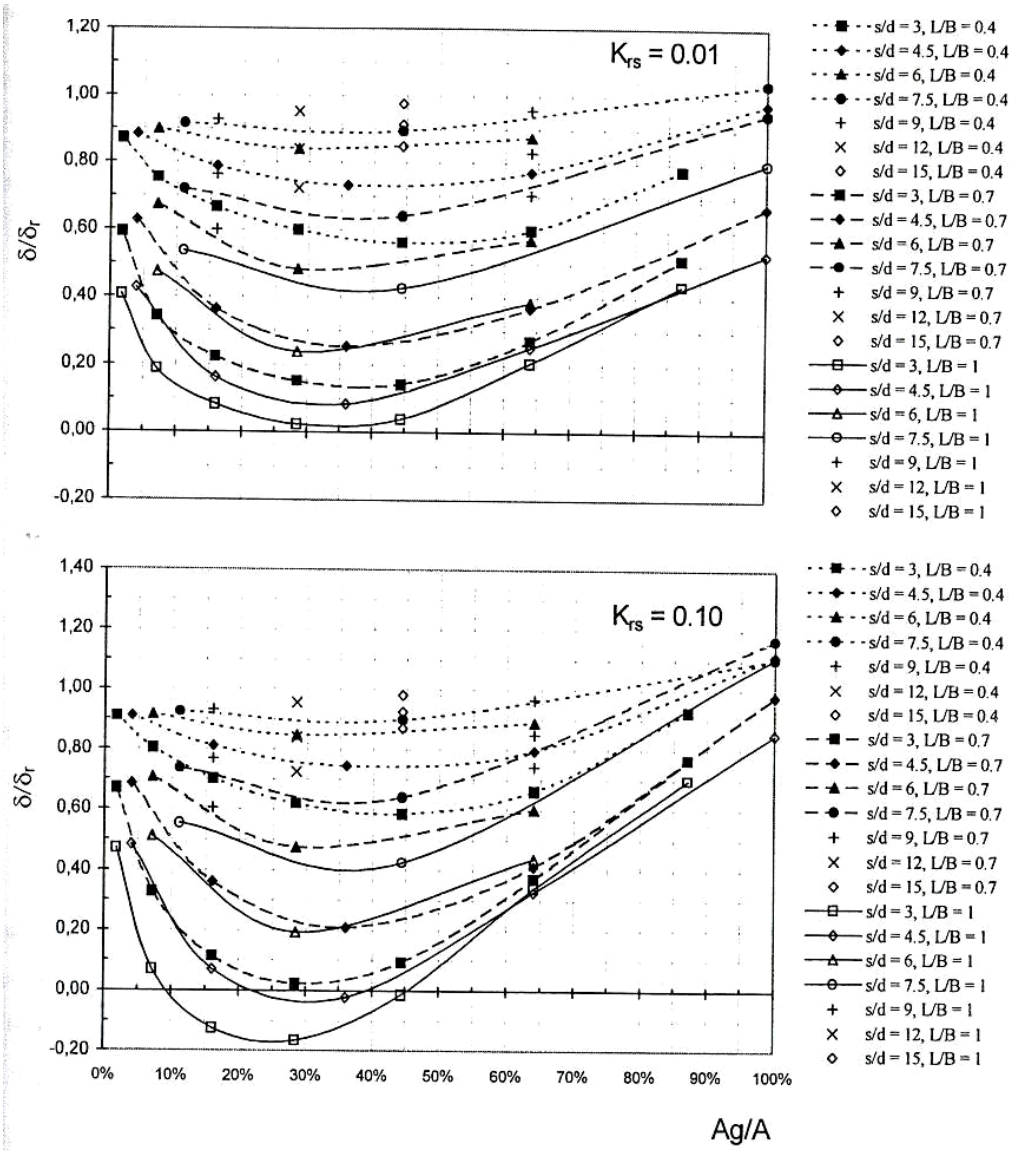

Figure 2.20c Influence of pile group size on differential settlement (Sanctis et al.2002)

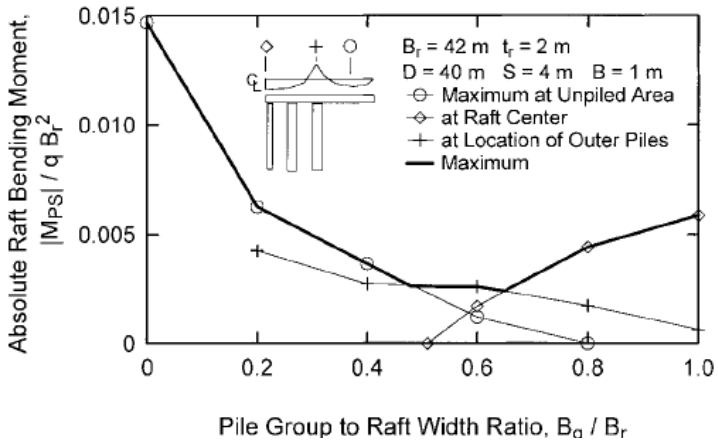

Figure 2.20d Influence of pile group size on Raft bending moment (Prakoso et al.2001)

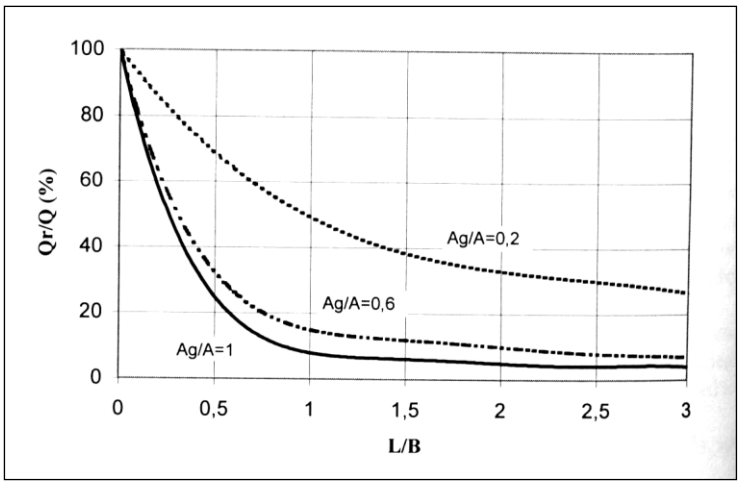

Figure 2.20e Influence of pile group size on load sharing of Raft (Sanctis et al.2002)

2.5.4 Pile Length and Diameter

Influence of varying pile length

Poulos (2001b) studied the effect of varying pile length on maximum settlement, differential settlement between the centre and outer piles, maximum moment in the raft, and portion of load carried by the piles and raft (figure 2.21). The analyses showed that the settlement, differential settlement and maximum moment decrease with increasing pile length, while the proportion of load carried by the piles increases. The same trends of the behavior were observed by Prakoso et al. (2001), Shen et al. (2000), Russo and viggiani (1997), Clancy et al. (1996),

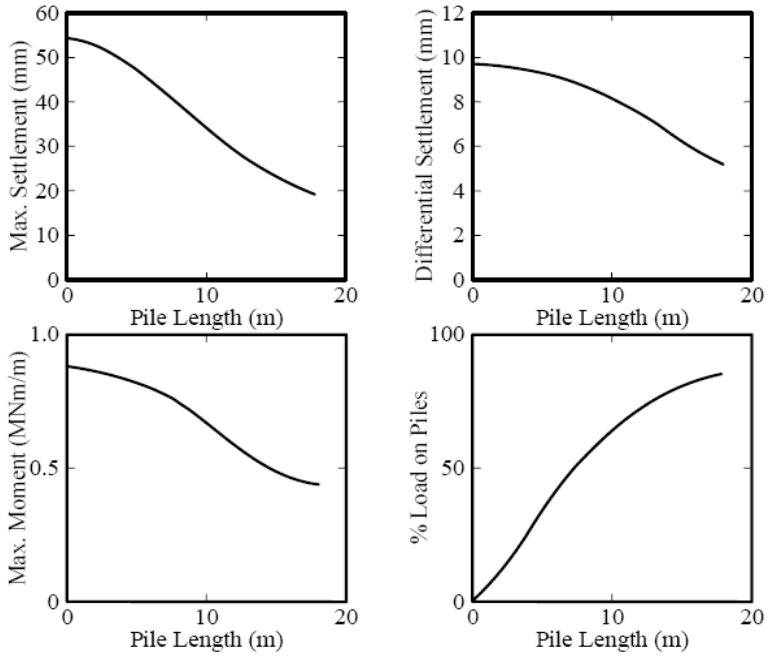

Figure 2.21 Influence of pile length variation on load settlement behavior of piled raft Foundation (0.5 m raft with 9 piles subjected to 12 MN load)

Influence of varying pile diameter

The pile diameter variation has important influence on frictional bearing capacity of free standing piles. The increasing pile diameter yields increasing pile shaft peripheral area that increases the pile bearing capacity. However Prakoso et al. (2001) found insignificant influence of varying pile diameter on the average and differential settlement (figure 2.22) and suggested for smaller pile diameter to reduce settlement of any type. Obviously, a further investigation is required to solve this contradiction and to estimate the interaction influence on pile diameter, which may play the key role in this respect.

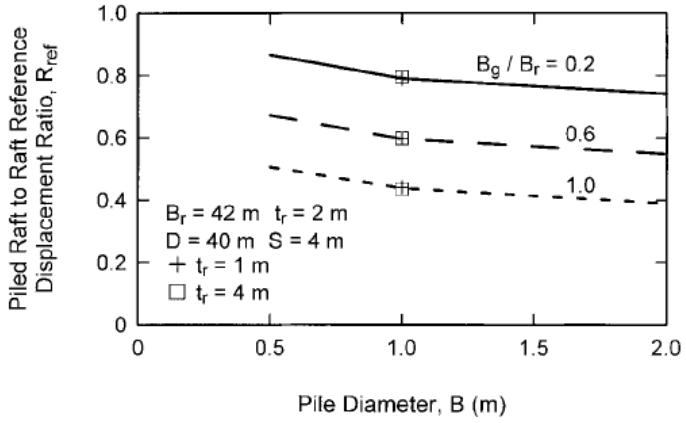

(a) Average settlement vs. Pile diameter

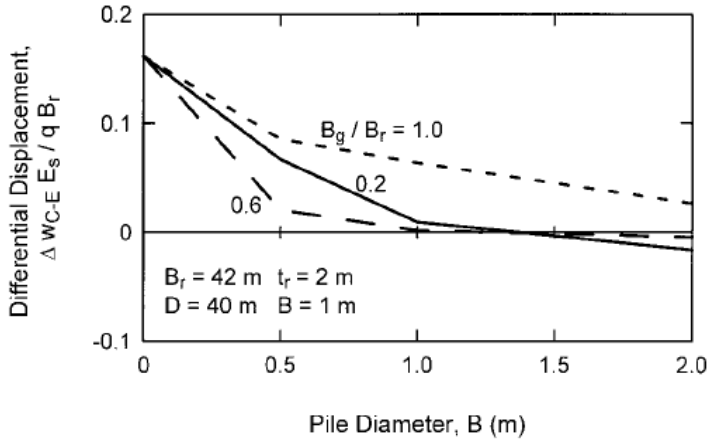

(b) Differential settlement vs. Pile diameter

Figure 2.22 Effect of varying pile diameter on (a) Average settlement (b) Differential settlement

Figures 2.21 and 2.22 indicate that increasing pile length could be a more effective design strategy for improving foundation performance than increasing the number of piles.

2.5.5 Type of Load

Poulos (2001a) showed the influence of concentrated and uniformly distributed load with varying pile number on maximum and differential settlement, maximum moment and load portion carried by the pile group and raft (figure 2.23). The maximum settlement for small number of pile is larger for concentrated loading than that of uniformly distributed loading. For large number of pile, the loading type has no effect on settlement. The settlement pattern is identical in both cases. The loading type also has almost no effect on the load portion carried by the pile group as shown in the figure, although, it influences the load distributions among the piles.

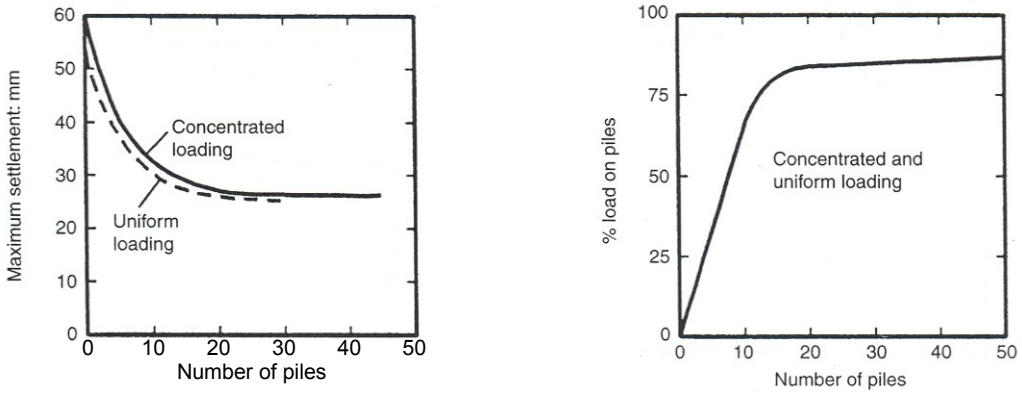

Figure 2.23 Effect of load type and number of piles on load settlement of piled raft foundation (total applied load 2 MN)

2.6 Summary

This chapter reviewed the literature on pile raft, available in English literature. The advantage, disadvantage and the limitations of each method has been described. In a nutshell, the so far developed analytical methods are incapable of capturing the pile raft behavior, because they are elastic in nature (based on Mindlin's and Boussinesq's equations for load settlement behavior) and based on the relative movement between two circular cap pile unit that neglects the simultaneous effects of surrounding units. At the same time, it avoids the cap peripheral stress (shear, flexural, punching) and twisting moment contribution to resist the settlement. The plate on spring, 2-D FE analysis and the hybrid approaches are incapable of analyzing the torsional behaviour and the material variations in the third axis. Therefore, only 3-D FEM is the most effective tools to simulate the complex behaviour of this type of foundation. The same conclusion was drawn by Katzenbach, Arslan, Reul, Randolph, Poulos and other modern researchers.

A number of 3-D numerical models has been developed and studied to offset the limitations of these models, but no attempt is found to develop an analytical model on the basis of these numerical models. Moreover, these analytical models were reported only for assessing the total settlement behaviour, but the prediction of the differential settlement behaviour and utilization of ultimate bearing capacity is yet to be done. In fact, to predict the total or differential settlement, the accurate prediction of full pile resistance of each individual pile in the group is vital. This work was intended to perform this investigation and thereby to develop the analytical model for the maximum and differential settlement. The analytical model for load sharing was intended to develop in

order to predict the load, transmitted by the raft directly to the soil. To develop the aforementioned models extensive parametric studies were required to be done. All these studies were performed on the basis of the 3-D numerical models, developed in 3-D finite element code ABAQUS. The following studies were made during the process of developing the analytical model for the load sharing, maximum and differential settlement.

01. To develop the numerical model.

a) Influence of the shape of the pile (Square, Octagonal, circle) on FEM calculation

b) Extent of stress influence zone along the three axes.

c) Influences of step time increments and stress applications

d) Influence of finite element number on the output

e) Sensitivity analysis / mesh refinement

02. To develop analytical model for load sharing, maximum and total settlement.

a) Influences of raft stiffness on bearing behavior

b) Influences of raft sizes on the settlement profile

c) Influences of Pile spacing of the pile group

d) Influences of pile length on the bearing behavior

e) Influences of pile diameter on the settlement behavior

f) Influence of internal frictional angle on settlement

g) Influence of soil cohesion on the settlement behavior.

03. To develop optimistic design strategy

a) The studies mentioned in step 02 above are sufficient to develop an optimistic design strategy for this purpose.

Chapter 3

Numerical Model

3.1 Introduction

The complex piled raft behaviour simulation in analytical method is tedious because the problem is three dimensional in nature and the complexity involved in the interaction process among its various components. The literature review in the previous chapter explains that only the three dimensional finite element analyses could be the versatile tool to analyze the complex behaviour of this type of foundation

In this chapter, the development of the three dimensional numerical model and its validation was depicted in the first part. The developed numerical model was then used to study the influences of various foundation parameters on its bearing behavior.

3.2 Numerical Modeling

The steps involved in developing the numerical model can be depicted by the flow chart below (figure 3.1). The appropriate elasto-plastic constitutive law for the soil continuum, the geometric modeling of the contact zone and other parts along with the numerical step by step simulation, are the major parts of the numerical model. The subsequent sections describe the steps involved in developing the model in ABAQUS environment.

On the basis of online resource study for a suitable 3-D finite element code for pile raft foundation, ABAQUS is deemed to be appropriate for this work. The available 3D FE codes for this type of foundation are: PLAXIS 3D foundation, version-2, developed by

PLAXIS VB, Netherland (http://www.plaxis.nl); FLAC 3D, version 4, developed by ITASCA (http://www.itascacg.com) and ABAQUS developed by ABAQUS Inc, now belongs to Simulia Inc, headquartered in USA (http://www.simulia.com)

The PLAXIS 3D code is completely new and no research was found to use this for the 3-D analysis of piled raft foundation. FLAC-3D is a finite-difference program which has mathematical limitations in computations (Poulus 1994). ABAQUS, on the other hand, is used by the recent researchers of this field (Garcia 2006, Reul 2006). Concordia University has the privileges of using 20 licences of the academic version which has a node limitation of 100,000 along with other limitations. The available academic version in Concordia University is sufficient for this work.

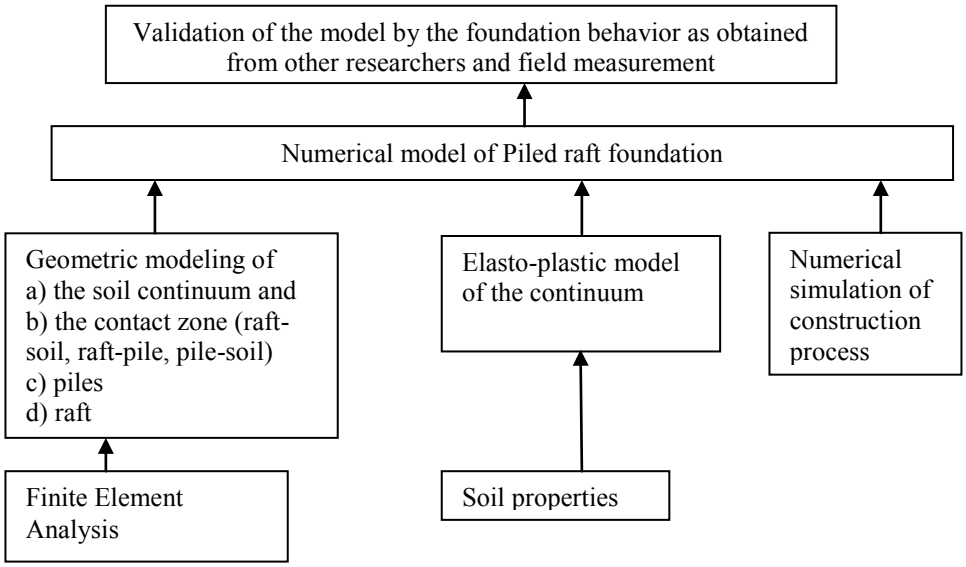

Figure 3.1 Steps in numerical model development

3.2.1 Elasto-Plastic Model of the Continuum (Material Modeling)

The available theory for elasticity was developed and established on the basis of homogenous and isotropic behaviour of construction material (e.g. metal like steel, iron, rubber etc.). The strong ionic bond in between the particles holds the elastic property within the elastic limit. Soil, on the other hand, is an anisotropic, non-homogenous, three-phase material, where a little (cohesive soil) or no (granular) bonding force in between the particles exists. Therefore, the behaviour of soil mass, which is a combination of a number of discrete particles, cannot be modeled by the pure elastic theory. Hence, the researcher's represent the soil stress-strain constitutive behaviour by means of elasto-plastic, visco-plastic or some visco-hypo-plastic models, which are the combination of the elastic, plastic and or viscous theory, obtained from mechanics of material.

Soil is a three phase medium, consists of solid, water and air. In absence of suitable theory to convert this three phase medium into a single phase, it is considered as a single phase isotropic medium. The modified Drucker-Prager/Cap model is used as the constitutive model for the modeling of soil continuum for this work. Since, the investigations would be three dimensional in nature and the Cap constitutive model contains both elastic and plastic behaviour, it is essential to extend the one dimensional Hook's law in to three dimensional coordinate and express all the three dimensional stress components of normal (σ) and shear (τ) stress into matrix form, in order to facilitate analysis and explain the cap constitutive model.

3-D Stresses in Soil Mass

The stresses in soil mass are expressed by the normal (σ) and shear (τ) stress. The stress state at a point within a soil mass can be represented by an infinitesimal (very small) cube with three stress components on each of its six sides (one normal and two shear components), as shown in Figure 3.2

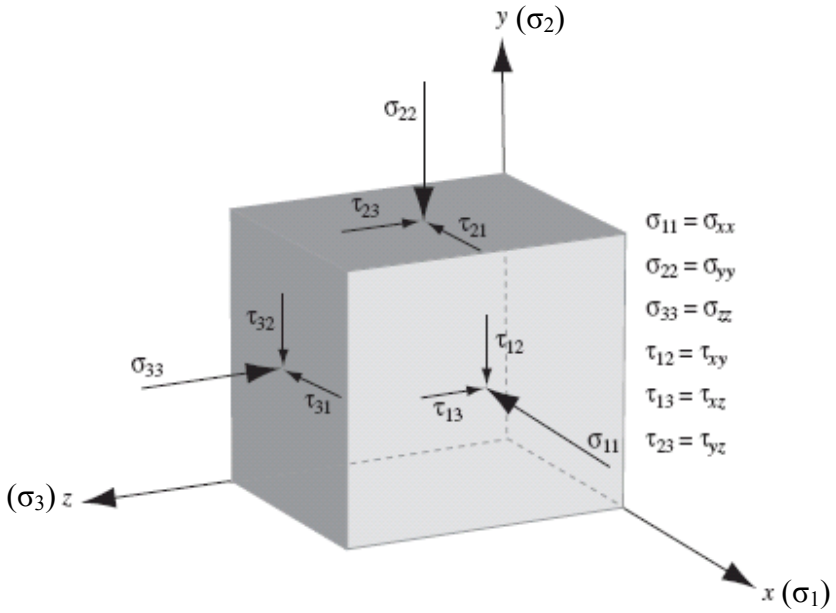

Figure 3.2 Stress on a soil particle in three dimensional space

These stress components can be organized into the "stress matrix" as shown below.

$$\begin{pmatrix} \sigma_{11} & \tau_{12} & \tau_{13} \\ \tau_{21} & \sigma_{22} & \tau_{23} \\ \tau_{31} & \tau_{32} & \sigma_{33} \end{pmatrix} \qquad (3.1)$$

This arrangement of the nine stress components is also known as "stress tensor". To satisfy the static equilibrium (moment equilibrium), the shear component across the diagonal are identical (i.e., $\tau_{12} = \tau_{21}$, $\tau_{13} = \tau_{31}$ and $\tau_{23} = \tau_{32}$).

Elasticity

The universal Hook's law is valid for isotropic, linear, elastic material, while, soil is an anisotropic, nonlinear, inelastic material. Therefore, to apply Hook's law to estimate stress and strain, necessary idealization to the soil mass is required. As a part of this work, the one dimensional Hook's law for isotropic linear elastic medium is extended into three dimensional perspectives in the following paragraph.

The simplest stress-strain relationship of Hook's law ($\sigma = E\varepsilon$) for one dimensional linear elastic isotropic material can be applied to the three dimensional stress condition of the infinitesimal soil element of figure 3.2 above by introducing Poisson's ratio (ν) as below

By definition, Poisson's Ratio, $\nu = \dfrac{Lateral\ Strain}{Axial\ (Longitudinal)\ Strain} = -\dfrac{\varepsilon_{22}}{\varepsilon_{11}} = -\dfrac{\varepsilon_{33}}{\varepsilon_{11}}$ (3.2)

Since the soil is considered isotropic, therefore the Young's modulus of elasticity (E), the Poisson's ratio (ν), the shear modulus of elasticity (G) are the same in all directions i.e. orientation independent. Therefore, the longitudinal stress (σ_{11}) causes the longitudinal strain (ε_{11}) in σ_{11} direction and associated lateral strains at the same time of same amount (due to material isotropy) in other two directions (σ_{22} and σ_{33}). From the above equation these lateral strains can be expressed as

$$\varepsilon_{22} = \varepsilon_{33} = -\nu\varepsilon_{11} = -\nu\sigma_{11}/E \qquad (3.3)$$

Combining the strains in each direction, to get the total in that direction, the following equations result.

Strain (ε_{11}) in σ_{11} direction, $\varepsilon_{11} = \frac{1}{E}\left(\sigma_{11} - \nu\sigma_{22} - \nu\sigma_{33}\right)$ (3.4)

Strain (ε_{22}) in σ_{22} direction, $\varepsilon_{22} = \frac{1}{E}\left(\sigma_{22} - \nu\sigma_{33} - \nu\sigma_{11}\right)$ (3.5)

Strain (ε_{33}) in σ_{33} direction, $\varepsilon_{33} = \frac{1}{E}\left(\sigma_{33} - \nu\sigma_{11} - \nu\sigma_{22}\right)$ (3.6)

Now from the definition of Bulk modulus of elasticity

$$\textit{Shear Strain}, \quad \gamma_{12} = 2\varepsilon_{12} = \frac{\tau_{12}}{G} = \frac{2(1+\nu)}{E}\tau_{12}$$
$$or, \quad \varepsilon_{12} = \frac{(1+\nu)}{E}\tau_{12} \tag{3.7}$$

$$\textit{Similarly}, \quad \gamma_{23} = 2\varepsilon_{23} = \frac{\tau_{23}}{G} = \frac{2(1+\nu)}{E}\tau_{23}$$
$$or, \quad \varepsilon_{23} = \frac{(1+\nu)}{E}\tau_{23} \tag{3.8}$$

$$and \quad \gamma_{31} = 2\varepsilon_{31} = \frac{\tau_{31}}{G} = \frac{2(1+\nu)}{E}\tau_{31}$$
$$or, \quad \varepsilon_{31} = \frac{(1+\nu)}{E}\tau_{31} \tag{3.9}$$

Therefore, the total three dimensional strain can be represented in matrix form as below

$$\begin{pmatrix} \varepsilon_{11} \\ \varepsilon_{22} \\ \varepsilon_{33} \\ \varepsilon_{12} \\ \varepsilon_{13} \\ \varepsilon_{23} \end{pmatrix} = \begin{bmatrix} 1/E & -\nu/E & -\nu/E & 0 & 0 & 0 \\ -\nu/E & 1/E & -\nu/E & 0 & 0 & 0 \\ -\nu/E & -\nu/E & 1/E & 0 & 0 & 0 \\ 0 & 0 & 0 & 1/2G & 0 & 0 \\ 0 & 0 & 0 & 0 & 1/2G & 0 \\ 0 & 0 & 0 & 0 & 0 & 1/2G \end{bmatrix} \begin{pmatrix} \sigma_{11} \\ \sigma_{22} \\ \sigma_{33} \\ \tau_{12} \\ \tau_{13} \\ \tau_{23} \end{pmatrix} \tag{3.10}$$

Now, equating G = E/2(1+ν) in the above equation and inverting, the three dimensional stresses on the element can be determined as

$$\begin{pmatrix}\sigma_{11}\\ \sigma_{22}\\ \sigma_{33}\\ \tau_{12}\\ \tau_{13}\\ \tau_{23}\end{pmatrix} = \frac{E}{(1+\nu)(1-2\nu)}\begin{bmatrix}1-\nu & \nu & \nu & 0 & 0 & 0\\ \nu & 1-\nu & \nu & 0 & 0 & 0\\ \nu & \nu & 1-\nu & 0 & 0 & 0\\ 0 & 0 & 0 & 1-2\nu & 0 & 0\\ 0 & 0 & 0 & 0 & 1-2\nu & 0\\ 0 & 0 & 0 & 0 & 0 & 1-2\nu\end{bmatrix}\begin{pmatrix}\varepsilon_{11}\\ \varepsilon_{22}\\ \varepsilon_{33}\\ \varepsilon_{12}\\ \varepsilon_{13}\\ \varepsilon_{23}\end{pmatrix} \quad (3.11)$$

These generalized Hooke's law expression for three dimensional stress and strain condition of an element can be applied to determine the one dimensional (uniaxial) stress and strain as well as the plane strain (two-dimensional) and plane stress (two-dimensional) by means of putting the non relevant parameters to zero.

Plasticity

The plasticity of a material is characterized by its irreversible strain property, which is due to the permanent dislocation of the particles. Soil, in fact, is a granular material; therefore, the plastic behaviour is more dominant than the elastic behaviour. The Hook's law is unique to explain the constitutive relationship within elastic limit, however, for plasticity; no such unique constitutive model is available. Plasticity theory was originally developed to simulate the metal behaviour and now, similar models are available to calculate the irreversible strains in concrete, soils and polymers.

Among the various available plastic models, the Modified Drucker–Prager/Cap Model, Modified Cam Clay Model and Lade's Single Hardening Model are frequently used by the Geotechnical researchers in order to decompose strains into elastic and plastic regimes. The main limitation of modified Cam clay model is that its formulations are based on the triaxial stress condition, in which the intermediate and the minor principal

stresses are equal ($\sigma_2 = \sigma_3$). Similarly, the Lade's Single Hardening Model has the limitations of involving 11 parameters, those can be determined from three consolidated drained (CD) triaxial compression tests and one isotropic compression test along with additional assumptions on plastic strain rate vectors. More limitations of these models are summarized in Gens and Potts (1988) as well as in Yu H S (1995, 1998)

An ideal plasticity model should include (1) a yield criterion that predicts material behavior whether it is elastic or plastic, (2) a strain hardening rule that controls the shape of the stress–strain response during plastic straining, and (3) a plastic flow rule that determines the direction of the plastic strain increment caused by a stress increment. The Modified Drucker-Prager/Cap Model has a clear yield criterion to distinguish the elastic and plastic behavior with its work hardening and flow rule predicting capability. The Cap model is appropriate to soil behavior, because it is capable of considering the effect of stress history, stress path, dilatancy, and the effect of the intermediate principal stress.

The Drucker-Prager model and its subsequent modifications are expressed in terms of invariants of deviator stress, which is particularly useful for problems involving three-dimensional stress conditions and plane strain condition; those are common in geotechnical engineering. A brief summary of stress and strain invariants that is used frequently in this thesis are presented here, which will facilitate the reader to perceive the model conveniently.

a) Stress Invariants

The stress invariants of the stress tensor or stress matrix of equation 3.1 above can be expressed in terms of its first (I_1), second (I_2) and third (I_3) stress invariant as

$$I_1 = \sigma_{11} + \sigma_{22} + \sigma_{33} \tag{3.12}$$

$$I_2 = \begin{vmatrix} \sigma_{11} & \tau_{12} \\ \tau_{21} & \sigma_{22} \end{vmatrix} + \begin{vmatrix} \sigma_{22} & \tau_{23} \\ \tau_{32} & \sigma_{33} \end{vmatrix} + \begin{vmatrix} \sigma_{11} & \tau_{13} \\ \tau_{31} & \sigma_{33} \end{vmatrix} \tag{3.13}$$

$$I_3 = \begin{vmatrix} \sigma_{11} & \tau_{12} & \tau_{13} \\ \tau_{21} & \sigma_{22} & \tau_{23} \\ \tau_{31} & \tau_{32} & \sigma_{33} \end{vmatrix} \tag{3.14}$$

Three other invariants, J_1, J_2 and J_3, known as invariants of the stress tensor and related to the aforementioned stress invariants as

$$J_1 = I_1 = \sigma_{11} + \sigma_{22} + \sigma_{33} \tag{3.15}$$

$$J_2 = \frac{1}{2} I_1^{\,2} - I_2 \tag{3.16}$$

$$J_3 = \frac{1}{3} I_1^{\,3} - I_1 I_2 - I_3 \tag{3.17}$$

b) Stress Decomposition

To estimate the effect caused by the deviator stress and hydrostatic stress, the stress matrix of equation 3.1 can be decomposed into a deviator stress matrix and a hydrostatic stress matrix as shown below. This decomposition is convenient for soil modeling as most of them assume that the distortion of soil is caused by deviator stresses and that the soil volume change is caused by hydrostatic stresses.

$$\underset{Stress\,Matrix}{\begin{pmatrix}\sigma_{11} & \tau_{12} & \tau_{13}\\ \tau_{21} & \sigma_{22} & \tau_{23}\\ \tau_{31} & \tau_{32} & \sigma_{33}\end{pmatrix}}=\underset{Deviator\,Stress\,Matrix}{\begin{pmatrix}S_{11} & \tau_{12} & \tau_{13}\\ \tau_{21} & S_{22} & \tau_{23}\\ \tau_{31} & \tau_{32} & S_{33}\end{pmatrix}}+\underset{Hydrostatic\,Stress\,Matrix}{\begin{pmatrix}p & 0 & 0\\ 0 & p & 0\\ 0 & 0 & p\end{pmatrix}} \tag{3.18}$$

Therefore, $$\underset{Deviator\,Stress\,Matrix}{\begin{pmatrix}S_{11} & \tau_{12} & \tau_{13}\\ \tau_{21} & S_{22} & \tau_{23}\\ \tau_{31} & \tau_{32} & S_{33}\end{pmatrix}}=\underset{Stress\,Matrix}{\begin{pmatrix}\sigma_{11} & \tau_{12} & \tau_{13}\\ \tau_{21} & \sigma_{22} & \tau_{23}\\ \tau_{31} & \tau_{32} & \sigma_{33}\end{pmatrix}}-\underset{Hydrostatic\,Stress\,Matrix}{\begin{pmatrix}p & 0 & 0\\ 0 & p & 0\\ 0 & 0 & p\end{pmatrix}} \tag{3.19}$$

or, $$\begin{pmatrix}S_{11} & \tau_{12} & \tau_{13}\\ \tau_{21} & S_{22} & \tau_{23}\\ \tau_{31} & \tau_{32} & S_{33}\end{pmatrix}=\begin{pmatrix}\sigma_{11}-p & \tau_{12} & \tau_{13}\\ \tau_{21} & \sigma_{22}-p & \tau_{23}\\ \tau_{31} & \tau_{32} & \sigma_{33}-p\end{pmatrix} \tag{3.20}$$

Thus the invariants of the deviator stress can be determined from this deviator stress matrix, which are very useful for three dimensional elasto-plastic modeling of any type. The stress invariants and stress invariant tensor are notated here as I_{1D}, I_{2D}, I_{3D} and J_{1D}, J_{2D}, J_{3D} respectively and can be expressed as

$$J_{1D}=I_{1D}=S_{11}+S_{22}+S_{33}=(\sigma_{11}-p)+(\sigma_{22}-p)+(\sigma_{33}-p)=0 \tag{3.21}$$

$$where,\ mean\ stress,\ p=\frac{\sigma_{11}+\sigma_{22}+\sigma_{33}}{3}=\frac{J_1}{3}$$

$$\begin{aligned} similarly,\quad J_{2D} &= J_2-\frac{J_1^{\,2}}{6}\\ &=\left(\frac{1}{2}I_{1D}^{\,2}-I_{2D}\right)-\frac{J_1^{\,2}}{6}=\frac{J_1^{\,2}}{3}-I_{2D}\\ &=\frac{1}{6}\left[(\sigma_{11}-\sigma_{22})^2+(\sigma_{22}-\sigma_{33})^2+(\sigma_{33}-\sigma_{11})^2\right]+\tau_{12}^{\,2}+\tau_{23}^{\,2}+\tau_{31}^{\,2}\end{aligned} \tag{3.22}$$

and $J_{3D} = J_3 - \frac{2}{3} J_1 J_2 + \frac{2}{27} J_1^3$ (3.23)

Physically, J_1 (= I_1) indicates the effect of mean stress, J_2 represents the magnitude of shear stress and J_3 determines the direction of shear stress. These three parameters are frequently used to describe the soil elasto-plasticity.

Drucker and Prager (1952) are the pioneers to introduce a yield surface that takes into account the effect of water in the soil mass and thereby introduced the elasto-plastic model in the geotechnical engineering. This yield surface was developed on the basis of the generalized Mohr-Coulomb hypothesis. Drucker et al. (1957) extended this theory by introducing a work hardening plastic spherical cap with the yield surface in order to offset the limitation of overestimating the plastic dilatancy of the previously developed yield surface. The previous basic fundamental theory of soil mechanics developed by Mohr-Coulomb, Karl Terzaghi, Gorge Meyerhof, Brinch Hansen, Rankin and others are essentially based on the assumption that soil is perfectly plastic (Drucker et al. 1957)

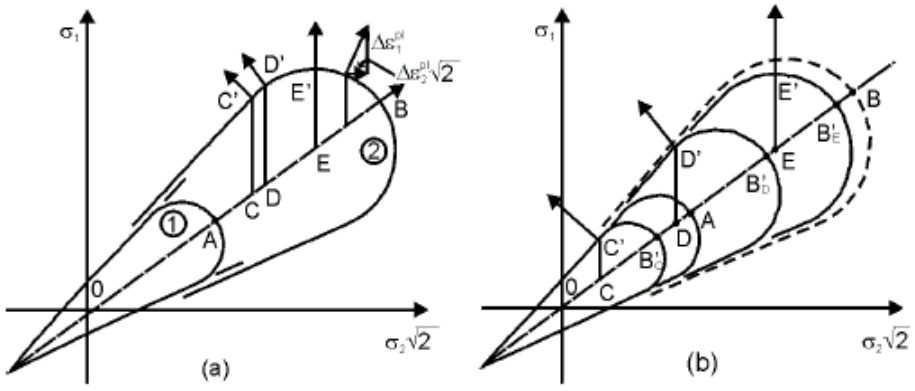

Figure 3.3 Modified Cap Model proposed by Drucker et al.(1957)

The shape of the spherical cap was replaced by an elliptical cap as proposed by DiMaggio and Sandler (1971), where the authors summarized a number of researches done on the cap shape to make the model more representative to the measured behavior. This shape standardization investigation is still in progress. They also modified the Drucker-Prager linear yield surface to a nonlinear yield surface in order to accommodate the effect at high pressure level at which a soil passes to a fluid state (figure 3.4).

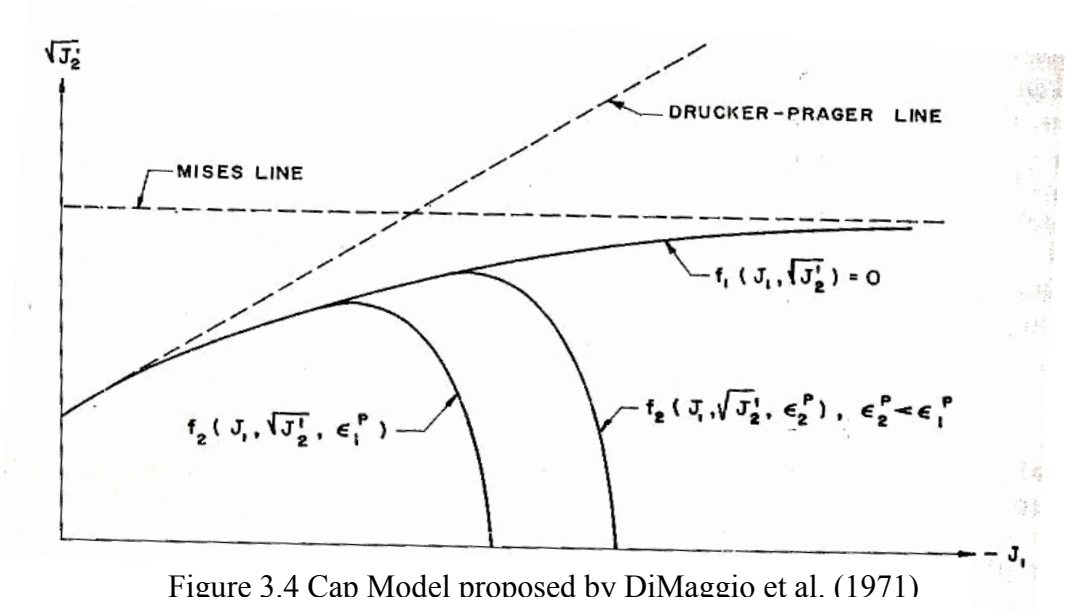

Figure 3.4 Cap Model proposed by DiMaggio et al. (1971)

It can be commented on DiMaggio-Sandler yield surface that the friction angle of the soil decreases with increasing hydrostatic stress. Moreover, a horizontal tangent parallel to J_1 axis could be decisive for the smooth transition from nonlinear yield surface to the elliptical cap surface.

Sandler, DiMaggio and Baladi (1976) generalized the above model, outlined the procedure for fitting the cap and extended its applicability for ground shock calculation,

while, Sandler and Rubin (1979) published the FORTRAN source code for the model. The effective stress versions of the cap model are found in Baladi and Rohani (1979a and 1979b) for saturated soil. Bethe et al. (1980) proposed only a plane cap to couple with the yield surface of Drucker-Prager while Resende et al. (1985) proposed a hyperbolic cap to couple with the Drucker-Prager yield surface. However, the full coupling mechanism between the yield surface and the plastic dilatancy controlled cap remain unavailable in the model so far developed.

To simulate the elasto-plastic behavior of soil, the Drucker-Prager yield surface is coupled with the elliptical dilatancy controlled cap of DiMaggio et al. (1971) in this thesis. To offset the limitation of coupling between these two surfaces and thereby to make a smooth transition from the yield surface to the elliptical cap surface, a transition surface is introduced to fit the modified Drucker-Prager model in ABAQUS environment. Figure 3.5 below describes this modified Drucker-Prager model in *p-t* plane and its three yield surfaces are defined subsequently.

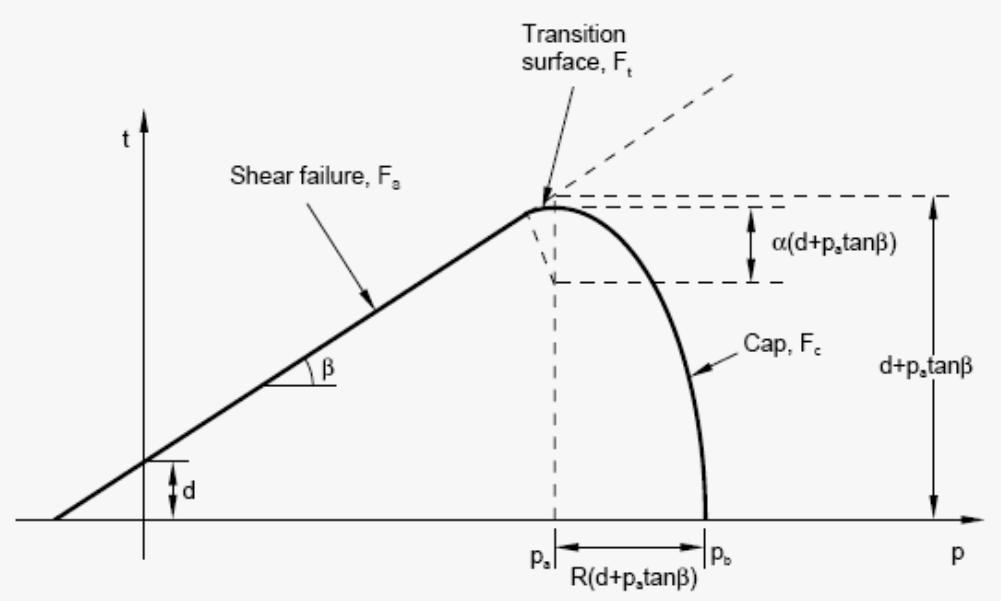

Figure 3.5 Modified Drucker-Prager/Cap model yield surfaces in the *p-t* plane

The Drucker-Prager Yield or Shear Failure Surface

The Drucker-Prage yield surface is a pressure dependent shear failure surface (F_s), which is a perfectly plastic yield surface (no hardening). Changes of stress inside the yield surfaces cause elastic deformations, while changes of stress on the yield surfaces cause plastic deformations. The elastic behavior is modeled as the generalized Hook's law explained in the previous section and the Drucker-Prager shear failure or yield surface is expressed as

$$F_s = t - p\tan\beta - d = 0 \tag{3.24}$$

where,

p = equivalent pressure/normal stress = $(\sigma_1 + \sigma_2 + \sigma_3)/3$

t = the deviatoric stress, $t = \frac{q}{2}\left[1 + \frac{1}{K} - \left(1 - \frac{1}{K}\right)\left(\frac{r}{q}\right)^3\right]$ (3.25)

where, q = Von Mises equivalent stress for triaxial compression that gives the failure combination of three principal stress and defined as

$$q = \sqrt{\frac{1}{2}[(\sigma_1 - \sigma_2)^2 + (\sigma_2 - \sigma_3)^2 + (\sigma_3 - \sigma_1)^2]} \tag{3.26}$$

K = Shape parameter of yield surface F_s $\quad (0.778 \leq K \leq 1)$

$= q_E / q_K$

$= \frac{3 - \sin\phi'}{3 + \sin\phi'}$ ABAQUS Analysis Manual, page 18.3.1.22] (3.27)

Where, q_E and q_k are the yield stress in tri-axial tension and yield stress in tri-axial compression respectively. For $q_E = q_K = K = 1$, no third stress invariant effects are taken into account. In such a case, the deviator stress, t is equal to the Mises equivalent stress, q (equation 3.25 above), and the yield surface has a von Mises (circular) section in the deviator stress plane as shown in figure 3.6

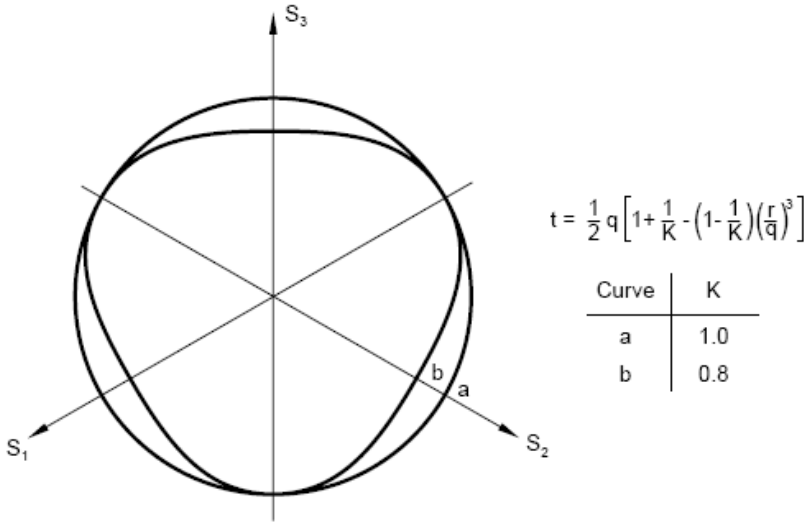

Figure 3.6 Typical yield/flow surface in the deviatoric plane

.

r = Third invariant of deviator stress

$$r = \left(\frac{9}{2} S.S : S\right)^{\frac{1}{3}} \quad \text{where, stress deviator, } S = \sigma + pI$$

$$r = \left(\frac{27}{2} J_{3D}\right)^{\frac{1}{3}} = \left(\frac{27}{2} J_3 - 9J_1J_2 + J_1^3\right)^{\frac{1}{3}} \tag{3.28}$$

β = Material (Soil) angle of friction in p-t plane and its relation with Mohr-Coulomb frictional angle (φ) is, $\tan\beta = \dfrac{6\sin\varphi'}{3-\sin\varphi'}$ (3.29)

d = Material (Soil) cohesion in p-t plane and its relation with Mohr-Coulomb cohesion (c) is, $d = (1-\dfrac{1}{3}\tan\beta)\dfrac{\cos\phi'}{1-\sin\phi'} * 2c'$ (3.30)

The Elliptical Cap Yield Surface

The elliptical cap yield surface, with an eccentricity of R (constant for a material and also known as material parameter) in the p-t plane is given as

$$F_c = \sqrt{(p - p_a)^2 + \left(\frac{Rt}{1 + \alpha - \alpha / \cos\beta}\right)^2} - R(d + p_a \tan\beta) = 0 \tag{3.31}$$

where, p_a is an evolution parameter that controls the hardening–softening behavior as a function of the volumetric plastic strain and can be calculated as

$$p_a = \frac{p_b - Rd}{1 + R\tan\beta} \tag{3.32}$$

The hardening–softening behavior is simply described by a piecewise linear function relating the mean effective (yield) stress and the volumetric plastic strain $p_b = p_b\left(\varepsilon_{vol}^{pl}\right)$ as shown in Figure 3.7. This function can be obtained from the results of one isotropic consolidation test with several unloading–reloading cycles.

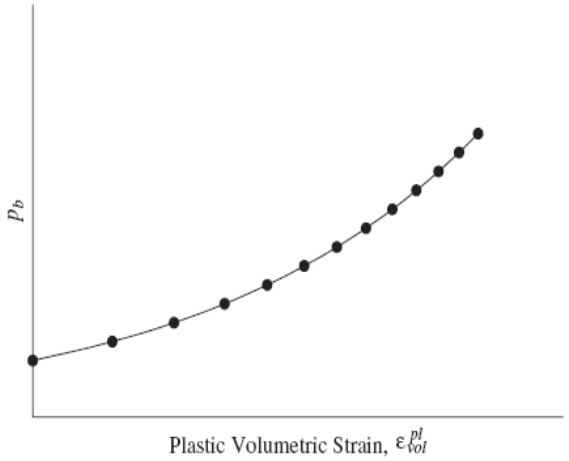

Figure 3.7 Typical cap hardening behavior

Parameter α is a small number (typically, 0.01 to 0.05) and is used to define a smooth transition surface between the Drucker-Prager shear failure surface and the elliptical cap surface. Obviously, for a value of α = 0 indicates no transition zone is allowed in between the shear failure and cap surface.

This elliptical cap intersects the mean effective stress (p) axis at right angle. The movement of the cap is controlled by the increase or decrease of the plastic volumetric strain. Plastic volumetric compaction of the material (when yielding on the cap) causes hardening, while volumetric plastic dilation (when yielding on the shear failure surface) causes softening.

The Transition Yield Surface

The coupling between the Drucker-Prager yield surface and the elliptical cap is made by a smooth transition curve surface which is defined as

$$F_t = \sqrt{(p - p_a)^2 + \left[1 - \left(1 - \frac{\alpha}{\cos\beta}\right)(d + p_a \tan\beta)\right]^2} - \alpha(d + p_a \tan\beta) = 0 \qquad (3.33)$$

3.2.2 Selection of Finite Element

The available elements for three dimensional analyses are the hexahedral, tetrahedral and the wedge as shown in figure 3.12 below. For a same volume of continuum, hexahedral with its eight nodes rather than four nodal tetrahedral or six nodal wedges would be more accurate and involve least computing costs.

This is because, to generate a hexahedral element, a minimum of five tetrahedral elements (figure 3.8a) or two elements of wedge (figure 3.8b) are required. Consequently, for first order elements, the number of nodes increased to 12 for wedge elements and 20 for tetrahedral which is 1.5 and 2.5 times to that of 8 nodded hexahedral brick element. For higher order element the number of nodes increases exponentially. Since the computational cost is directly related to the number of nodes, 8 nodded first order brick element is therefore a realistic consideration.

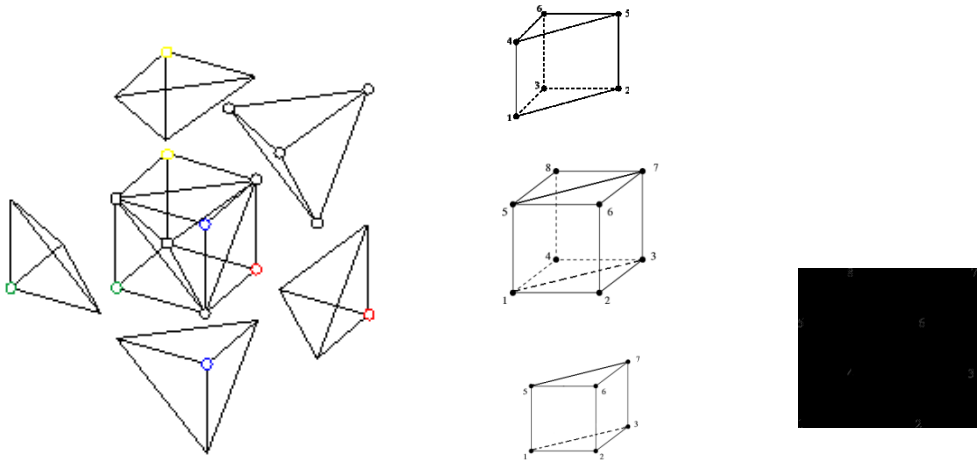

a) Tetrahedron b) Wedge c) Hexahedron

Figure 3.8 Geometry of 3-D finite elements

Apart from the computational cost, the hexahedral element is more accurate than the other two. This is because the increased number of elements in wedge or tetrahedral for the same volume of continuum results in increased number of discretization error, because these elements cannot assume all the displacement fields, handled by the hexahedral element. Besides accuracy, meshes comprised of hexahedrons are easier to

visualize than meshes comprised of tetrahedrons or wedges. In addition, the reaction of hexahedral elements to the applied loads, more precisely corresponds to loads under real world conditions [Hibbit et al. 2007]. The eight-node hexahedral elements are, therefore, superior to other elements as it provides fast, less expensive and more accurate formulation for finite element analysis, which is more precise to the real world.

The soil continuum and raft has consistent shape to accommodate this hexahedral element, but for the widely constructed circular shape pile, discretization can be easier with the tetrahedral and wedge shaped element. However, a study can be performed to investigate the influence of various pile shapes (circular, octagonal and rectangular) on the pile raft bearing behavior.

3.2.3 Net Discretization

The discretization of the soil, raft and pile into finite element influence directly the simulated output of the modeled piled raft behavior. Generally, the finer the element the more accurate would be the result. Conversely, the increased number of finite element contributes to the increased number of nodes, which in turn, increase the computational process of the program. The available teaching version of ABAQUS 6.9-1 for this research work has a node limitation of 100,000 nodes for the whole model. To be limited within this restriction, it is essential to study the influence of discretization technique.

The ABAQUS has the facility to perform the analysis by using the axisymmetric boundary condition. Therefore, only one quarter of the whole model is sufficient to simulate and thus to mesh. Since, the continuum elements in the vicinity of raft and piles are the major concern, the meshing strategy was carefully considered to obtain the finer elements in those regions. Some special partition techniques were used to make a smooth transition of element sizes from the finer to the larger one (figure 3.9). During this process the bias and aspect ratio were kept within the specified limit to run the program successfully. The ABAQUS advantage of notification regarding the bad elements at the beginning of running any job analyses ensures the quality of the elements. Its capability to query, repair, replace and remove the elements provides a strong basis of simulation. Both the graphic interface (ABAQUS cae) and input file on "TXC" text editor were used to create nodes, elements etc. and the global coordinate system was used.

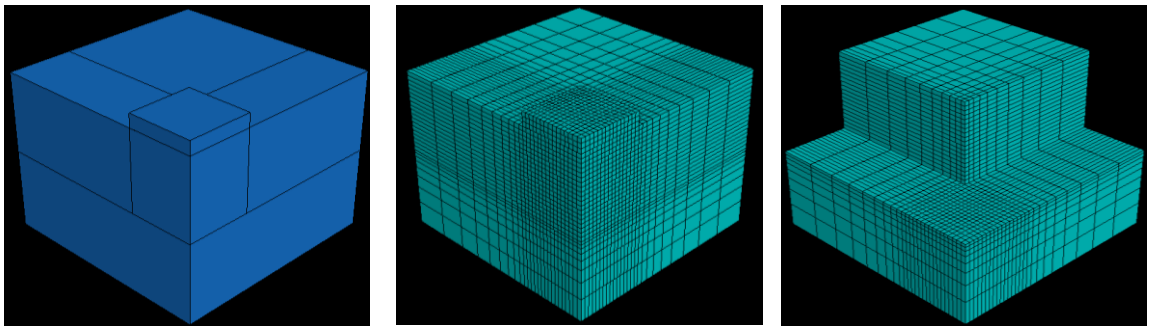

a) Partition b) Mesh c) Inside elements

Figure 3.9 a) Partition, b) Meshing and c) inside elements

3.2.4 Modelling of the Contact Zone

The realistic analysis of soil-structure systems requires considerations of the interaction or coupling between the structural and geologic media (Desai 1987). This interaction is generally handled through the use of contact or interface element for which there is a vast body of literature that encompass the fields of geo-mechanics, engineering mechanics and computational mechanics.

Three contact zones are required to be modeled in piled raft foundation, the pile-soil, the raft-soil and the pile-raft. To model the contact behavior among the soil and pile/raft surface material, it is essential to obtain the friction factor between these materials which is again a function of surface roughness, porosity, adhesion etc. Several procedures and methods are available in literature from which Das (2007) summarized three widely accepted methods (α, β and λ method) based on empirical formulas to calculate the friction factor for clay and pile material. Here only the formula in α method is described below.

According to α method, the friction factor, $f = \alpha c_u$

Where, α = empirical adhesion factor can be estimated from figure 3.10 below.

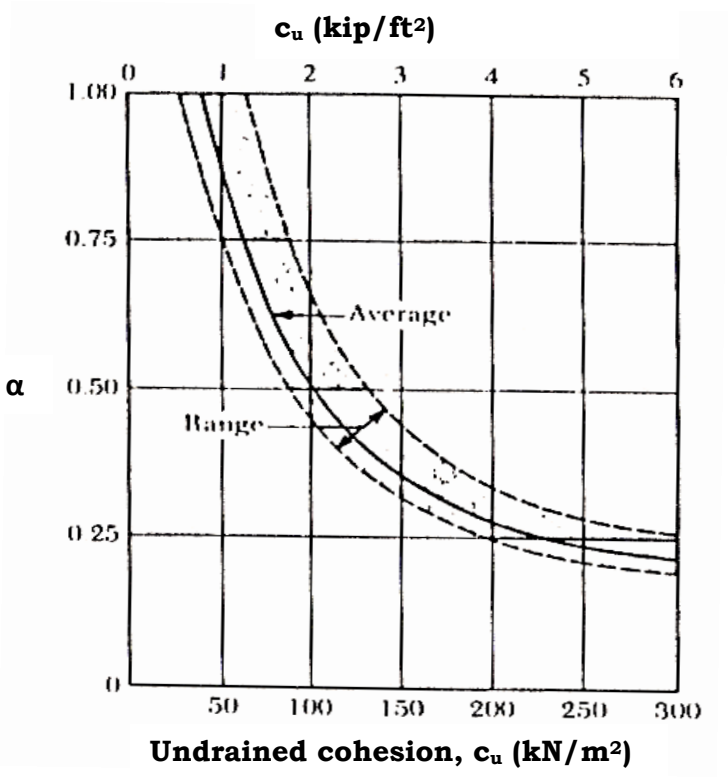

Figure 3.10 Variation of α with undrained cohesion, c_u

Several other semi-empirical equations to estimate α, are available in the literature (e.g., API, 1984; Semple and Ridgen, 1984; Fleming et al., 1985). Budhu (1999) summarized several of these equations to estimate α. The empirical equation by API (1984), as stated below, can be used along with the value from figure 3.10 above.

$$\begin{aligned} \alpha &= 1 - \frac{c_u - 25}{90} \qquad for\ 25\ kPa < c_u < 70\ kPa \\ &= 1.0 \qquad for\ c_u \le 25\ kPa \\ &= 0.5 \qquad for\ c_u \ge 70\ kPa \end{aligned} \tag{3.34}$$

Similarly, for pile in sand, this friction factor can be given as stated in Das (2007)

$$\begin{aligned} f &= K\sigma'_z \tan\delta \qquad for\ z = 0 - L' \qquad where,\ L' = effectove\ length = 15D \\ &= f_{zL'} \qquad for\ z = L'\ to\ L \end{aligned}$$

where, K = effective earth coefficient = 1-sinφ for bored pile

σ'_z = effective vertical stress at depth z

δ = soil pile frictional angle = 0.5φ ~ 0.8φ

Judgment is applied to choose the value of δ and some correlations are available in the literature of Bhusan (1982), Meyerhof (1976) for low and high displacement driven pile. The empirical formula to predict K is also different for driven pile and available in Das (2007). Since piled raft foundation is erected on the bored pile, those formulas are not mentioned here.

A direct shear test can give this friction factor, but the limitation regarding the in-situ concrete surface roughness of the pile and raft should exist there. These limitations can be offset by selecting the friction factor on trial and error basis, until the model behavior becomes consistent with the measured field behavior.

The numerical treatment of contact problems involves the formulation of the geometry, the statement of interface laws, the variational formulation and the development of algorithms (Wriggers 1995). To simulate the interaction or contact behavior, specially, for the soil, pile and raft, the following concepts are available in the literature.

- The use of one dimensional interface element in geotechnical applications are the *p-y*, *t-z* and *Q-z* springs and was first introduced by McClelland et al. (1958) and Reese et al. (1956). These springs are usually so called Winkler spring model Recently, Taciroglu et al. (2005) combines one dimensional frictional, drag and

gap elements with a nonlinear spring element in parallel connection to model gap, stick and slip behavior at the soil pile interface. These elements are empirically based and calibrated to load test data. In piled raft foundation this element is used by Griffith et al. (1991), Clancy et al. (1993), Poulos (1994), Horikoshi et al. (1998) Russo (1998), Kim et al. (2001) and Kitiyodem et al. (2002, 2003, 2005) as detailed in literature review of this dissertation.

- The use of zero thickness interface element was developed by Goodman et al. (1968), which requires the use of high stiffness values to prevent penetration of the contact bodies. Such high stiffness values generally lacks physical meaning (Desai et al. 1984).To improve this aspect and general element performance, modifications have been made by Ghaboussi et al. (1973), and Herman (1978). Two and three dimensional iso-parametric zero thickness elements with improved numerical performance were subsequently developed by Beer (1985), and Gens (1988).
- The use of thin layer interface element was first proposed by Zienkiewicz (1970) and later expanded by Pande et al. (1979), Desai (1981), Desai et al. (1984), and Sharma et al. (1992). For this element, the tangent matrix is developed to account for normal, shear and coupled responses at the interface. The element is found to simulate stick, slip, debonding and rebonding behavior reasonably well. Desai et al. (1988) developed a constitutive model for this type of interface element to capture the cyclic behavior in dynamic soil-structure interaction problems. Boudzid et al. (2004) developed a closed form solution with enhanced computational efficiency for thin layer interface element in axi-symmetric

problems. However, the thin layer interface element does not allow for large slip or large deformation at interface and ignoring the thickness may lead to numerical instabilities.

- The use of the so-called master-slave concept, developed by Wriggers (1995), includes the numerical formulation of the contact geometries and the interface constitutive laws for both the normal and tangential stress components in the contact area. Different variational formulations can be applied to treat the variational inequalities due to contact along with the algorithm. This concept is widely used now due to its response closest to the measured behavior and it is capable of simulating large deformations

The widely accepted master-slave concept has been used in this work, where the pile and raft has been treated as master surface and soil surface as slave surface. To choose between the 'node to surface contact' and 'surface to surface' contact option, the surface to surface contact is more accurate, as shown by Hibbitt et al. (2007) in figure 3.11. This surface to surface discretization technique has been used in this work. Again to define the mechanical tangential behavior, the penalty type frictional constraint enforcement method rather than Lagrange method is justified in order to formulate the stiffness (penetration in other words) of the contact surfaces. Lagrange method requires the multiplier that increases the computational cost of the analysis by adding more degrees of freedom to the model and often by increasing the number of iterations required to obtain a converged solution. The Lagrange multiplier formulation may even prevent convergence of the solution (Hibbitt 2007),

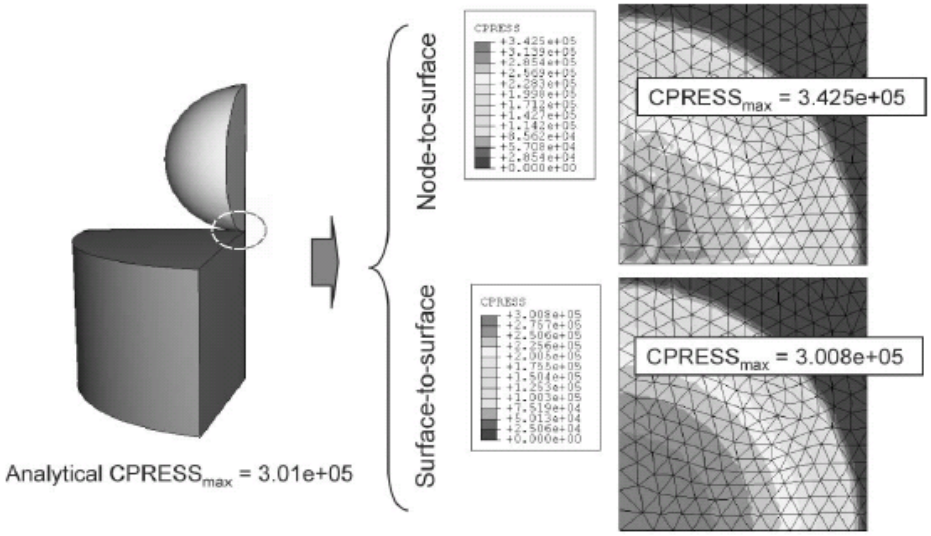

Figure 3.11 Comparison of contact pressure accuracy for node to surface and surface to surface contact discretizations.

3.2.5 Geometric Modeling of the Continuum

The soil is considered as an isotropic homogenous single phase medium. To limit the computation cost of the numerical simulation, it is essential to set the suitable boundary extent and the boundary condition of the selected continuum. Figures 3.12a), 3.12b) and 3.12c) below depict the boundary conditions used in this work to idealize the numerical simulation. In all cases no x, y or z translations at the bottom nodes were allowed.

Figure 3.12a) is the full scale (simulation of the whole) soil block under consideration, while figure 3.12b) is for the case, where the ABAQUS advantage of analyzing the quarter symmetry of the whole, was taken into account. Because of the symmetry, one fourth of the model was simulated, setting the boundary condition along the mid axis as

XSIMM (symmetry about plane x = constant) and YSIMM (symmetry about plane y = constant) as shown in figure 3.12b). No x-translation is allowed in yz plane and no y-translation is allowed on xz plane. Similarly, in figure 3.12b), the rotational degree of freedom Rx and Rz in xz plane are not allowed and the same for Ry and Rz in yz plane. Besides the translational degree of freedom in x,y and z direction, the rotational degree of freedom were notated as Rx, Ry and Rz in these figures. Figure 3.12c) represents the boundary conditions applied for the 2D-axisymmetric analysis used in this research.

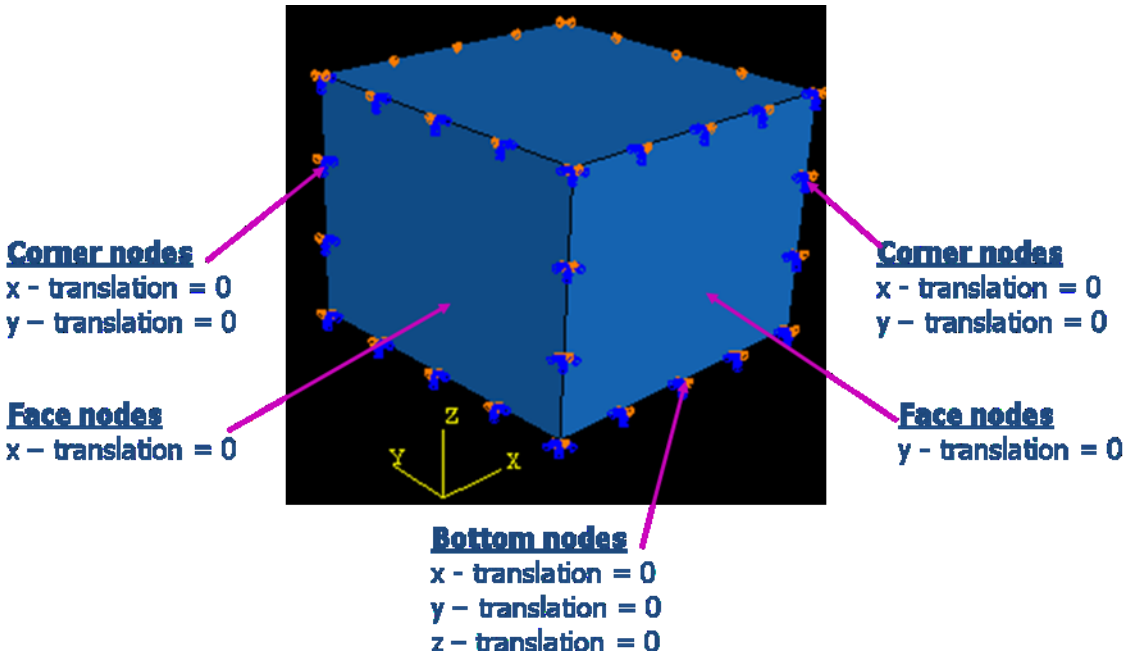

Figure 3.12 a) Boundary condition of a 3-D model.

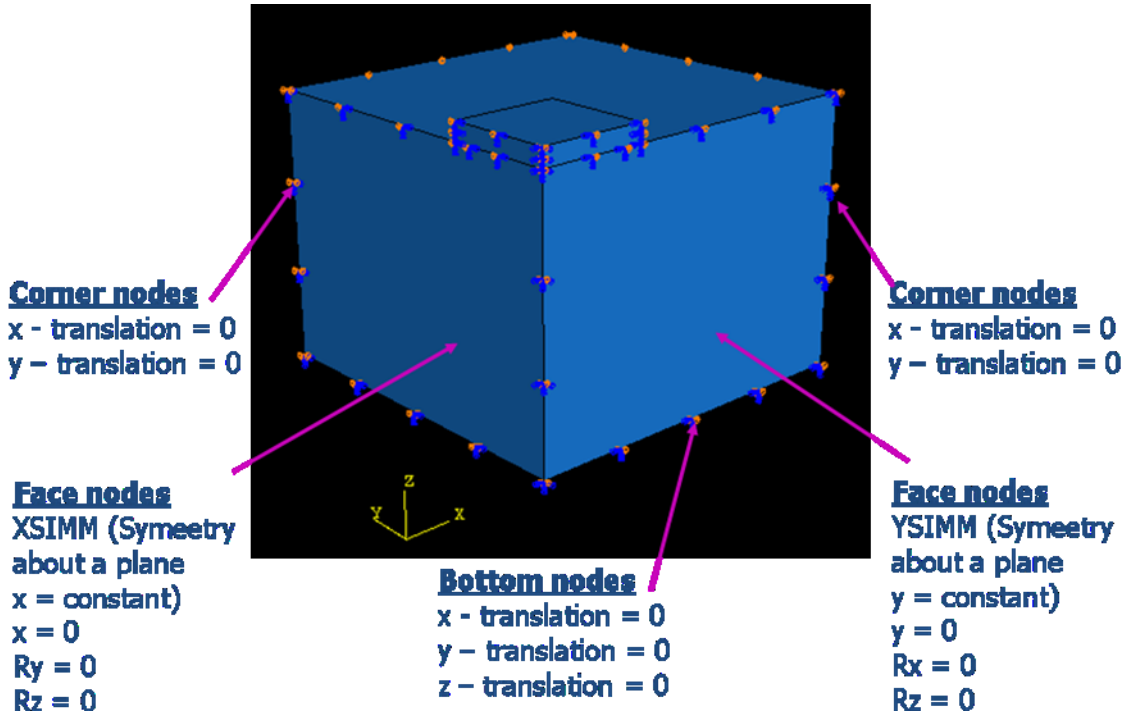

Figure 3.12 b) Boundary condition of a 3-D quarter symmetry model.

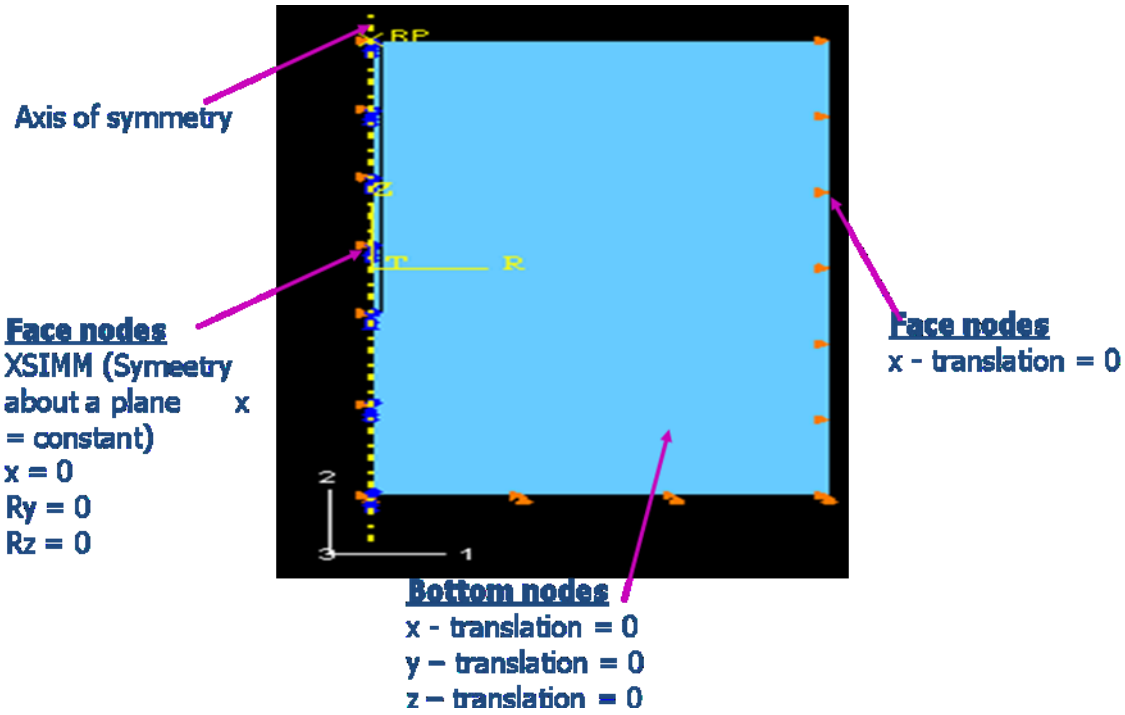

Figure 3.12 c) Boundary condition of a 2-D axi-symmetry model.

In order to set the boundary extent of the continuum to reduce the analysis or computational cost (time, resources like RAM, processor speed etc.), a number of elastic, elasto-plastic simulations of the soil continuum have been performed. Both the stress and strain variation with the length, breadth and depth were investigated. It is concluded that the horizontal length extent of 30D (30 times of the pile diameter) and vertical depth extent of 2L (two times the pile length) is sufficient after which no appreciable stress and strain variation effect was observed. Figure 3.13a) and 3.13b) are the contour plot of displacement components (lateral displacement component, U2 and vertical displacement,U3) from the output of such an investigation. The figures represent the quarter cut central axis view of a soil continuum of 80x80x30m with 16 piles of 15x1m (LxD) having a raft of 14x14x2m subjected to a uniformly distributed load of 0.5MPa. At this load, the vertical settlement of the raft top centre element is observed as 497mm, while no influence is observed at the bottom (contoured by the orange color in figure 3.13b).

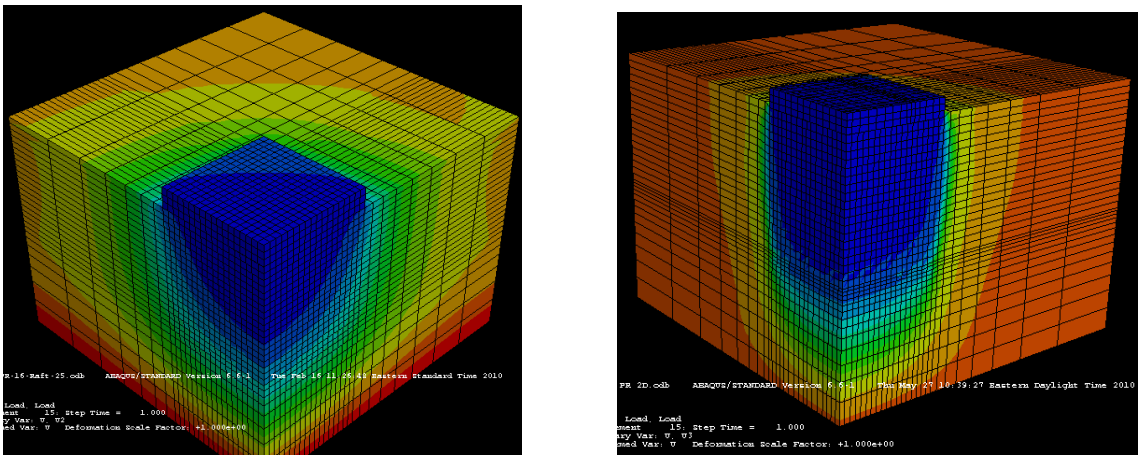

Figure 3.13 Displacement contour for a) lateral component,U2 and for (b) vertical component, U3

The boundary extent was also investigated on a 2D-axisymmetric model for a single pile of 16m length and 0.6m diameter. The vertical stresses along various paths in the continuum were observed. It is concluded that the vertical stress variation after a depth of 1.6L is negligible (figure 3.14a) and the same is true for a lateral distance of about 16D (figure 3.14b). Therefore, the boundary extent of 30D in lateral and 2L in vertical direction is justified.

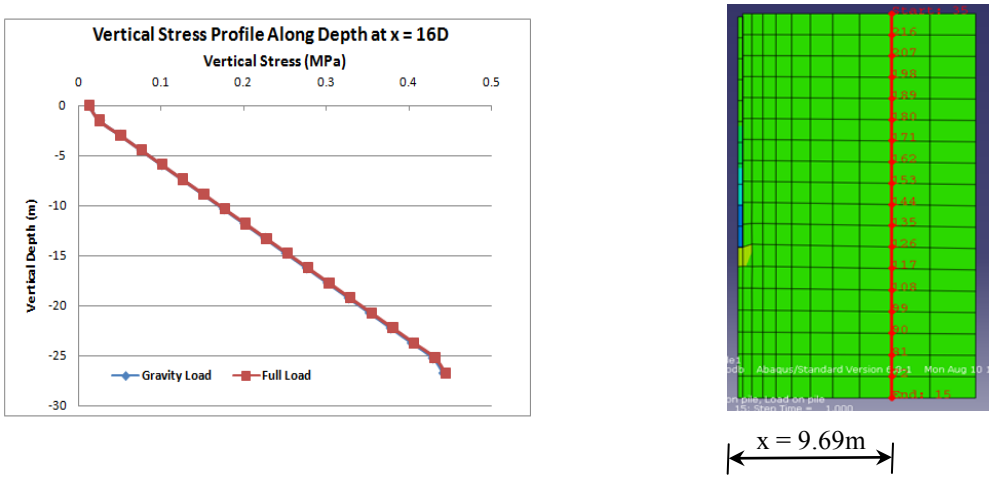

a) Vertical stress profile along depth at x = 9.6m

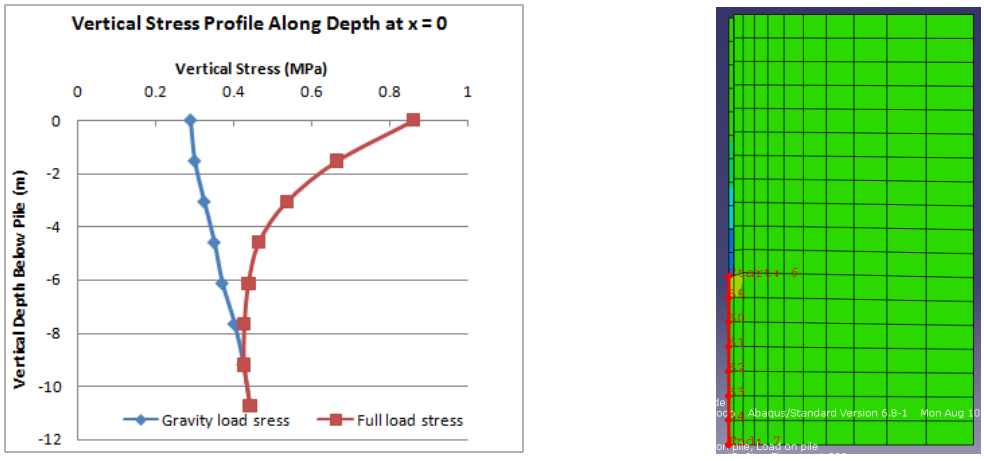

b) Vertical stress profile along depth at x = 0m

Figure 3.14 Vertical stress variations with depth

3.2.6 Sensitivity Analysis / Mesh Refinement

Several finite element analyses were performed to investigate the influence of number of elements and their sizes on the bearing behavior of pile raft foundation. These were done by varying their number and sizes keeping material properties and all other parameters constant. For simplicity, the 2D-axisymmetric analysis output is depicted below. This type of investigation was performed before finalizing the element geometry of each model. For the soil continuum, the bias and aspect ratio were varied as shown in table 3.1 below and its observed consequences on the bearing behavior of pile shaft and tip are shown in figure 3.15 below. The pile tip bearing resistance was determined from the stress of adjacent soil element of the tip. Similarly, the shaft resistance was determined by integrating the adjacent soil element stresses along the shaft. The study shows that after a certain size, no more mesh refinement is required. For this soil geometry and property, the meshing of 20 elements along the lateral (x) direction with a bias of 10 is justified.

Table 3.1 Sensitivity analysis of soil continuum element for a load of 1.15 MN

Element				Load (MN) shared by	
Number*	**Bias**	**Length**	**Depth**	**Bottom**	**Shaft**
10	5	0.578	1.45	0.11	1.04
20	5	0.184	0.73	0.22	0.93
20	20	0.112	0.73	0.24	0.91
40	20	0.057	0.37	0.25	0.90

*Number of soil element along X direction

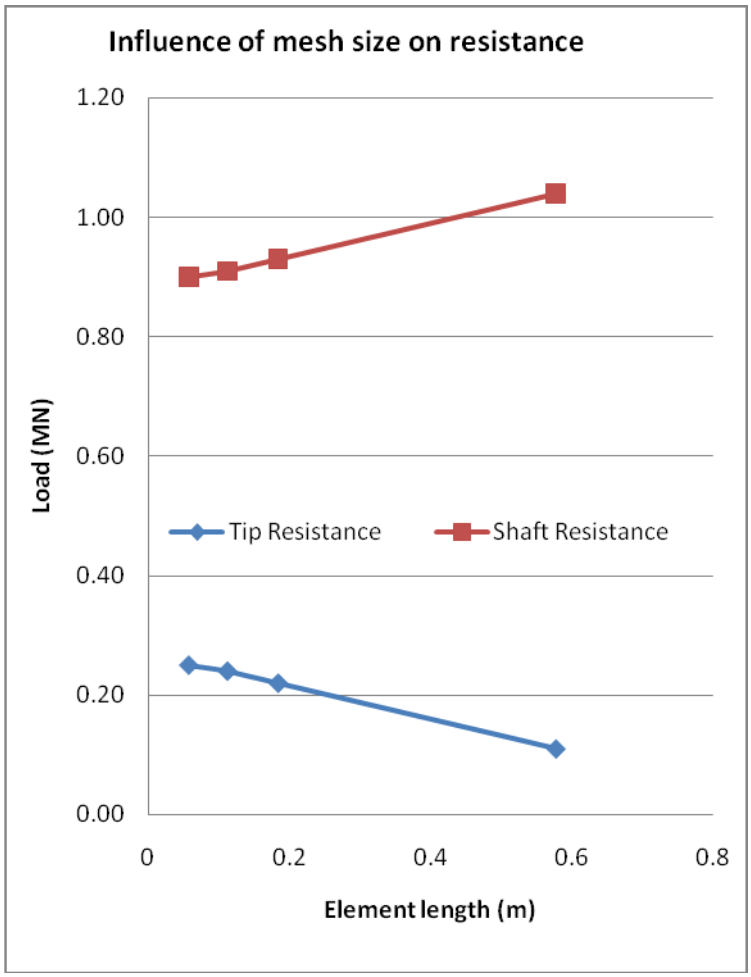

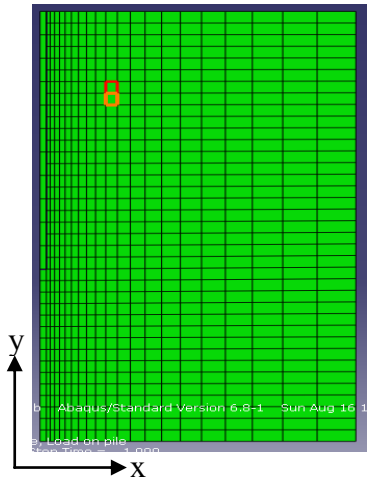

Element length variation along X axis

Figure 3.15 Influence of soil element size on bearing resistance

Another investigation was performed to study the influence on bearing behavior by varying the pile elements bias and aspect ratio. For this study, the material properties, geometric properties of pile and soil were kept constant. The twenty soil elements, with a bias of 10 as obtained from the previous study, were kept unchanged during this pile

elements size influence study. The pile elements' sizes were varied both in vertical and horizontal direction. The simulated output shows no significant influence of finer elements as shown in tables 3.2, 3.3 and figures 3.16 a) & b) respectively. The very minor change corresponds to an aspect ratio of 1.2 [for 0.3x0.36m size] diminished again at an aspect ratio of 1.25 [0.3x0.24m size].

Table 3.2 Sensitivity analysis of Pile element for a load of 1.15 MN

Element				**Load (MN) shared by**	
Number*	**Bias**	**Length**	**Depth**	**Bottom**	**Shaft**
11	1	0.3	1.45	0.22	0.93
22	1	0.3	0.73	0.22	0.93
44	1	0.3	0.36	0.24	0.91
66	1	0.3	0.24	0.22	0.93

*Number of pile element along vertical (y) direction

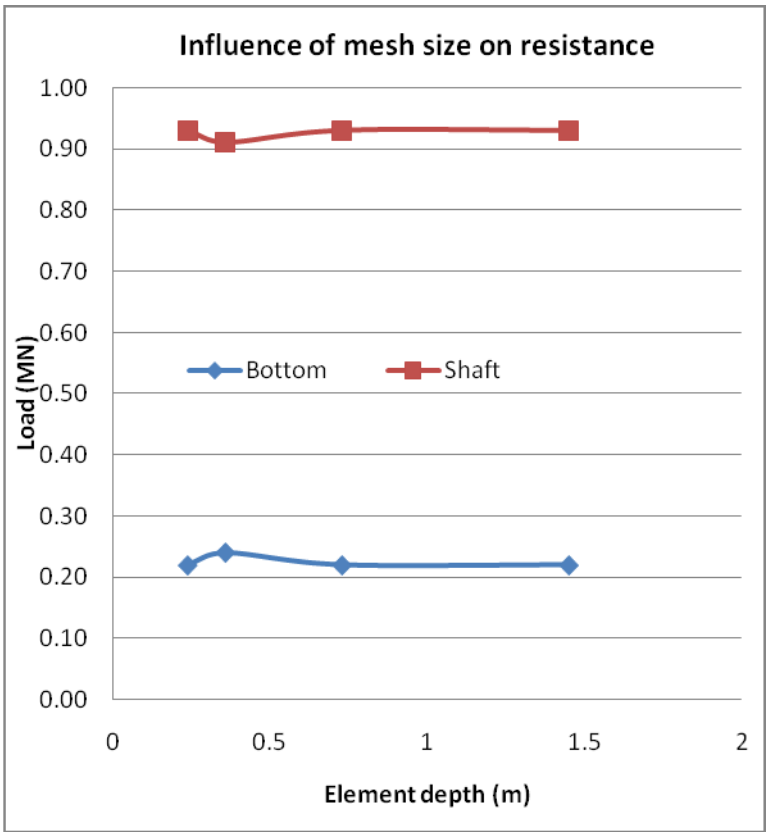

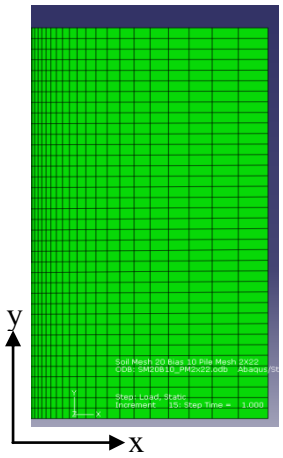

Element depth variation along Y axis

Figure 3.16a) Influence of Pile element size (vertically) on bearing resistance

Table 3.3 Sensitivity analysis of Pile element for a load of 1.15 MN

Element				Load (MN) shared by	
Number*	**Bias**	**Length**	**Depth**	**Bottom**	**Shaft**
1x22	1	0.3	0.73	0.22	0.93
2x22	1	0.15	0.73	0.21	0.94
3x22	1	0.1	0.73	0.21	0.94
4x22	1	0.075	0.73	0.21	0.94

*Number of pile element along horizontal (x) direction

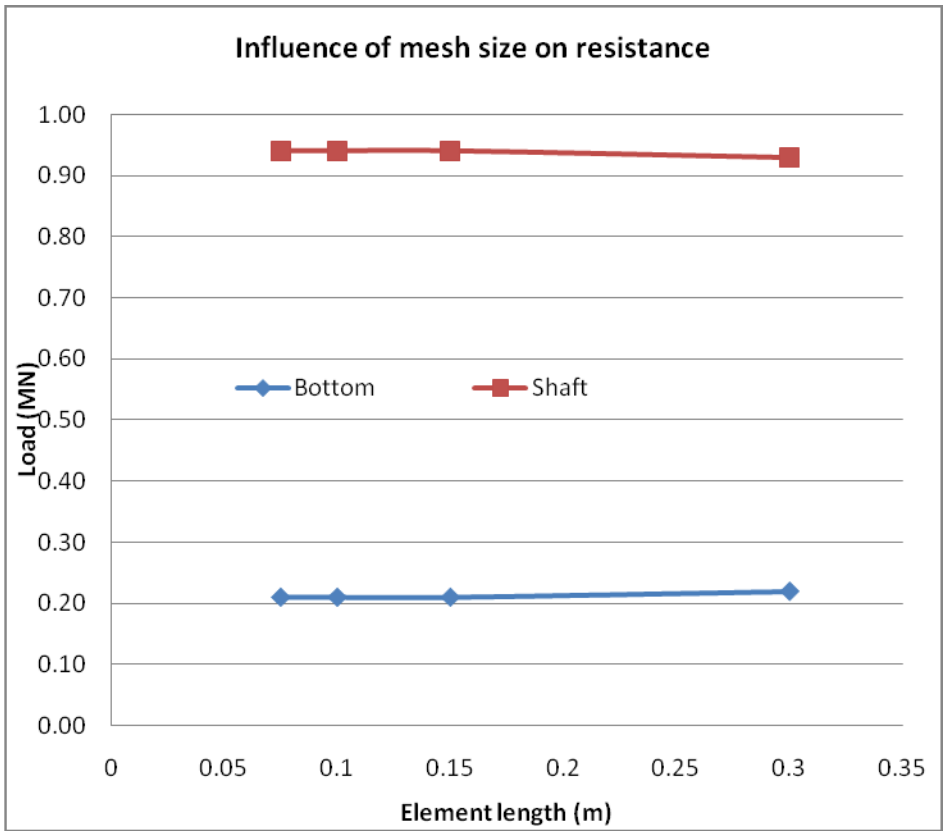

Figure 3.16b) Influence of Pile element size (laterally) on bearing resistance

3.2.7 Analysis Step Time Increment

In ABAQUS, analyses are performed according to the sequence of applied loads, which has been defined in different steps. The geostatic step immediately after the initial step establishes the geostatic equilibrium with the gravitational loads and forces. External loads can be applied in the next step or on the successive steps. The load application in a step is usually defined by the step time increment for a stress controlled analysis and the same is true for a strain controlled analysis where, given displacement was applied in a predefined sequence of step increment. The output of predefined field variables (reaction

forces, stresses, displacements etc.) is obtained in each step increment of analysis. However, for any cases where the deformation is too large in a step increment of load, ABAQUS fails to converge and aborts. At large displacements, ABAQUS step increment tends towards the minimum value, as specified in step definition (e.g. 10^{-07}), resulting in a very expensive simulation.

To reduce the computational cost (time, memory, disk space etc), an investigation was performed to observe the influence of step time increment on the analysis output. A plot of these applied loads and number of increments (figure 3.17a) shows that the required number of increments grows exponentially with the increased load, especially after a certain load, which is much closer to the distortion load (the load that causes too large settlement that ABAQUS fails to converge, even after invoking the large displacement theory with the full Newton's Ruphson iteration technique).

Pile load capacity is determined by the load value corresponding to the intersection of the tangent drawn along the initial curve on displacement axis and on the end curve portion as shown in figure 3.17b). The plot shows that this slope is almost constant after 4.5 MN of load and curve (a) shows that after this 4.5MN, the number of increment grows at an extreme high rate, because the slope of (a) curve is almost straight upward. Therefore, for further study on same material and configuration, pile load of 4.5MN application is justified.

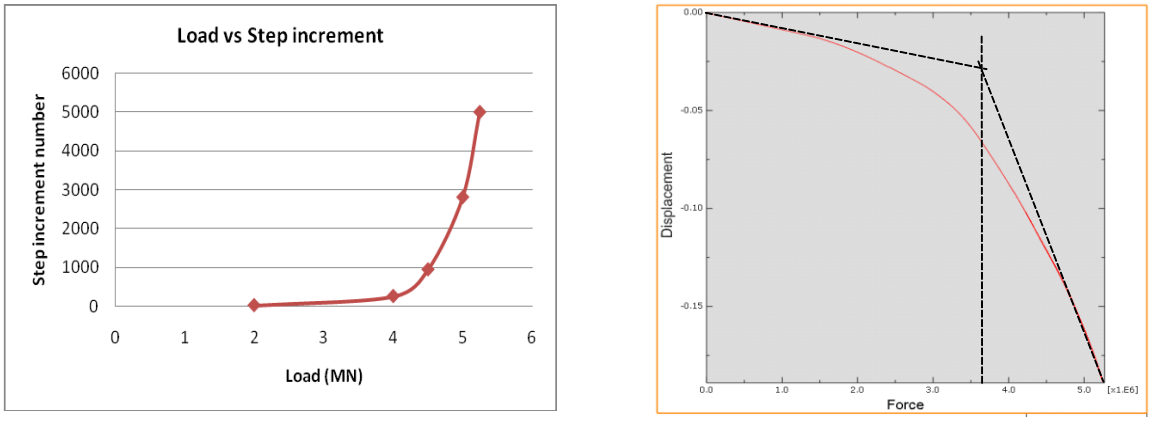

Figure 3.17 Influence of step time increment on analysis output

3.2.8 Geometric Modeling of the Pile

The circular pile is most commonly used in structural construction. On the other hand, the numerical simulation can be best performed by considering the octagonal or square cross-sectional shape of the pile. The simplification of circular pile to square one leads to considerable savings in the number of finite elements and thus, in the calculation time period. As explained in the previous section, hexahedrons are the best choice for the three dimensional analysis, so to accommodate these elements for a fast, less expensive and more accurate simulation, the consideration of square pile is decisive.

This simplification needs an investigation for the influence of the pile shape (circular, square and octagonal) on its bearing behavior for same peripheral surface area (figure 3.18 below). The same peripheral surface area was taken into account, because for this type of foundation, frictional resistance is the main concern rather than the tip resistance.

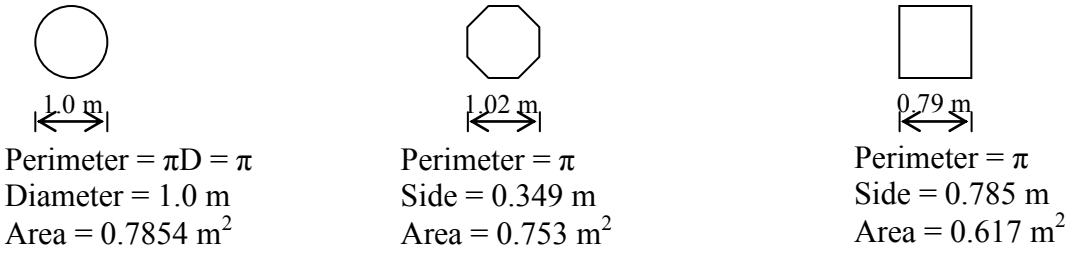

Figure 3.18 Commonly used pile shapes

The numerical simulation output in the form of load settlement curve for the circular, octagonal and square pile shapes have been depicted in figure 3.19 below for the identical parametric condition. The output shows that the circular shape settles a little bit more than octagonal, while the square one also settles more than the octagonal. However, no significant difference in magnitude has been observed. Therefore, the square shaped pile can be used for this work without establishing any correlation to the circular one.

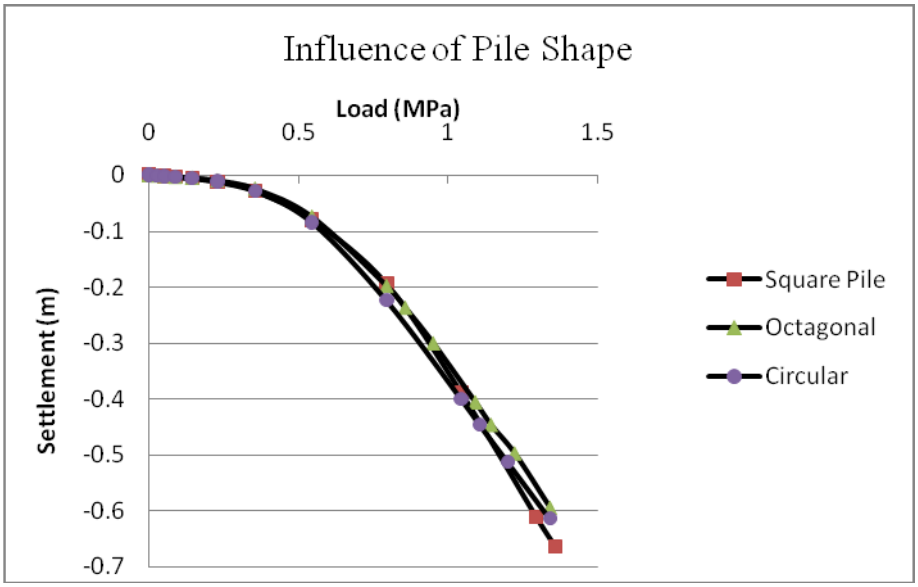

Figure 3.19 Influence of pile cross-sectional shape on the settlement

3.3 Model Validation

The previous sections detail the process of developing the numerical model and the associated investigation to predict the real field value. This predicted value and phenomena have to be confirmed with the realistic physical processes before the model is accepted and applied to simulate the real world problems. In fact, the numerical model is a complex system of equations, wrapped with boundary conditions and compared with a physical model data (Physical Validation) or with an accepted numerical model data (Numerical Validation). This validation is the only way to justify the predictions of a numerical model to the true physics concerned.

The model reported in the American Society of Civil Engineers (ASCE) Technical Committee – 18 (TC -18) report in 2001, has been used in this thesis for validation purpose. The simulated output for this model by various simplified, approximate and rigorous technique, as depicted in this report, should be the versatile tool for proper validation. The model geometry and material properties are mentioned in table 3.4 below

Table 3.4 Model geometry and material properties of ASCE TC 18 pile raft

	Soil	Pile	Raft
Size (m)	20x20x20	0.5(D)x10(L) S =1m (laterally) and 2m (longitudinally)	10x6x0.5
Unit weight, γ (kg/m^3)	1700	2500	2500
Elastic Modulus, E (MPa)	20	30,000	30,000
Poisson's Ratio, ν	0.3	0.2	0.2
Load (MN)	Self Weight	Self Weight	Self Weight + 2MN on middle row and 1MN on sides row of piles

One quarter of the foundation has been taken into account (figure 3.20a) for simulation purpose and the necessary axi-symmetric boundary condition for this quarter symmetric model, as explained in section 3.2.3 and shown in figure 3.10b), has been applied. The middle three piles in transverse direction were subjected to the concentrated load of 2MN, while the edge piles were subjected to the concentrated load of 1MN. The simulated pressure profile (figure 3.20b) shows that the pile spaced at 1m centre to centre, - shares the pressure while, the pile at 2m distance apart works as an individual pile

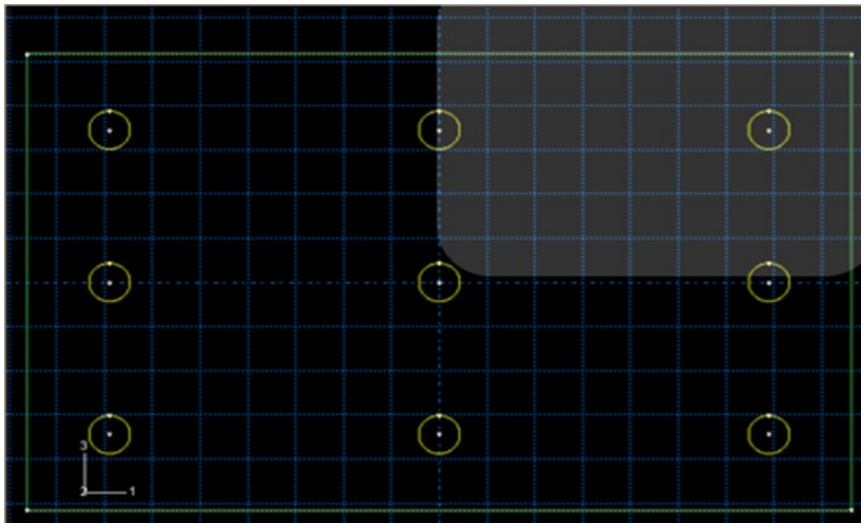

Figure 3.20 a) Quarter axi-symmetry of the plan

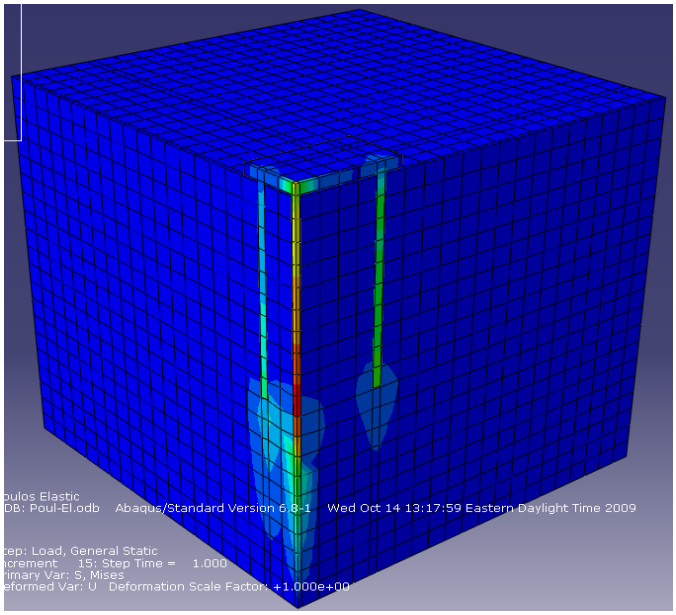

Figure 3.20 b) Pressure bulb of quarter cut pile raft

An excellent agreement is observed with the studies, cited in the ASCE - TC18 report as shown in figure 3.20c) below. The ABAQUS 3D simulated output is identical with those of Poulos-Davis-Randolph (PDR), Geotechnical Analysis of Raft with Piles (GARP5), Geotechnical Analysis of Strip on Piles (GASP) and conservative to the output of FLAC 2D and 3D. It can be noted that FLAC software coding is based on the finite difference formulation and even 2D and 3D are not giving the same output as reported in the figure. ABAQUS, on the other hand, is pure finite element software, based on strong solid mechanics principles and the obtained output has the resemblance of strong theoretical and real world situation.

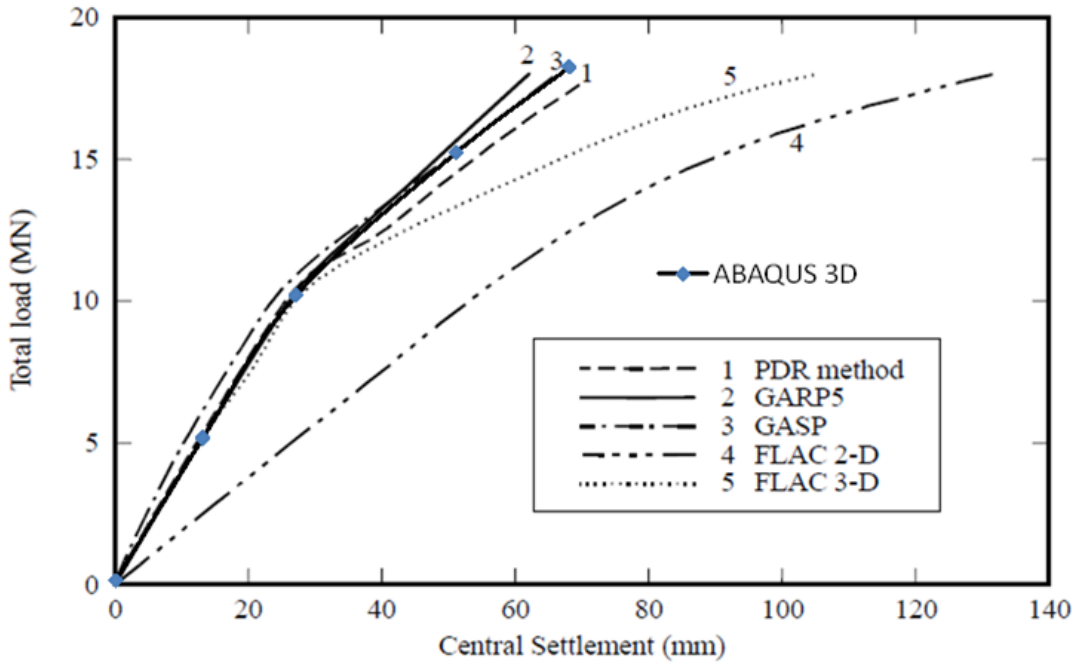

Figure 3.20 c) Load settlement curve for the validation

3.4 Justification of Piled Raft Foundation

The piled raft foundation is a new concept and to justify its necessity over the existing shallow (Raft) and deep (pile) foundation, an investigation was performed on an un-piled raft (UPR), a pile group (PG) of 64 piles without any cap and a pile raft (PR) combining the above two. The quarter symmetric cut views of these models are shown in figure 3.21 below. All these three models have been simulated for identical material property and loading condition, while the raft has a dimension of 24x24x2m and the square piles in the group have the length of 15m, sides of 0.8m (which is equivalent to the perimeter of 1m diameter) at the spacing of 3D (= 3.0m c/c).

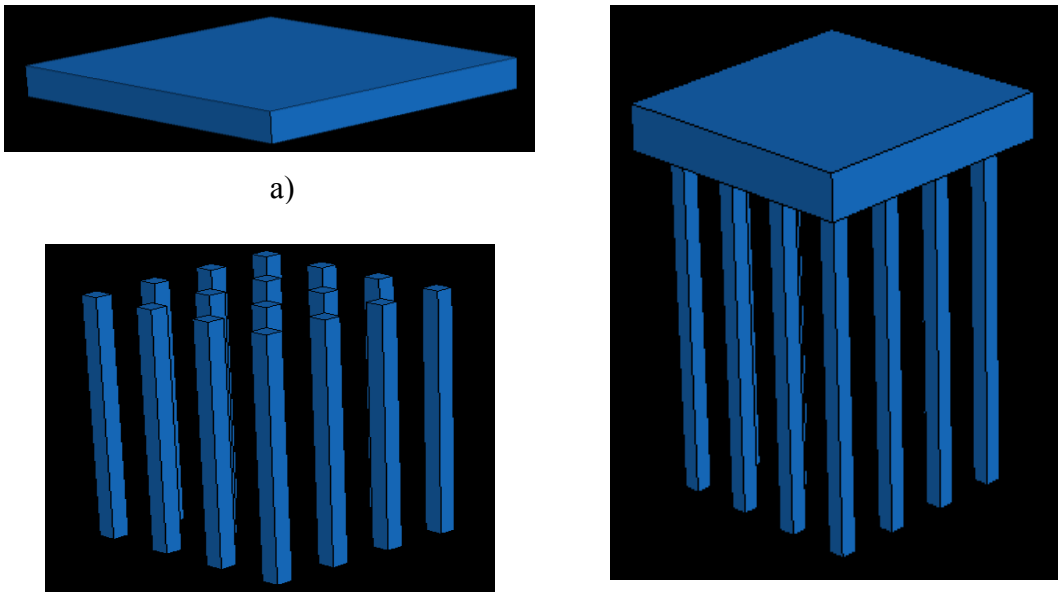

Figure 3.21 Quarter cut view of a) Raft, b) Pile group without raft or cap and c)

The material properties used in the rest of this research is adopted from Katchebach [2000] as shown in table 3.6 below and the associated volumetric plastic hardening property is as depicted in figure3.22. The derived parameter for modified Drucker-Prager cap plasticity model is shown in table 3.6 below. All of these are used as ABAQUS input parameter to define the material property.

Table 3.5 Subsoil properties of Frankfurt clay and limestone (Katzenbach 2000)

Parameter	Unit	Clay	Limestone
Young modulus, *E*	MPa	$E = 45 + \left[\tanh\left(\frac{z-30}{15}\right)+1\right]0.7z$	2000
Poisson's ratio, *v*		0.15	0.25
Unit weight, γ	kN/m^3	19	22
Angle of internal friction, φ	degree	20	15
Cohession, c'	kPa	20	1000
Natural water content. *w*	%	34	
Liquid limit. *LL*	%	74	
Consistency index, I_c		0.82	

*z is the depth below the ground surface and the equation is proposed by Reul 2004.

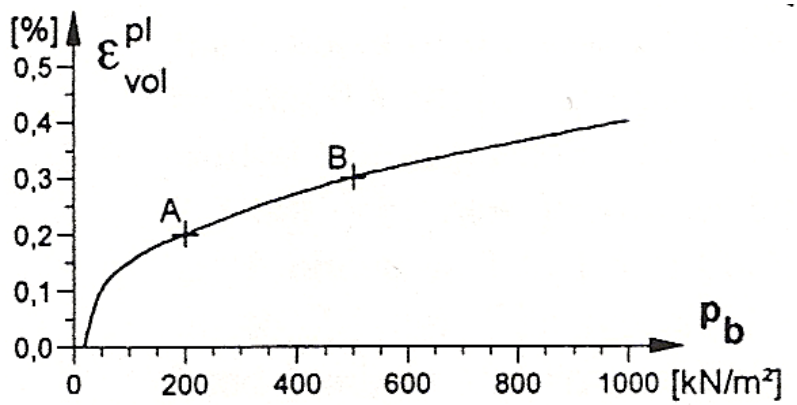

Figure 3.22 Volumetric plastic hardening properties of Frankfurt clay (Katzenbach 1997)

Table 3.6 Material properties used in numerical model

Parameter	Unit	Clay	Lime stone	Pile	Raft
Young modulus, *E*	MPa	54	2000	25000	34000
Poisson's ratio, *v*		0.15	0.25	0.2	0.2
Unit weight, γ	kN/m^3	19	22	25	25
Submerged unit weight, γ'	kN/m^3	9	12	15	15
Earth pressure coefficient at rest, k_0		0.72 for $0 \leq z < 25$ 0.57 for $z \geq 25$		0.5	
Angle of internal friction, φ	degree	20	15		
Cohession, c'	kPa	20	1000		
Cap parameter					
d	kPa	42.42	2114		
β	degree	37.67	29.53		
α		0	0.001		
K		0.795	0.841		
R		0.1	0.01		

The simulated ABAQUS output for a Uniformly Distributed Load (UDL) of 0.5MPa are shown in load settlement plot of figure 3.23 below. At this loading condition, the settlements of UPR, PG and PR are obtained 500mm, 560mm and 196 mm respectively, i.e., the settlement reduction is more than 60% by the combination. The same is observed even for a lower load e.g. for a 100mm settlement both the UPR and PG can withstand of an UDL of 0.21MPa while for the PR an UDL of 0.31MPa is required, which is 50% greater than that of the other two. This additional bearing resistance, obtained from the raft or cap of pile group, is ignored in conventional group pile theory. For structural reason, i.e. to maintain structural integrity, to provide a base of the structure, pile group cap or raft is a must. Therefore, proper design of pile and raft on the basis of accurate estimation of the load resistance of both components can yield an economical savings of more than 50% along with the greater reliability.

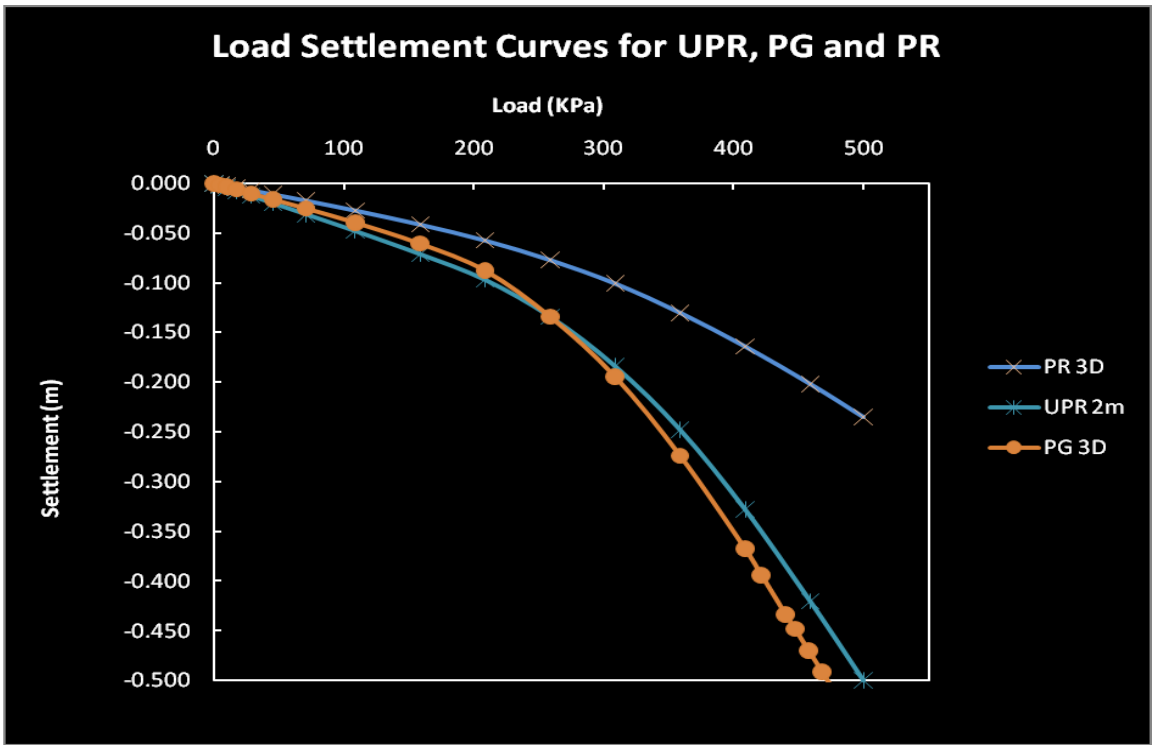

Figure 3.23 Load settlement behavior of Raft, Pile Group and Pile raft

3.5 Influence of Pile Spacing

The major question for the group pile is the spacing for the piles. It dictates not only the number of piles and thereby construction cost, but also provides the structural safety by means of stiffness of the structure. The conventional group pile theory implies that the group action is no more valid for pile spacing greater than 2.5D [Das 2007] but this theory does not take into account the bearing contribution of the raft. Investigation was therefore made to observe the influence of pile spacing on pile raft foundation behaviour.

Eight models for various pile spacing were developed and simulated for this purpose. To model the soil continuum, the same properties, boundary condition and modeling technique, mentioned in the previous section, were used. The concrete property for raft

and piles is same as in previous section and the same UDL of 0.5MPa was applied on raft top in each case. The pile length of 15.0m with perimeter equivalent to a 1.0m diameter of circular pile was used. The rest geometric properties of rafts and piles of various configurations are as below

Table 3.7 Geometric properties of pile raft models

Pile Spacing	Raft Size (LxBxD)	No of Piles
2D, 3D, 4D & 6D	24x24x2	144, 64, 36 & 16
7D	28x28x2	16
8D	32x32x2	16
10D	40x40x2	16

The numerical analysis output of ABAQUS for the pile spacing, ranging from 2D to 10D along with that for UPR, obtained from previous section for identical situation, have been plotted in load settlement behaviour as shown in figure 3.25 below.

The output shows that the settlement increases with the increase in pile spacing and the load bearing capacity increases sharply for the spacing smaller than 6D. Conversely, the settlement is worse than that of an un-piled raft (UPR) for pile spacing greater than 7D. Therefore, for pile spacing equal or greater than 7D, only the raft footing is sufficient to withstand the structural load.

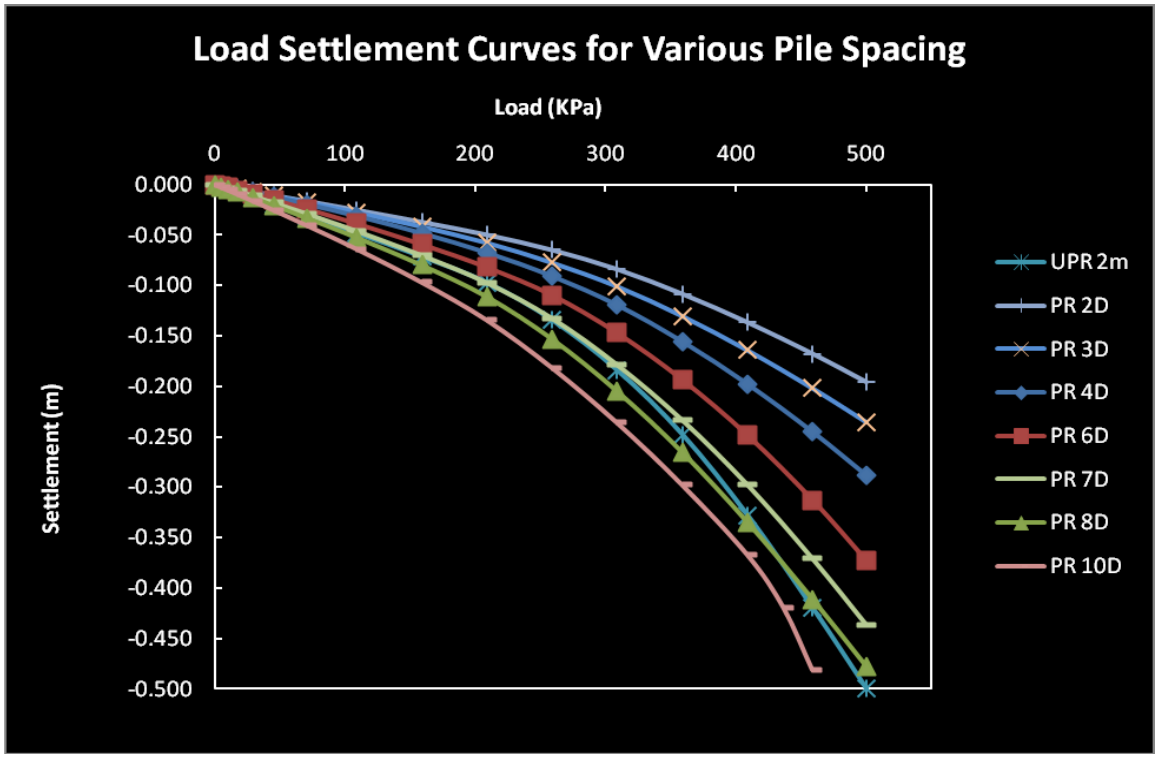

Figure 3.25 Influence of pile spacing on load settlement behavior

Another distinct representation can be obtained from the settlement plot for various pile spacing, subjected to a load of 0.3MPa as a reference. The plot in figure 3.26 below depicts that the slope of the curve is constant up to 6D, after which, it changes dramatically and seems to attain another constant slope again, just after the pile spacing of 8D. This slope changing pattern is identical for any other magnitudes of load, because the pattern of load settlement curves for different spacing are identical as shown in figure 3.25 above. This phenomenon dictates that the pile spacing for pile raft foundation should not be greater than 6D. Before concluding on maximum spacing for this type of foundation, it is essential to observe the raft top deflection at this spacing.

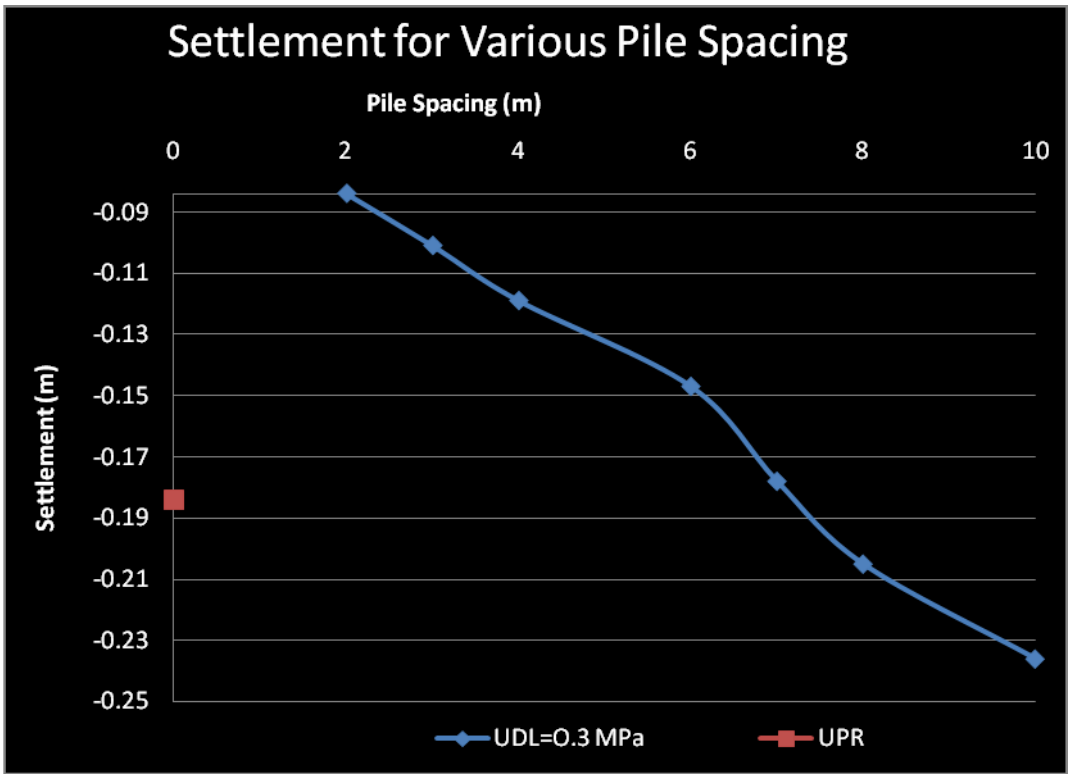

Figure 3.26 Settlement for various pile spacing

The concern regarding the abrupt raft top deflection (differential settlement) for the pile raft foundation of 6D spacing, was also investigated and the contour plot of the raft deflection from ABAQUS output is depicted in figure 3.27 below. To obtain the deflected raft top shape in two dimensional representations, plotting of raft top settlement along raft centerline, center piles and along raft diagonal path were shown in figure 3.28. Since, these are the output of quarter symmetric analyses, where point A is the raft centre, B and C are mid peripheral and corner points, the curves in figure 3.28 are plotted on true horizontal distance from the raft centre. The raft top settlement profiles along centre line, centre pile lines and diagonal indicates that the raft settlement takes the shape of a bowl

with the maximum is at centre. The settlement pattern has no irregularity or abrupt differential settlement. The same is observed by Horikoshi and Randolph (1996 & 1998) in their so called centrifuge model. Therefore, it could be concluded that the maximum pile spacing for pile raft foundation, should not be greater than six times the pile diameter.

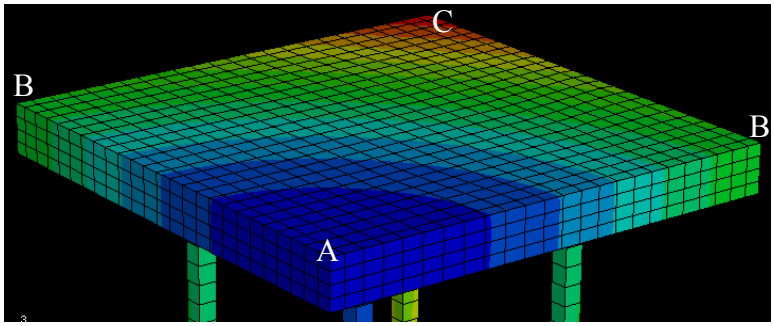

Figure 3.27 Raft top settlement contour for a pile spacing of 6D

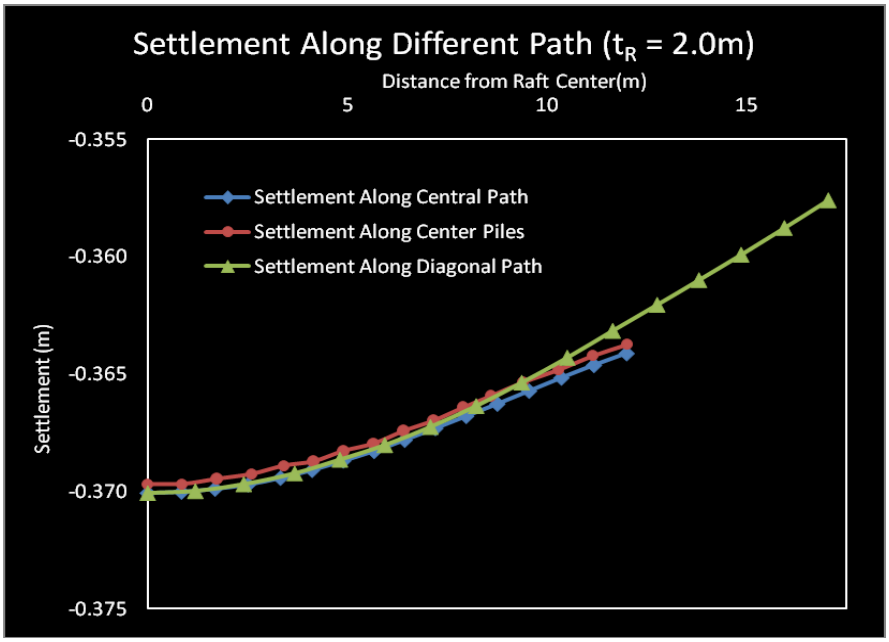

Figure 3.28 Raft top settlement profile

Besides the load settlement behavior, the influences of spacing on the raft centre settlement and differential settlement have been investigated. Considering the constructional aspect and simplicity, both the raft centre and differential settlements have been plotted for the pile spacing of 4D, 6D and 8D, as shown in figure 3.29 and 3.30 below.

The raft centre settlements for the various spacing imply that the settlement increases with the increase in spacing. Figure 3.29 implies the relationship in between them is almost directly proportional. The differential settlement plot against spacing, on the other hand, shows no significant changes for a pile spacing of up to 6D, after which it increases with the pile spacing (figure 3.30). The differential settlement is in between the centre and the corner point of the raft.

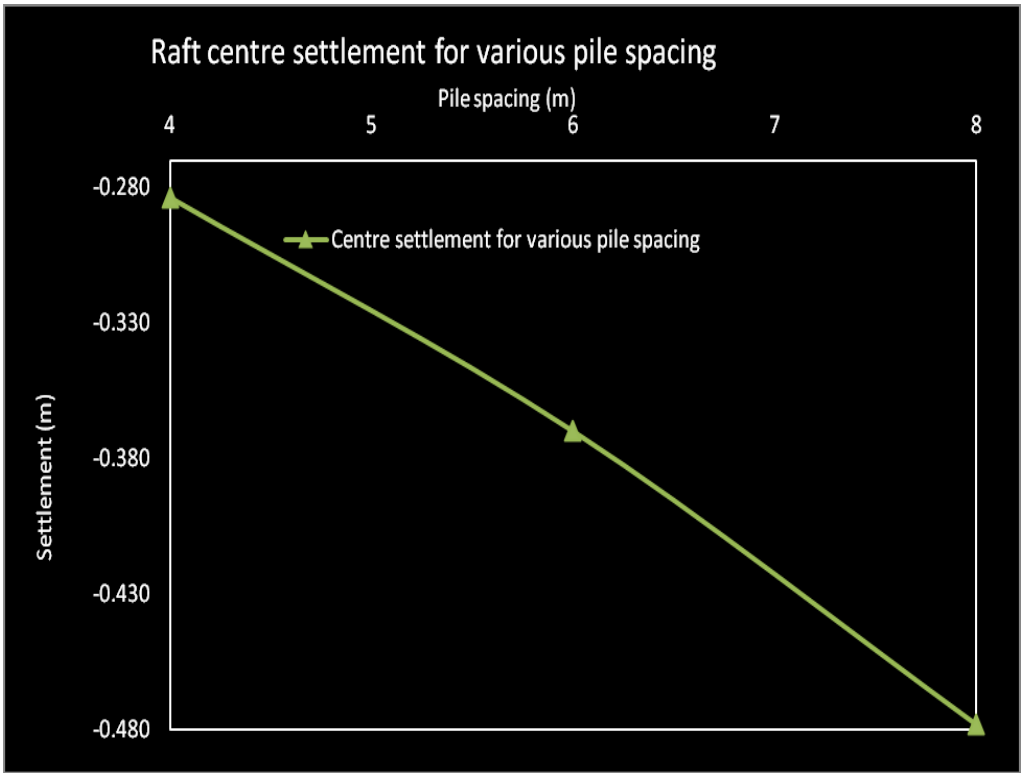

Figure 3.29 Raft centre settlement for various pile spacing

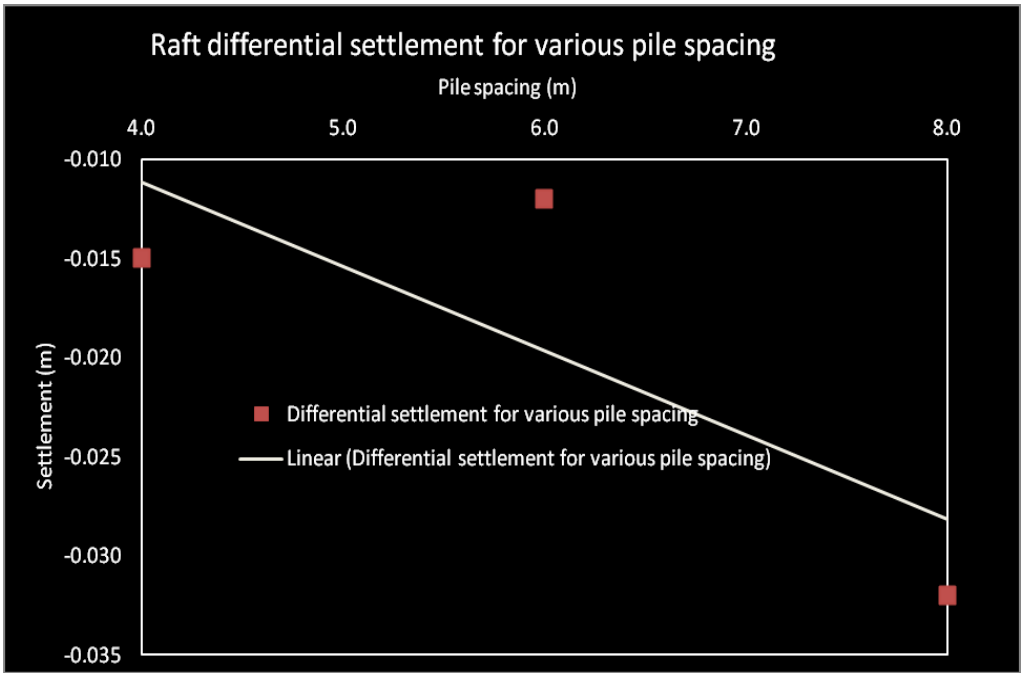

Figure 3.30 Raft differential settlements for various pile spacing

3.6 Influence of Pile Length

Pile length plays the major role in transmitting the load as observed in section 3.4 above. For clayey soil, the pile group acts as floating pile and all the load transmission is accomplished by the pile shaft friction. This shaft friction occurs on the peripheral surface area of each of the pile in the group. This peripheral area of the pile is again a direct function of the pile length and its diameter.

To capture the influence of pile length on the load settlement behaviour of piled raft, nine models have been developed for the varying pile length of 5m, 10m and 15m. These three types of pile length have been simulated numerically for 4D, 6D and 8D pile spacing, where the geometric properties (raft dimensions and pile diameter) are as mentioned in

table 3.7 above. To model the soil continuum, the same properties, boundary condition and modeling technique, mentioned in the previous section, were used. The concrete property for raft and piles is same as in previous section and the same UDL of 0.5MPa was applied on Raft top in each case.

The simulated output of the numerical analyses by means of ABAQUS 3D FE software, in the form of raft top settlement, has been depicted in figure 3.31 to 3.33 below. The settlement pattern of the raft top is same for all the pile spacing and length variation. However, this pattern for 8D pile spacing (figure 3.33) is steeper, which reflects the more differential settlement for 8D spacing of any pile length.

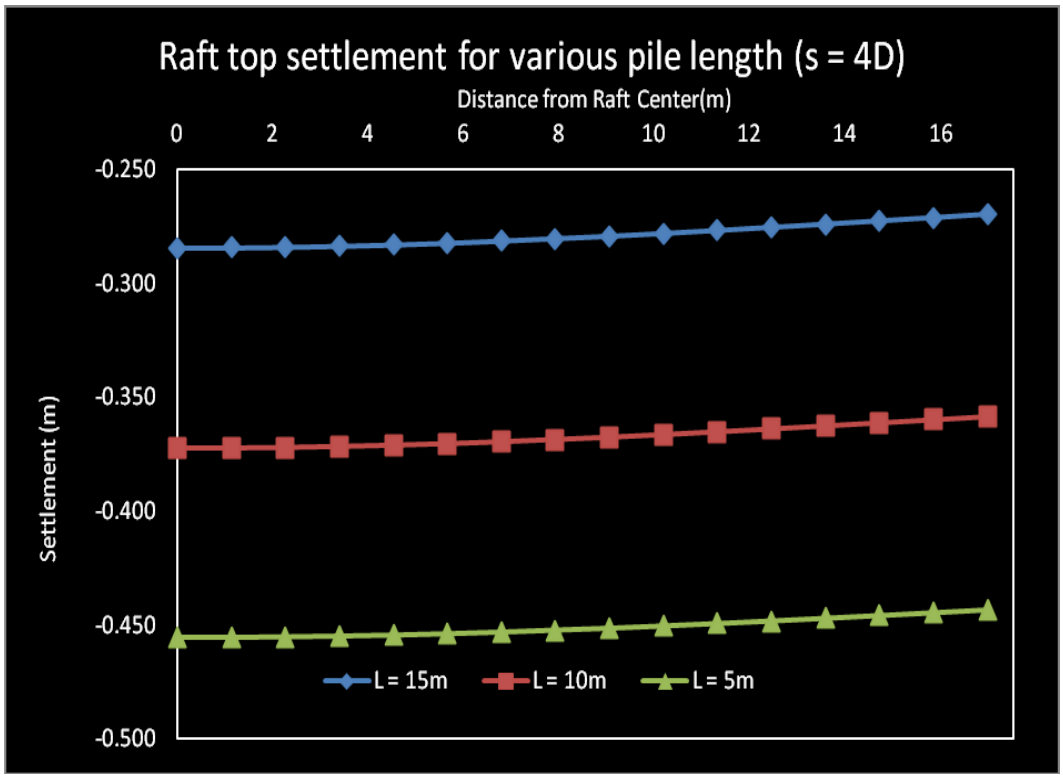

Figure 3.31 Raft top settlement for various pile length (s =4D)

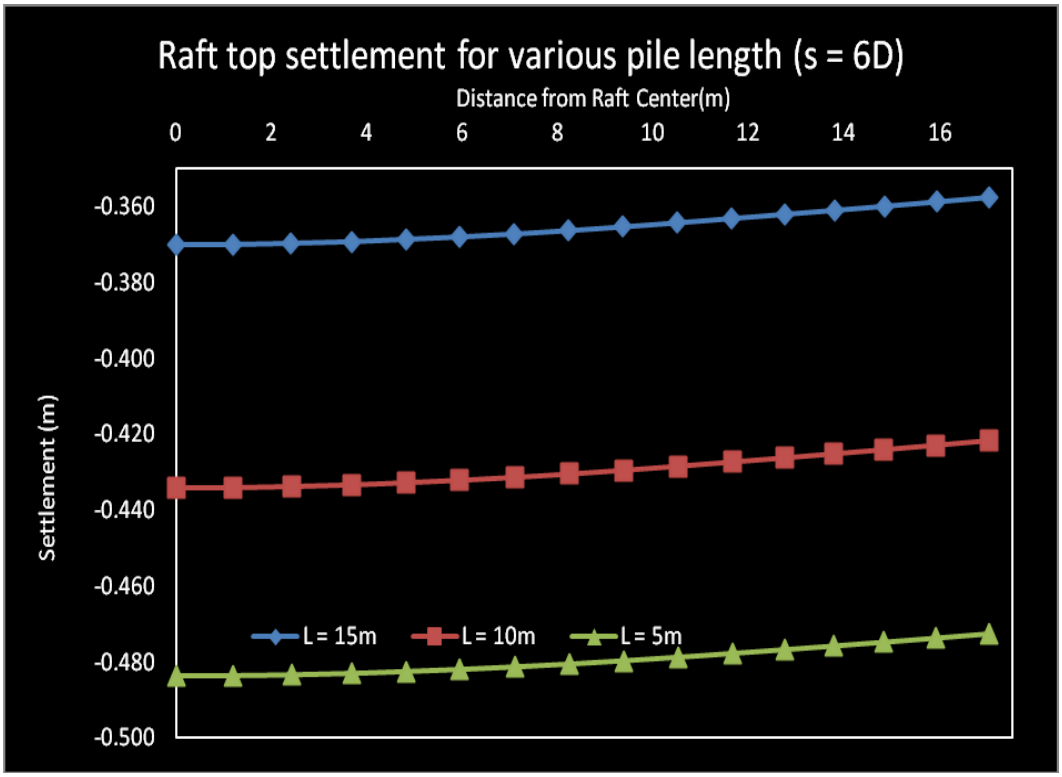

Figure 3.32 Raft top settlement for various pile length (s =6D)

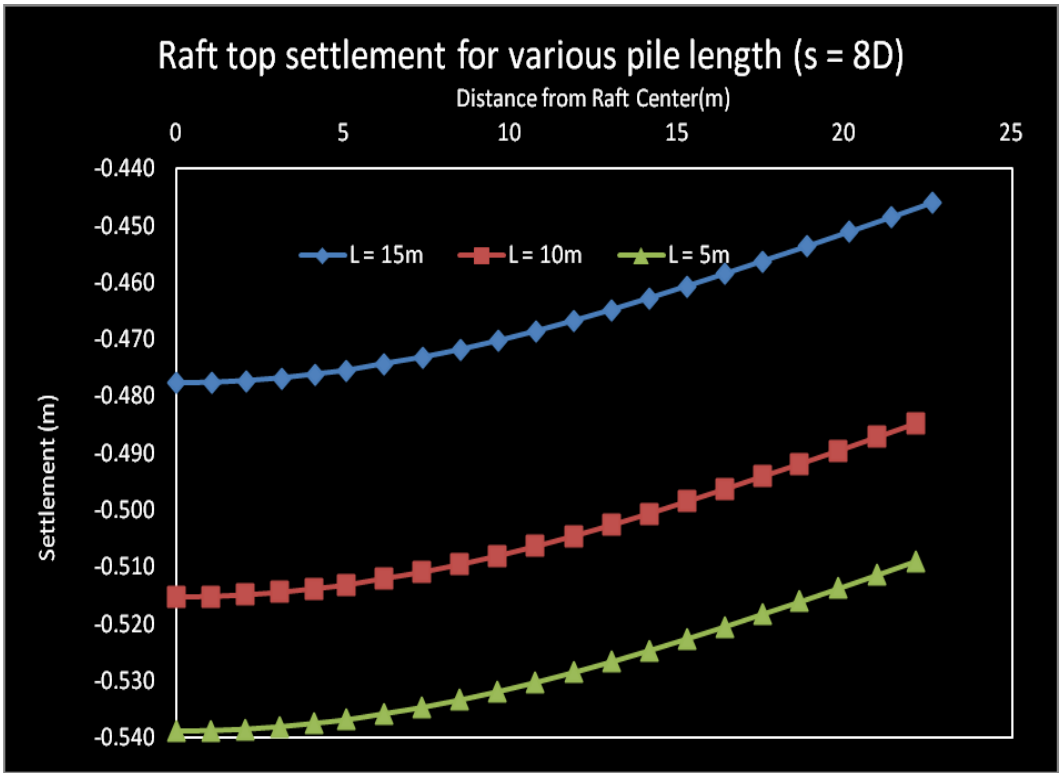

Figure 3.33 Raft top settlement for various pile length (s =8D)

Besides the raft top settlement profile, the influence of pile length on raft centre settlements have been investigated for each of the 4D, 6D and 8D pile spacing. For each case, the centre point settlement is decreased with the increased pile length as shown in figure 3.34. Table 3.8 below depicts the effective reduction in settlement with the increased pile length for each type of spacing. These studies were performed for 4D, 6D & 8D spacing, because the range of effective pile spacing is from 4D to 7D, which is observed in section 3.5 above. The settlement reduction rate for the same raft centre with increased pile length again varies with the pile spacing. Figure 3.34 dictates that the settlement reduction rate is steeper for smaller pile spacing and flatter for the larger pile spacing. It can be concluded therefore, the larger spacing of the piles reduces the effectiveness of increased pile length. So to develop the optimum design strategy a balance in between the spacing and pile length should be established.

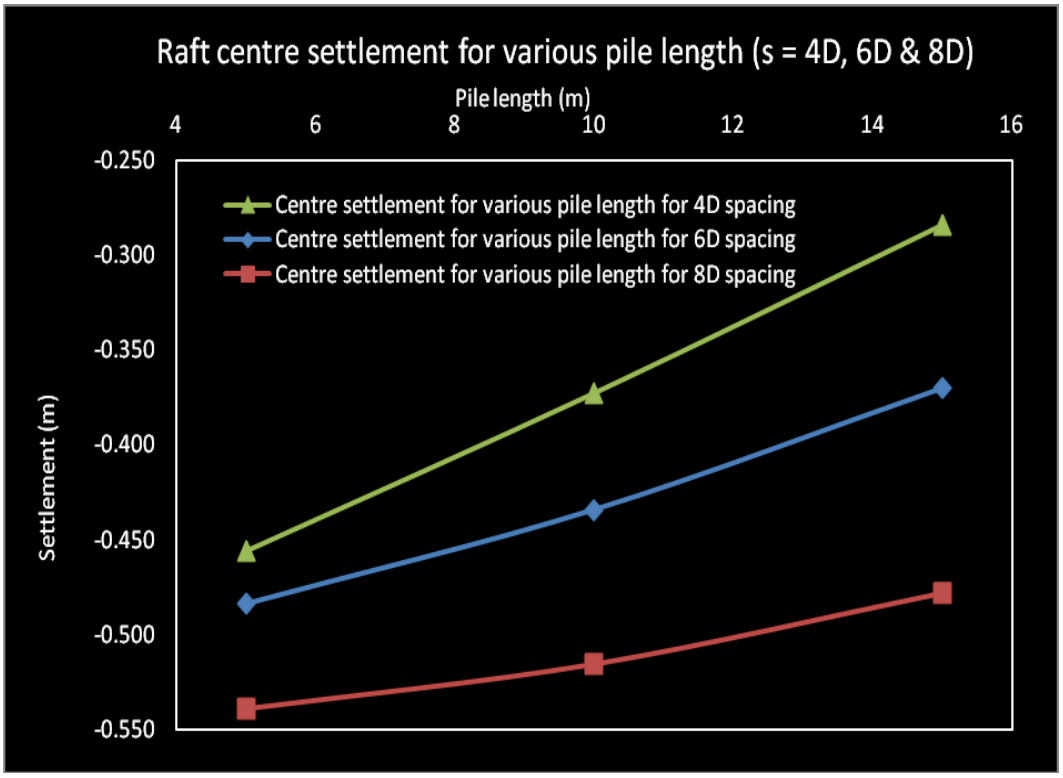

Figure 3.34 Raft centre settlement for various pile length

Table 3.8 Raft centre settlement for various pile length

Pile length (m)	5	10	15
Centre settlement for 4D spacing (m)	-0.456	-0.373	-0.284
Centre settlement for 6D spacing (m)	-0.484	-0.434	-0.370
Centre settlement for 8D spacing (m)	-0.539	-0.515	-0.478
Reduced settlement for 4D spacing (m)	-	0.083	0.089
Reduced settlement for 6D spacing (m)	-	0.050	0.064
Reduced settlement for 8D spacing (m)	-	0.024	0.037

Further numerical investigation was done with these 3D finite element models to study the pile length variation effects on the differential settlement of the pile raft. The settlement difference between the raft centre and corner point has been taken into consideration for this purpose. Figure 3.35 below depicts the differential settlement variation with varying pile length for the pile spacing of 4D, 6D and 8D. The differential settlement does not vary significantly with the pile length variation and the patterns for all the spacing are same. Though the large magnitudes in the differential settlements are observed for the pile spacing of 8D (Figure 3.35 and 3.33), the length does not have any influence on the differential settlement as the rate of differential settlement does not vary significantly with the changes in pile length for any spacing of pile (Table 3.9).

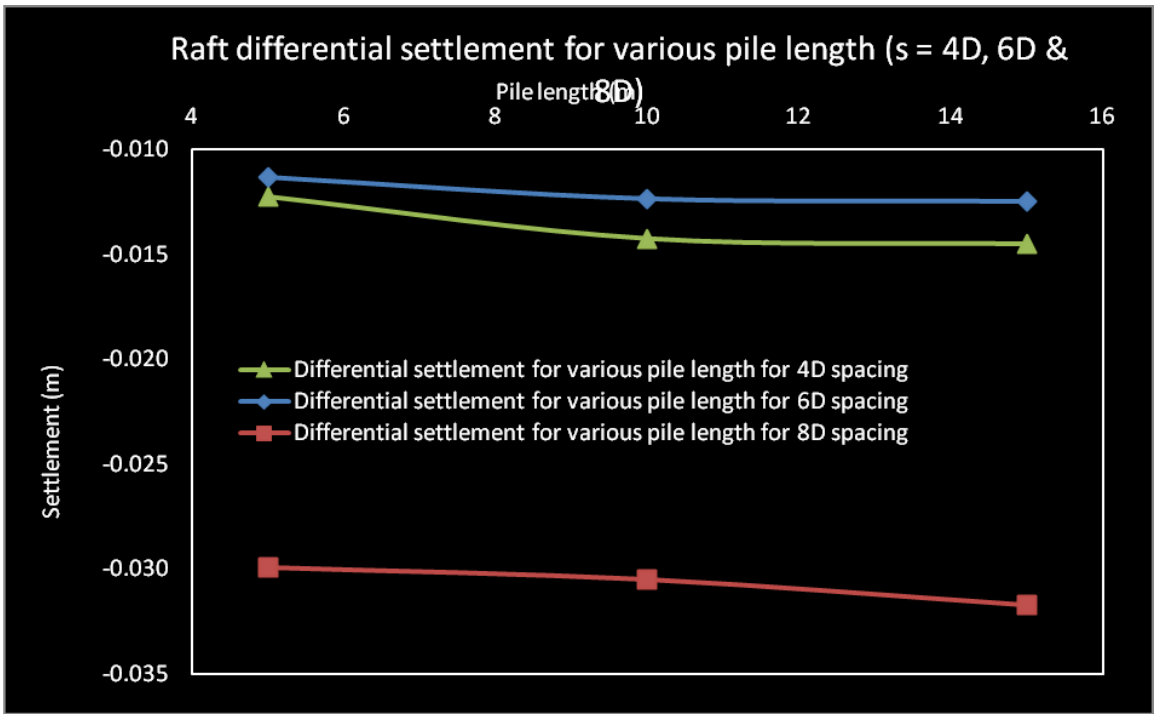

Figure 3.35 Raft differential settlements for various pile length

Table 3.9 Raft differential settlement for various pile length

Pile length (m)	5	10	15
Differential settlement for 4D spacing (m)	-0.011	-0.012	-0.012
Differential settlement for 6D spacing (m)	-0.012	-0.014	-0.015
Differential settlement for 8D spacing (m)	-0.030	-0.030	-0.032
Reduced differential settlement for 4D spacing (m)	-	-0.001	0.0
Reduced differential settlement for 6D spacing (m)	-	-0.002	-0.001
Reduced differential settlement for 8D spacing (m)	-	0.0	-0.002

3.7 Influence of Pile Size

The pile size is another important parameter in transmitting the load to the soil. The load bearing capacity of an end bearing pile has a direct second order exponential relationship

to the pile cross-sectional dimension. This cross-sectional dimension in the form of perimeter determines the shaft load bearing capacity in a direct first order relationship.

The load settlement behaviour of piled raft have been observed by simulating the nine models, developed for the varying pile size of 0.4m, 0.8m and 1.2m sides of square cross-section. These three types of pile size categories have been simulated numerically for 4D, 6D and 8D pile spacing with the geometric properties (raft dimensions and pile diameter) as mentioned in table 3.7 above. To model the soil continuum, the same properties, boundary condition and modeling technique mentioned in the previous section were used. The concrete property for raft and piles is same as in previous section and the same UDL of 0.5MPa was applied on Raft top in each case.

The numerical simulated analysis output by ABAQUS in the form of raft top settlement has been depicted in figure 3.36 to 3.38 below. The settlement pattern of the raft top is same for all the pile spacing and size variation. The settlement is observed greater for 0.4x0.4m size and reduced gradually as the pile size increased. The settlement intensity varies with the pile spacing. For smaller pile spacing, the pile raft settles in a greater magnitude than that of the bigger size piles (figure 3.36). This tendency is reduced as the pile spacing increased. Figure 3.37 depicts the uniform settlement for various pile sizes for the spacing of 6D and figure 3.38 depicts the reverse characteristics of figure 3.36 i.e the biggest sized piles (1.2x1.2m) settle less than the other two sizes.

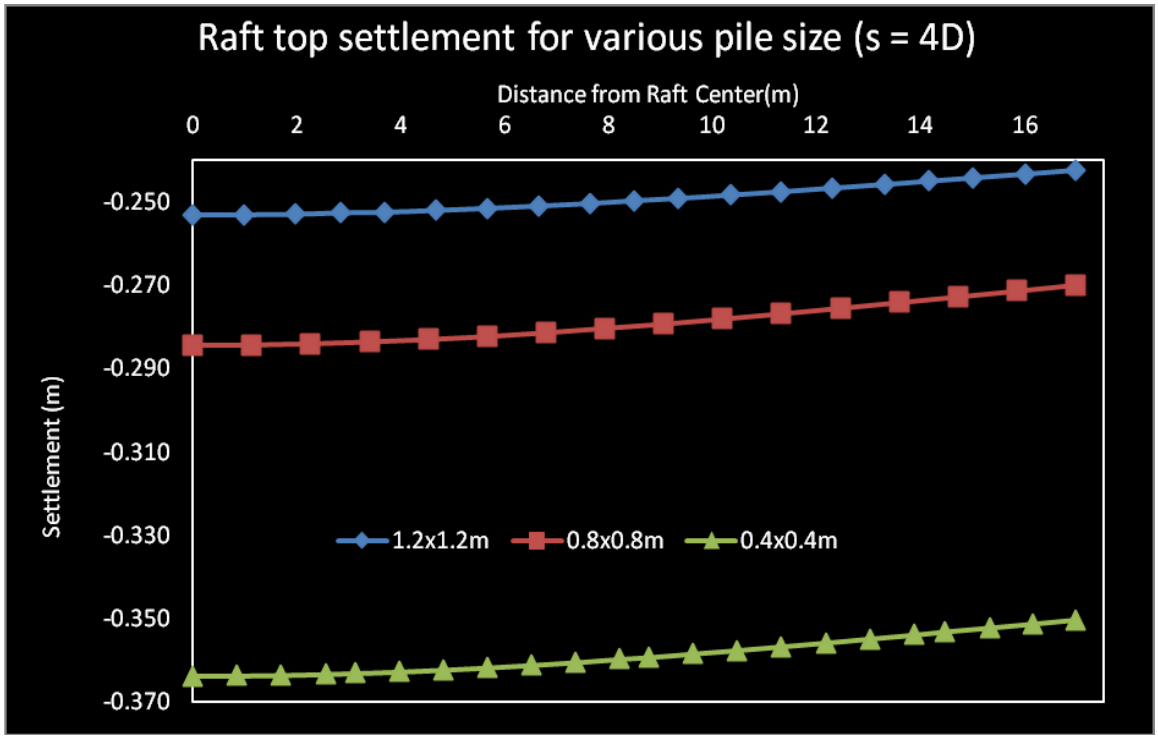

Figure 3.36 Raft top settlements along diagonal path for various pile size (s = 4D)

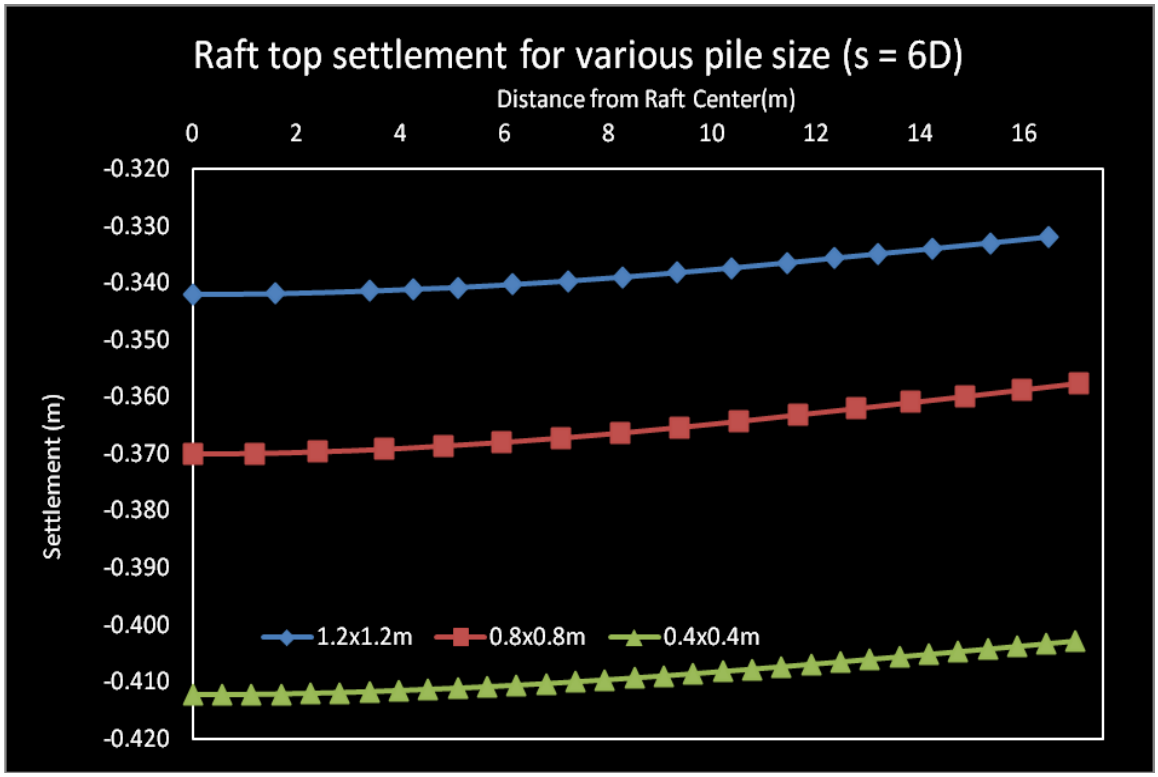

Figure 3.37 Raft top settlements along diagonal path for various pile size (s = 6D)

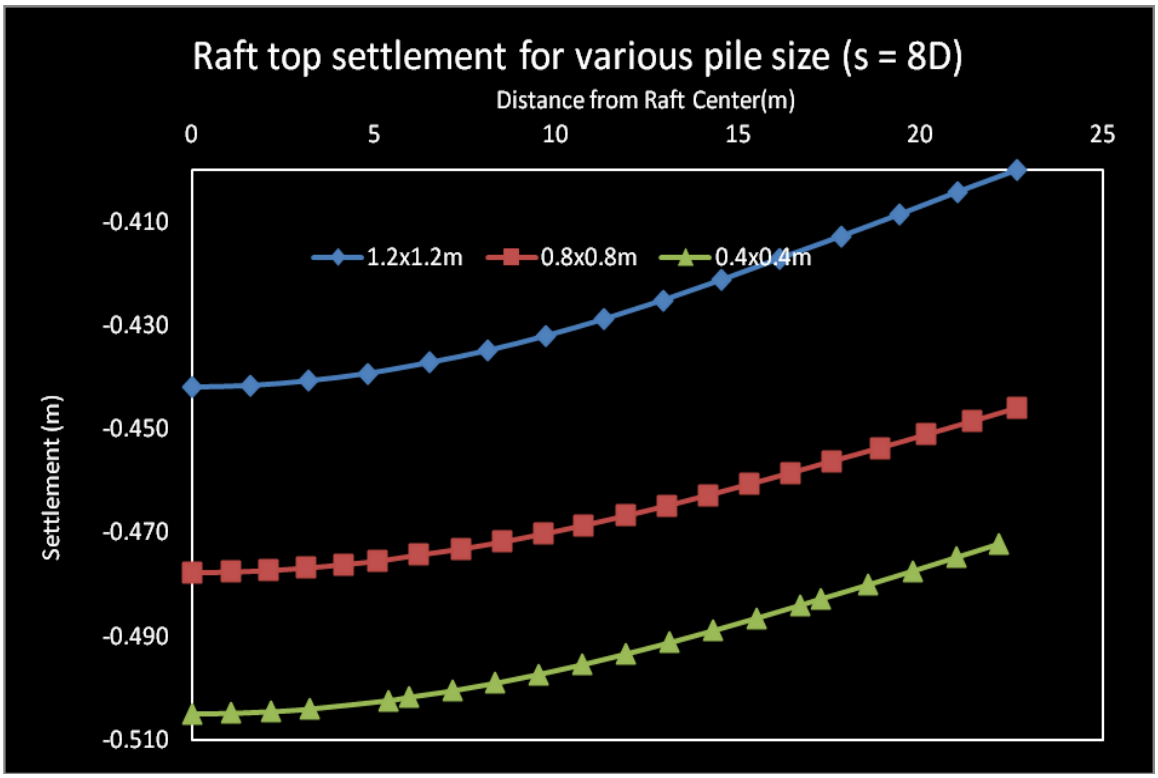

Figure 3.38 Raft top settlements along diagonal path for various pile size (s = 8D)

The raft centre settlements for varying pile sizes have been investigated for each case of 4D, 6D and 8D pile spacing. In each case, the centre point settlement is decreased with the increased pile sizes, as shown in figure 3.39. Table 3.10 below depicts the effective reduction in settlement with the increased pile sizes for each type of spacing. The settlement reduction rate for the same raft centre with increased pile size, again, varies with the pile spacing. Figure 3.39 dictates that the settlement reduction rate is steeper for smaller pile spacing and flatter for the larger pile spacing. It can be concluded therefore, the larger spacing of the piles reduces the effectiveness of increased pile sizes. This phenomenon is similar to the influences of pile length on settlement behavior. A cost

effective design strategy requires the optimization of length and cross-sectional area to reduce the settlement with minimum pile material usage.

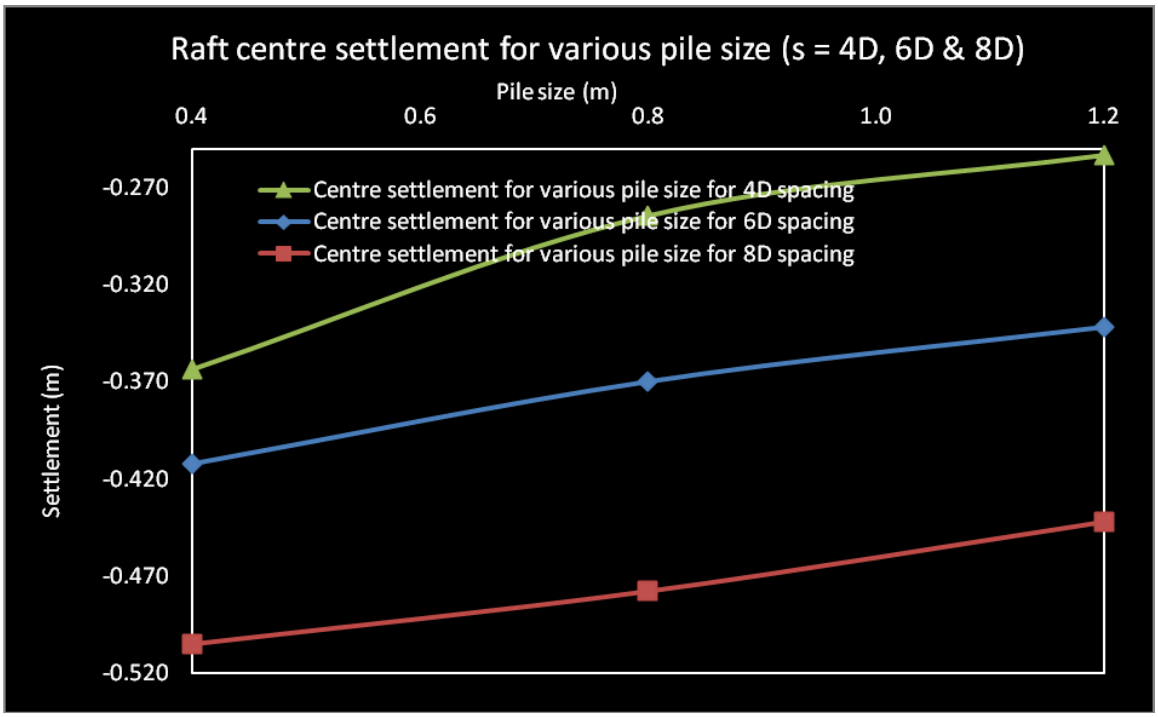

Figure 3.39 Raft centre settlement for various pile spacing

Table 3.10 Raft centre settlement for various pile size

Pile size (m)	0.4	0.8	1.2
Centre settlement for 4D spacing (m)	-0.364	-0.284	-0.253
Centre settlement for 6D spacing (m)	-0.412	-0.370	-0.342
Centre settlement for 8D spacing (m)	-0.505	-0.478	-0.442
Reduced settlement for 4D spacing (m)	-	0.080	0.031
Reduced settlement for 6D spacing (m)	-	0.042	0.028
Reduced settlement for 8D spacing (m)	-	0.027	0.036

The influence of pile size variation on the differential settlement of piled raft foundation has been investigated with the 3-D finite element model. The settlement difference between the raft centre and corner point has been taken into consideration for this

purpose. Figure 3.40 below depicts the differential settlement variation with varying pile sizes for the pile spacing of 4D, 6D and 8D. The differential settlement does not vary significantly with the pile size variation for 4D and 6D spacing and the variation patterns are same for these two types of pile spacing. However, the differential settlement is observed in a significant amount for the pile spacing of 8D. The different pattern of the change in differential settlement is also observed for the pile spacing of 8D (Figure 3.40). Table 3.11 summarizes the numerical values of the changes in differential settlement in tabular form.

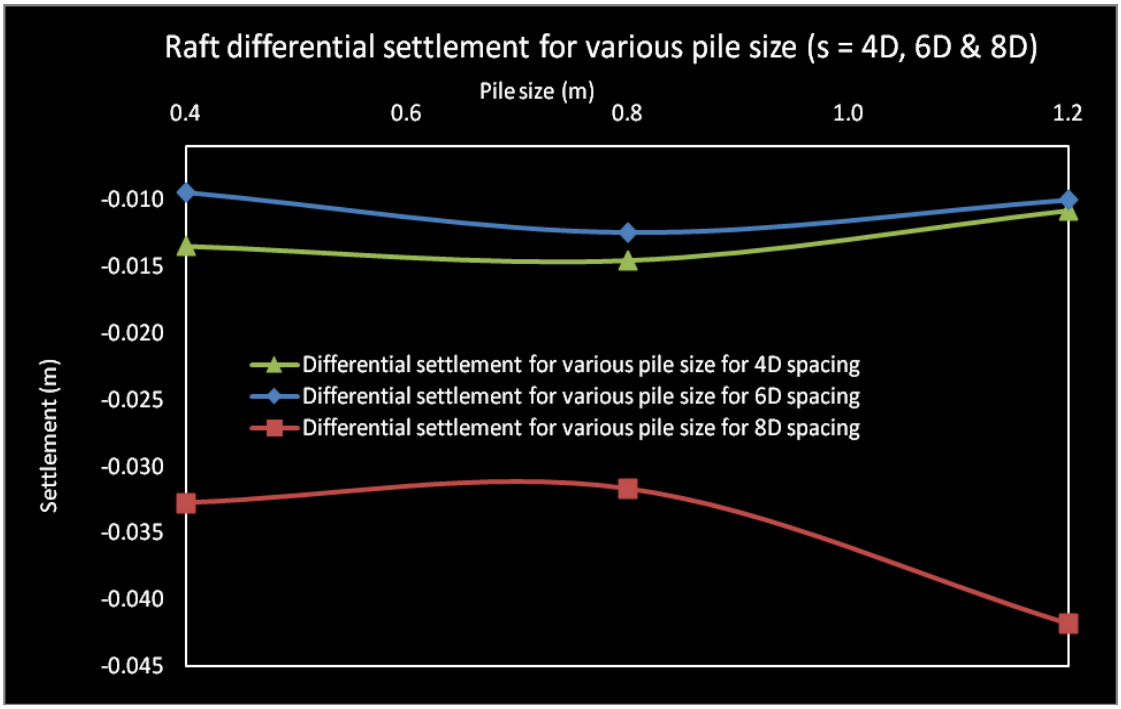

Figure 3.40 Raft differential settlements for various pile size

Table 3.11 Raft differential settlement for various pile size

Pile size (m)	0.4	0.8	1.2
Differential settlement for 4D spacing (m)	-0.013	-0.015	-0.011
Differential settlement for 6D spacing (m)	-0.009	-0.012	-0.010
Differential settlement for 8D spacing (m)	-0.033	-0.032	-0.042
Reduced differential settlement for 4D spacing (m)	-	-0.002	0.004
Reduced differential settlement for 6D spacing (m)	-	-0.003	0.002
Reduced differential settlement for 8D spacing (m)	-	0.001	-0.010

3.8 Influence of Raft Thickness or Raft Stiffness

The previous section signifies the raft stiffness has the influence on the structural integrity of the combined pile raft foundation. This structural component is sand-witched between the action reaction forces from the applied load and the soil bearing capacity. This action reaction interaction along with the punching shear tendency from pile or super structural column or any other concentrated load, has to be taken into account before setting the raft stiffness. For simplicity, for a 0.5MPa UDL on square rafts of 24x24m and of different thicknesses have been investigated to the raft thickness influences on pile raft foundation behavior. The material property is as mentioned in table 3.7 above. The modeling technique, boundary condition and analysis technique are as mentioned in the previous sections.

The numerical investigation output for varying raft thickness of 0.5, 1.0, 1.5, 2.0 and 2.5m, was plotted in the form of load settlement behavior of the piled raft foundation, as shown in figure 3.41 below. The raft top centre point settlement is plotted here for a typical pile spacing of 6D. The settlement profile of various thickness indicate that raft thickness of 1m or less yield a load settlement behavior, which is inferior to that of raft only footing of identical condition. This observation can be viewed by another plotting of settlements profile for various raft thickness (figure 3.42 below), subjected to an UDL of 0.3 MPa as reference. The plot implies that the settlements reduce sharply from a raft thickness of 1.0m to 1.5m and increase again after a raft thickness of 2.0m. The increased settlement after raft thickness of 2.0m is due to the increased self weight of increased raft thickness.

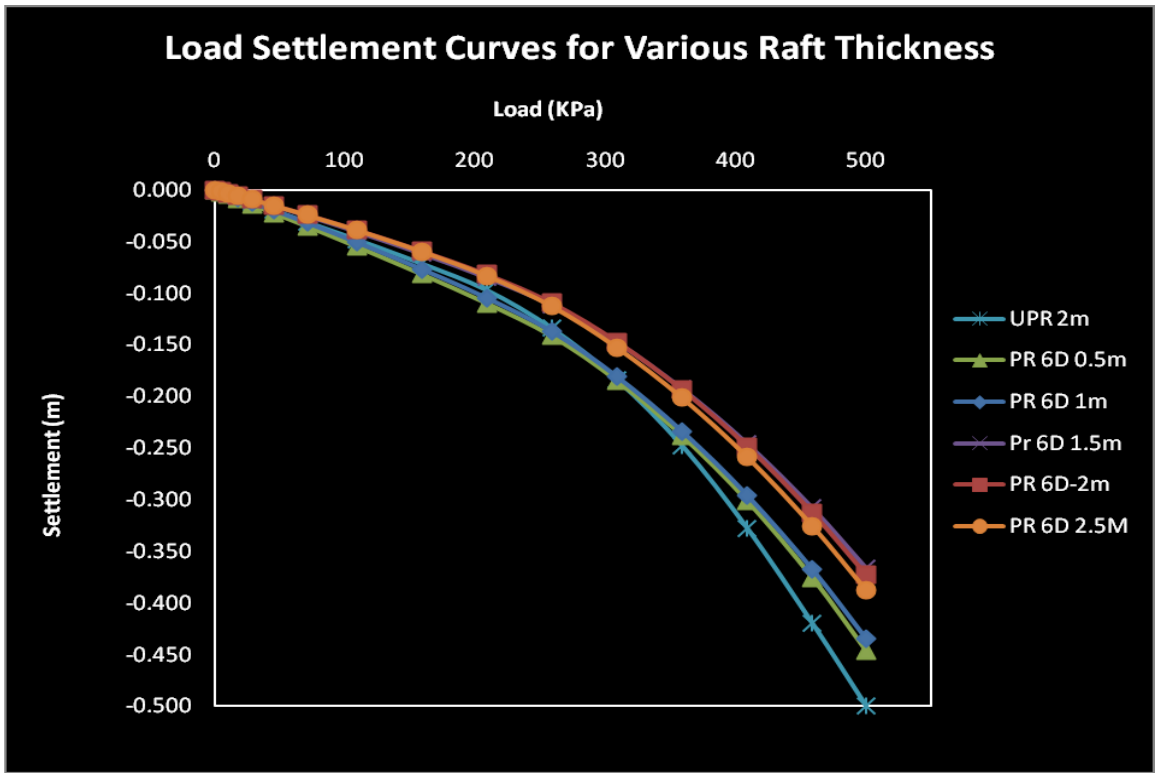

Figure 3.41 Raft centre settlement for various raft thickness

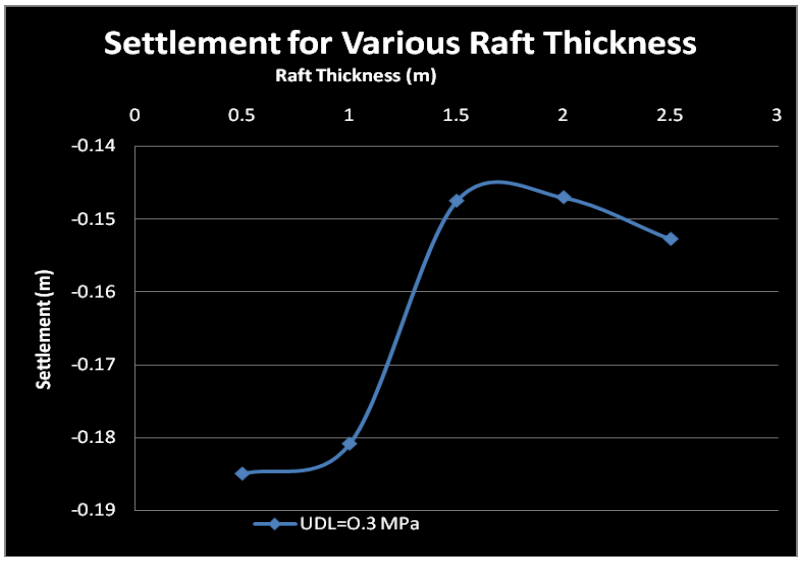

Figure 3.42 Raft centre settlement for 0.3MPa UDL and for various raft thickness

To observe the stiffness influence on the raft top settlement pattern, several investigations were performed. The objective is to find the sudden change in deflection due to inadequate stiffness of the raft. The raft top settlement along centre lines, centre piles and along diagonal piles were plotted for various raft thickness as shown in figure 3.31 to 3.35 below. These studies were performed on 24mx24m square raft of varying thicknesses with a pile spacing of 6D and subjected to a UDL of 0.5MPa. The abrupt changes in settlement profile are observed in the vicinity of piles, located at 3m and 9m from the centre of the 0.5m thick raft (figure 3.43). Obviously, this large differential settlement is the failure case of the raft, as it exceeds the concrete strain limit. The same is observed for 1.0m thick raft (figure 3.44), however, the changes are milder. For a raft thickness of 1.5m, the shape is rather regular and bowl shape deflection is observed (figure 3.45). The same is true for 2.0 and 2.5m thick raft as shown in figure 3.46 and 3.47 respectively, with an additional settlement caused by the additional self weight. However, the changes in differential settlement of incremental points are gradual for the 1.5m, 2.0m & 2.5m thick raft and the absence of abrupt changes in differential settlement for these thicker raft, confirms the non-failure state of raft component.

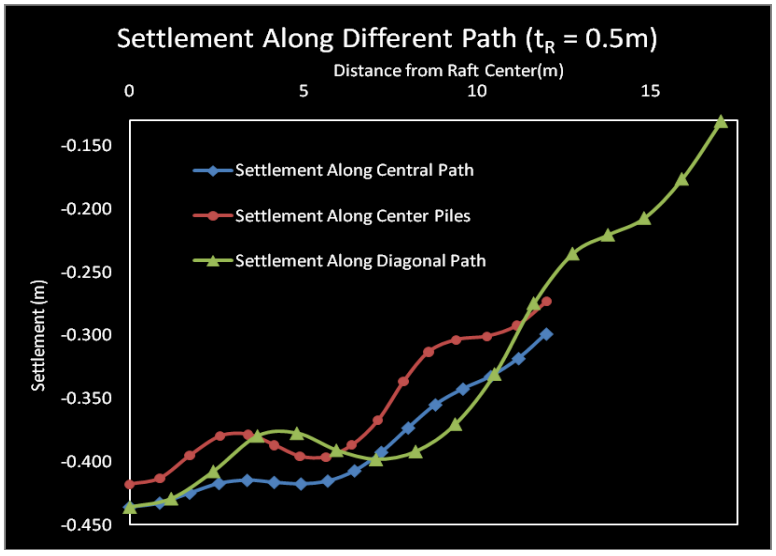

Figure 3.43 Raft top settlement profile for 0.5m thick raft

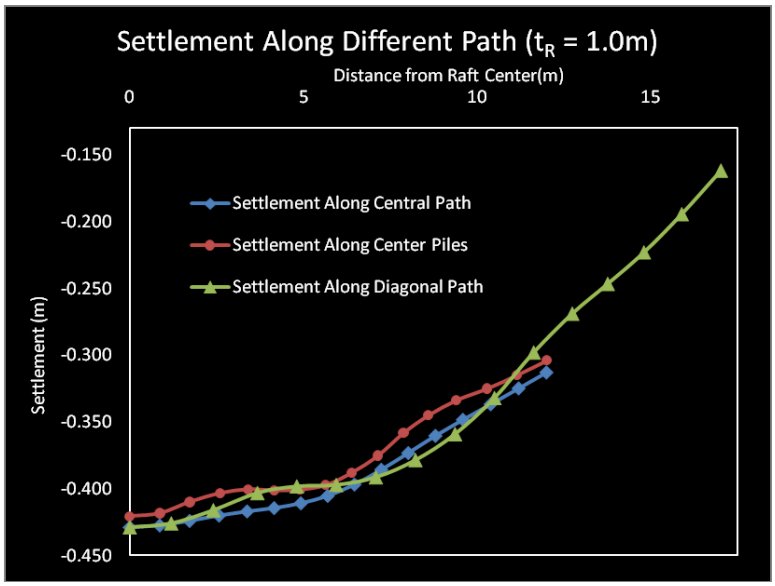

Figure 3.44 Raft top settlement profile for 1.0m thick raft

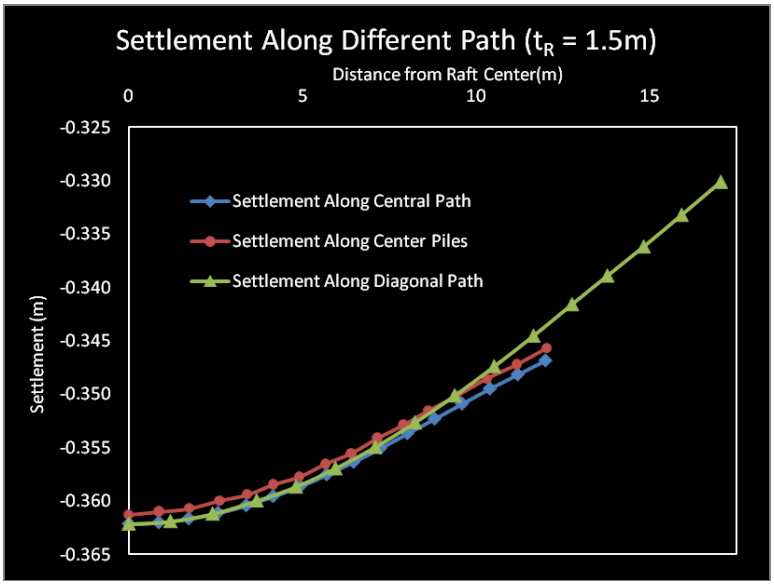

Figure 3.45 Raft top settlement profile for 1.5m thick raft

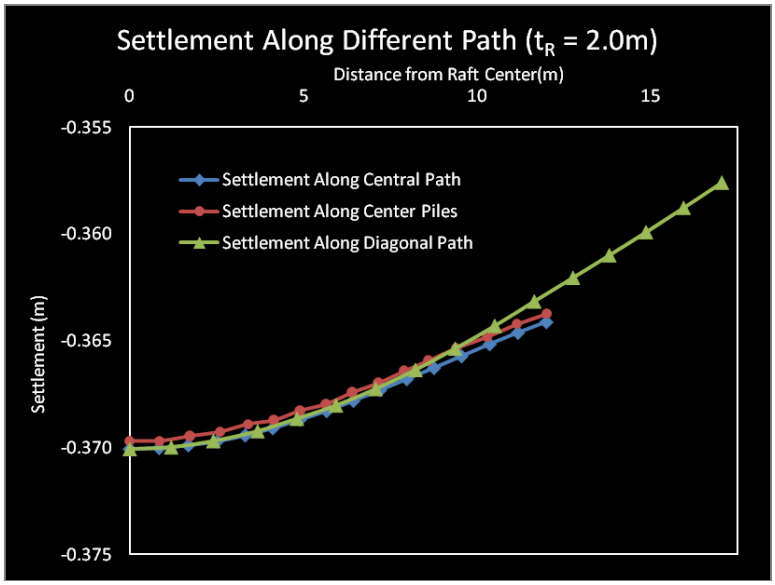

Figure 3.46 Raft top settlement profile for 2.0m thick raft

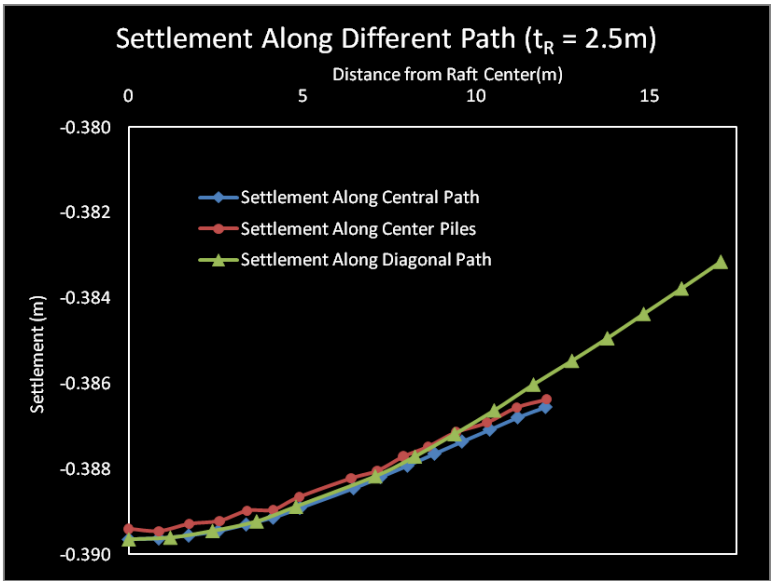

Figure 3.47 Raft top settlement profile for 2.5m thick raft

Another set of investigation, in this context, was performed to observe the influence of raft thickness on the maximum differential settlement magnitudes. The previous investigations and the material mechanics theory dictates that the maximum differential settlements occur between the raft centre and its corner point. Therefore, the settlements of these two points of various raft thickness, have been plotted as shown in figure 3.48 and tabulated in table 3.12. Figure 3.48 and table 3.12 indicate that the raft centre settlement increases with the increased raft thickness and the differential settlement does not change after a raft thickness of 1.5m. The tabulated value also indicates that the strain, corresponds to a raft thickness lesser than 1.5m, is larger than the concrete crushing strain value of 0.003 [ACI 318-02]. In contrast, the differential settlement for the same points of 2.0m and 2.5m thick raft, are only 6mm and 3mm respectively; which are equivalent to the strain value of 0.0004 and 0.0002 respectively. Figure 3.48 depicts the influences and their profiles in graphical form and dictates that the raft thickness of 2.0m is the best for this configuration of pile raft and for the properties of relevant components.

Table 3.12 Raft top differential settlement for various raft thickness

Raft thickness (m)	Settlement (m)			Strain
	Centre	Corner	Differential	
0.50	-0.2987	-0.13005	-0.16866	0.01
1.00	-0.31273	-0.16154	-0.15118	0.009
1.50	-0.34684	-0.33006	-0.01678	0.001
2.00	-0.36411	-0.35759	-0.00652	0.0004
2.50	-0.38655	-0.38315	-0.00339	0.0002

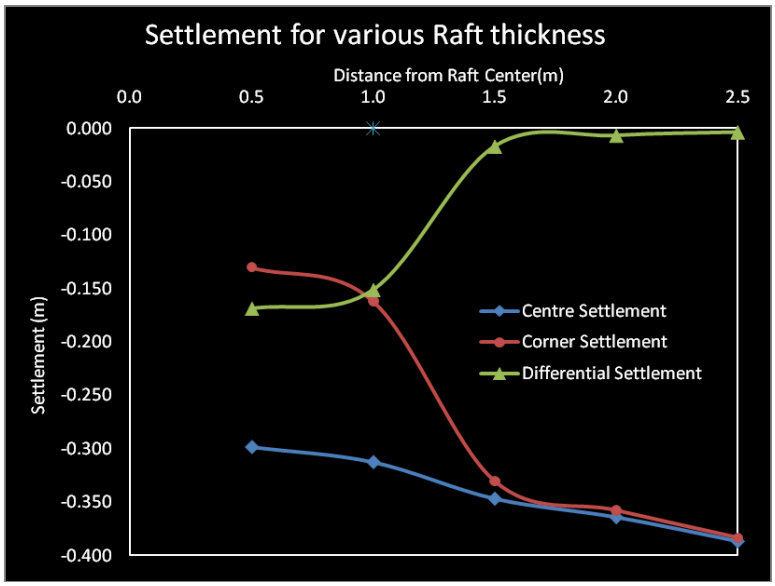

Figure 3.48 Raft top centre, corner and differential settlement profile for various raft thickness

3.9 Influence of Angle of Internal Friction (φ)

Besides the influence of the geometric properties, discussed in section 3.5 to 3.8 above, the mechanical properties (e.g elasticity, plasticity etc.) of the foundation materials have significant influences on the foundation behavior. The concrete elastic modulus is thousand times greater than the soil modulus of elasticity. Therefore, the influence of concrete elastic modulus needs not to be investigated. The soil stiffness, on the other hand, is mainly influenced by its cohesion (c) and angle of internal friction (φ). In this section the influence of angle of internal friction on the settlement behavior of pile raft foundation is depicted.

Three models have been simulated for internal frictional angle of 10^o, 15^o and 20^o, in ABAQUS 3D finite element analysis platform, in order to study the influences. The modified Drucker-Prager cap plastic model is used to model the soil plasticity (discussed in section 3.2.1) and is valid for the K (the shape parameter of yield surface F_s) value of $0.778 \leq K \leq 1$). This in turns dictates that this model is valid for the angle of internal friction up to 22^o (can be calculated from equation 3.30). The cap plasticity parameters β, d and K are calculated from equations 3.29, 3.30 and 3.27 respectively for various values of soil angle of internal friction (φ') as shown in table 3.13 below. The rest parameters and geometry are same as mentioned in the previous section but the raft thickness is fixed to 2.0 meter.

Table 3.13 Cap plasticity parameters for various ϕ'

ϕ' (Degree)	10	15	20
β (Degree)	20.21	29.38	37.67
D (Pa)	41819	42346	42425
K	0.891	0.841	0.795

The simulated output in the form of load settlement plot is shown in figure 3.49 below. A large reduction is observed with the increasing internal frictional angle from 10^o to 15^o. This change is not so sharp for the next transition from 15^o to 20^o. This profile can be explained well from figure 3.50 below.

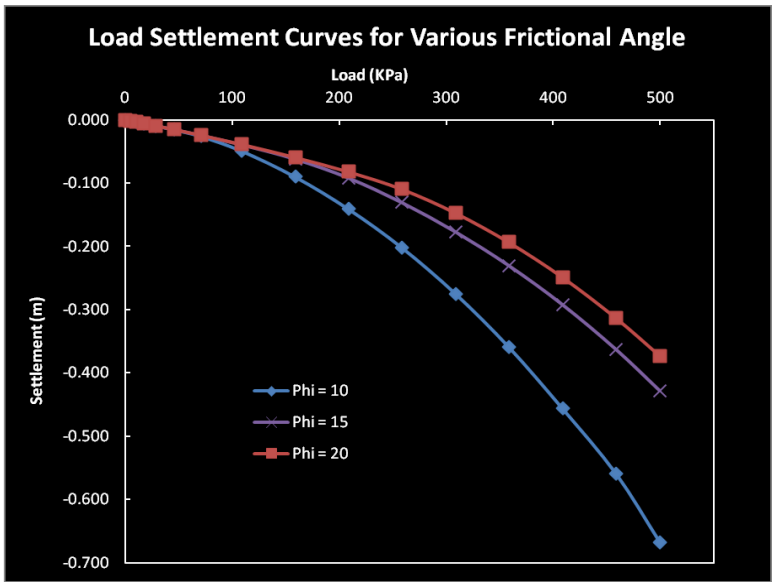

Figure 3.49 Load settlement curve for various internal frictional angle of soil

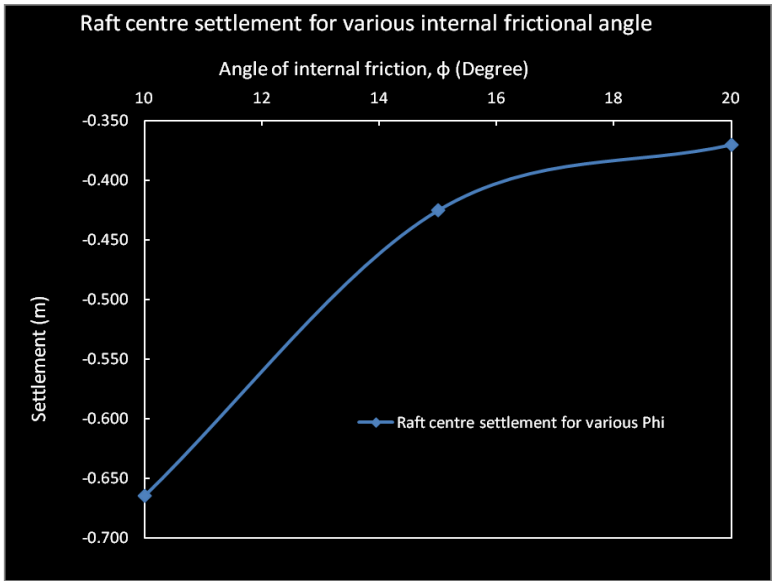

Figure 3.50 Raft top centre settlement for various internal frictional angle of soil

To observe the raft top settlement profile and thereby to estimate the differential settlement, the settlement along the raft central axis, along the top of central group of pile

and along diagonal path were simulated for each of the 10^o, 15^o and 20^o of φ' value (figure 3.51, 3.52 and 3.53 below). In all cases the raft top takes the bowl shape form after settlement and the curvature rate diminishes with the reduced angle of internal friction.

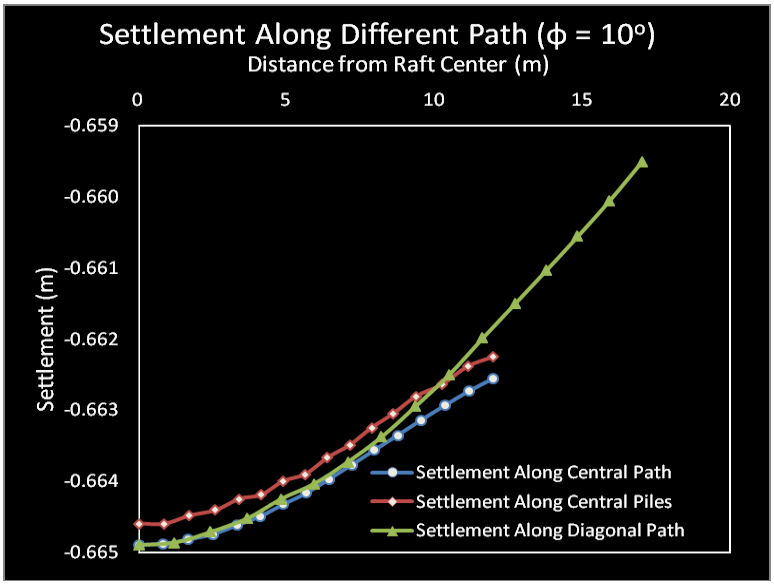

Figure 3.51 Raft top settlement along different path for φ' = 10^o

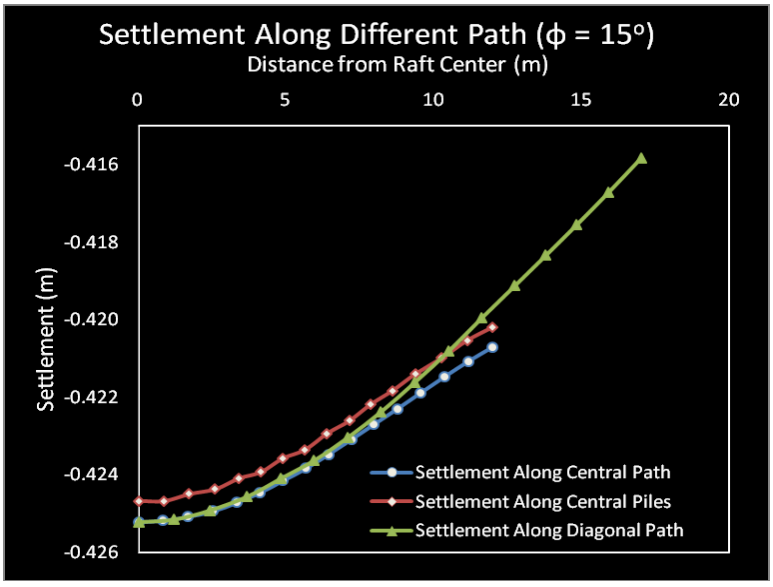

Figure 3.52 Raft top settlement along different path for φ' = 15^o

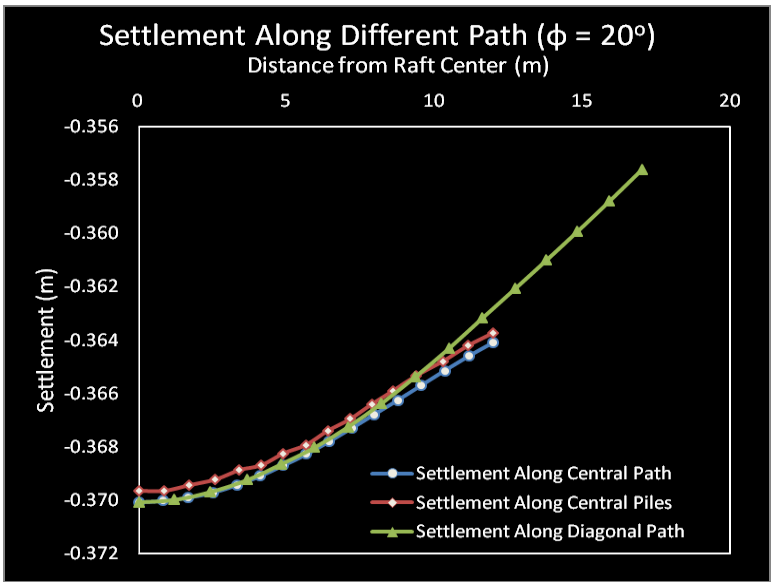

Figure 3.53 Raft top settlement along different path for φ ' = 20°

The differential settlement between the raft top centre and corner point, for various angle of internal friction, is shown in table 3.14 below. A lower value of differential settlement in the raft is observed for the lower value of soil internal frictional angle, while it is higher for its greater value. This is because the higher φ provides greater stiffness to the soil that causes the stiffer raft to settle more in the center than the corner point. The change in differential settlement with increasing φ is shown in figure 3.61 below.

Table 3.14 Differential settlement for various internal frictional angle of soil

Angle of internal friction, ϕ	Settlement (m)		
	Centre	Corner	Differential
10	0.665	0.660	0.005
15	0.425	0.416	0.009
20	0.370	0.358	0.012

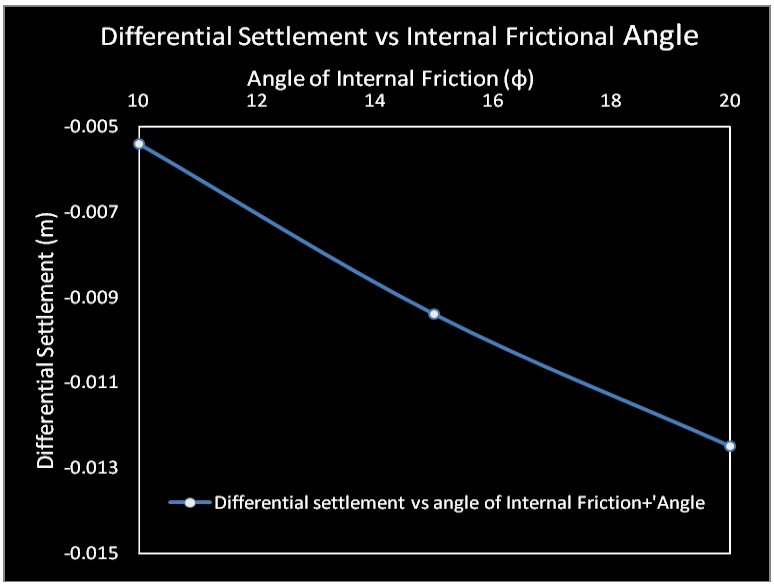

Figure 3.54 Differential settlement vs internal frictional angle

3.10 Influence of Soil Cohesion (c)

Cohesion is the dominant mechanical property of clayey soil that provides resistance to deformation. To study its influence on the pile raft foundation behavior, four models have been simulated for the cohesion value of 10, 20, 30 & 40 kPa. The corresponding cap plasticity parameters d, calculated from equation 3.30, are 21212, 42425, 63637 and 84849 kPa respectively. Since k and β are φ dependent variables, they remain constant for this set of study to 0.795 and 37.67 (determined from equation 3.27 and 3.29). The geometric configuration and properties of the foundation are same as in previous section.

The load settlement plot for the various soil cohesion values as shown in figure 3.55 below indicates that the settlement reduces with increased cohesion value. Figure 2.56 shows that the change in settlement reduction rate is sharp for lower value of cohesion

and has a diminishing tendency for progressive higher values of cohesion. This property is helpful to the designer to fix the allowable settlement corresponding to the cohesion obtained from experimental data.

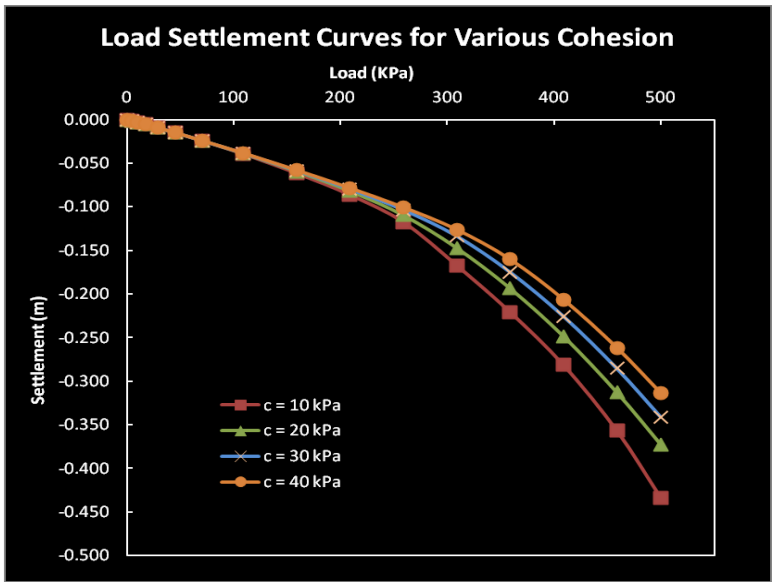

Figure 3.55 Load settlement curves for various cohesion

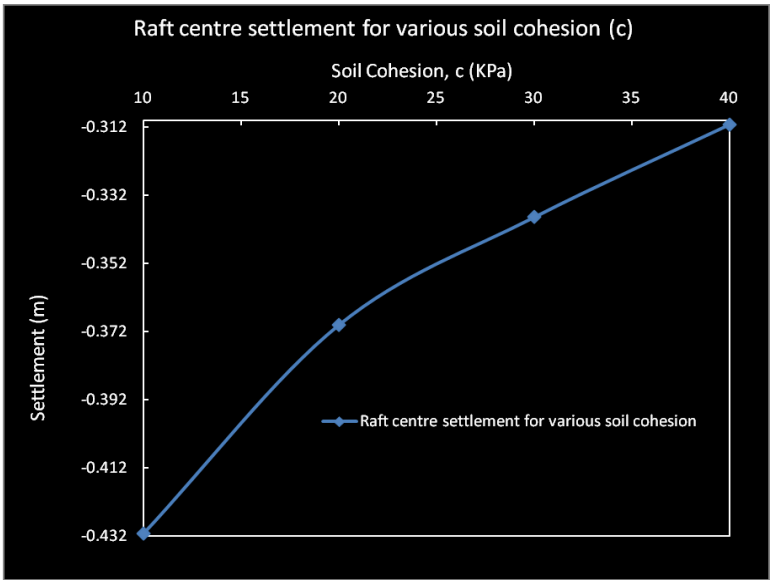

Figure 3.56 Raft centre settlement for various soil cohesion

The influence of the soil cohesion on raft top surface is observed from the simulated settlement output for various cohesion values of soil. To depict the deflected raft top pattern, settlement along the raft central axis, along the top of central group of pile and along diagonal path were plotted for each of the 10, 20, 30 and 40 kPa of c ' value (figure 3.57, 3.58, 3.59 and 3.60 below). In all cases the deflected raft top takes the bowl shape form and the rate of change in settlement decreases with the increased cohesion value.

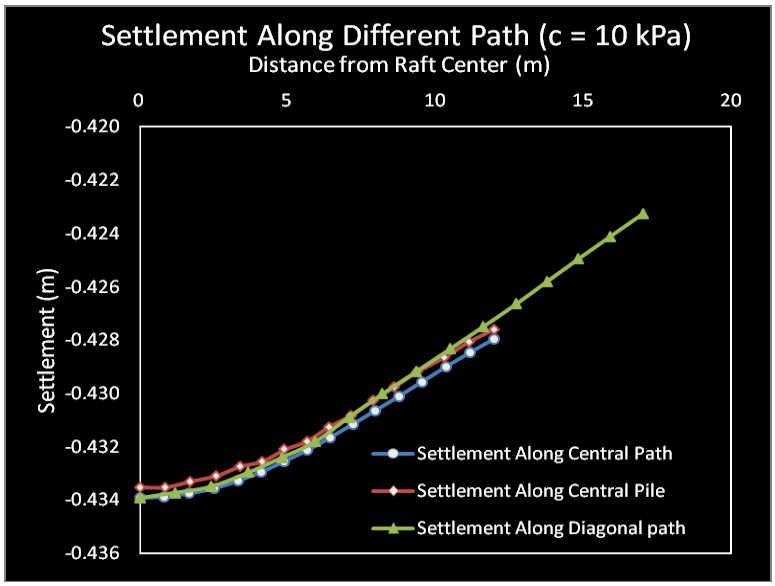

Figure 3.57 Raft top settlement along different path for c = 10 kPa

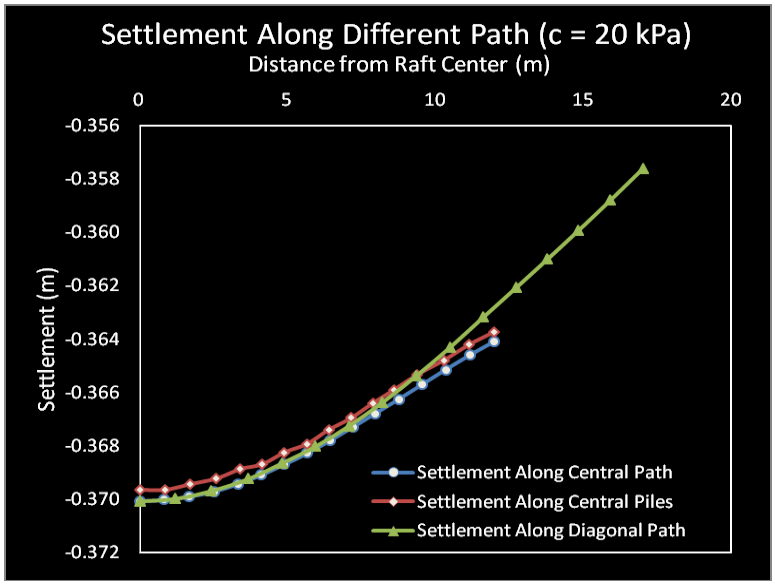

Figure 3.58 Raft top settlement along different path for c = 20 kPa

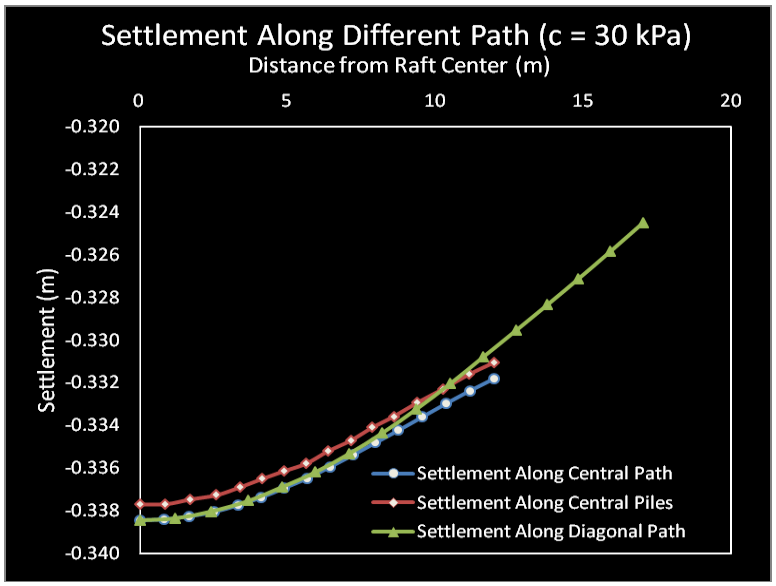

Figure 3.59 Raft top settlement along different path for c = 30 kPa

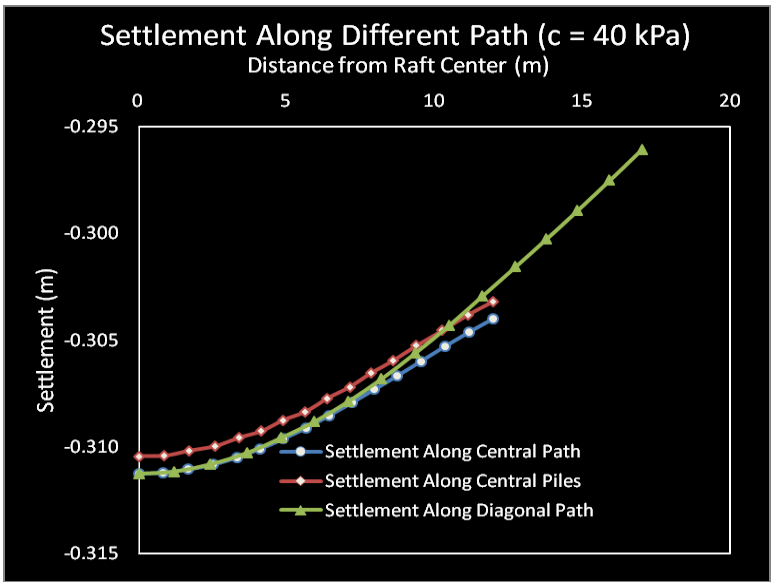

Figure 3.60 Raft top settlement along different path for c = 40 kPa

The differential settlement between the raft top centre and corner point, for various soil cohesions, is shown in table 3.15 below. A lower value of differential settlement in the raft is observed for the lower value of soil cohesion, while it is higher for the greater

value of c. This is because the higher c provides greater stiffness to the soil that causes the stiffer raft to settle more in the center than the corner point. The change in differential settlement with increasing c is shown in figure 3.61 below.

Table 3.15 Differential settlement for various cohesion value of soil

Soil cohesion, c (kPa)	Settlement (m)		
	Centre	Corner	Differential
10	0.434	0.423	0.011
20	0.370	0.357	0.013
30	0.339	0.325	0.014
40	0.311	0.296	0.015

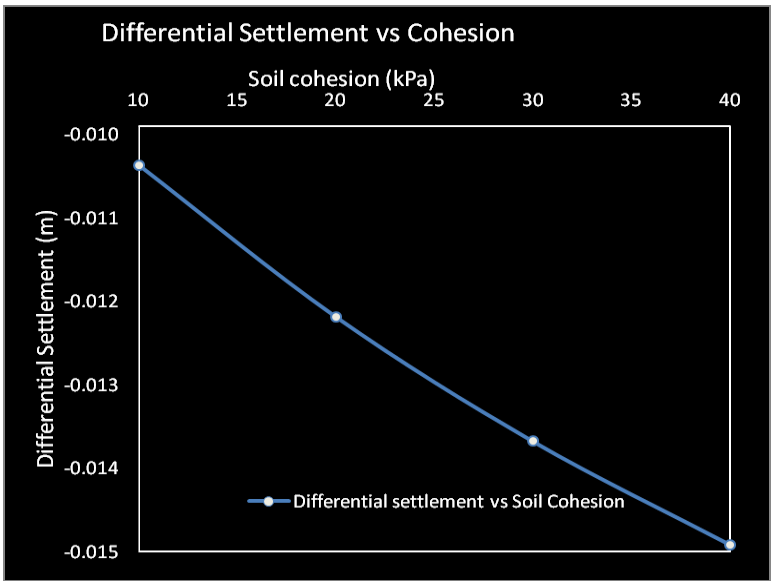

Figure 3.61 Differential settlement vs soil cohesion

3.11 Load Sharing Between Pile Group and Raft

The study in the previous section clearly focussed on the necessity of estimating the load resistance of the structural components of this type of foundation. The design formulation for the pile raft foundation entirely depends on the accurate prediction of the load sharing. This load sharing again depends on the soil property, raft geometry, pile geometry (diameter, length) and its spacing.

Investigation was made for a soil continuum having the property mentioned in table 3.2 for various spacing, ranging from 2D to 7D, keeping all other parameter constant. The load shared by the raft and pile group is shown in tabular and graphical form below (table 3.16 and figure 3.62).

Table 3.16 Load sharing between Raft and Pile group

Pile Spacing	Applied UDL (MPa)	Load Shared (MPa)		Load Shared (%)	
		Raft	Piles	Raft	Pile
7D	0.5	0.337	0.163	67%	33%
6D	0.5	0.330	0.170	66%	34%
4D	0.5	0.183	0.317	37%	63%
3D	0.5	0.073	0.427	15%	85%
2D	0.5	0.068	0.432	14%	86%

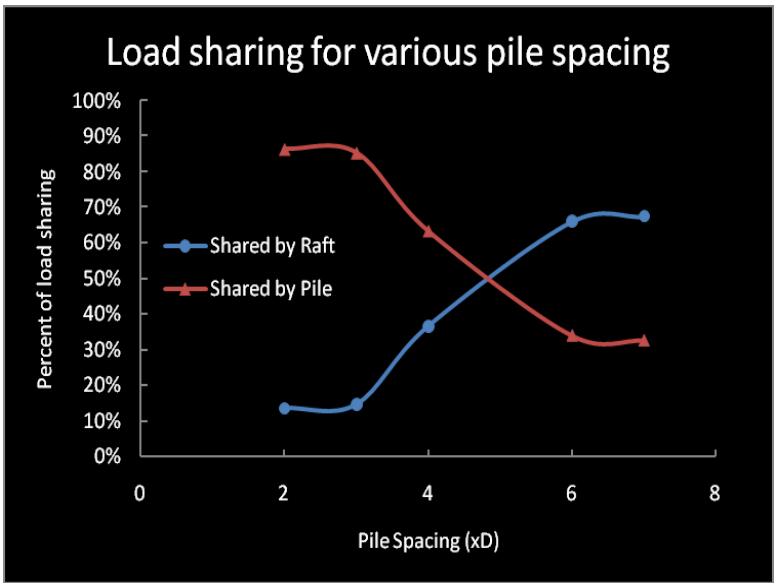

Figure 3.62 Load sharing between raft and piles for various pile spacing

The figure and table above indicates that for a pile spacing of 2D, the pile group (consists of 144 piles) withstand the major portion (86%) of the applied load and the reverse scenario is observed with the increased pile spacing. A nearly flat slope of the load sharing curve is observed at 2D & 3D (64 piles) as well as 6D & 7D spacing, while a sharp change is noticed in between 3D and 6D. Since, the previous study, in section 3.5, dictates that the pile spacing greater than 7D is worse than a raft only foundation (figure 3.25), no attempt therefore, was made in this study for a pile spacing greater than 7D. This load sharing study implies that a 50-50 percentage of load sharing between the pile group and raft can be achieved for a pile spacing of 5D. Figure 3.49 is a versatile tool for the designer, to select the optimum geometric parameter of the structural components.

3.12 Summary

The various components and the process of developing the numerical model in 3-D finite element code have been detailed in this chapter. To reduce the resource cost, the ABAQUS axi-symmetric facility of 3-D finite element analysis has been used. The optimum and careful technique is used in selecting the element, setting the boundary limit, partitioning and net discretization, step time increment and in setting up the geostatic condition by introducing initial stress to the soil continuum. The influence of the geometric properties of the foundation components and the mechanical properties of soil, on the foundation behavior have been simulated and detailed in this chapter. This parametric study provides the basis of developing the analytical models, described in the following chapter.

Chapter 4

Analytical Model

4.1 Introduction

The three dimensional numerical simulation of the piled raft foundation for various configuration and stiffness in the previous chapter indicates that the raft centre settles more than the corner. It gives a bowl shape deflection pattern of the raft of sufficient stiffness. From the obtained deflected shapes of the raft top, analytical models are developed in this chapter and calibrated with the respective numerical models to finalize the analytical models.

This chapter is composed of the development of three analytical models and their validations. The first one is the load sharing model that is capable of estimating the load portion shared by the raft and pile group for various geometric and loading configurations. The second one is the maximum settlement model and the third one is the differential settlement model. Each of these models has been validated with the research data available in various publications.

4.2 Analytical Model for Load Sharing

4.2.1 Model Development

The numerical load sharing study in the previous chapter (section 3.11) indicates that for smaller pile spacing the major load proportion is carried by the pile group and for larger pile spacing the major load proportion is carried by the raft, this is in good agreement

with Randolph (1998). Therefore, to proceed for the development of load sharing model, Randolph approach is taken into consideration.

The Randolph (1983) development for a single pile with circular cap unit is applicable to piled raft having a pile group of more than one pile. To extend this single pile cap unit theory to pile group with raft, modification to the pile raft interaction factor (α_{rp}) needs to be done. Rewriting the equation (2.8) of chapter 2 by replacing the pile cap stiffness (K_{pc}) by the pile raft stiffness (K_{pr}) of pile raft foundation as

$$k_{pr} = \frac{k_p + (1 - 2\alpha_{rp})k_r}{1 - \alpha_{rp}{}^2 k_r / k_p} \tag{4.1}$$

Where, K_p and K_r are the stiffness's of pile group and raft in isolation, i.e the separate calculation for pile group without raft and the raft without pile group need to be performed by means of suitable theory. Several theories are available to estimate both the pile group and raft stiffness in isolation. For K_p, the theory of Randolph & Wroth (1978, 1979), extended by Chow (1986) and Fleming et al. (1992), is most popular. For this work, the equation provided by Randolph & Wroth (1978) for this purpose, is used as

$$k_p = \frac{E_p R_a}{E_s} \tag{4.2}$$

Where, E_p is the elastic modulus of pile material, E_s is the elastic modulus of surrouding soil or more precisely an average secant deformation modulus of soils along the pile shaft. R_a is the ratio of pile section to area bounded by pile outer circumference and is expressed as

$$R_a = \frac{A_1}{A_2}$$

Where, A_1 = average area of pile and

A_2 = Area of pile section

For the analysis of this work the rigid pile will be considered for which $R_a = 1$, so the pile stiffness equation reduces to

$$k_p = \frac{E_p}{E_s} \tag{4.3}$$

Similarly, for raft stiffness K_r, the equation for rigid raft by Brown (1975) has been used in this work and the equation is

$$k_r = \frac{4E_r B_r t_r^{\,3}(1-v_s^{\,2})}{3\pi E_s L_r^{\,4}(1-v_r^{\,2})} \tag{4.4}$$

Where, E_r, L_r, B_r, t_r, v_r are raft modulus of elasticity, length, breadth, thickness, Poisson's ratio and E_s, v_s are soil modulus of elasticity and Poisson's ratio respectively.

The load sharing equation for the pile group by Randolph is

$$P_p = \frac{\left[1-k_r(\alpha_{rp}/K_p)\right]w_{pr}}{1/k_p - k_r(\alpha_{rp}/k_p)^2} \tag{4.5}$$

The above equation can be simplified by replacing w_{pr} with P/k_{pr} as below

$$P_p = \frac{\left(k_p - k_r\alpha_{rp}\right)}{1-\alpha_{rp}^{\,2}k_r/k_p}.\frac{P}{k_{pr}} \tag{4.6}$$

$$\frac{P_p}{P_p + P_r} = \frac{k_p - k_r \alpha_{rp}}{k_{pr}(1 - \alpha_{rp}^2 k_r / k_p)} \qquad \text{[Since, } P = P_p + P_r\text{]} \tag{4.7}$$

Similarly, the load sharing equation for raft can be calculated as

$$P_r = \frac{\left[(k_r / K_p) - k_r(\alpha_{rp} / K_p)\right] w_{pr}}{1/k_p - k_r(\alpha_{rp}/k_p)^2} \tag{4.8}$$

$$P_r = \frac{(1 - \alpha_{rp})}{1/k_r - \alpha_{rp}{}^2 / k_p} w_{pr} \tag{4.9}$$

$$P_r = \frac{(1 - \alpha_{rp})}{1/k_r - \alpha_{rp}{}^2 / k_p} \cdot \frac{P}{K_{pr}} \tag{4.10}$$

$$\frac{P_r}{P_p + P_r} = \frac{(1 - \alpha_{rp})}{K_{pr}/k_r - K_{pr}\alpha_{rp}{}^2 / k_p} \tag{4.11}$$

The raft pile interaction factor (α_{rp}) is then calculated from its basic definition in stiffness matrix as follows

$$\begin{bmatrix} 1/k_p & \alpha_{pr}/k_r \\ \alpha_{rp}/k_p & 1/k_r \end{bmatrix} \begin{bmatrix} P_p \\ P_r \end{bmatrix} = \begin{bmatrix} w_p \\ w_r \end{bmatrix} \tag{4.12}$$

The settlement of pile (w_p) and raft (w_r) are the same at their interface and considered as the combined pile raft settlement (w_{pr}). Therefore, the raft pile interaction factor (α_{rp}) can be obtained from equation (4.12) as

$$\alpha_{rp} \frac{P_p}{k_p} + \frac{P_r}{k_r} = w_r = w_{pr} \tag{4.13}$$

$$\alpha_{rp} = \frac{k_p}{P_p}(w_{pr} - \frac{P_r}{k_r}) \tag{4.14}$$

In a similar fashion the pile raft interaction factor (α_{pr}) can be calculated as

$$\frac{P_p}{k_p} + \alpha_{pr}\frac{P_r}{k_r} = w_p = w_{pr} \tag{4.15}$$

$$\alpha_{pr} = \frac{k_r}{P_r}(w_{pr} - \frac{P_p}{k_p}) \tag{4.16}$$

The following steps are to be followed to develop the interaction chart

01. Obtain the value of k_p and k_r from equation (4.3) and (4.4) above

02. Assume a value of α_{rp} and find the value of k_{pr} from equation (4.1) above

03. Obtain the load carried by pile and raft from equation (4.5) and (4.9) respectively

04. Use equation (4.14) to obtain the actual value of α_{rp}

05. The chart was developed for various K_{pr}, pile and raft configuration (both geometric and mechanical)

06. The chart for the raft pile interaction for this work was developed for the value of k_p and k_r from the numerical analysis of individual pile group and raft instead of equation (4.3) and (4.4) above. In the next step the w_{pr}, P_p and P_r are determined from the numerical analysis of combined pile raft and α_{rp} or α_{pr} are calculated from equation (4.14) and (4.16) respectively.

4.2.2 Validation of the Interaction Factor

Before developing the pile raft interaction chart on the basis of 3D FE analysis by ABAQUS and for actual pile spacing variation, rather than the single pile cap unit interaction factor developed by Clancy et al. (1993), it is essential to validate the numerical model. The developed interaction chart of Clancy et al. (1993) is on the basis

of single pile with cap of various diameters to indicate the pile spacing (figure 4.1). For the same parameters (table 4.1), the developed interaction factors for same cap sizes and pile dimensions of Clancy et al. were developed and depicted in figure 4.3. The interaction factors developed by Clancy et al. (1993) is depicted in figure 4.2 in order to validate with that obtained by current analysis as shown in figure 4.3. The comparison clearly shows the identical characteristics and a very good agreement in between them.

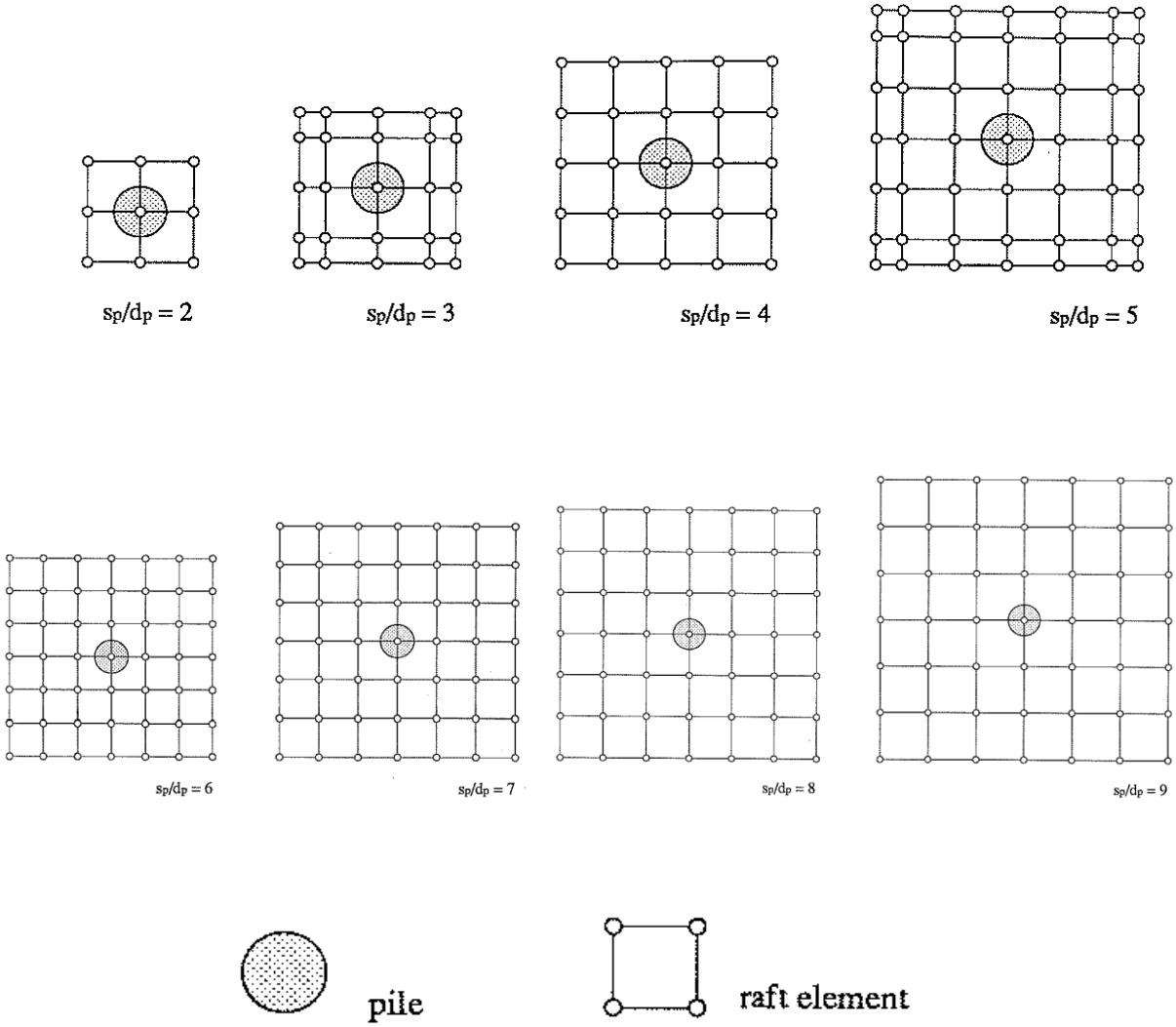

Figure 4.1 Single pile cap configurations for various spacing

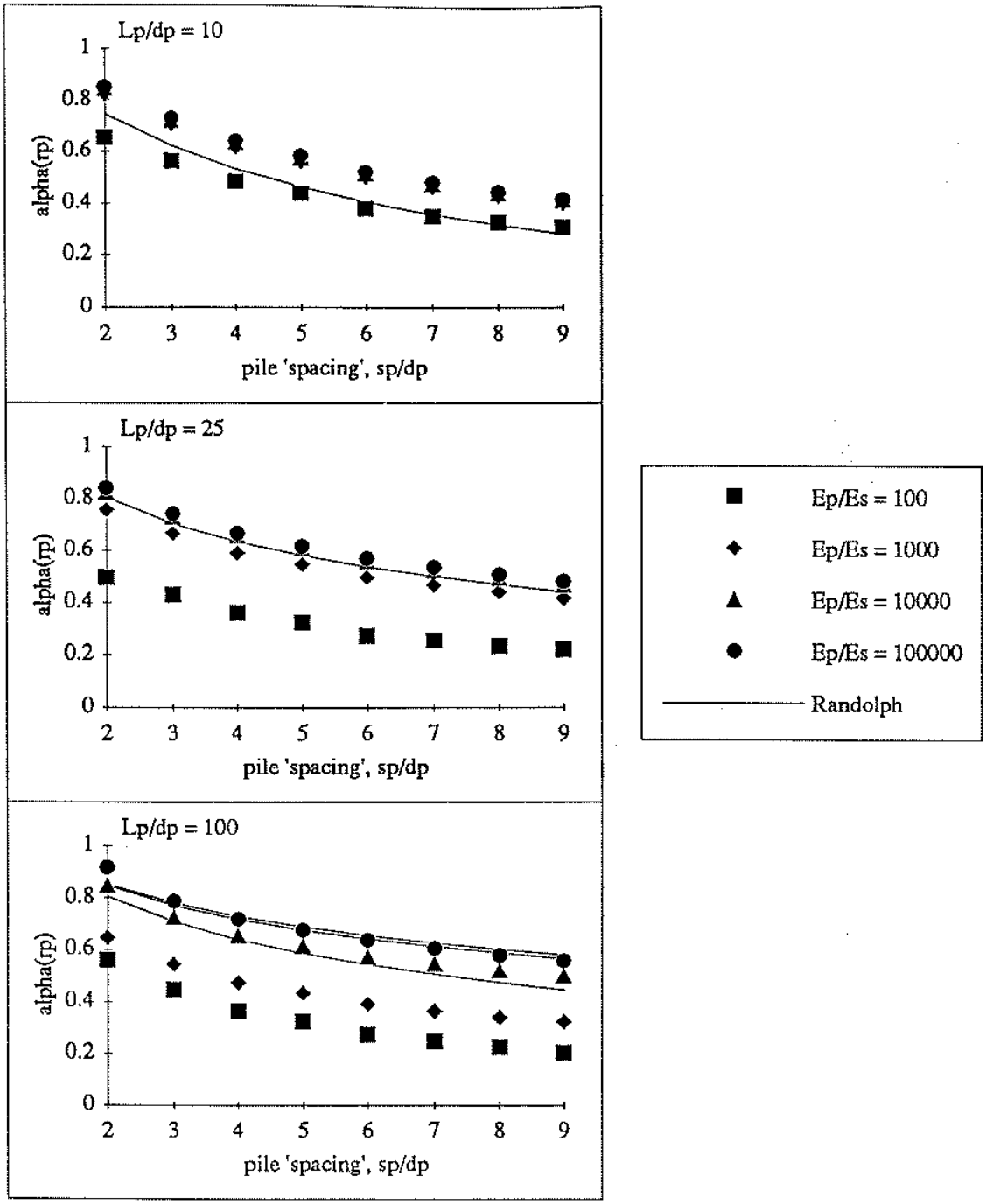

Figure 4.2 Single pile cap interaction factor by Clancy et al. (1986)

Table 4.1 Data from Clancy et al. (1993) used for validation purpose

Soil		Pile		Raft		Dimensionless Group	
E_s	250 Mpa	E_p	$25x10^3$MPa - $25x10^6$MPa	E_r	10^{10}MPa	$K_p = E_p/E_s$	10^2 - 10^5
v_s	0.5	v_p	0.3	v_r	0.3	$K_{r(Brown)}$	
		d_p	1.0 m	t_r	1.0 m	L_p/d_p	10 - 100
		L_p	10 - 100 m	B_r	2 - 8 m	S_p/d_p	2 - 8
						L_r/B_r	1

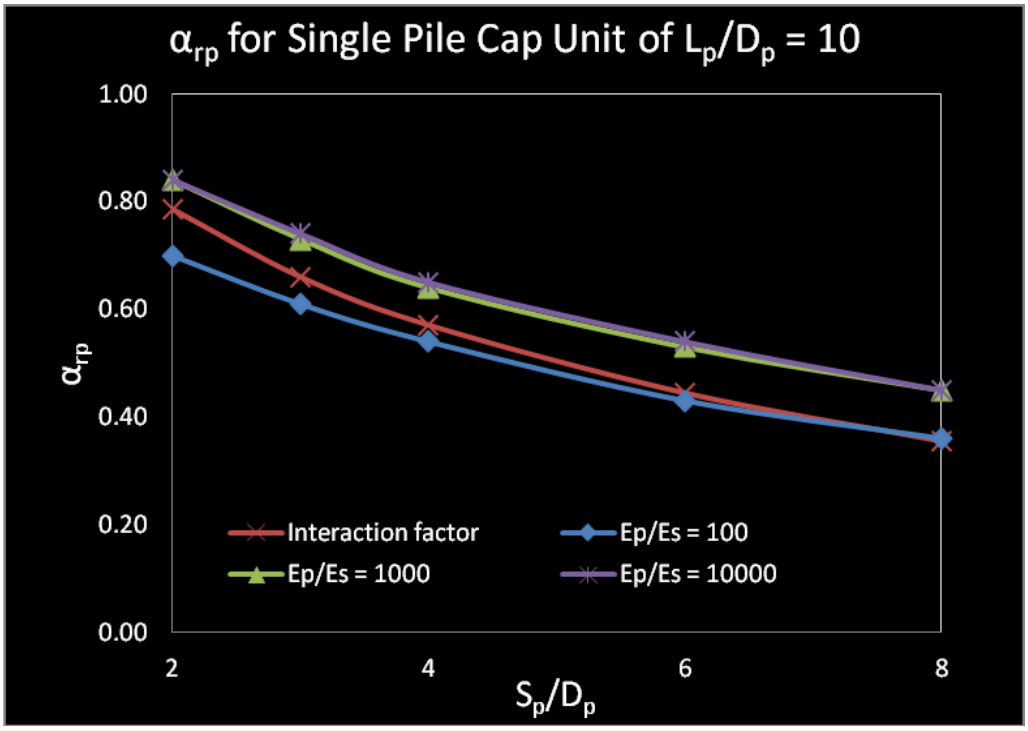

Figure 4.3a Single pile cap interaction factor for $L_p/d_p = 10$

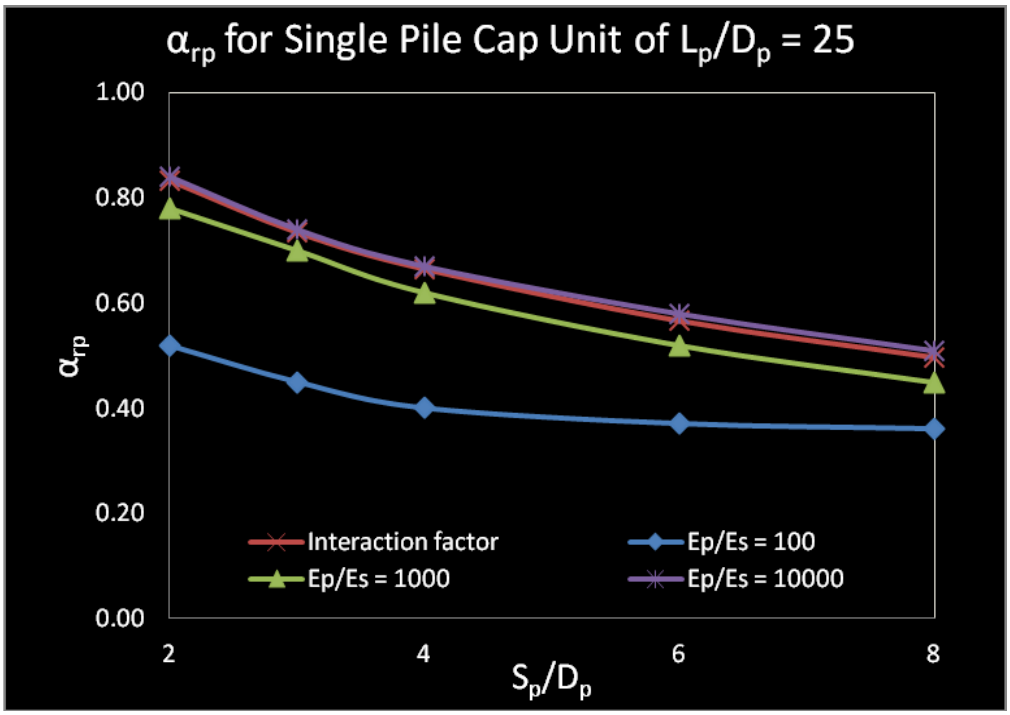

Figure 4.3b Single pile cap interaction factor for $L_p/d_p = 25$

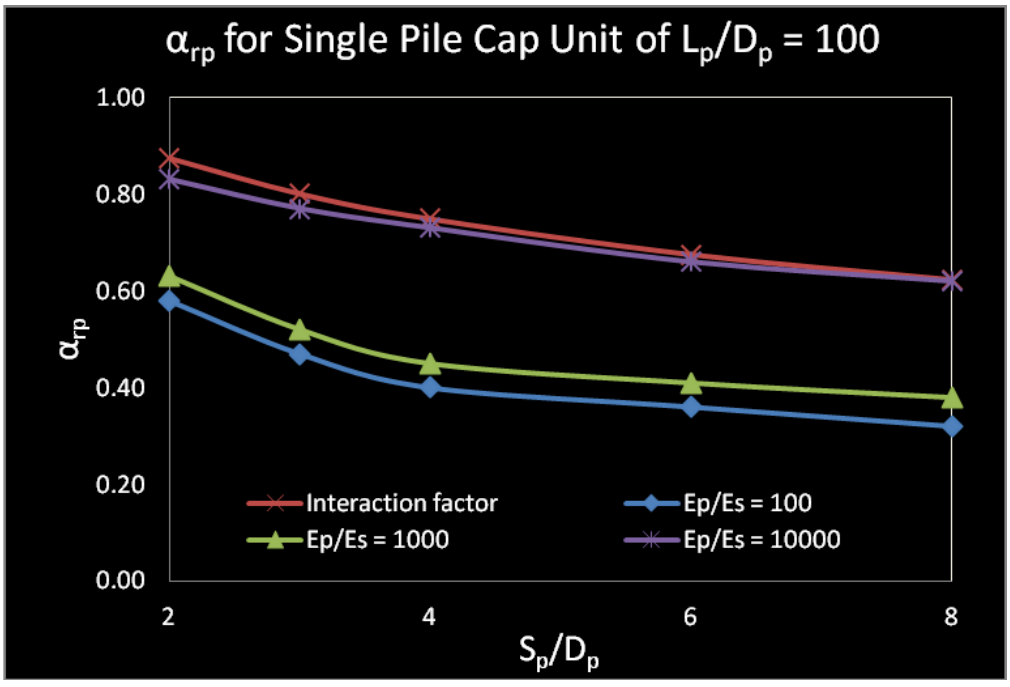

Figure 4.3c Single pile cap interaction factor for $L_p/d_p = 100$

4.2.3 Development of the New Interaction Factors

To offset the limitation of single pile cap interaction factors, as developed by Clancy et al. (1993), the new interaction factors have been developed as shown in figure 4.4 below. In this case, all possible ranges of elastic modulus, slenderness ratio of pile are included. The pile spacing range for these interaction factors are kept limited to 4D to 8D. This is because, the parametric studies in chapter 3 of this thesis shows that spacing greater than 7D is ineffective. On the otherhand majority of the load is carried by the pile group when the piles are spaced in less than two times of their diameter. The data used for this purpose is shown in table 4.2 below and the developed interaction chart is shown in figure 4.4 below.

Table 4.2 Data used to develop interaction factors for piled raft analysis

Soil		Pile		Raft		Dimensionless Group	
E_s	250 Mpa	E_p	$25x10^3$MPa - $25x10^6$MPa	E_r	10^{10}MPa	$K_p = E_p/E_s$	10^2 - 10^5
v_s	0.5	v_p	0.3	v_r	0.3	$K_{r(Brown)}$	
		d_p	1.0 m	t_r	2.0 m	L_p/d_p	10 - 100
		L_p	10, 25 & 100 m	L_r	24 & 32 m	S_p/d_p	2 - 8
		s_p	2D – 4D, 6D 8D	B_r	24 m 32 m	n	144, 64, 36, 16 16

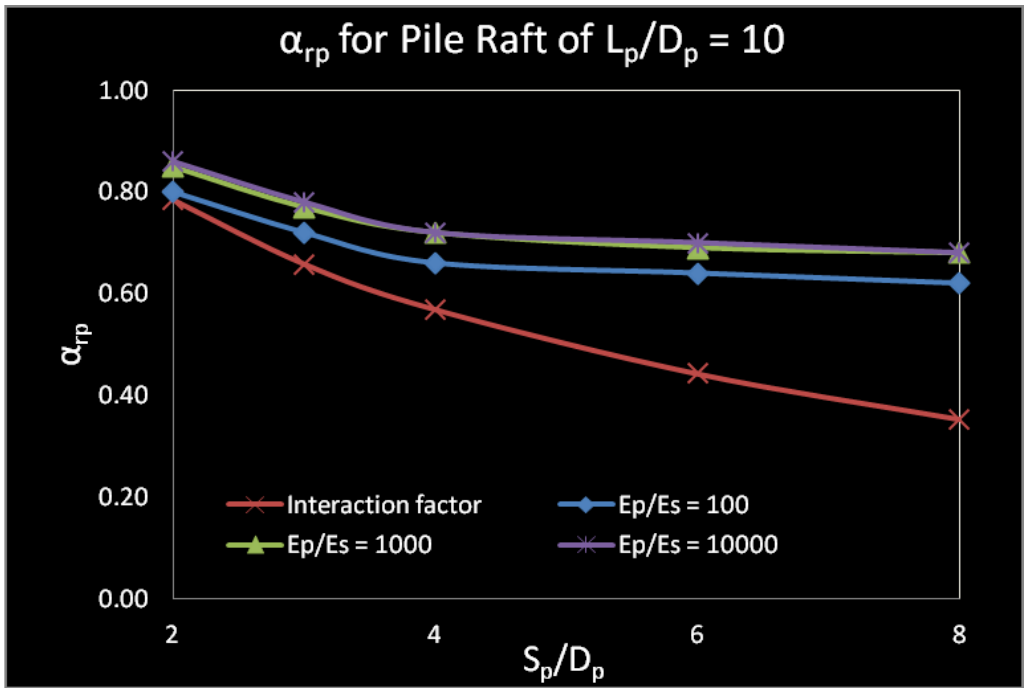

Figure 4.4a Pile Raft interaction factor for $L_p/d_p = 10$

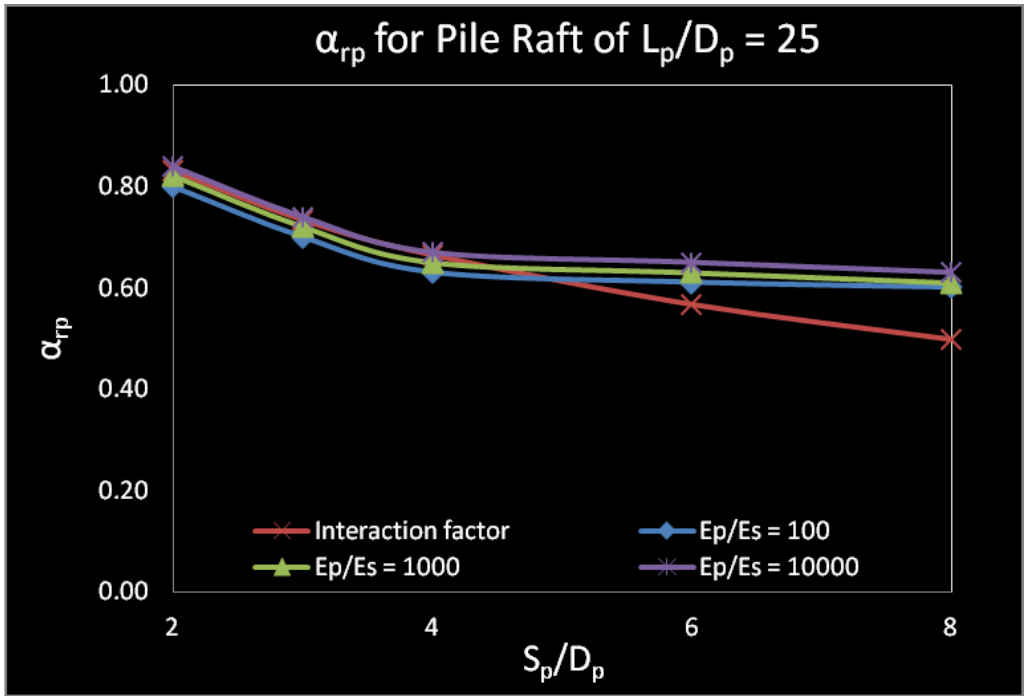

Figure 4.4b Pile Raft interaction factor for $L_p/d_p = 25$

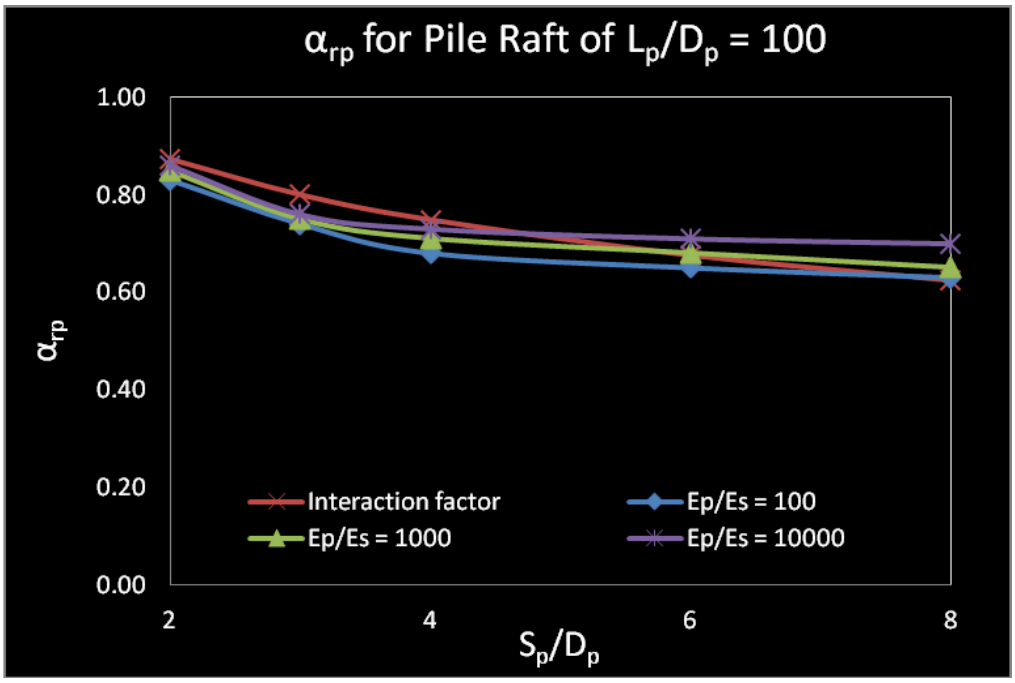

Figure 4.4c Pile Raft interaction factor for $L_p/d_p = 100$

4.2.4 Worked out Example

To demonstrate the utilization of the above developed interaction factors, a raft supported by a pile group of 6x6 is taken as an example. Numerical analyses were performed to obtain the value of K_p and K_r in isolation. The data used to develop the numerical models are as in table 4.3 below

Table 4.3 Data used for worked out example

Soil		Pile		Raft		Dimensionless Group	
E_s	250 Mpa	E_p	$25x10^3$MPa	E_r	$25x10^3$MPa	$K_p = E_p/E_s$	100
v_s	0.5	v_p	0.3	v_r	0.3	$K_{r(Brown)}$	
		d_p	1.0 m	t_r	2.0 m	L_p/d_p	25
		L_p	25 m	L_r	36 m	S_p/d_p	4
		s_p	4D	B_r	36 m	n	36

The values of K_p and K_r from individual pile group and raft analysis were found as 13.17 and 11.19 MN/mm respectively. From the developed chart above the value of α_{rp} can be estimated as 0.66 corresponding to the $E_p/E_s = 100$, $L_p/D_p = 25$ and $s_p/D_p = 4$. Then from equation 4.1 the value of K_{pr} can be calculated as

$$k_{pr} = \frac{13.17 + (1 - 2 * 0.66) * 11.19}{1 - 0.66^2 * 11.19 / 13.17} = 15.22 MN / mm$$

And from equation (4.7) the load shared by pile group can be estimated as

$$\frac{P_p}{P_p + P_r} = \frac{13.17 - 11.19 * 0.66}{15.22 * (1 - 0.66^2 * 11.19 / 13.17)} = 0.60$$

Obviously the raft will carry 40% of the total load and can also be calculated by equation (4.11) above.

4.3 Analytical Model for Maximum Settlement

4.3.1 Development of the Maximum Settlement Model

The analytical model for maximum settlement has been developed on the basis of the parametric studies conducted in the previous chapter of section 3.5 to 3.11. However, to capture the settlement profile corresponding to each of the contributing components, a more intensive analysis and a number of numerical models have been developed and simulated. The influences of each of these parameters have been expressed in some mathematical formulations. These individual contributions of the parameters were then

captured in a single mathematical model by means of statistical regression analysis technique.

Obviously, this development is comprised of multiple steps. In the first step, the empirical equation for each contributing parameter has been developed to capture its influence on the maximum settlement of the foundation. In the second step, additional data was generated by means of inter or extrapolation to fit the data. Finally, statistical multiple regression analyses were performed to capture the contribution of each parameter to the maximum settlement of the pile raft foundation.

4.3.1.1 The Load - Settlement Relationship in Empirical Form

The influence of load on settlement can be depicted based on the 3D numerical analysis of ABAQUS for a pile raft foundation of 24x24x2m raft supported by the pile group. Each pile in the group has a lateral dimension of 0.8mx0.8m that gives an equivalent pile diameter of 1.0m. The pile length is considered as 15m with the spacing of 6D. The soil, pile and raft properties used in this simulation are same as mentioned in table 3.2 in the previous chapter. The numerical output of the study on raft centre settlement for various loading conditions keeping all other parameters constant has been depicted in figure 4.5 below.

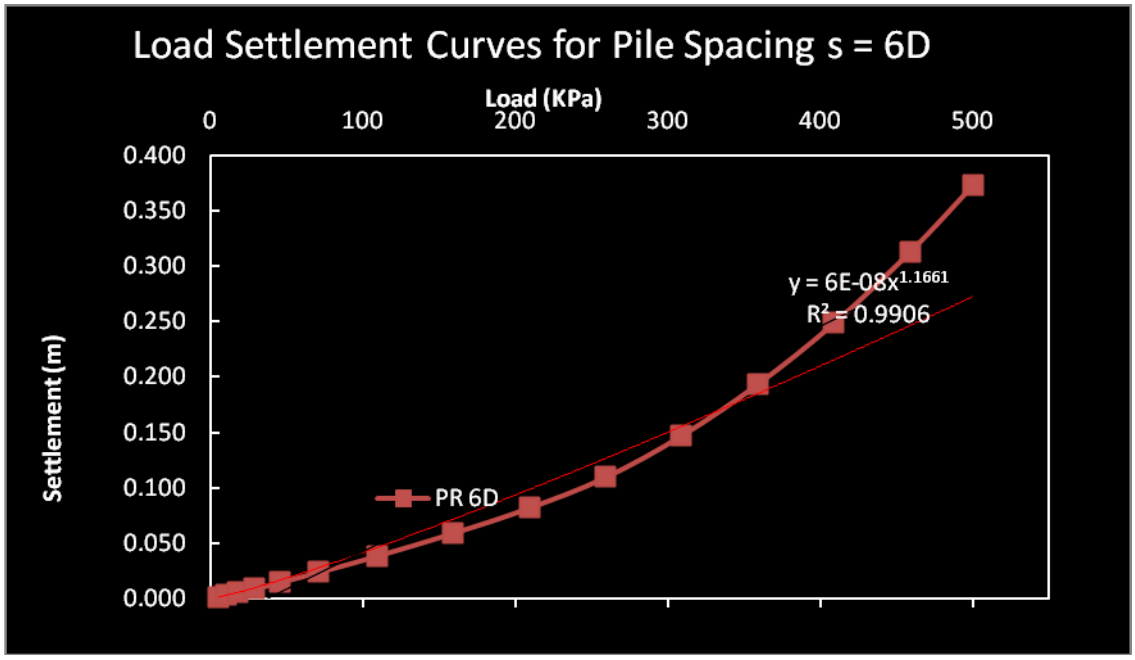

Figure 4.5 Load settlement relationships

The empirical equation to express the load settlement relationship can be expressed in equation (4.17) with a Pearson`s coefficient of determination, $R^2 = 0.9906$. This closer to unity value of R^2 indicates the goodness of data fit for the curve that depicts the load settlement relationship.

$$y = 6x10^{-8}w^{1.1661} \qquad (4.17)$$

4.3.1.2 The Pile Spacing - Settlement Relationship in Empirical Form

The influences of spacing on settlement have been detailed in section 3.5 of the previous chapter of this work. The raft and pile geometry are same as mentioned in section 4.3.1.1 above, only the variation is in pile spacing. Figure 4.6 below represents the relationship between the various pile spacing and settlement behavior. However, in this case, load and rest parameters were kept constant to capture the pile spacing or in other words, the pile number effect on the settlement.

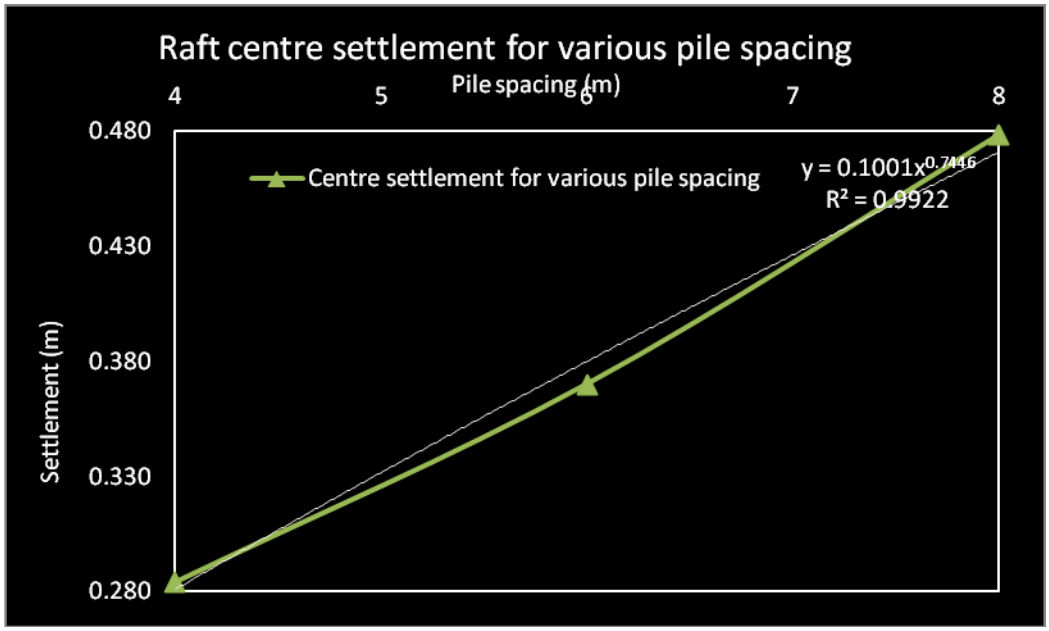

Figure 4.6 Pile spacing settlement relationship

The empirical equation to fit the data in its best fitting status with a R^2 value of 0.9922 can be expressed in equation (4.18). This analytical relation is to capture the spacing influence on settlement while other variables were kept constant.

$$y = 0.1001s^{0.7446} \tag{4.18}$$

4.3.1.3 The Pile Length - Settlement Relationship in Empirical Form

The pile length has an inverse relationship to the settlement. This phenomenon has been well depicted in section 3.7 of chapter 3. The same mechanical characteristics of soil and pile have been used as in section 3.7 and all other geometrical properties were kept constant except the length of the piles under the raft. The length influence on raft top centre settlement obtained by the 3D numerical analysis has been depicted in figure 4.7.

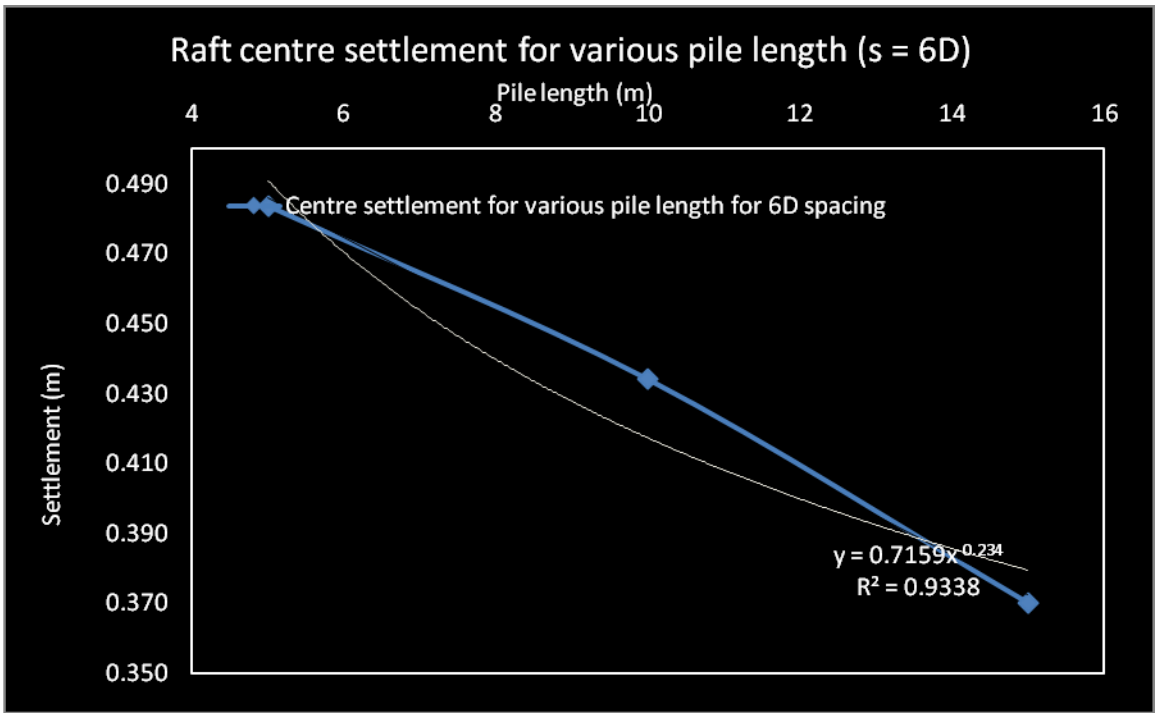

Figure 4.7 Pile length settlement relationship

The inverse relationship of pile length to the settlement can be expressed empirically in mathematical form with a best fitting coefficient (R^2) of 0.9338 as shown in equation (4.19) below.

$$y = 0.7159L^{-0.234} \tag{4.19}$$

4.3.1.4 The Pile Diameter - Settlement Relationship in Empirical Form

The similar inverse relationship of pile length to the settlement is found in the case of pile diameter to settlement as observed in section 3.8 of chapter 3. The term diameter is used literally, although, the square cross sections of varying sides have been used in numerical analysis to fit in the 3D octahedron element. Considering the floating pile characteristics of more frictional resistance than to tip resistance, the pile sizes used in this study were 0.4x0.4m, 0.8x0.8m & 1.2mx1.2m to yield an equivalent diameter effect of 0.5m, 1.0m & 1.5m respectively. The details have been discussed in section 3.8. The same mechanical characteristics and geometrical properties of soil, pile and raft have been used as mentioned in the previous sections and only the sides of square pile were varied. The inverse relationships of the settlement with the varying lateral dimension (width and breadth), along with the mathematical relationship are depicted in figure 4.8 below.

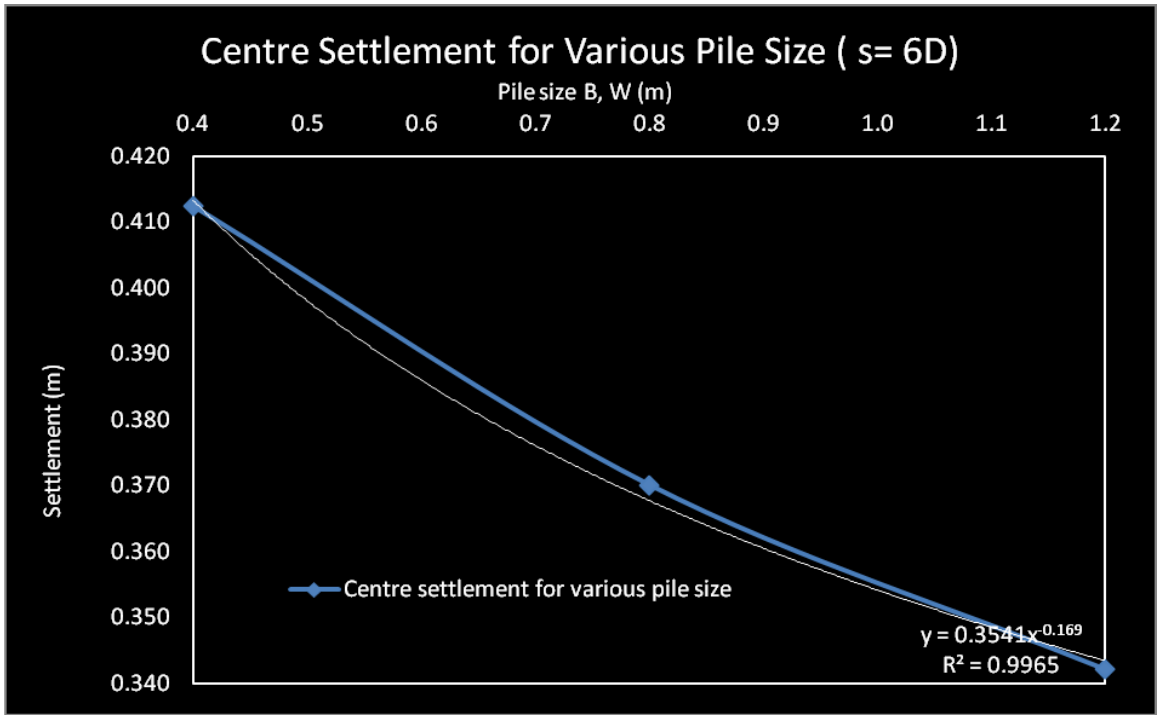

Figure 4.8 Pile size settlement relationships

The inverse relationship of pile size to the settlement can be expressed empirically in mathematical form with a best fitting coefficient (R^2) of 0.9965 as shown in equation (4.20) below. However, to express in terms of diameter the equation can be modified to equation (4.21).

$$y = 0.3541B^{-0.169} \quad (4.20)$$

$$y = 0.3541((B \times \frac{\pi D}{4B})^{-0.169}$$

$$y = 0.0.278B^{0.169} \quad (4.21)$$

4.3.1.5 The Raft Thickness Settlement Relationship in Empirical Form

The raft thickness has the direct influence on settlement as it superimposes to its load contribution on the foundation. This direct relationship has been shown as a 3D numerical analysis output of ABAQUS in section 3.9 of the previous chapter. The influences of raft thickness on foundation settlement have been expressed in mathematical formulation as shown in figure 4.9 below. In this case, only the raft thicknesses were varied and the rest parameters were kept unchanged (e.g the mechanical and geometric properties of soil, pile and raft).

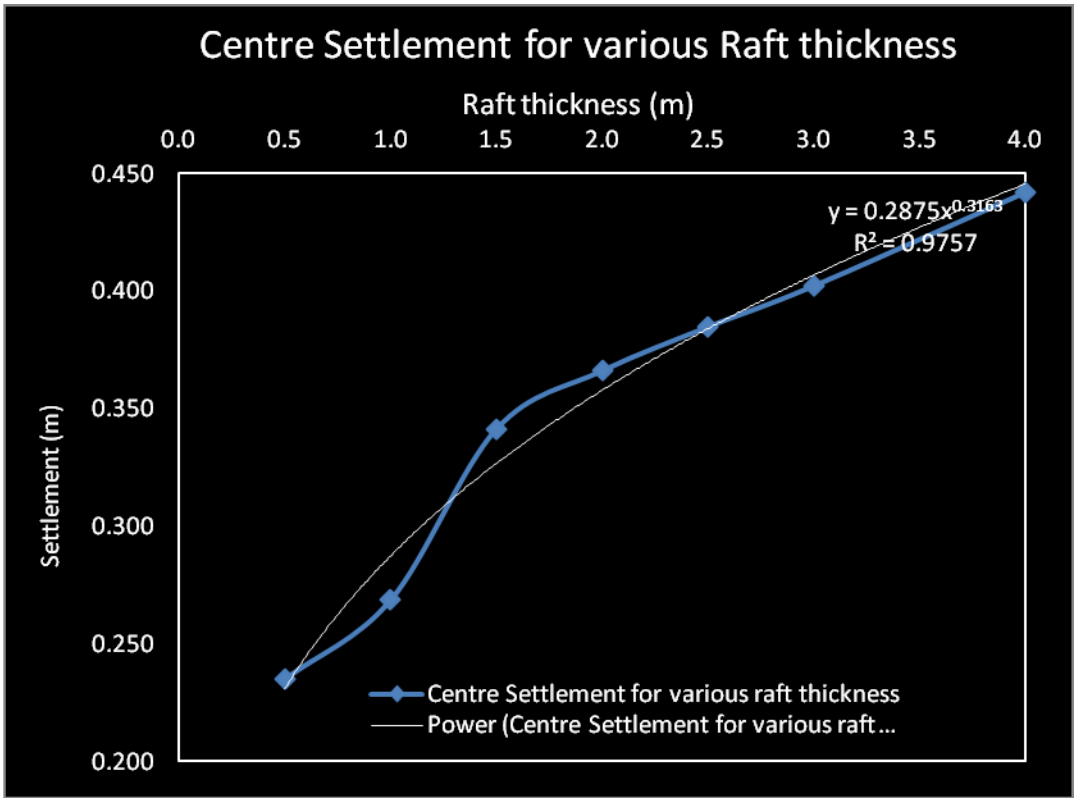

Figure 4.9 Raft thickness settlement relationship

The mathematical relationship to capture the raft thickness influence on settlement as depicted in figure 4.9 can be expressed as shown in equation (4.22) with a fitness of 0.9757 of the data as shown by their R^2 value.

$$y = 0.2875T^{0.3163} \tag{4.22}$$

4.3.1.6 The Angle of Internal Friction - Settlement Relationship in Empirical Form

The angle of internal friction of soil (φ) has an inverse influence on foundation settlement. The influences of various φ on soil settlement has been studied and depicted in section 3.10. Figure 4.10 below represents the correlation between them in mathematical form with a fitness coefficient of 0.9617. To develop this study, only the angle of internal friction was varied and the rest geometrical and mechanical properties were kept unchanged. The relationship is shown in equation 4.23 below.

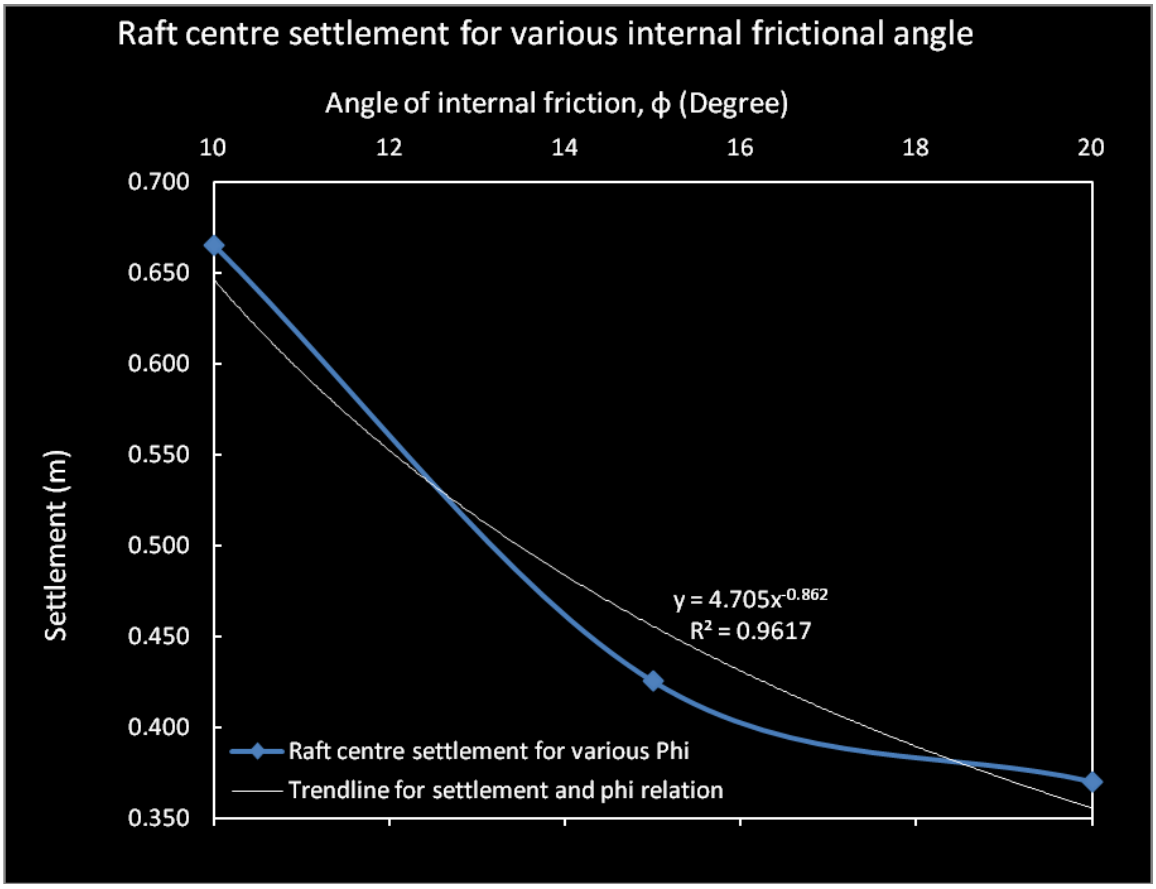

Figure 4.10 Angle of internal friction - settlement relationship

$$y = 4.705\varphi^{-0.862} \quad (4.23)$$

4.3.1.7 The Soil Cohesion - Settlement Relationship in Empirical Form

The soil cohesion contributes directly to the strength property of soil. It therefore, has an inverse influence on foundation settlement. The influences of various cohesions on soil settlement has been studied and depicted in section 3.11 of the previous chapter. Figure 4.11 below represents the correlation between them in mathematical form with a R^2 value of 0.997. The mathematical expression for the relationship between these two parameters is shown in equation 4.24 below.

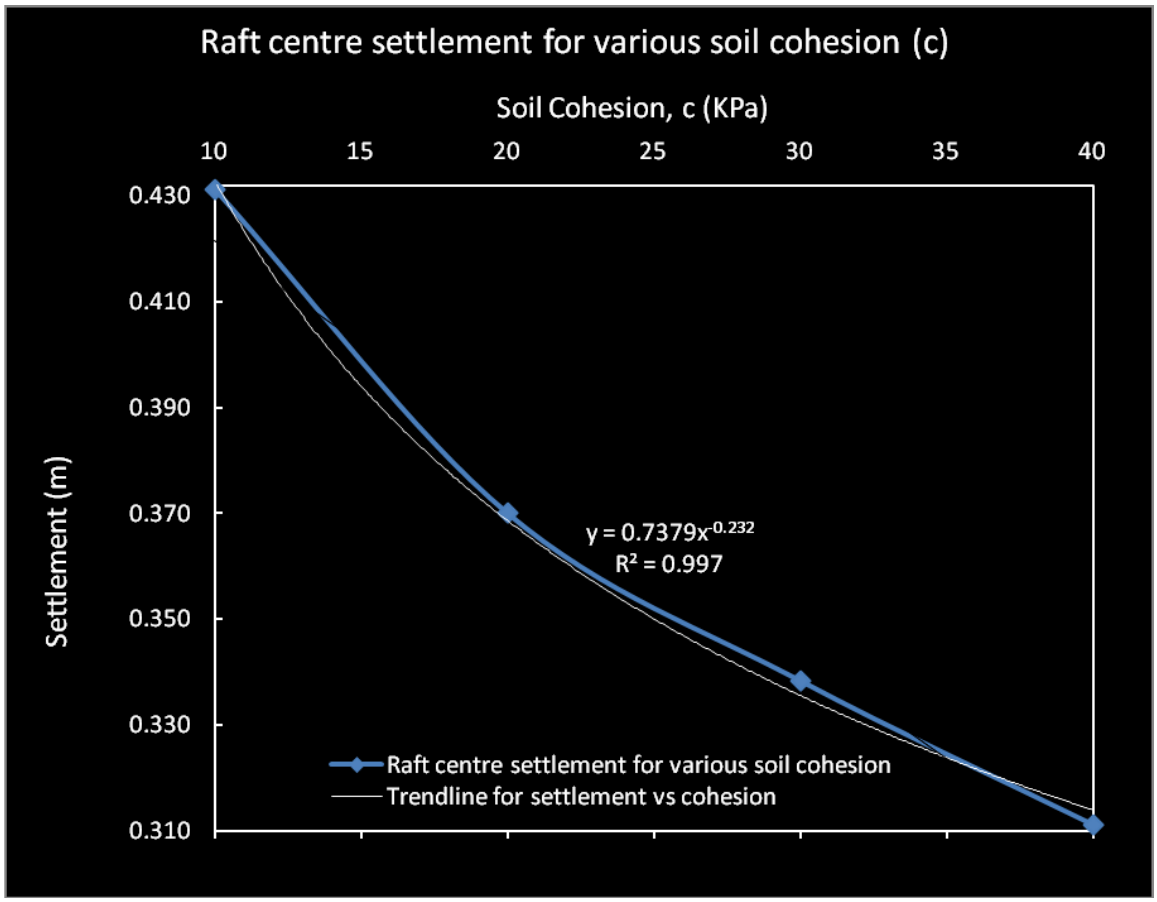

Figure 4.11 Raft thickness settlement relationship

$$y = 0.7379c^{-0.232} \quad (4.24)$$

4.3.2 The Regression Analysis

To capture the influences of the above mentioned foundation parameters in a single analytical model, the modeling technique of design concept, based on statistical theory, is used. Since for a single dependent variable (y, the settlement), seven independent variables come into play for this type of foundation, Multiple Regression Analysis (MRA) technique is therefore used to model the settlement pattern analytically.

The regression equation establishes a linear relationship between a response variable and the several possible predictor variables by the method of least squares. The Regression equation or Regression Model correlates the response or dependent variable (y) and the explanatory or predictor or independent variables (x) as follows.

$$y = f(x_1, x_2, \ldots\ldots x_p) + \varepsilon \qquad (4.25)$$

$$\text{i.e} \qquad y = \beta_0 + \beta_1 x_1 + \beta_2 x_2, \ldots\ldots + \beta_p x_p + \varepsilon \qquad (4.26)$$

where, β_0, β_1, β_2…… β_p are (the unknown constants to be determined) known as regression parameters or coefficients. ε is the error or random disturbance and known as residual. The regression coefficients β_0, β_1, β_2…… β_p have been determined in this work by the method of least square as shown below by equation (4.27) & (4.28) respectively

$$\beta_0 = \bar{y} - \beta_i \bar{x}\iota \qquad (4.27)$$

and $$\beta_i = \frac{\sum_{i=1}^{n} x_i y_i - n\bar{x}\bar{y}}{\sum_{i=1}^{n} x_i^2 - n\bar{x}^2} \quad (4.28)$$

Equations (4.27) & (4.28) are the principle equations. To capture all the parametric equations variables mentioned in the previous section along with their T-tests, significance tests and analysis of variance, the calculation will be tedious and may cause human errors. Therefore, statistical software MINITAB has been used for Multiple Regression Analysis.

The accuracy of statistical multiple regression analyses depends on the conformity of its dependent variables. The first step therefore is to test the data for their conformity. The data for the response variable (settlement) are collected from its relation to the predictor variables (load, pile spacing, size, raft thickness, internal frictional angle and soil cohesion) as shown in the figures 4.5 to 4.11. The range of the plotted settlement varies from parameter to parameter. In some cases, the output is limited to a lower range (380mm to 410mm of figure 4.8) and in some cases to a higher range (375mm to 670mm of figure 4.10). Therefore, to obtain the same response variable, the predicator variables were inter or extrapolated on the basis of their governing empirical equations (4.17 to 4.24), developed in section 4.3.1. Table 4.4 below summarizes the inverse form of the equations to generate

the data for the specific value of the response variable. The generated data used for multiple regression analysis is shown in table 4.5 below.

Table 4.4: Equations to generate the data for regression purpose

Settlement for load	$y = 6E\text{-}08w^{1.1661}$	w=(y/0.00000006)^(1/1.167)
Settlement for spacing	$y = 0.1001S^{0.7446}$	S = (y/0.1001)^(1/0.7446)
Settlement for length	$y = 0.7159L^{-0.234}$	L = (y/0.7159)^(1/-0.234)
Settlement for size	$y = 0.3541D^{-0.169}$	D = (y/0.3541)^(1/-0.169)
Settlement for thickness	$y = 0.2875T^{0.3163}$	T = (y/0.2875)^(1/0.3163)
Settlement for internal frictional angle	$y = 4.705\phi^{-0.862}$	ϕ = (y/ 4.705)^(1/-0.862)
Settlement for soil cohesion	$y = 0.7379c^{-0.232}$	c = (y/0.7379)^(1/-0.232)

Table 4.5: Generated data for regression purpose

Settlement (m)	Load (Pa)	Spacing (m)	Length (m)	Size (m)	Thickness (m)	Internal frictional angle (^{o})	Cohession (Pa)
0.200	388546	2.533	232.682	29.378	0.317	39.00	277860
0.225	429808	2.968	140.657	14.633	0.461	34.02	167240
0.250	470418	3.419	89.664	7.845	0.643	30.11	106196
0.275	510450	3.885	59.666	4.463	0.869	26.96	70420
0.300	549964	4.367	41.137	2.667	1.144	24.37	48396
0.325	589009	4.863	29.220	1.661	1.473	22.21	34275
0.350	627626	5.372	21.288	1.071	1.862	20.38	24903
0.375	665850	5.893	15.852	0.712	2.316	18.81	18497
0.400	703710	6.427	12.031	0.486	2.841	17.45	14005
0.425	741234	6.972	9.285	0.340	3.441	16.27	10784
0.450	778442	7.528	7.273	0.242	4.122	15.22	8429
0.475	815356	8.095	5.772	0.176	4.891	14.30	6677
0.500	851993	8.672	4.636	0.130	5.752	13.47	5353

The key output of multiple regression analysis by the statistical software MINITAB is described in the following tables. Table 4.6 displays that the P values of each predicator are 0, which rejects the null hypotheses and signifies strongly that the multiple regression

model is extremely effective to express the dependent variable (settlement) in terms of the predicator variables. The large T values indicate their extreme location with high confidence level and the almost 0 value of the standard error of the coefficients (β_i) reflects the accuracy of the model. A further accuracy of the response variable (y, settlement) is estimated by the standard error test of MINITAB output, which shows it as highly significant (s = 3.5 x 10^{-9}) with a R^2 = 100.00%. Therefore, the data fit in the model is perfect with no error. However, it notifies about the 'unusual observation' for the first two rows of data of table 4.5 above.

Table 4.6 Confidence interval and significance level (T & P) tests of the variables

Predictor	Coef	SE Coef	T	P
Constant	-0.0315647	0.0003237	-97.51	0.000
Load (Pa)	0.00000049	0.00000000	679.23	0.000
Spacing (m)	0.0125592	0.0000444	283.04	0.000
Length (m)	-0.00047885	0.00002492	-19.22	0.000
Size (m)	-0.00002966	0.00000198	-15.01	0.000
Thickness (m)	-0.00014758	0.00000329	-44.89	0.000
Internal frictional angle (^{o})	0.00025375	0.00000558	45.45	0.000
Cohession (Pa)	0.00000040	0.00000002	19.09	0.000

The analysis of variance (ANOVA), as shown in table 4.7, is simply a reassurance of the T-test of table 4.6 above. In fact, F is nothing but T-square. The lowest p-value suggests that the coefficients of the predicator variables (β_i) play significant roles in the model. The sum of square (SS) and the mean square (MS) of errors of the regression is almost 0 of this analysis. The residual errors in all the cases are zero.

Table 4.7 Analysis of variance (ANOVA)

Source	DF	SS	MS	F	P
Regression	7	0.113750	0.016250	1.32846E+15	0.000
Residual Error	5	0.000000	0.000000		
Total	12	0.113750			

Based on the above analysis, the MINITAB yields the regression model as

Settlement (m) = - 0.0316 + 0.00000049 Load (Pa) + 0.0126 Spacing (m)
- 0.000479 Length (m) - 0.000030 Size (m) - 0.000148 Thickness (m)
+ 0.000254 Internal frictional angle (^{o}) + 0.000000 Cohession (Pa)

$$\mathbf{y = - 0.0316 + 4.9*10^{-7}*w + 0.0126*S - 4.79*10^{-4}*L - 3*10^{-5}*D - 1.48*10^{-4}*T + 2.5*10^{-4}*\varphi + 4*10^{-7}*c} \quad (4.29)$$

The above tables indicate the accuracy of the model from statistical view point. The developed regression model (equation 4.29) is validated with the data used for regression purpose (table 4.5). Inserting the load, spacing, length, size, thickness, internal frictional angle and cohesion parameters from the table 4.5 into equation (4.29), the model response found (second last column of table 4.8 below) is in excellent agreement with the model input data.

Table 4.8 Validation of the statistical regression model with the generated data

Settlement (m)	Load (Pa)	Spacing (m)	Length (m)	Size (m)	Thickness (m)	Int. fric. angle (^{o})	Cohesion (Pa)	Model response(m)	Difference (m)
0.200	388546	2.533	232.682	29.378	0.317	39.00	277860	0.199	0.001
0.225	429808	2.968	140.657	14.633	0.461	34.02	167240	0.224	0.001
0.250	470418	3.419	89.664	7.845	0.643	30.11	106196	0.249	0.001
0.275	510450	3.885	59.666	4.463	0.869	26.96	70420	0.274	0.001
0.300	549964	4.367	41.137	2.667	1.144	24.37	48396	0.299	0.001
0.325	589009	4.863	29.220	1.661	1.473	22.21	34275	0.323	0.002
0.350	627626	5.372	21.288	1.071	1.862	20.38	24903	0.348	0.002
0.375	665850	5.893	15.852	0.712	2.316	18.81	18497	0.373	0.002
0.400	703710	6.427	12.031	0.486	2.841	17.45	14005	0.398	0.002
0.425	741234	6.972	9.285	0.340	3.441	16.27	10784	0.423	0.002
0.450	778442	7.528	7.273	0.242	4.122	15.22	8429	0.448	0.002
0.475	815356	8.095	5.772	0.176	4.891	14.30	6677	0.473	0.002
0.500	851993	8.672	4.636	0.130	5.752	13.47	5353	0.498	0.002

4.4 Validation of the Analytical Model for Maximum Settlement

To validate the analytical model, the 3D FEM simulation of the load settlement behavior of a piled raft foundation by Maharaj (2003 b) are taken into account. The mechanical and geometrical properties are shown in table 4.9 below.

Table 4.9 Pile raft foundation data (Maharaj 2003 b)

Soil		Pile		Raft		Dimensionless Group	
E_s	25 Mpa	E_p	$2x10^3$ - $2x10^6$MPa	E_r	$2x10^3$ - $2x10^6$MPa	$K_p = E_p/E_s$	80-80000
v_s	0.45	v_p	0.3	v_r	0.3	$K_{r(Brown)}$	
		d_p	0.5 m	t_r	4.0 m	L_p/d_p	96
		L_p	48 m	L_r	16 m	S_p/d_p	8
		s_p	4 m	B_r	16 m	n	16

The pile and raft geometrical properties are entered into equation (4.29) for varying load and the obtained load settlement curve is plotted on Maharaj (2003 b) plot as depicted in figure 4.12 below. The analytical model is in good agreement for settlement up to 470mm after which, the analytical model responds in a stiffer response than that of Maharaj (2003 b).

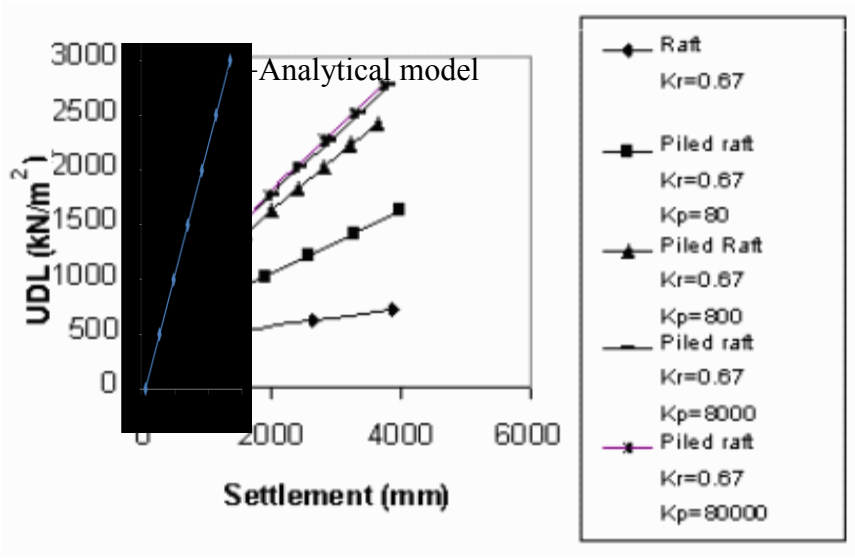

Figure 4.12 The maximum settlement analytical model validation with Maharaj (2003 b)

4.5 Analytical Model for Differential Settlement

4.5.1 Development of the Differential Settlement Model

The three dimensional numerical simulation of the piled raft foundation for various configurations and mechanical properties, depicted in the previous chapter, indicates that the raft centre settles more than any other points in the raft. This yields a bowl shape to the deflected raft with sufficient stiffness. The analytical model development for differential settlement consists of three steps. In the first step, the foundation parameters responsible to cause the differential settlement have been identified. The second step

consists of identifying the raft top deflection shape pattern. In the third step, the differential settlement analytical model is formulated in terms of its contributing factors identified in the first step, in order to capture the settlement pattern obtained in the second step.

4.5.2 Differential Settlement Contributing Parameters

The settlement of pile raft foundation is a function of the applied load, the geometric and mechanical properties of raft, pile and soil. To capture the raft top settlement profile corresponding to each of the contributing components, extensive analyses on a number of numerical models have been performed and the output have been depicted in the subsequent sections.

The load settlement plot for various pile spacing, depicted in figure 3.25 of the previous chapter, indicates that the pile raft is effective for a pile spacing of less than 7D. On the other hand, majority of the load is carried by the pile group for pile spacing less than 4D. Therefore, the influence of each pile raft settlement contributing factors have been studied and depicted in this thesis for the pile spacing of 4D to 8D. In these studies the load is considered as uniformly distributed on the top surface of square rafts. Therefore, the maximum differential settlement is the settlement difference in between the centre and corner point of the raft top surface.

The plotting of differential settlement variation with the increased load for the pile spacing of 4D, 6D & 8D, as shown in figure 4.13 below, indicates no significant load

effect on the differential settlement above the load of 300 kPa. Even the maximum differential settlement is observed as 0.08% for 4D and 6D and 0.18% for 8D pile spacing.

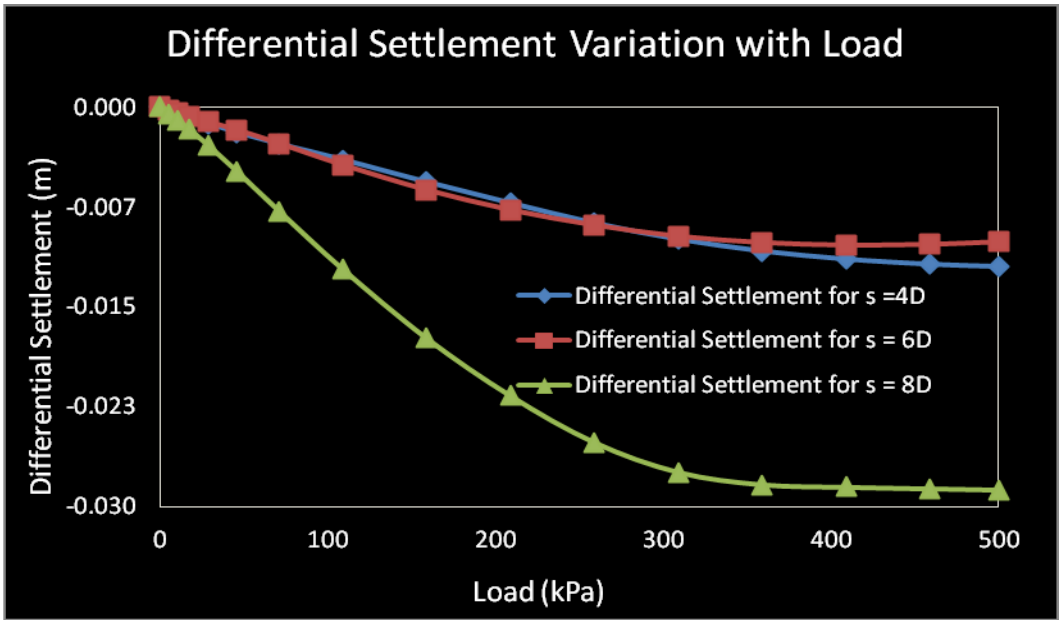

Figure 4.13 Differential settlement variations with load

Flatter changes in differential settlements are observed in the case of pile length and size variation as shown in figure 4.14 and 4.15 below. Therefore, no significant influence of load, pile length and size on differential settlement is observed. However, the differential settlement variation is observed as highly significant with the variation of pile spacing and raft thickness as obtained from the 3-D finite element analysis and depicted in figure 4.16 and 4.17 below.

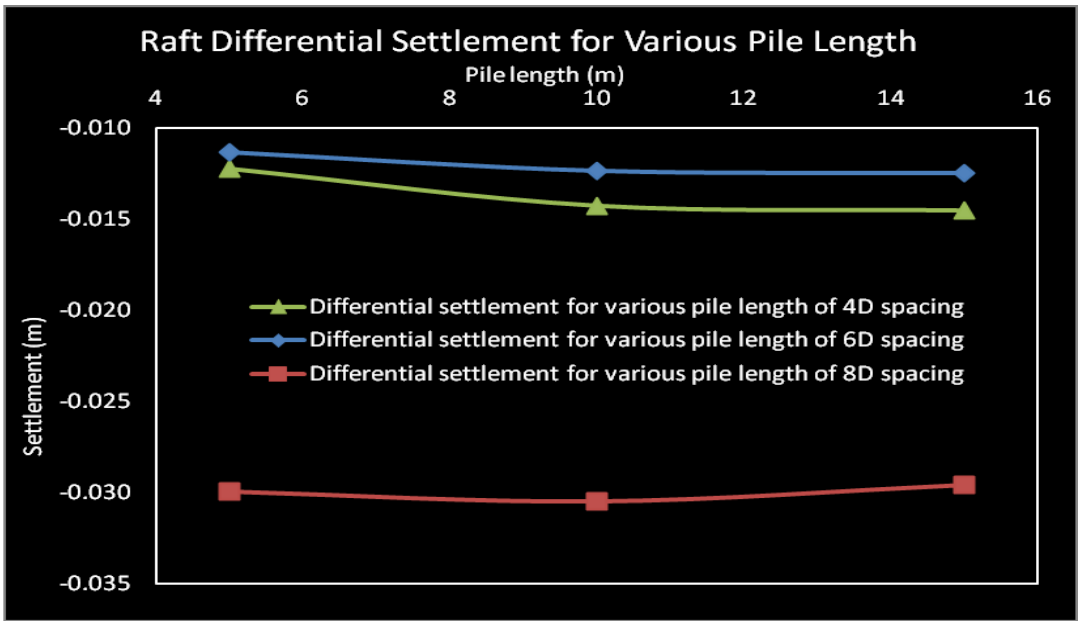

Figure 4.14 Differential settlement variations with length

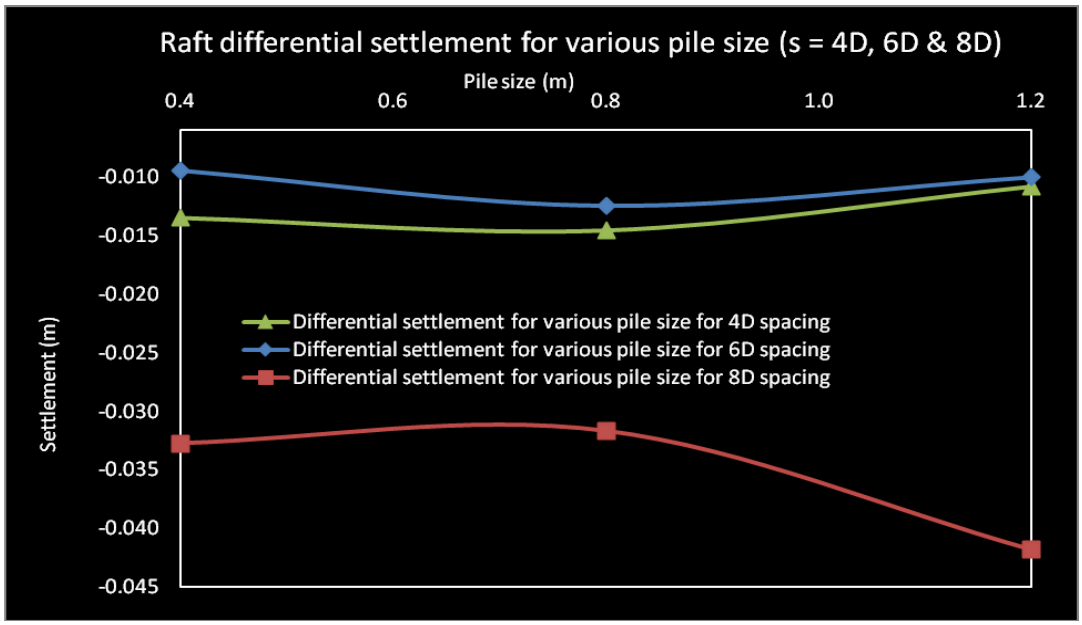

Figure 4.15 Differential settlement variations with pile size

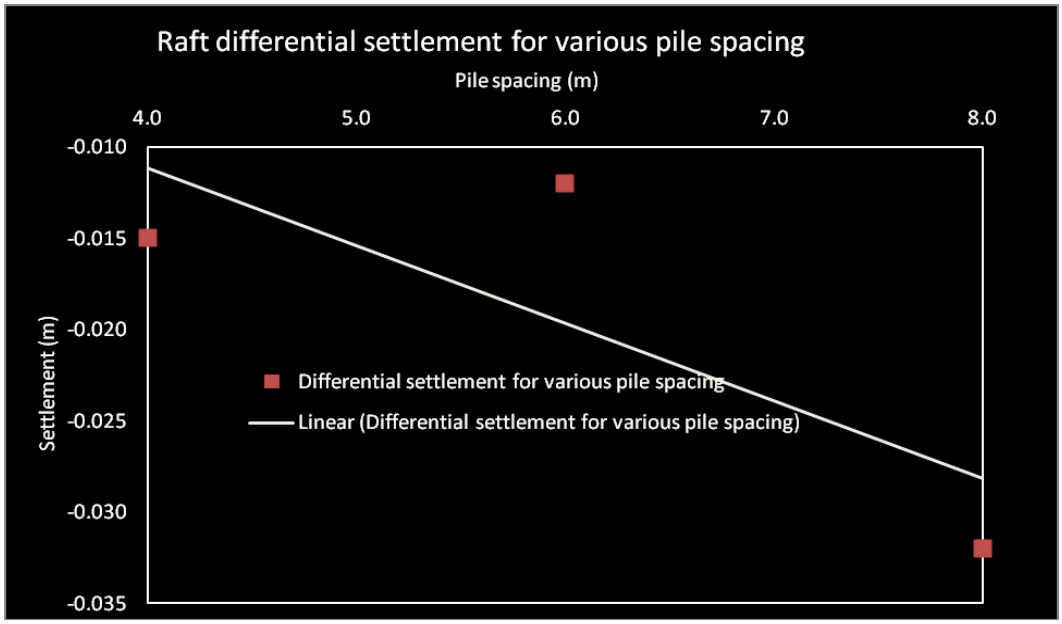

Figure 4.16 Differential settlement variations with pile spacing

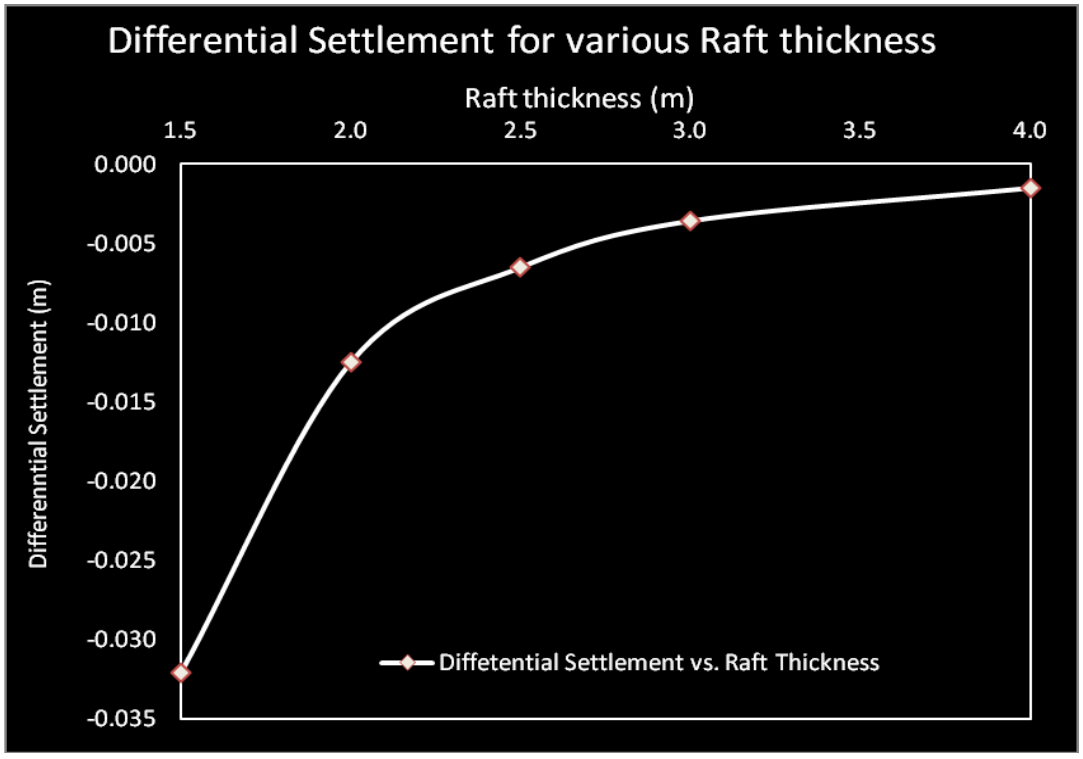

Figure 4.17 Differential settlement variations with raft thickness

4.5.3 The Raft Top Settlement Profile

Once the differential settlement contributing factors have been identified, the next step is to depict the raft top settlement profile for each of the contributing factors, in order to capture the settlement pattern. Figures 4.19 to 4.21 depict the raft top settlement profile for various raft spacing and figures 4.22 to 4.26 depict the same for the raft thickness of 1.5 to 4.0m. The reason of selecting this range of raft thickness is that the differential settlement below 1.5m thick raft is greater than the concrete fracture strain value and on the other hand, the differential settlement is not significant for thicker raft (figure 4.17 as well as figures 4.22 to 4.26).

The raft top settlement profiles for each of the figures 4.19 to 4.26 have been investigated and plotted along three individual paths. The raft central path passes through the centre axis of the raft, the central pile path passes through the top of the central pile group and the diagonal path connects the raft centre and corner point. A depiction of these three profile paths is available on figure 4.18 below.

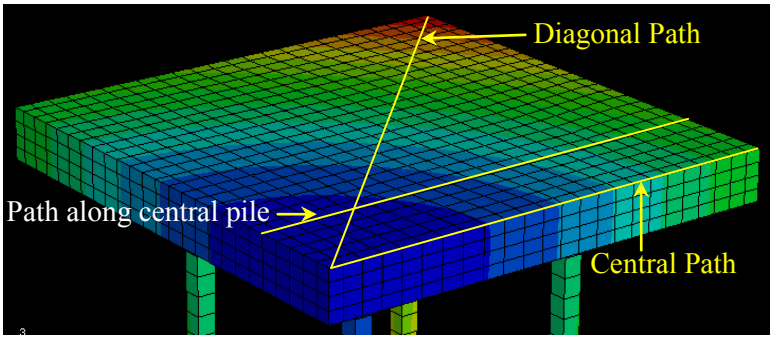

Figure 4.18 Raft top path definition

In all the cases, it is observed that the settlement profiles have the same bowl or dish shape pattern with the maximum settlement is at centre. It is also observed that the settlement profile along diagonal path could be the representative of the settlement profile along any path on the raft top surface.

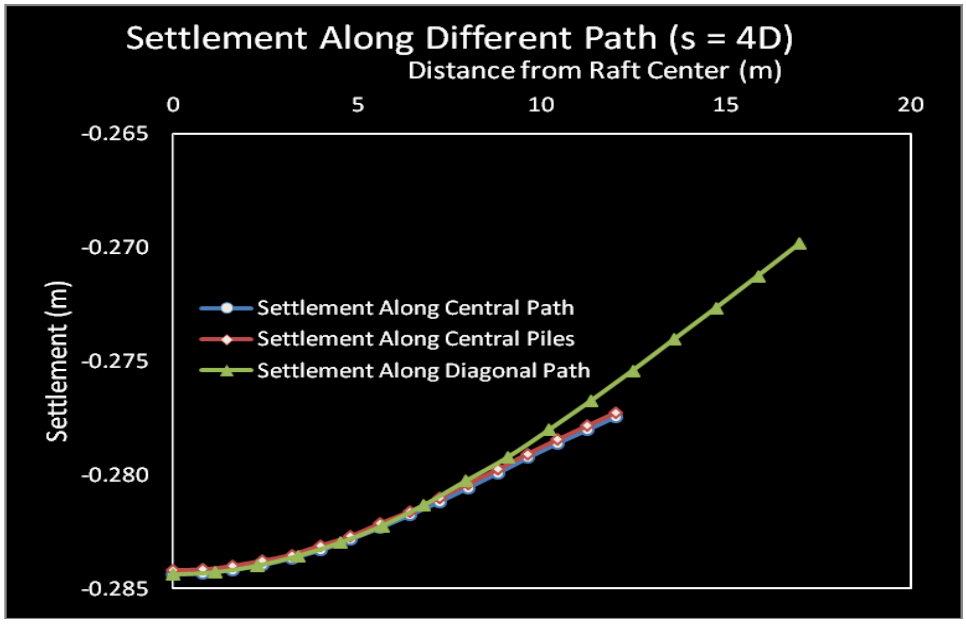

Figure 4.19 Raft top settlement profile along different path (s = 4D)

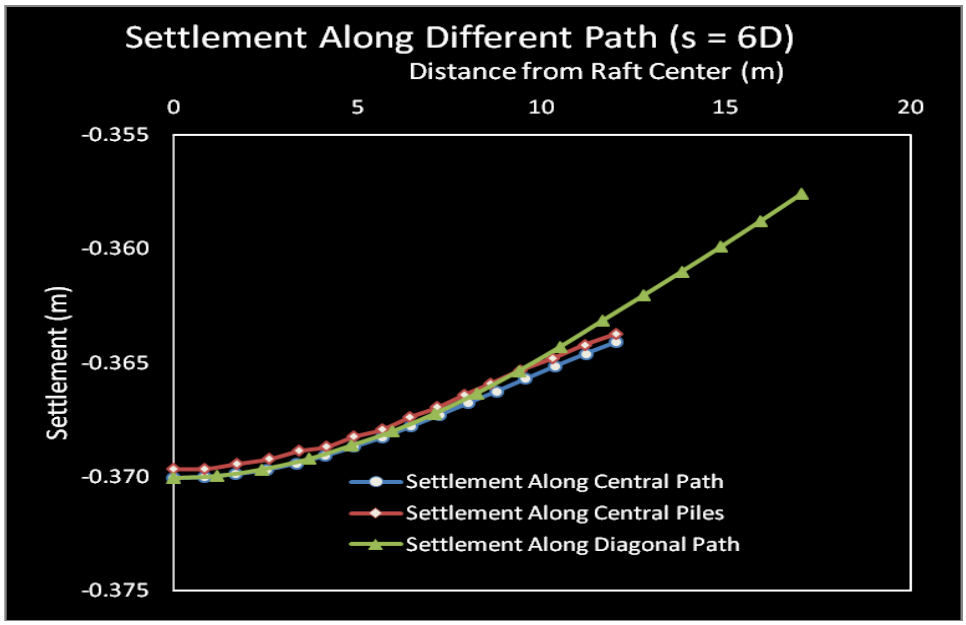

Figure 4.20 Raft top settlement profile along different path (s = 6D)

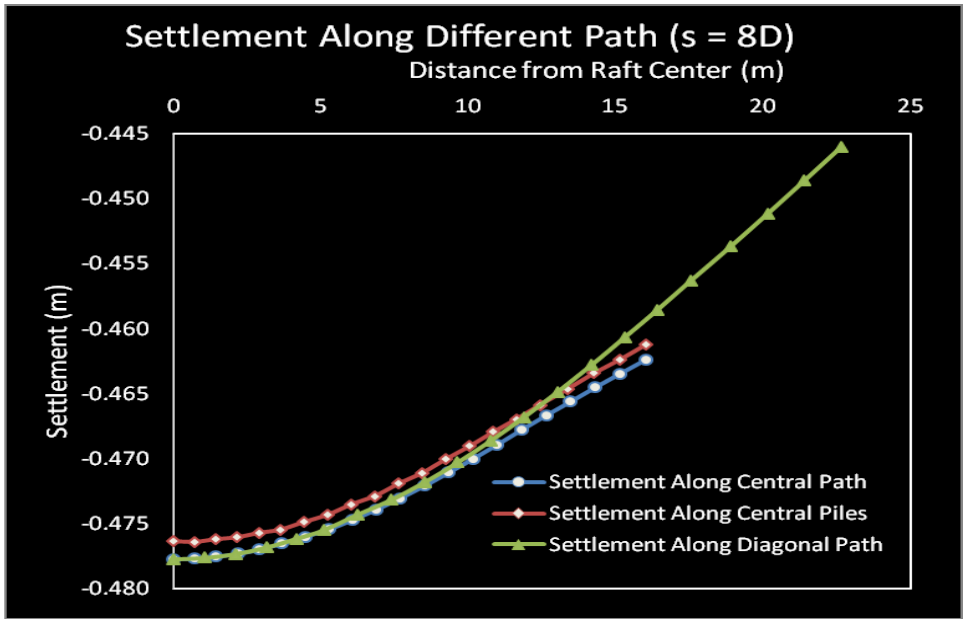

Figure 4.21 Raft top settlement profile along different path (s = 8D)

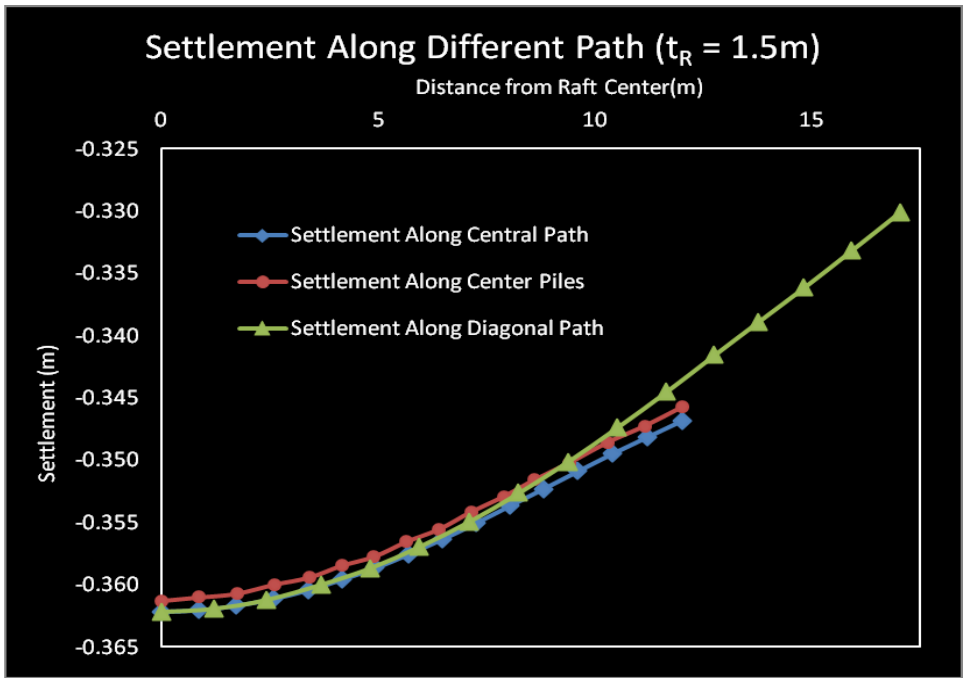

Figure 4.22 Raft top settlement profile along different path (t_R = 1.5 m)

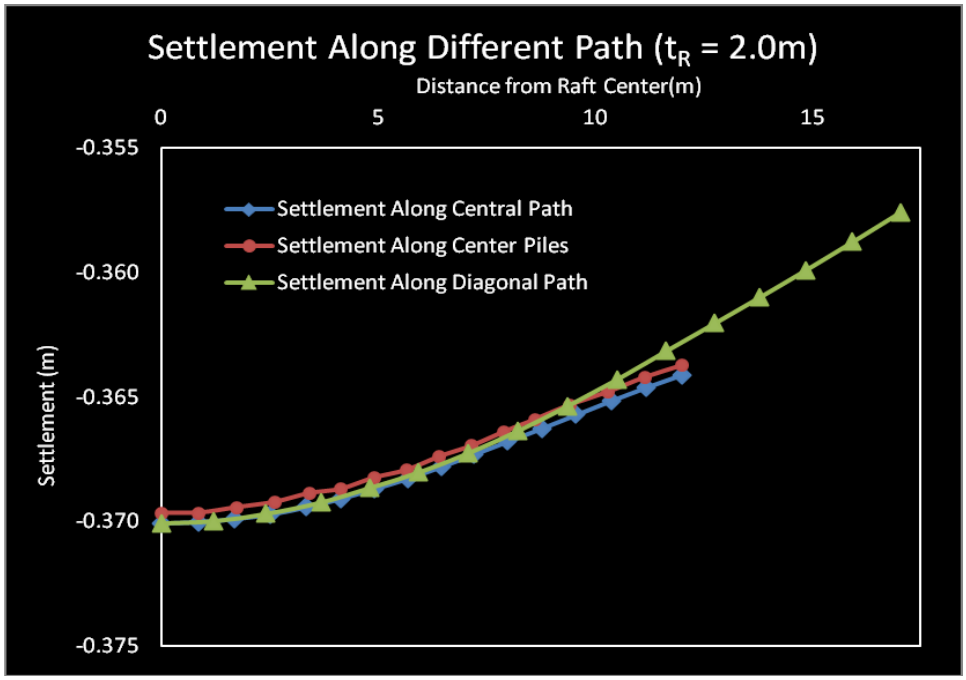

Figure 4.23 Raft top settlement profile along different path (t_R = 2.0 m)

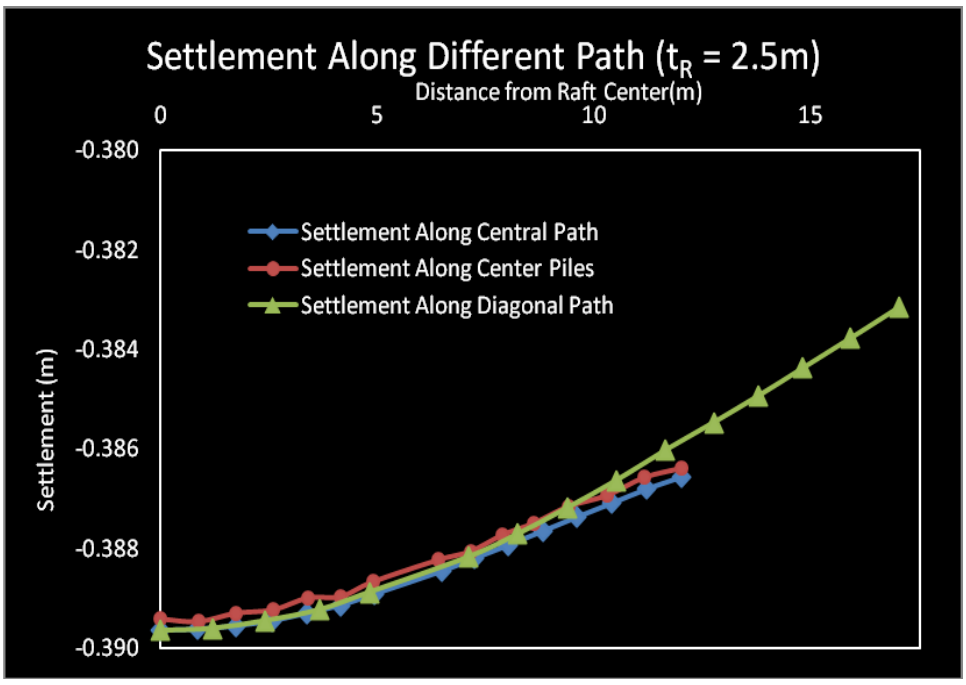

Figure 4.24 Raft top settlement profile along different path (t_R = 2.5 m)

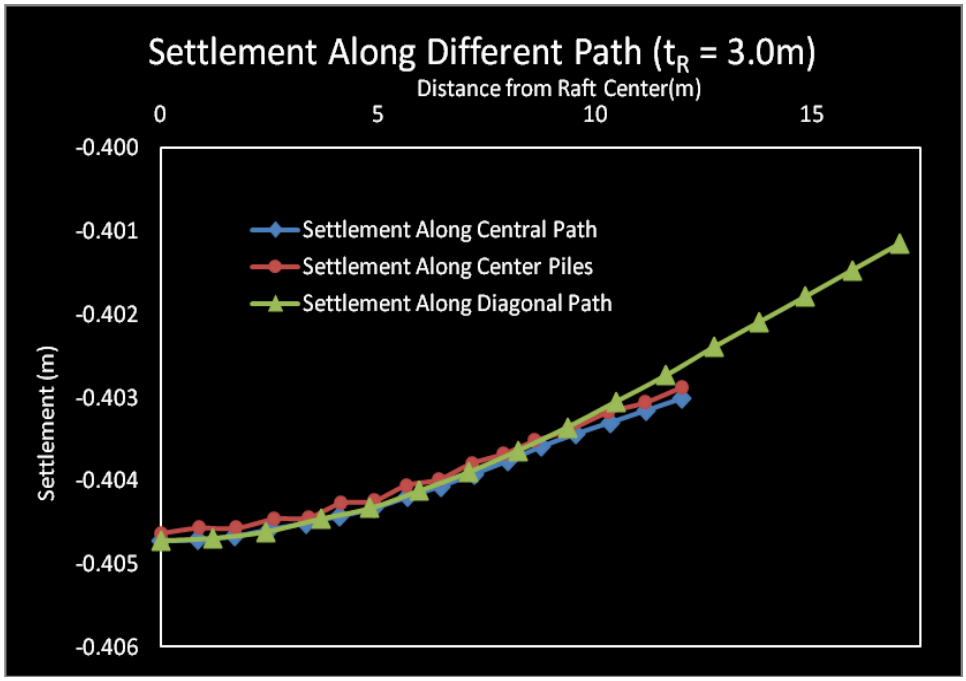

Figure 4.25 Raft top settlement profile along different path (t_R = 3.0 m)

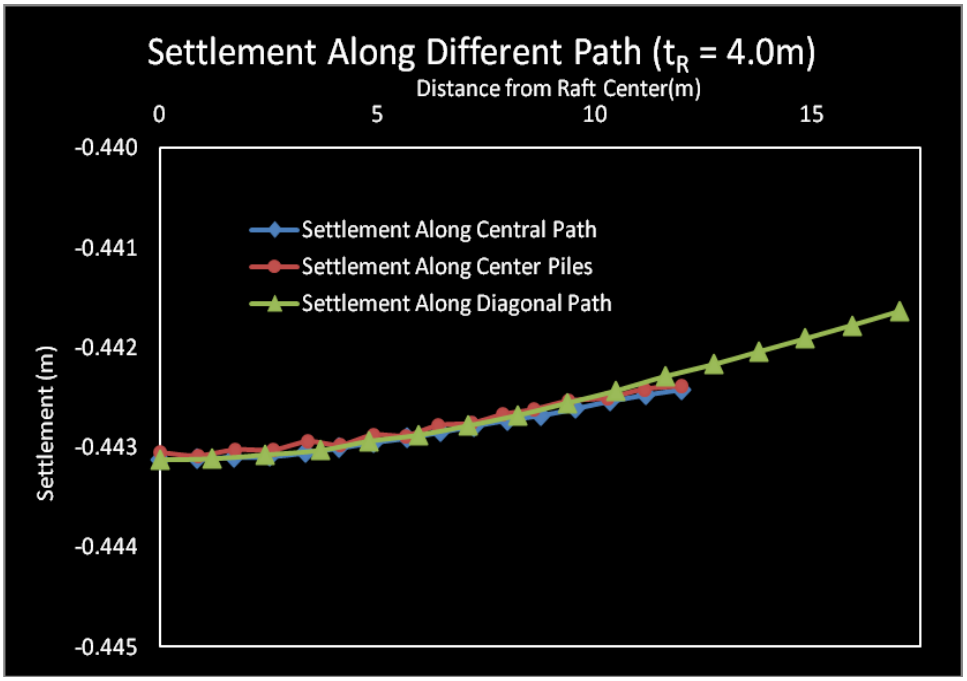

Figure 4.26 Raft top settlement profile along different path (t_R = 4.0 m)

4.5.4 Analytical Model for Differential Settlement

Raft thickness and pile spacing have been identified as the contributing factors to differential settlement in the previous section. Figures 4.19 to 4.26 conclude that the raft top settlement along diagonal path is the representative pattern of the settlement profile along any path on the raft top. Therefore, the observed bowl shape raft top deflection pattern can be expressed in terms of parabolic equation and its coefficients can be investigated to observe the influence of raft thickness and pile spacing on the coefficients. The parabolic equation to capture the bowl shape pattern can be written as

$$y = ax^2 + bx + c \tag{4.30}$$

where, y is the vertical deflection at any point on the raft top surface, x is the horizontal or lateral distance from the raft centre or point of maximum settlement. Coefficients a, b and c are to be investigated from the numerical analysis. To finalize the differential settlement analytical model, the parabolic coefficients have been expressed in terms of raft thickness and pile spacing as described in the subsequent sections.

4.5.4.1 Differential Settlement Model in Terms of Raft Thickness

To express the parabolic bowl shape deflection of raft top, the raft thicknesses were varied from 1.5m to 4.0m at an incremental raft thickness of 0.5m for each of the pile spacing of 4D, 6D and 8D. The ABAQUS 3D finite element simulation of fifteen numerical models yield the raft top deflection curves as shown in figures 4.27, 4.29 and 4.31 respectively. The corresponding mathematical model to capture each of the curve shapes along with their fitness coefficients are shown in table 4.10, 4.11 & 4.12 respectively. The coefficients of the representative parabolic curves for each case have

been plotted in terms of raft thickness to express its relation in terms of raft thickness as shown in figures 4.28, 4.30 & 4.32.

For 4D spacing

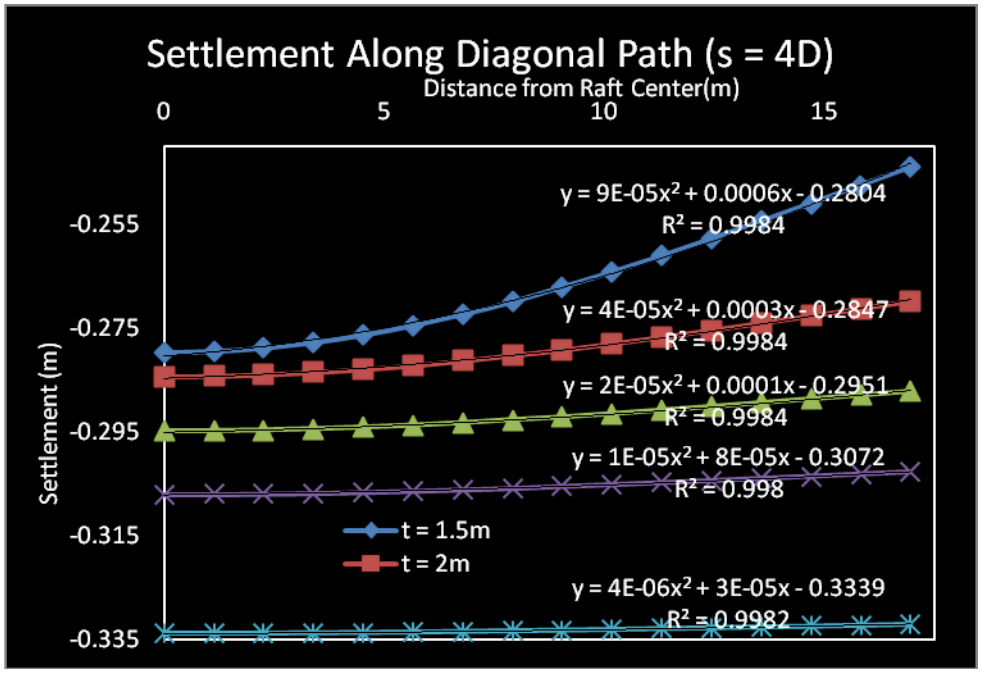

Figure 4.27 Differential settlements for various raft thickness of 4D spacing

Table 4.10 Differential settlement equation for various raft thickness of 4D pile spacing

Thickness (m)	Equation	R^2	a	b	c
1.5	$y = 9E\text{-}05x^2 + 0.0006x - 0.2804$	0.9984	0.00009	0.0006	0.2804
2.0	$y = 4E\text{-}05x^2 + 0.0003x - 0.2847$	0.9984	0.00004	0.0003	0.2847
2.5	$y = 2E\text{-}05x^2 + 0.0001x - 0.2951$	0.9984	0.00002	0.0001	0.2951
3.0	$y = 1E\text{-}05x^2 + 8E\text{-}05x - 0.3072$	0.9980	0.00001	0.00008	0.3072
4.0	$y = 4E\text{-}06x^2 + 3E\text{-}05x - 0.3339$	0.9982	0.000004	0.00003	0.3339

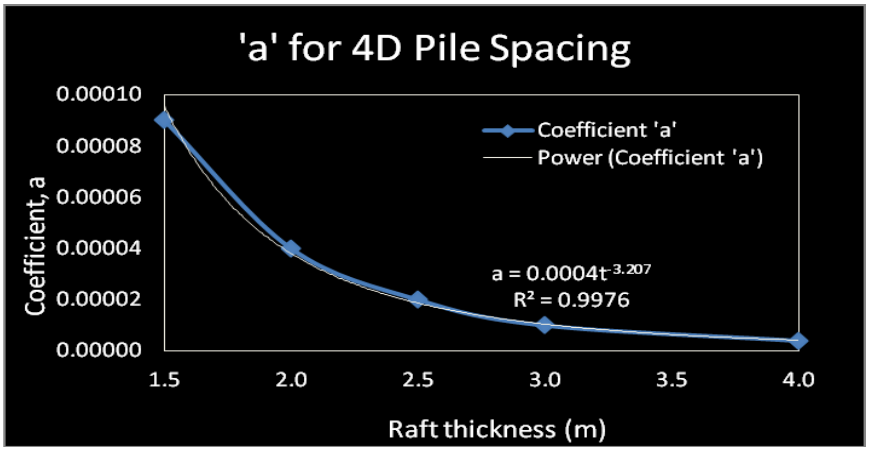

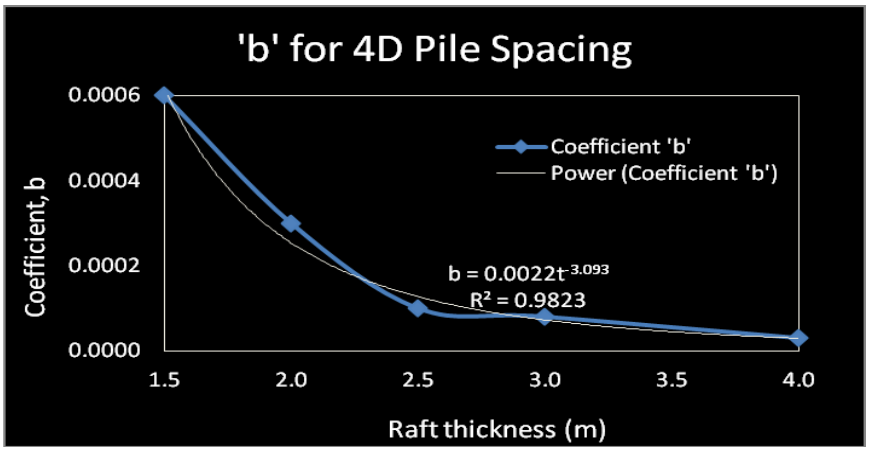

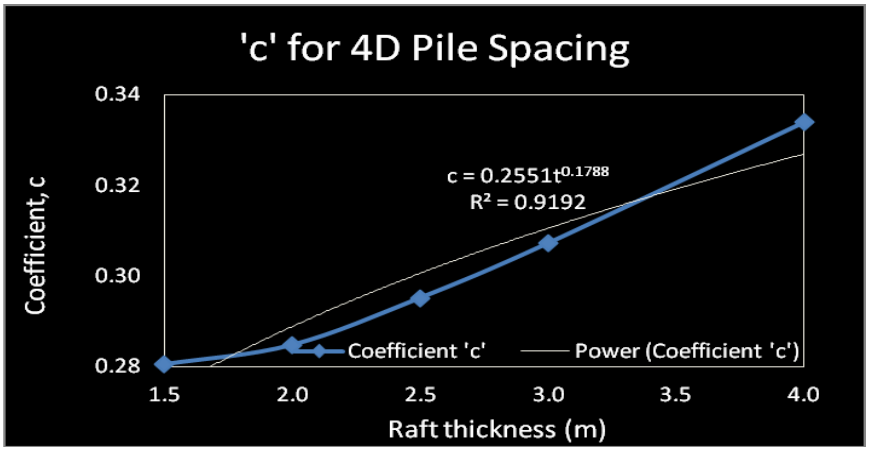

Figure 4.28 Parabolic coefficients relationship to various raft thickness for 4D spacing

The equation becomes $y = 0.0004t^{-3.207}x^2 + 0.0022t^{-3.093} - 0.2551t^{0.1788}$ (4.31)

For 6D spacing

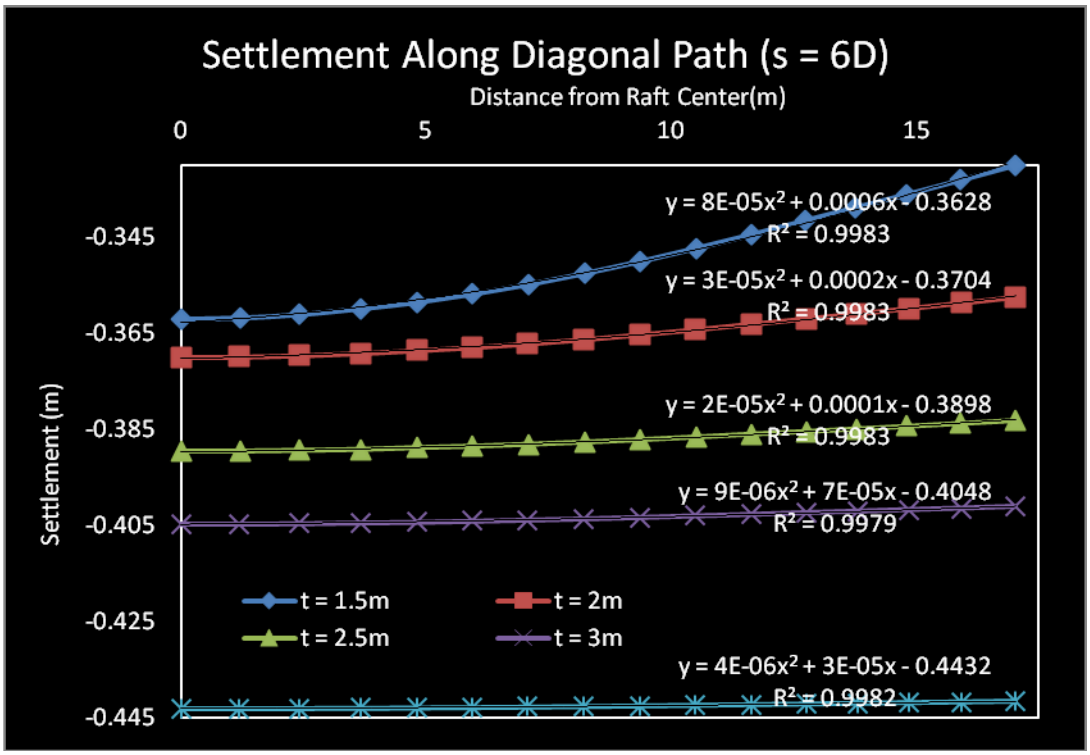

Figure 4.29 Differential settlements for various raft thickness of 6D spacing

Table 4.11 Differential settlement equation for various raft thickness of 6D pile spacing

Thickness (m)	Equation	R^2	a	b	c
1.5	$y = 8E\text{-}05x^2 + 0.0006x - 0.3628$	0.9983	0.00008	0.0006	0.3628
2.0	$y = 3E\text{-}05x^2 + 0.0002x - 0.3704$	0.9983	0.00003	0.0002	0.3704
2.5	$y = 2E\text{-}05x^2 + 0.0001x - 0.3898$	0.9983	0.00002	0.0001	0.3898
3.0	$y = 9E\text{-}06x^2 + 7E\text{-}05x - 0.4048$	0.9979	0.000009	0.00007	0.4048
4.0	$y = 4E\text{-}06x^2 + 3E\text{-}05x - 0.4432$	0.9982	0.000004	0.00003	0.4432

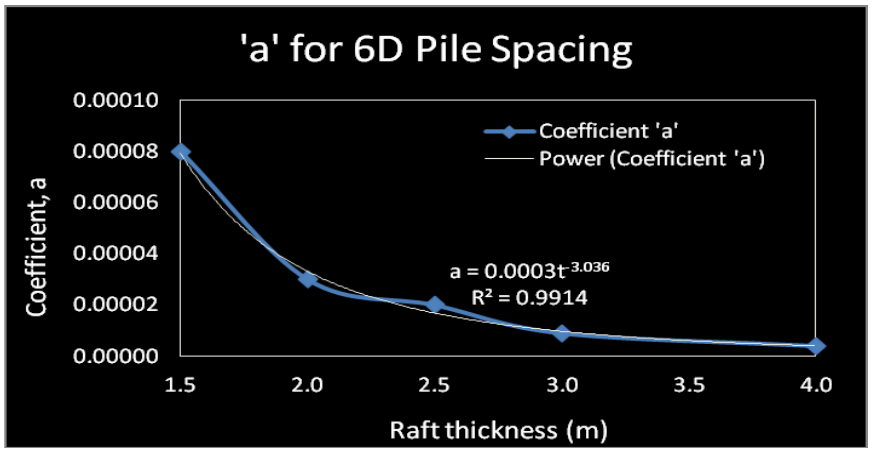

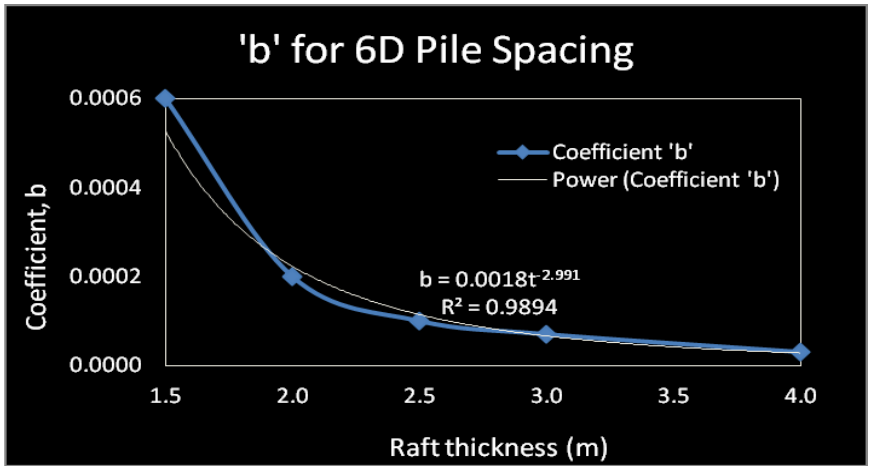

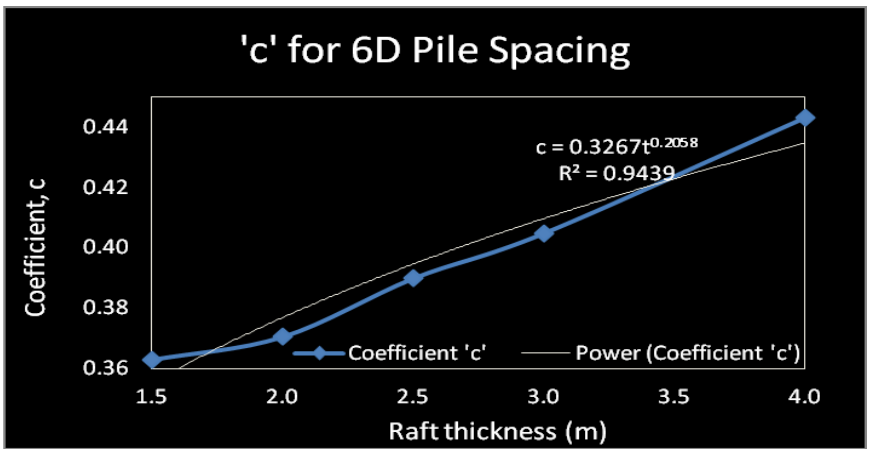

Figure 4.30 Parabolic coefficients relationship to various raft thickness for 6D spacing

And the equation becomes, $y= 0.0003t^{-3.036}x^2 + 0.0018t^{-2.991}x - 0.3267t^{0.2058}$ (4.32)

For 8D spacing

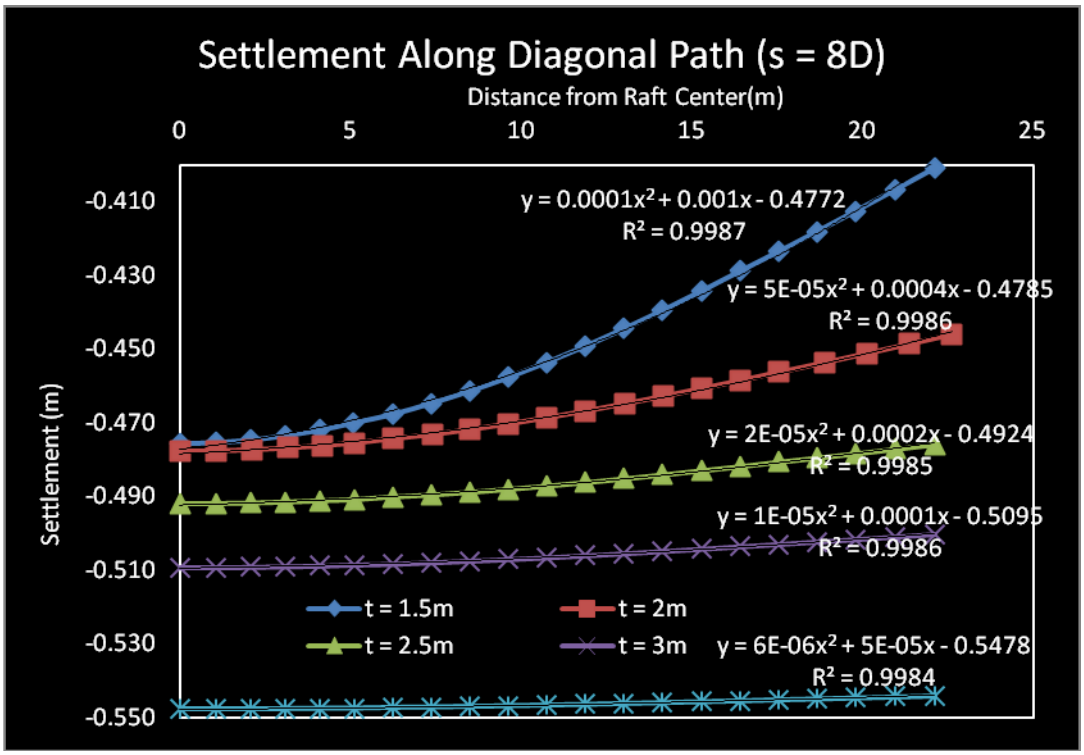

Figure 4.31 Differential settlements for various raft thickness of 8D spacing

Table 4.12 Differential settlement equation for various raft thickness of 8D pile spacing

Thickness (m)	Equation	R^2	a	b	C
1.5	$y = 0.0001x^2 + 0.001x - 0.4772$		0.0001	0.001	0.4772
2.0	$y = 5E\text{-}05x^2 + 0.0004x - 0.4785$		0.00005	0.0004	0.4785
2.5	$y = 2E\text{-}05x^2 + 0.0002x - 0.4924$		0.00002	0.0002	0.4924
3.0	$y = 1E\text{-}05x^2 + 0.0001x - 0.5095$		0.00001	0.0001	0.5095
4.0	$y = 6E\text{-}06x^2 + 5E\text{-}05x - 0.5478$		0.000006	0.00005	0.5478

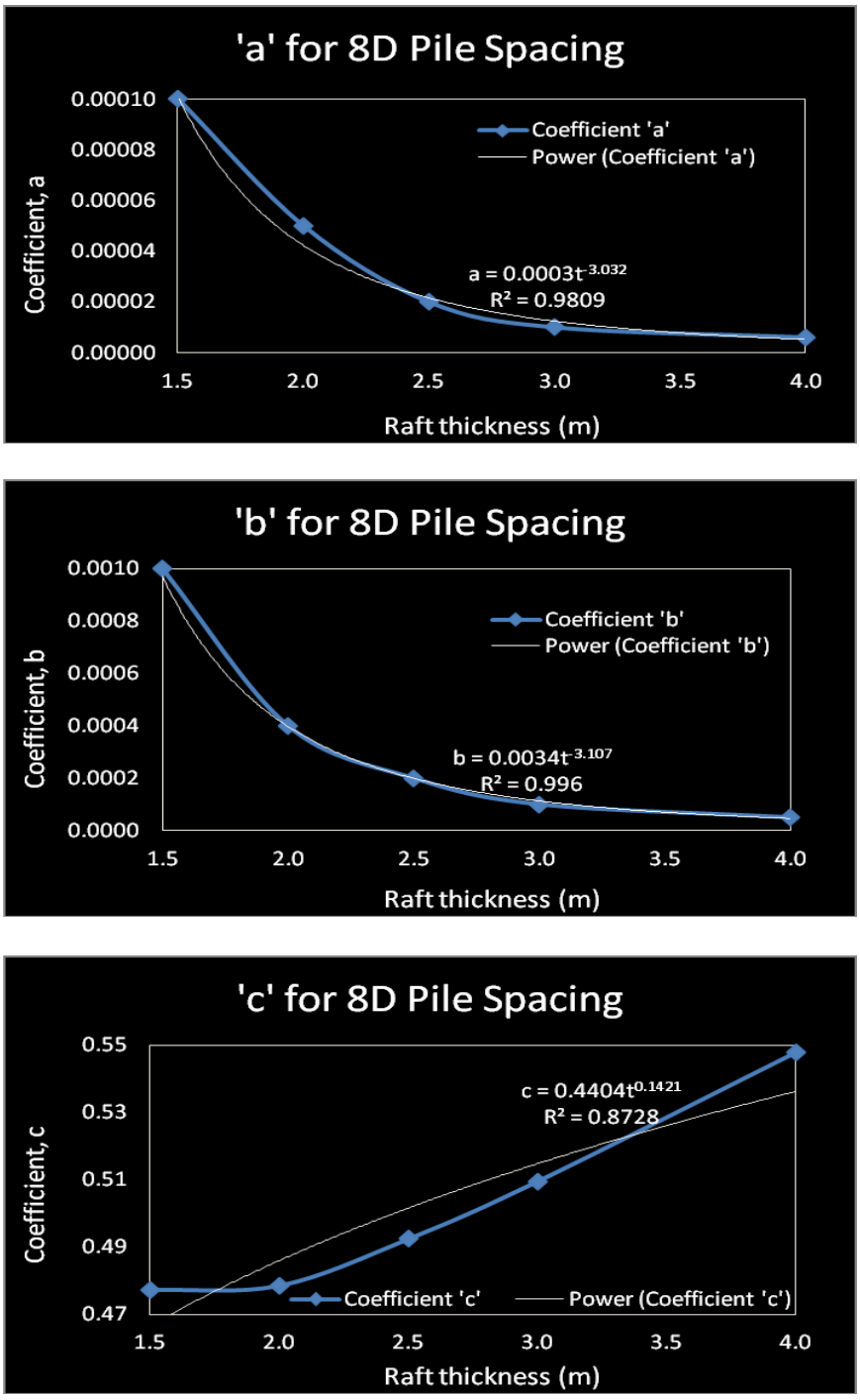

Figure 4.32 Parabolic coefficients relationship to various raft thickness for 8D spacing

The equation becomes $y = 0.0003t^{-3.032}x^2 + 0.0034t^{-3.107} - 0.4404t^{0.1421}$ (4.33)

4.5.4.2 Differential Settlement Model in Terms of Pile Spacing

To express the parabolic coefficients in terms of pile spacing, the 3-D numerical sumulated output of 15 models, under identical boundary, loading, material and geometric condition, were studied. Only the raft thcikness were varied from 1.5m to 4.0m. The output are plotted for 4D, 6D & 8D pile spacing as shown in figures 4.33, 4.35, 4.37, 4.39 & 4.41. The respective mathematical model to capture each of the curve shapes along with their fitness coefficients are shown in tables 4.13, 4.14, 4.15, 4.16 & 4.17 respectively. The coefficient of the representative parabolic curves for each case have been plotted in terms of pile spacing as shown in figures 4.34, 4.36, 4.38, 4.40 and 4.42 respectively.

For 1.5m raft thickness

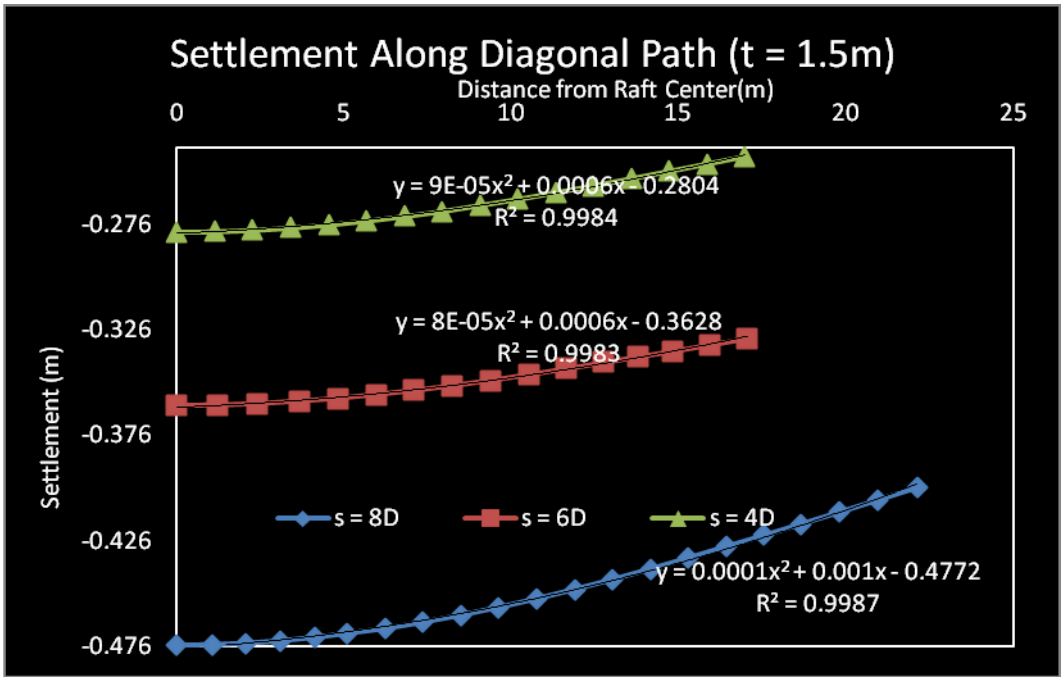

Figure 4.33 Differential settlement for various pile spacing of 1.5m thick raft

Table 4.13 Differential settlement equation for various pile spacing of raft thickness 1.5m

Spacing	Equation	R^2	a	b	C
4D	$y = 9E\text{-}05x^2 + 0.0006x - 0.2804$	0.9984	0.00009	0.0006	0.2804
6D	$y = 8E\text{-}05x^2 + 0.0006x - 0.3628$	0.9983	0.00008	0.0006	0.3628
8D	$y = 1E\text{-}04x^2 + 0.001x - 0.4772$	0.9987	0.00010	0.0010	0.4772

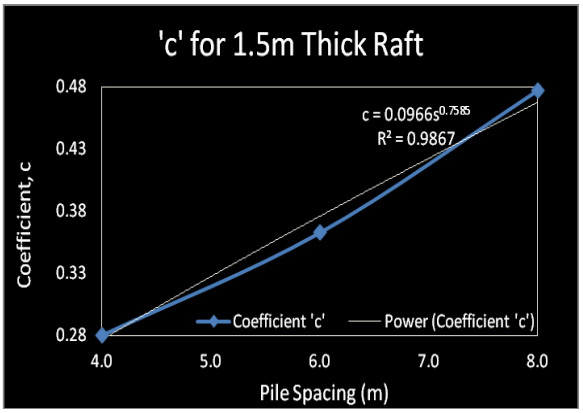

Figure 4.34 Parabolic coefficient ‘c’ for various pile spacing of 1.5m thick raft

Table 4.13 indicates that the parabolic coefficients ‘a’ and ‘b’ do not vary significantly with the pile spacing while, coefficient ‘c’ varies significantly with the pile spacing. Coefficient ‘c’ is therefore expressed in terms of pile sapcing as depicted in figure 4.34 above. The parabolic equation is therefore expressed in terms of the average value of coeficient ‘a’ and ‘b’ of table 4.13, and the power value of ‘c’ obtained from figure 4.34 above, as

$$y = 9E\text{-}05x^2 + 6E\text{-}04x - 0.0966s^{0.7585} \qquad (4.34)$$

The same raft top delection pattern and effects of the curves coefficients have been found for varying pile spacing for each raft thickness of 2.0, 2.5, 3.0 and 4.0m. The deflected curves obtained from numerical output, developed coefficients plots and their tabular representation for each type of raft thickness, have been depicted in the subsequent figures (figure 4.35 to 4.42) and in tables (Table 4.14 to 4.17). It is concluded that the change in pile spacing have no influence on deflected curve coefficients 'a' and 'b'. However, coefficient 'c' varies with the spacing. Therefore, the differential settlement equation developed for each raft thickness ignores the pile spacing effects on coefficients 'a' and 'b' and their average values are taken into consideration.

For 2.0m raft thickness

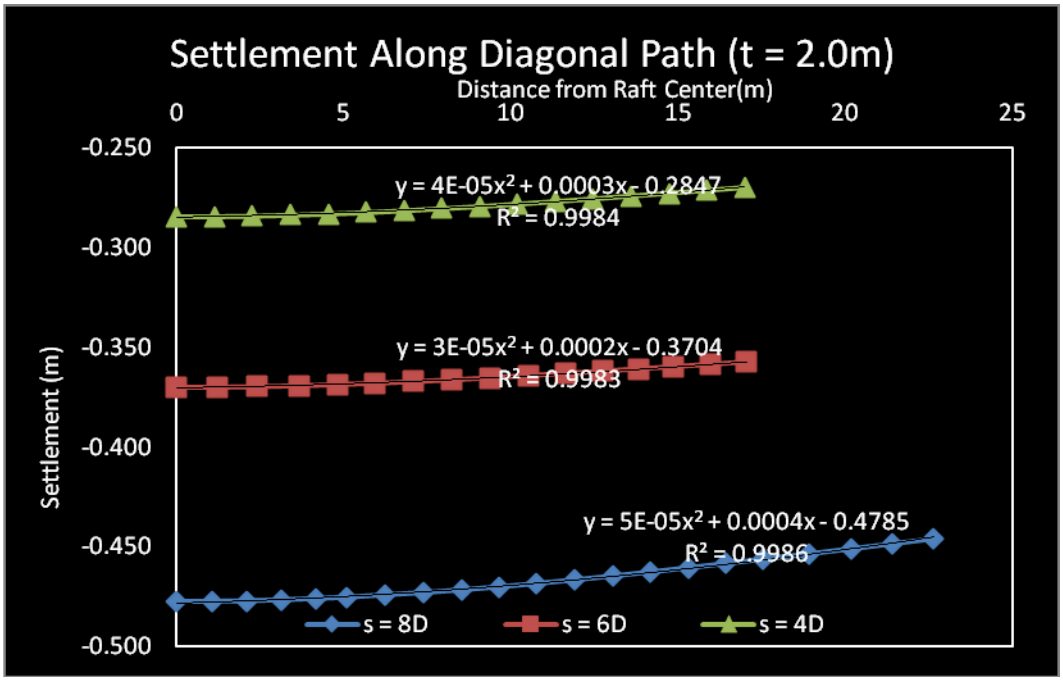

Figure 4.35 Differential settlement for various pile spacing of 2.0m thick raft

Table 4.14 Differential settlement equation for various pile spacing of raft thickness 2.0m

Spacing	Equation	R^2	a	b	c
4D	$y = 4E\text{-}05x^2 + 0.0003x - 0.2847$		0.00004	0.0003	0.2847
6D	$y = 3E\text{-}05x^2 + 0.0002x - 0.3704$		0.00003	0.0002	0.3704
8D	$y = 5E\text{-}05x^2 + 0.0004x - 0.4785$		0.00005	0.0004	0.4785

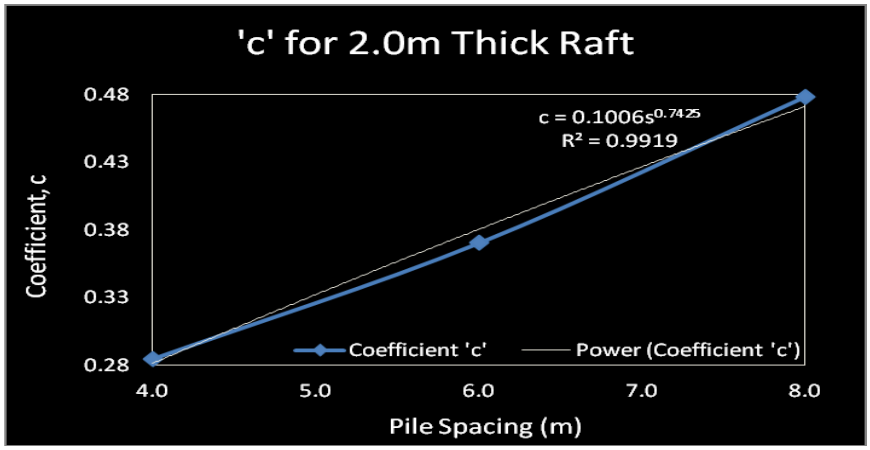

Figure 4.36 Parabolic coefficient 'c' for various pile spacing of 2.0m thick raft

The differential settlement equation for raft thickness of 2.0m becomes

$$y = 4E\text{-}05x^2 + 3E\text{-}04x - 0.1006s^{0.7425} \quad (4.35)$$

For 2.5m raft thickness

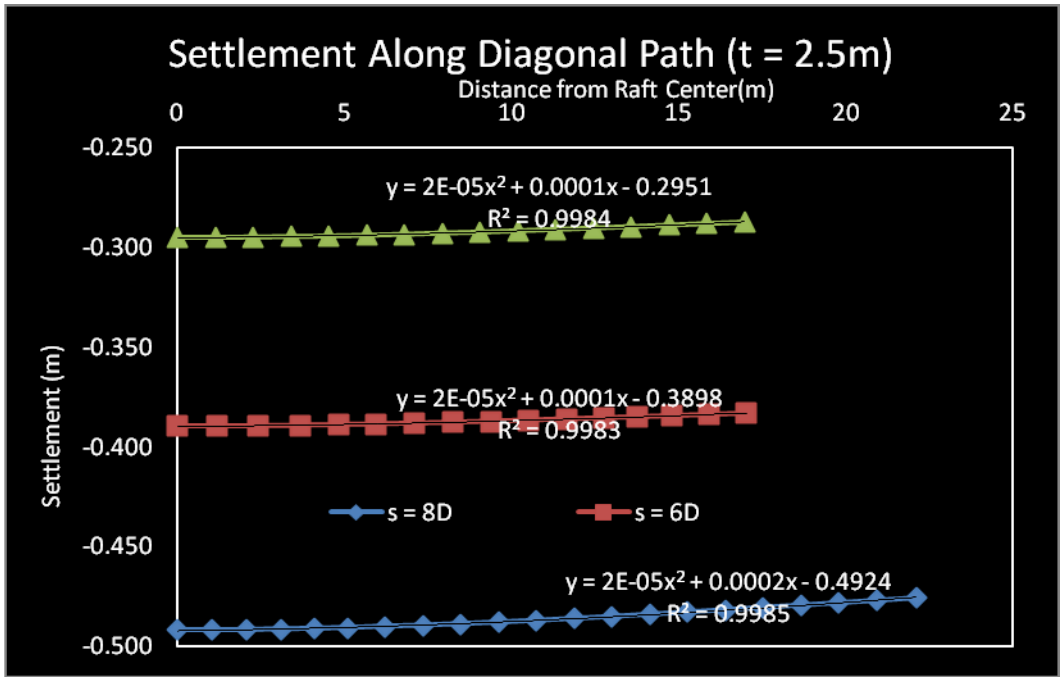

Figure 4.37 Differential settlement for various pile spacing of 2.5m thick raft

Table 4.15 Differential settlement equation for various pile spacing of raft thickness 2.5m

Spacing	Equation	R^2	a	b	c
4D	$y = 2E\text{-}05x^2 + 0.0001x - 0.2951$		0.00002	0.0001	0.2951
6D	$y = 2E\text{-}05x^2 + 0.0001x - 0.3898$		0.00002	0.0001	0.3898
8D	$y = 2E\text{-}05x^2 + 0.0002x - 0.4924$		0.00002	0.0002	0.4924

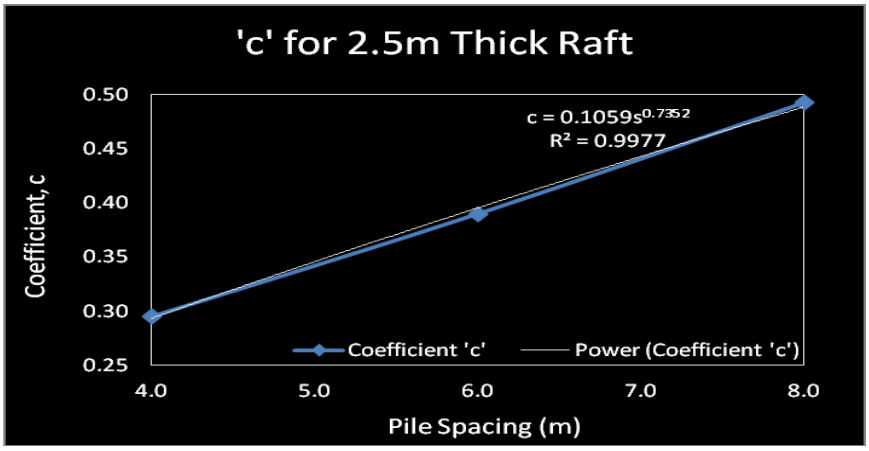

Figure 4.38 Parabolic coefficient 'c' for various pile spacing of 2.5m thick raft

The differential settlement equation for raft thickness of 2.5m becomes

$$y = 2E\text{-}05x^2 + 1E\text{-}04x - 0.1059s^{0.7352} \quad (4.36)$$

For 3.0m raft thickness

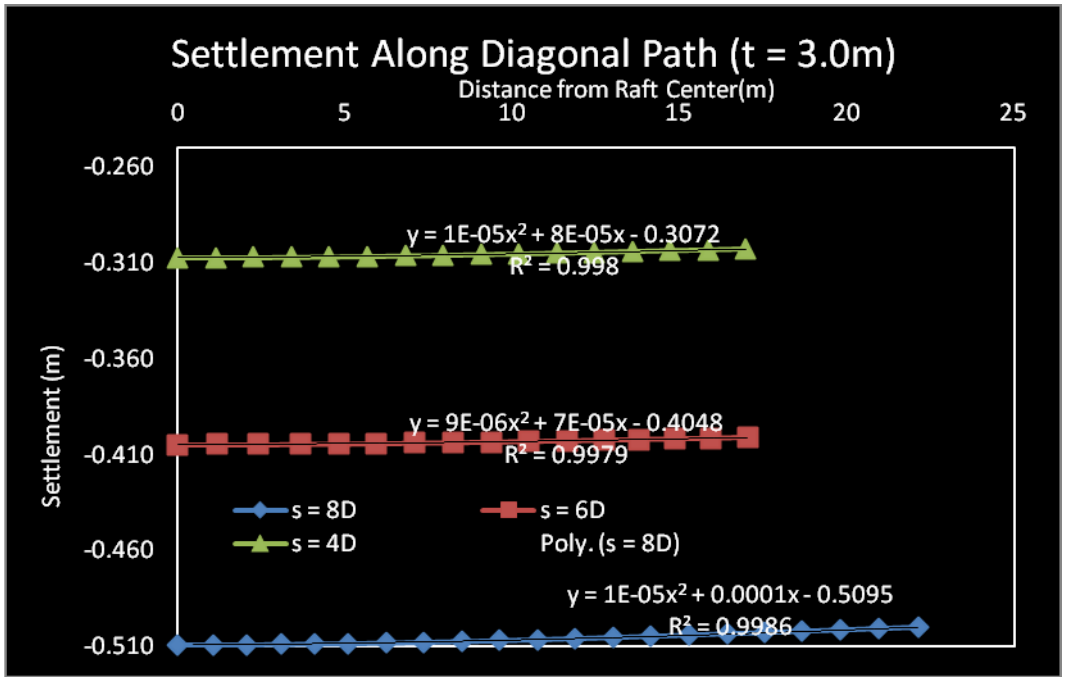

Figure 4.39 Differential settlement for various pile spacing of 3.0m thick raft

Table 4.16 Differential settlement equation for various pile spacing of raft thickness 3.0m

Spacing	Equation	R^2	a	b	c
4D	$y = 1E\text{-}05x^2 + 8E\text{-}05x - 0.3072$		0.00001	0.00008	0.3072
6D	$y = 9E\text{-}06x^2 + 7E\text{-}05x - 0.4048$		0.000009	0.00007	0.4048
8D	$y = 1E\text{-}05x^2 + 0.0001x - 0.5095$		0.00001	0.0001	0.5095

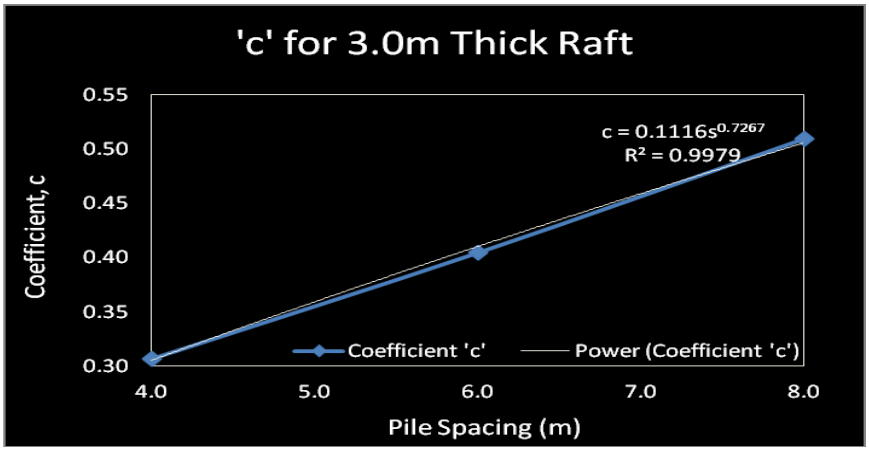

Figure 4.40 Parabolic coefficient 'c' for various pile spacing of 3.0m thick raft

The differential settlement equation for raft thickness of 3.0m becomes

$$y = 1E\text{-}06x^2 + 8E\text{-}05x - 0.1116s^{0.7267} \quad (4.37)$$

For 4.0m raft thickness

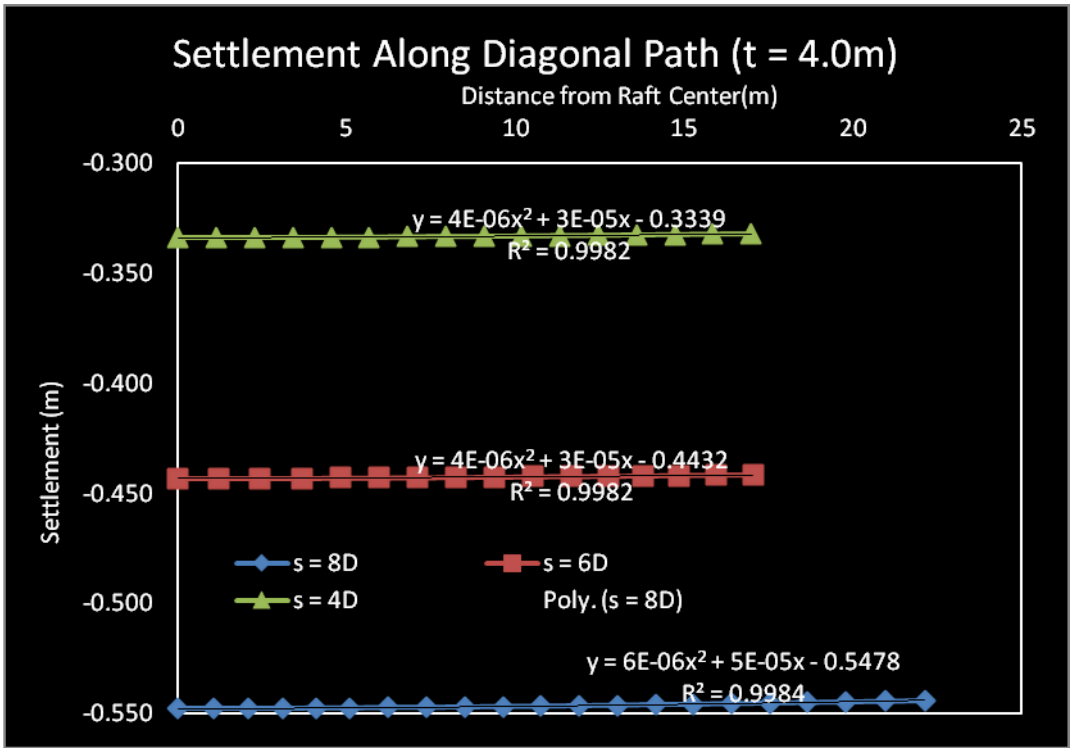

Figure 4.41 Differential settlement for various pile spacing of 4.0m thick raft

Table 4.17 Differential settlement equation for various pile spacing of raft thickness 4.0m

Spacing	Equation	R^2	a	b	c
4D	$y = 4E\text{-}06x^2 + 3E\text{-}05x - 0.3339$		0.000004	0.00003	0.3339
6D	$y = 4E\text{-}06x^2 + 3E\text{-}05x - 0.4432$		0.000004	0.00003	0.4432
8D	$y = 6E\text{-}06x^2 + 5E\text{-}05x - 0.5478$		0.000006	0.00005	0.5478

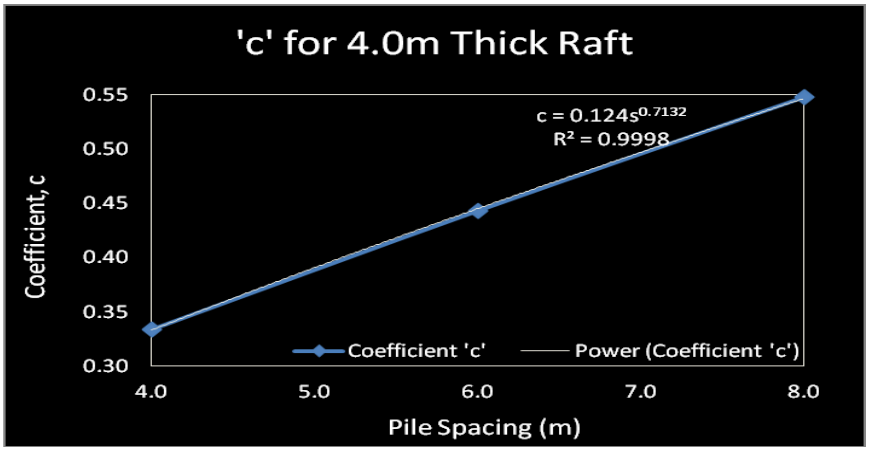

Figure 4.42 Parabolic coefficient 'c' for various pile spacing of 4.0m thick raft

The differential settlement equation for raft thickness of 4.0m becomes

$$y = 4E\text{-}06x^2 + 3E\text{-}05x - 0.124s^{0.7132} \quad (4.38)$$

4.5.5 The Differential Settlement Model

To finalize the differential settlement model in terms of raft thickness and spacing, the equations obtained in sections 4.5.4.1 & 4.5.4.2 are repeated below.

Differential settlement equations in terms of raft thickness

4D $$y = 0.0004t^{-3.207}x^2 + 0.0022t^{-3.093}x - 0.2551t^{0.1788} \quad (4.31)$$

6D $$y = 0.0003t^{-3.036}x^2 + 0.0018t^{-2.991}x - 0.3267t^{0.2058} \quad (4.32)$$

8D $$y = 0.0003t^{-3.032}x^2 + 0.0034t^{-3.107}x - 0.4404t^{0.1421} \quad (4.33)$$

Differential settlement equations in terms of pile spacings

t = 1.5m $y = 9E\text{-}05x^2 + 6E\text{-}04x - 0.0966s^{0.7585}$ (4.34)

t = 2.0m $y = 4E\text{-}05x^2 + 3E\text{-}04x - 0.1006s^{0.7425}$ (4.35)

t = 2.5m $y = 2E\text{-}05x^2 + 1E\text{-}04x - 0.1059s^{0.7352}$ (4.36)

t = 3.0m $y = 1E\text{-}06x^2 + 8E\text{-}05x - 0.1116s^{0.7267}$ (4.37)

t = 4.0m $y = 4E\text{-}06x^2 + 3E\text{-}05x - 0.1240s^{0.7132}$ (4.38)

The above sets of equations indicate that 'a' and 'b' vary with raft thickness (t) and can be expressed in terms of 't', while 'c' varies with pile spacing (s) and can be expressed in terms of 's'. The above equations also indicate that 'a' and its associated power components do not vary, it can therefore be taken as $0.0003t^{-3}$ without any further treatment. Coefficient 'b' has a minor variation and a weighted average is applied to balance in between the power components and coefficient components to yield the 'b' value of $0.002t^{-3}$.

A similar approach has been used to finalize the 'c' value in the model. Based on equations 4.31, 4.32 & 4.33, the power of 't' is fixed at 0.18 by weighted average technique and the coefficients of 0.2551, 0.3267 & 0.4404 of the equations are plotted against spacing in order to express them in terms of pile spacing and to yield a power relationship of 0.78, as shown in figure 4.43 below.

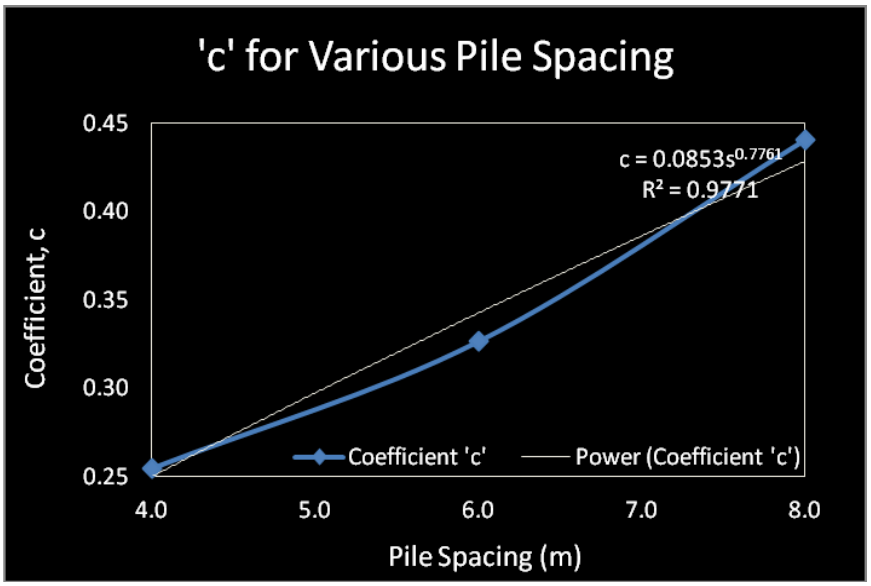

Figure 4.43 Coefficients for various pile spacing

Therefore, the final equation can be standardized as below.

$$y = 0.0003t^{-3}x^2 + 0.002t^{-3}x - 0.085s^{0.78}t^{0.18} \quad (4.39)$$

or in an approximate form of

$$y = 0.0003t^{-3}x(x + 6) - 0.085s^{0.78}t^{0.18} \quad (4.40)$$

where, 'y' is the vertical displacement of any point on the raft at a distance of 'x' from raft centre to the periphery, 't' is the raft thickness and 's' is the pile spacing.

4.5.6 Validation with the Numerical Model

The developed analytical model in equation (4.40) is validated with those of the numerical models discussed earlier for the raft of 24x24x2m for 4D and 6D pile spacing and of 32x32x2m raft for 8D pile spacing. Equation (4.40) is used to estimate the raft

centre (for x = 0) and corner point settlement (x = $12*\sqrt{2}$ for 4D & 6D and x = $16*\sqrt{2}$ for 8D spacing). The comparison is shown in table 4.18 below.

Table 4.18 Validation of analytical model with the numerical model

Spacing	Settlement (numerical)		Settlement (Analytical)		Deviations* in %	
	Centre	Corner	Centre	Corner	Centre	Corner
4D	-0.284	-0.267	-0.284	-0.276	0.00	0.05
6D	-0.370	-0.357	-0.390	-0.381	0.12	0.14
8D	-0.478	-0.446	-0.488	-0.479	0.04	0.15

*The deviation percentages in settlement values have been calculated on the basis of the coreesponding values of numerical and analytical model, making the percentage on the half raft width (as the comparison is done for corner and centre points)

The settlement obtained from analytical model is greater than the numerical and the maximum deviation is shown corresponding to 6D spacing of about 0.14%. These deviations can be minimized by changing the exponential power of spacing from 0.78 to 0.76 as shown in equation (4.41) below. Table 4.19 shows that the deviation is minimum. Therefore, the proposed differential settlement model for pile raft foundation is

$$y= 0.0003t^{-3}x(x + 6) - 0.085s^{0.76}t^{0.18} \qquad (4.41)$$

Table 4.19 Validation of analytical model with the numerical model for $s^{0.76}$

Spacing	Settlement (numerical)		Settlement (Analytical)		Deviations* in %	
	Centre	Corner	Centre	Corner	Centre	Corner
4D	-0.284	-0.267	-0.276	-0.268	-0.05	0.01
6D	-0.370	-0.357	-0.376	-0.368	0.03	0.06
8D	-0.478	-0.446	-0.468	-0.460	-0.05	0.06

*The deviation percentages in settlement values have been calculated on the basis of the coreesponding values of numerical and analytical model, making the percentage on the half raft width (as the comparison is done for corner and centre points)

4.6 Design Strategy

This study clearly gives the interaction factors based on the actual pile raft and its configurations. Therefore, the load sharing can easily be estimated by the interaction chart provided in figure 4.4 with the related equations mentioned in section 4.2. Once the load carried by the raft and pile group is obtained, it is convenient to the designers to design the raft and the pile group. The study clearly shows that pile spacing greater than 7D is ineffective, and in that case, an individual raft is good enough to withstand the applied load. On the other hand, pile spacing less than 4D, makes the raft contribution ineffective, because majority of the load is carried by the pile group in that case.

Each code has its specified settlement allowances or limit. The maximum settlement can be estimated for any type of soil and foundation components of any type of mechanical and geometrical properties from equation (4.29). Equation (4.29) basically yields the centre point or maximum settlement of the raft, which is important to estimate rather than the average settlement or total settlement.

Once the foundation centre point settlement is estimated, equation (4.41) can be applied to estimate the settlement at any point on the foundation top with the following modification.

$$y= 0.0003t^{-3}x(x + 6) - y_{centre} \qquad (4.42)$$

where, y_{centre} is the raft centre settlement mentioned in equation (4.29).

Chapter 5

Conclusions and Recommendations

5.1 Introduction

The pile raft foundation is a complex system and its stress distributions are three dimensions in nature. Attempt has been made in this work to capture these effects by means of three dimensional finite element software ABAQUS simulations. These simulations and the output yields some remarks which are summarised stepwise in the next section and in the following section recommendations have been made for future works.

5.2 Conclusions

The concluding remarks below are according to the development of the models

01. On developing the numerical model.

    Extent of stress influence zone exists in a maximum of twice the pile length in vertical direction and about 30 times the pile diameter in lateral direction.

    Conventionally, the finer the finite element the more precise is the result, but after a certain limit, the finer element does not yield any significant influence on the output. To reduce the computational cost, it should be limited to its optimum.

    The time increments of any analysis step should be limited to its optimum as excessive step time increments would not influence the output significantly.

The pile cross-sectional shapes (square, octagonal, circle) have minor influences on its load settlement behavior as obtained from 3D FEM analysis of ABAQUS.

02. On the basis of parametric study

Pile raft increase the load resistance of about 40% than that of individual pile group or mat foundation.

Pile spacing more than 7D is ineffective.

An optimization among the pile length, diameter and spacing should be established in order to develop a cost effective foundation with minimum total and differential settlement.

Similarly, thicker raft is effective in reducing differential settlement; however, it contributes to the maximum settlement because of its self weight. A thinner raft, on the other hand, is susceptible to the differentials settlement and punching shear. Therefore, an optimization needs to be established.

At smaller pile spacing, piles take the greater portion of the load and at larger pile spacing; the major load portion is carried by the raft.

03. On load sharing model

The value of pile raft interaction factor increases with the increase of pile stiffness (E_p/E_s), however, for greater stiffness (E_p/E_s =1000 or more), the interaction factors do not vary significantly with the pile-soil stiffness.

Pile raft interaction factor decreases with increased pile spacing i.e. greater pile spacing is less susceptible to the interaction in between piles and raft.

Pile raft interaction factor increases with the increase in slenderness ratio (L_p/d_p). However, this increment is less for small pile spacing as compared to large pile spacing.

04. On centre settlement model

The raft top centre settles more than any other point of the foundation.

The raft top centre settlement has been captured by an analytical model based on the statistical multiple regression technique.

The various points of raft top settle in a pattern to yield a bowl shape of the deflected raft top.

05. On differential settlement model

The bowl shape deflection of the raft top is parabolic in nature.

The bowl shape raft top settlement profile has been modeled in terms of raft thickness which is capable of estimating the settlement of any point on the raft top, and thereby, the settlement of any individual pile of pile group under the raft.

5.3 Recommendation for Future Works

The pile raft foundation is a new concept and a lot of investigation needs to be done to expose the interaction among the foundation components. Therefore, it is essential to

- Investigate the full scale model tests under various conditions and configurations.
- Collect the data of the instrumented pile raft foundation of various buildings.
- Estimate the pile raft interaction factors for plastic soil with varying mechanical and geometrical properties of the foundation components to establish the interaction factor charts.
- Study the statistical interaction influences of the multiple regression models. This is because raft thickness, size, pile dimensions (diameter and length) with spacing contribute to the total load of the foundation, and in this work, the load is considered as an independent variable.
- Study the influences of pore water pressure, stage construction on pile raft foundation.

- Establish the safety factor for this type of foundation as no code has been finalized yet.
- Develop the models for layered soil.
- Develop the theory of mixing as soil is a three phase medium.

REFERENCES

1. Ahner, C., and Soukhov, D., (1999), "Safety Concept in Codified Design of piled raft foundation (CPRF)", LACER 4, 403 - 412. Universität Leipzig

2. Ahner, C., Soukhov, D., and Konig, G., (1998), "Reliability Aspects of Design of Combined Piled-Raft Foundation (CPRF)", 2nd Int. PhD Symposium in Civil Engineering Budapest.

3. Ahner C., Soukhov D. (1996): Combined Piled-Raft Foundation (CPRF) "Safety Concept", Lacer 1, 333-345, Universität Leipzig

4. Ai Z.Y., Han J, Yan Y. (2005), "Elastic Analysis of Single Pile-Rigid Circular Raft System in Layered Soil", Advances in Deep Foundations, ASCE, Geotechnical Special Publications 132.

5. Anagnostopoulos, C. & Georgiadis, M. (1998), "A Simple Analysis of Piles in Raft Foundation. Geotechnical. Engineering, vol 29, No.1, 71-83.

6. Baladi, G. Y., Rohani, B. (1979a), "Elastic-plastic model for saturated sand"; Journal of the Geotechnical Engineering Division, Proc. ASCE, Vol. 105, No. GT4, 465-480.

7. Baladi, G. Y., Rohani, B. (1979b), "An Elastic-plastic Cnstitutive Model for Saturated Sand Subjected to Monotonic and/or Cyclic Loadings". Proc. 3rd ICNMG, Aachen, 389-404, Rotterdam: Balkema.

8. Barthe K. J., Snyder M.D. (1980), "On Some Current Procedures and Difficulties in FE Analysis of Elasto-plastic Rresponse", Computers and structures, Vol.12, 607 – 624.

9. Basile, F. (2000), "Non Linear Analysis of Pile Group", Discussion Proc. ICE, Geotechnical Engineering, Vol.143, Oct, 241-244.

10. Booker, J. R., Poulos, H. G. (1976), "Analysis of Creep Settlement of Pile Foundations", ASCE, Vol. 102, No. 1, pp 1-14.

11. Brown P.T. (1969), Numerical Simulation of Uniformly Loaded Circular Rafts on Elastic Layers of Finite Depth, Geotechnique, Vol. 19, No. – 2, 301 – 306.

12. Burland, J.B., Kaira J.C. (1986), "Queen Elezabeth II Conference Centre, Gotechnical Aspects", Porc. ICE, part I, No.- 80, 1479 - 1503

13. Burland, J.B., Broms, B.B. and de Mello, V.F.B. (1977), "Behavior of Foundations and Structures", Proc.9 ICSMFE, Tokyo, 2, 495-546.

14. Butterfield, R. and Banerjee, P.K. (1971), "The Elastic Analysis of Compressible Piles and Pile Groups", Géotechnique 21, No. 1,43-60

15. Butterfield, R. and Banerjee, P.K. (1981), "The Problem of Pile Group – Pile Cap Interaction", Géotechnique, 21(2), 135-149.

16. Canadian Geotechnical Society (2006), "Canadian Foundation Engineering Manual", 4th edition, Printed in January, 2007.

17. Cao X.D., Wong H.I., Chang M.F. (2004), "Behavior of Model Raft Resting on Pile-Reinforced Sand", Journal of Geotechnical and Geoenvironmental Engineering, ASCE, 130 (2), 129-138.

18. Chow H.S.W., Small J.C (2006), "Analysis of Piled Raft Foundation with Piles of Different Lengths Subjected to Horizontal and Vertical Loading", NIMGE, Porc.6th European Conf. on NUMGE, Graz, Austria, 6-8 Septermeber, 2006, 583 – 588.

19. Chow H.S.W., Small J.C (2005), "Behavior of Pile Raft with Piles of Different Lengths and Diameter under Vertical Loading", ASCE, Advances in Deep Foundation. GSP 132

20. Chow H.S.W., Yong K.Y. (2001), "Analysis of Pile Raft Foundation Using a Variational Approach", ASCE, International Journal of Geomechanics, vol. 1 no.2, 129-147.

21. Chow H.S.W.(1987), "Iterative Analysis of Pile-Soil-Pile Interaction", Geotechnique 37, No. – 3, 321 - 333.

22. Clancy, P. and Randolph, M.F. (1996), "Simple Design Tools for Piled Raft Foundations", Géotechnique 46(2), 313-328.

23. Clancy, P. and Randolph, M.F. (1993), "An Approximate Analysis Procedure for Piled Raft Foundations", Int. J.Numer. and Analytical Methods in Geomech., London, 17(12), 849-869.

24. Clarke N.W.B., Watson J.B. (1936), "Settlement Records and Loading Data for Various Building Erected by the Public Works Department, Municipal Council, Shanghai", Proceedings of 1st ICSMFE, Cambridge, Mass, USA, June 1936 vol.2 pp 174-185.

25. Cooke R.W. (1986), "Piled Raft Foundation on Stiff Clays – A Contribution to Design Philosophy", Geotechnique 36. no.-2, 169-203

26. Cunha, R. P. and Poulos, H. G. and Small, J.C. (2001), "Investigation of Design Alternatives for a Piled Raft Case History", Géotechnique, Vol.127, (8), 635-641.

27. Das B.M. (2008), "Advanced Soil Mechanics", 3rd edition, Taylor & Francis, New York, NY.

28. Das B.M. (2007), "Principles of Foundation Engineering" 6th edition, Thomson, Canada.

29. Davis, E.H. and Poulos, H.G. (1972), "The Analysis of Piled Raft Systems", Aust. Geomechs.J. , G2: 21-27.

30. DiMaggio, F. L., Sandler, I. S. (1971), "Material model for granular soils". Journal of the Engineering Mechanics Division, Proc. ASCE, Vol. 97, No. EM 3, 935-950

31. Drucker, D. C., Prager, W. (1952), "Soil Mechanics and Plastic Analysis or Limit Design". Quarterly of Applied Mathematics, Vol. X, 157-165.

32. Drucker, D. C., Gibson, R. E., Henkel, D. J. (1957), "Soil mechanics and work-hardening theories of plasticity". Transactions ASCE, Vol. 122, 338-346.

33. Duncan J.M., Chang C.Y. (1970), "Nonlinear Analysis of Stress and Strain in Soils" Journals of the Soil Mechanics and Foundation Division, Proc. ASCE, vol. 96, SM 5, 1629-1653.

34. El-Mossallamy, Y. (2002), "Innovative Application Of Piled Raft Foundation In Stiff and Soft Subsoil", Geot. Spec. Pub. 116, ASCE, 1: 426-440.

35. Fleming W.C.K., Weltman A.I., Randolph M.F., Elson W.K. (1992), "Piling Engineering", 2nd edition, pp 179-214, Blackie.

36. Framk L., DiMaggio, Sandler I.S. (1971), "Material Model for Granular Soil", Journal of the Engineering Mechanics Division, ASCE, vol. 97 EM 3 pp. 935 - 950

37. Franke, E., Lutz, B. and El-Mossallamy, Y. (1994), "Measurements and Numerical Modelling of High-Rise Building Foundations on Frankfurt Clay", Geot. Spec. Pub. 40, ASCE, 2: 1325-1336, New York: American Society of Civil Engineers.

38. Franke R.,Guenot A., Humbert P. (1982), "Numerical Analysis of Contacts in Geomechanics", Proc. 4th ICNMG, Edmonton, vol. 1, 37-45, Rotterdam Balkema.

39. Fraser, R. A. and Wardle, L. J. (1976), "Numerical Analysis of Rectangular Rafts on Layered Foundations", Géotechnique 26, No. 4, 613.

40. Garcia F., Lizcano A, Reul O. (2006), "Visco-plastic Model Applied to The Case History of Piled Raft Foundation", Geocongress, ASCE.

41. Gens A., Potts D.M., (1988), "Critical State Models in Computational Geo-mechanics". Engineering Computations, vol. 5, issue 3, pp. 178 – 197. MCB UP Ltd.

42. Griffiths D.V., Clancy P. and Randolph M.F. (1991), "Piled raft foundation analysis by finite elements", Porc. 7th Int. Conf. Comput. Methods Adv. Geomech. Cairns, (2) 1153-1157, Rotterdam Balkema.

43. Griffiths, D. V. (1985), "Numerical modeling of interfaces using conventional finite elements". Proc. 5th ICNMG, Nagoya, 837-844, Rotterdam: Balkema

44. Griffiths, D. V. (1982), "Elasto-plastic analysis of deep foundations in cohesive soil". IJNAMG, Vol. 6, No. 2, 211-218.

45. Grycxmanski M., Majewski S (1997), "A study on elasto-plastic raft foundation-soil interaction", Proc. XIV ICSMFE, vol. 2, pp.983-986.

46. Gwizdata K., Tejchman A. (1997), "Numerival modelling of pile subsoil interaction", Proc. XIV ICSMFE, vol. 1, pp.673-676.

47. Guo, W. D. and Randolph M. F. (1999), "An Efficient Approach for Settlement prediction of Pile Groups", Géotechnique 49, No.2, 161-179.

48. Hain, S. J. & Lee, I. K. (1978), "The Analysis of Flexible Raft-Pile Systems", Géotechnique 28, No.1, 65-83

49. Hemsley J.A. (1998), "Elastic Analysis of Raft Foundation", Thomas Telford.

50. Han J., Ye S.L. (2006), "A Field Study on the Behavior of Foundations Underpinned by Micropiles", Canadian Geotechnical Journal, 43: 30–42.

51. Han, J., Ye, S.L. (2006). A field Study on the Behavior of Micropiles in Clay under Compression or Tension. Canadian Geotechnical Journal, 43: 19–29.

52. Hansbo, S. (1993), "Interaction Problems Related to the Installation of Pile Groups", Sem. on Deep Founds. on Bored and Auger Piles, BAP2, Ghent, 59-66.

53. Hansbo, S., (1993), "Interaction Problems Related to the Installation of Pile Groups", Sem. on Deep Founds. on Bored and Auger Piles, BAP2, Ghent, 59-66.

54. Hansbo, S. and Hoffman E (1973), "Gothenburg experiences concerning a difficult foundation problem and its unorthodox solution",

55. Hartmann F., Jahn P. (2001), "Boundary Element Analysis of Raft Foundations on Piles", Meccanica, vol. 36 pp.351 – 366,

56. Hassen G., Buhan P., (2006), "Elasto-plastic Multiphase Model for Simulating the Response of Piled Raft Foundations Subject to Combined Loadings", Int. J. Numer. Anal. Meth. Geomech. 2006; 30:843–864.

57. Herrmann L.R. (1978), "Finite Element Analysis of Contact Problems", Journal of The Engineering Mechanics Division, Porc. ASCE, vol. 104, EM – 5, 1043-1057

58. Hibbit H.D., Karlsson B.L, Sorrensen (2007), "ABAQUS Theory Mannul and all Manuals, Guide, Online support (2007 to present)",

59. Hooper, J.A. (1979), Review of Behavior of Piled Raft Foundations, Report No. 83. London: CIRIA.

60. Hooper, J.A. (1973), "Observations on the Behavior of a Piled-Raft Systems", Geotechnique, 28 (1): 65-83.

61. Horikoshi, K. and Randolph, M. F. (1998), "A Contribution to Optimum Design of Piled Rafts", Geotechnique, 48 (3): 301-317.

62. Horikoshi, K. and Randolph, M. F. (1997), "Optimum Design of Piled Raft Foundations", Proceed. XIV ICSMFE, Hamburg, vol. 2, pp.1073 - 1076.

63. Horikoshi, K. and Randolph, M. F. (1996), "Centrifuge Modeling of Piled Raft Foundation on Clay", Geotechnique, 46 (4): 741-752.

64. Horikoshi, K. and Randolph, M. F. (1997), "Optimum Design of Piled Raft Foundations", Proc., 14th Int. Conf. on Soil Mech. and Found. Engrg., Hamburg, Germany, 2, 1073-1076.

65. Horikoshi, K. and Randolph, M. F. (1996), "Centrifuge Modeling of Piled Raft Foundations on Clay", Geotechnique, 46 (4): 741-752.

66. Hu L, Pu J. (2004), "Testing and Modeling of Soil–Structure interface". Journal of Geotechnical and Geoenvironmental. Engineering, ASCE; vol. 130 no.-8, pp. 851–860.

67. Jardin R.J., Potts, D.M., Fourire A.B., Burland J.B. (1986), "Studies of the Influence of Nonlinear Stress-Strain Characteristics in Soil-Structure Interactions", Geotechnique 36 no.-3, pp. 377 – 396.

68. Kakurai, M., Yamashita, K. & M. Tomono 1987. Settlement Behavior of Piled Raft Foundation on Soft Ground. Proc. VIII Asian Conference on SMFE, Kyoto: 373-376.

69. Katzenbach, R., Schmitt A., Turek J. (2005). Assessing Settlementof High-rise Structures by 3D Simulations" Computer Aided Civil and Infrastucute Engineering. vol.20, 221-229,

70. Katzenbach, R., Arslan, U. & Moormann, C. (2000). Piled Raft Foundation Projects in Germany. Design Applications of Raft Foundations, 323-391, London: Thomas Telford.

71. Katzenbach, R., Arslan, U., Moorman, C. & Reul, O. (1998), "Piled Raft Foundation: Interaction Between Piles and Raft", Darmstadt Geotechnics (Darmstadt University of Technology), No. 4, 279-296.

72. Katzenbach, R., Arslan, U., Gutwald, J., Holzhauser, J., Quick, H. (1997a), "Soil-Structure Interaction of the 300 m High Commerzback tower in Frankfurt am Main. Measurements and Numerical Studies", Proc. XIV ICSMFE, Vol. 2, 1081-1084, Rotterdam: Balkema.

73. Katzenbach, R., Reul, O. (1997b), "Design and Performance of Piled Rafts". Proc. XIV ICSMFE, Hamburg, Vol. 4, 2253-2256, Rotter-dam: Balkema.

74. Katzenbach, R., Arslan, U. & Gutwald, J. (1994). A Numerical Study on Pile Foundation on the 300 m High Commerzbank Tower in Frankfurt am Main. 3rd European Conference on Numerical Methods in Geomechanics, Manchester, 271-277, Rotterdam: Balkema

75. Kim, K. N., Lee, S. H., Kim, S. K., Chung, C. K., Kim, M. M., and Lee, H. S. (2001), "Optimal Pile Arrangement for Minimizing Differential Settlements in Piled Raft Foundations", Computers and Geotechnics 28: 235-253.

76. Kitiyodom P, Matsumoto T. (2005), "A Simplified Analysis Method for Piled Raft Foundations Subjected to Ground Movements Induced by Tunneling". Int. J. Numer. Anal. Meth. Geomech., 2005; 29:1485–1507.

77. Kitiyodom P, Matsumoto T. (2003), "A Simplified Analysis Method for Piled Raft Foundations in Non-homogeneous Soils", Int. J. Numer. Anal. Meth. Geomech., 2003; 27:85–109.

78. Kitiyodom P, Matsumoto T. (2002), “A simplified analysis method for piled raft and pile group foundations with batter piles”. Int. J. Numer. Anal. Meth. Geomech., 2002; 26:1349–1369.

79. Kudella P., Reul O. (2002), ”Hypo-plastic Analysis of Piled Rafts”, Numerical Methods in Geotechnical Engineering - 2002, pp. 389 - 395

80. Kulhawy F.H., Prakoso W.A. (1997), “Panel Discussion: Some Observations on Piled Raft Foundation Analysis”, Proc. XIV ICSMFE, Hamburg, Vol. 4, 2261-2262, Rotter-dam: Balkema.

81. Kuwabara, F. (1989), “An Elastic Analysis For Piled Raft Foundations In A Homogeneous Soil”, Soils Found. 28, No. 1, 82-92.

82. Liang F.Y.(2004), “A Modified Variational Approach for the Analysis of Piled Raft Foundation”, Mechanics Research Communications 31 (2004) 593–604.

83. Liang F.Y., Chen L.Z., Shi X.G., “Numerical Analysis of Composite Piled Raft with Cushion Subjected to Vertical Load”, Computers and Geotechnics 30 (2003) 443–453.

84. Mandolini, A., and Viggiani, C. (1997), “Settlement of Piled Foundations”, Geotechnique, London, 47(4), 791-816.

85. Maharaja D.K., (2004), “Three Dimensional Nonlinear Finite Element Analysis to Study the Effect of Raft and Pile Stiffness on the Load –Saettlement B ehavior o fPiled Radft Foundations”, Electronic Journal of Geotechnical Engineering, 2004.

86. Maharaja D.K., (2003), “Load Settlement Behavior of Piled Raft Foundation by Three Dimensional Nonlinear Finite Element Analysis”, Electronic Journal of Geotechnical Engineering 2003.

87. Mendonca A.V., Puiva J.B, (2003), “An Elastostatic FEM/BEM Analysis of Vertically Loaded Eaft and Piled Raft Foundation”, Engineering Analysis with Boundary Elements 27 (2003) 919–933, Elsevier.

88. Mendonca A.V., Paiva J.B.. “A Bboundary Element Method for the Static Analysis of Raft Foundations on Piles”. Engng Anal Bound Elem 2000; 24:237–247. Elsevier.

89. Mets M., (1997), “Piled Raft Classification and Behavior”, Proc. XIV ICSMFE, Hamburg, vol. 4, pp. 2259-2260.

90. Novak J.L, Reese L.C., Wang S.T. (2005), “Analysis of Piled Raft Foundation with 3D Finite Element Method” Structures, ASCE,

91. Ottaviani, M. (1975), Three Dimensional Finite Element Analysis of Vertically Loaded Pile Groups", Geotechnique 25, no.- 2, 159-174.

92. Pellissier J. (1997), "A Raft Design Method for Swelling Clay", Proc. XIV ICSMFE, vol. 1 pp. 863-869.

93. Placzek D., Jentzsch E. (1997), "Piled raft foundation under exceptional vertical loads - Bearing behavior and settlement", XIV ICSMFE, vol. 2 pp. 1116-1118.

94. Poorooshasb H.B., Noorzad A. (1995), "Analysis of Piled Raft Foundation", Numerical Methods in Geomechanics, 565-571, Rotterdam Balkema.

95. Poulos, H.G. (2007), "Design Charts for Pile Supporting Embankments on Soft Clay", Journal of Geotechnical and Geo-environmental Engineering, ASCE, vol. 133, no.-5, 493-501.

96. Poulos, H.G. (2005), "Piled Raft and Compensated Piled Raft Foundation for Soft Soil Sites", Advances in Designing and Testing Deep Foundations, Geot. Spec. Pub. No. 129, ASCE, 214-234.

97. Poulos, H.G. (2002), "Simplified Design Procedure for Piled Raft Foundations", Deep Foundations 2002, ASCE Spec. Geot. Pub. No. 116, 1: 441-458

98. Poulos, H.G. (2001a), "Piled Raft Foundations: Design and Applications", Géotechnique 51, (2): 95-113.

99. Poulos, H.G. (2001b), "Methods of Analysis of Piled Raft Foundations", TC18 Report, Int. Society of Soil Mech. and Geot. Engineering.

100. Poulos, H.G., Small, J.C., Ta, L.D., Sinha, J. & Chen, L. (1997), "Comparison of Some Methods for Analysis of Piled Rafts. Proc. 14th Int. Conf. Soil Mech. Found. Eng, Hamburg 2, 1119-1124, Rotterdam: Balkema

101. Poulos, H.G. (1994), "An Approximate Numerical Analysis of Pile- Raft Interaction", Int. J. Numer. And Analytical Methods in Geomech., London, 18(2), 73-92.

102. Poulos, H.G. (1993), "Piled Rafts in Swelling or Consolidating Soils", Jnl. Geotechnical Div., ASCE, 119(2), 374-380.

103. Poulos, H.G. (1991), "Analysis of Piled Strip Foundations", Proc. of the 7th Int. Con. on Computer Methods and Advances in Geomechanics/Cairns/6-10 May 1991 : Computer methods and advances in geomechanics. Rotterdam Balkema. 183-191.

104. Poulos, H.G. (1989), "Pile Behavior: Theory and Application", Géotechnique 39, No. 3, 365-415.

105. Poulos, H.G. and Davis, E.H. (1980), "Pile Foundation Analysis and Design", John Wiley, New York.

106. Prakoso, W. A., and Kulhawy, F. H., (2002), "Contribution to Piled Raft Foundation Design", Discussion and Closures, J of Geotech. and Geoenv. Engg, ASCE, vol. 128 (8): 707-709.

107. Prakoso, W. A., and Kulhawy, F. H., (2001), "Contribution to Piled Raft Foundation Design", J of Geotech. and Geoenv. Engg, ASCE, vol 127(1): 17-24.

108. Price, G. and Wardle, I.F. (1986), "Queen Elizabeth II Conference Centre: Monitoring of Load Sharing Between Piles and Raft", Proc. Inst. Civ. Engrs., 80(1): 1505-1518.

109. Randolph, M.F. (1994a), "Design Methods for Pile Groups and Piled Rafts" Proc.XIII ICSMFE, New Delhi, Vol.5, 61-82, Rotterdam Balkema.

110. Randolph, M.F., Clancy P. (1994b), "Design and Performance of a Piled Raft Foundation", Proceedings on Settlement, ASCE< Geotechnical Special Publications 40. pp. 1315-1336.

111. Randolph, M.F., Clancy P. (1993), "Efficient Design of Piled Rafts", Proceedings of the 2nd International Geotechnical Seminar on Deep Foundation on bored and Auger Piles, Guent, Belgium, pp. 119 - 130.

112. Randolph, M.F. (1983), "Design of Piled Raft Foundations" Proc. Int. Symp. on Recent Developments in Laboratory and Field Tests and Analysis of Geotechnical Problems, Bangkok, pp 525-537.

113. Randolph M.F. (1981), "The Response of Flexible Piles to Lateral Loading", Geotechnique, Vol 31, No 2, pp 247-259.

114. Randolph M.F. (1981), "Piles Subjected to Torsion", J. of the Geot. Eng. Div., ASCE, Vol 107, No GT8, pp 1095-1111

115. Randolph, M.F. and Wroth C. P. (1979), "Analysis of Deformation of Vertically Loaded Pile Groups", Géotechnique, 29(4): 423-439.

116. Reese L.C., Wang S.T., Reuss R., (1993), "Test of Auger Piles for Design of Pile Supported Rafts", International Journal of Analytical and Numerical methods in Geomechanics, 22(6), 477-493.

117. Resende L., Martin J.B. (1985), "Formulation of Drucker-Prager Cap Model", Journal of Engineering Mechanics. ASCE, vol. 111 no. 7 pp 855 – 881.

118. Reul O., Krajewski W., Ripper P. (2006), Numerical Analysis of Foundations for High-Rise Buildings and Deep Excavations", FELSBAU 24, no.-2, pp. 22-30.

119. Reul & Randolph (2003). Piled rafts in Over-consolidated Clay-Comparison of In-situ Measurements and Numerical Analyses. Géotechnique, 2003, Vol. 1

120. Russo, G. (1998), "Numerical Analysis of Piled Rafts", Int. Journ. Analytical and Numerical Methods in Geomechanics, 22(6): 477-493.

121. Russo, G. and Viggiani, C. (1997), "Some Comments on the Analysis of Piled Rafts". Proceedings 14th ICSMFE, Hamburg, vol 4 pp 2263 – 2264, Rotterdam Balkema.

122. Sanctis, L D., Mandolini, A., (2006), "Bearing Capacity of Piled Raft on Soft Clay Soil", Journal of Geotechnical and Geo-environmental Engineering, ASCE, vol. 132, no.-12, pp.1600-1610 .

123. Sanctis, L D., Mandolini, A., Russo, G. and Viggiani, C. (2002), "Some Remarks on the Optimum Design of Piled Rafts", Geot. Spec. Pub. 116, ASCE, 1: 405-425.

124. Sandler, I. S., DiMaggio, F. L., Baladi, G. Y. (1976), "Generalized Cap Model for Geological Materials",. Journal of the Geotechnical Engineering Division, Proc. ASCE, Vol. 102, No. GT7, 683-699.

125. Schwab, H., H., Günding, N., Lutz, B. (1991), "Monitoring Pile Raft Soil Interaction". Proc. 3rd International Symposium on Field Measurements in Geo-mechanics, Oslo, 1-11, Rotterdam: Balkema

126. Selvadurai, A. P. S. (1979), "Elastic Analysis Of Soil- Foundation Interaction", In Developments In Geotechnical Engineering Vol. 17. Amsterdam: Elsevier.

127. Shen, W.Y., Chow, Y.K., and Yong, K.Y. (2000), "A Variational Approach For The Analysis Of Pile Group-Pile Cap Interaction", Geotechnique, 50(4): 349-357.

128. Sinha, J., and Poulos, H.G. (1997), "Piled Raft Foundation Systems in Swelling and Shrinking Soils", Proc., 14th Int. Conf. on Soil Mech. and Found. Engg., ABMS, Brazil, Vol.2, 1141-1144.

129. Small J.C., Zhang H.H., (2002), "Behavior of Piled Raft Foundation Under Lateral and Vertical Loading", The International Journal of Geomechanics. Vol. 2 no.- 1, pp 29 -85.

130. Small J.C., (2001), "Practical Solution to Soil-Structure Interaction Problem", Prog. Struct. Engg. Mater 2001, 3: 305 - 314.

131. Small J.C., Booker J.R., (1986), "Finite Layer Analysis of layered Elastic materials Using a Flexibility Approach, Part 2 – Circular and Rectangular loadings", International Journal for Numerical Methods in Engineering. Vol. 23, pp 959 - 978.

132. Small J.C., Booker J.R., (1984), "Finite Layer Analysis of layered Elastic materials Using a Flexibility Approach, Part 1 – Strip loadings", International Journal for Numerical Methods in Engineering. Vol. 20, pp 1025 - 1037.

133. Smith, I. M., Wang, A. (1998), "Analysis of Piled Rafts". International Journal of Numerical and Analytical Methods in Geo-mechanics, Vol. 22, 477-492

134. Sommer, H. (1993), "Development of locked stresses and negative shaft resistance at the piled raft foundation - Messeturm Frankfurt/Main". Proc. Deep Foundations on Bored and Auger Piles, 347-349, Rotterdam: Balkema.

135. Sommer, H., Tamaro, G., De Benedittis, G. (1991), "Messeturm: Foundation for Tallest Building in Europe", Proc.4th Int. Conf. Piling and Deep Foundations, Stresa, Balkema, Rotterdam, Vol. 1,139-146.

136. Sommer, H., Wittmann, P. and Ripper, P. (1985), "Piled Raft Foundation of a Tall Building in Frankfurt Clay", Proc.11 ICSMFE, San Francisco, 4:2253-2257.

137. Ta, L. D., and Small, J. C. (1997), "An Approximation for Analysis of Raft and Piled Raft Foundations", Computers and Geotechnics, vol. 20, no. – 2, 105-123.

138. Ta, L. D., and Small, J. C. (1996), "Analysis of Piled Raft Systems in Layered Soils", Int.J. Numer.and Analytical Methods in Geomech.,20, 57-72.

139. Terzaghi K. (1936), "Discussion Contribution", Proceedings of 1st ICSMFE, Cambridge, Mass, USA, June 1936 vol.3 pp 92-96.

140. Trochanis, A. M., Bielak, J., Christiano, P. (1991), "Three Dimensional nonlinear study of piles". Journal of Geotechnical Engineering, Proc. ASCE, Vol. 117, No. 3, 429-447.

141. Van Impe W.F., “TC 18 Activity Report – Summary”, Proc.XIV ICSMFE, Hamburg, Vol. 4, pp 2637 – 2640.

142. Vasquez L.G., Wang S.T., Isenhower W.M. (2006), “Estimation of the Capacity of the Piled Raft Foundations by Three Dimensional Nonlinear Finite Element Analysis”, Geocongress, ASCE sp. Publications 2006,

143. Wriggers, P. (2006), “Computational Contact Mechanics”, 2nd edition, Springer, New York.

144. Wriggers, P. (1995), “Finite Element Algorithms for Contact Problems”. Archives of Computational Methods in Engineering, Vol. 2, 4, 1-49.

145. Yamashita, K., Kakurai, M., Yamada, T., (1993), “Settlement Behavior of a Five Storied Building on Piled Raft Foundation”, Proc. of the 2nd Int. Geotechnical Seminar on Deep Found. on Bored and Auger Piles, Guent, Belgium, 350-356 Balkema, Rotterdam, Brooke.

146. Yang R. (2007), “Nonlinear Interaction of Pile-Soil-Raft During Consolidation”, Ph.D. Thesis, Dept. of BCEE, Concordia University.

147. Yu H.S. (1998), “CASM: A Unified State Parameter Model for Clay and Sand”, Int. J. Num. Anal. Meth. Geomech. Vol. 22, pp. 621-653.

148. Yu H.S. (1995), “A Unified Critical State Model for Clay and Sand”, Civil Engineering Research Report no.- 112.08.1995, University of Newcastle, NSW.

149. Zeevaert, L. (1957b), “Compensated Friction-Pile Foundation to Reduce the Settlement of Buildings on Highly Compressible Volcanic Clay of Mexico City”, Proc. 4th ICSMFE, London, v.2, pp. 81 - 86.

150. Zeevaert, L. (1957a), “Foundation Design and Behavior of Tower Latino Americana in Mexico City”,Geotechnique, v.7, no.-1, pp. 115 - 133.

151. Zhang H.H, Small J.C (2000), “Analysis of Capped Pile Groups Subjected to Horizontal and Vertical loads”, Computers and Geotechnics. Vol. 26, pp. 1 - 21.